

2016

Dry Powder Aerosol Nanocomposite Microparticles for the Treatment of Pulmonary Diseases

Zimeng Wang
University of Rhode Island

Follow this and additional works at: https://digitalcommons.uri.edu/oa_diss

Terms of Use

All rights reserved under copyright.

Recommended Citation

Wang, Zimeng, "Dry Powder Aerosol Nanocomposite Microparticles for the Treatment of Pulmonary Diseases" (2016). *Open Access Dissertations*. Paper 605.
https://digitalcommons.uri.edu/oa_diss/605

This Dissertation is brought to you by the University of Rhode Island. It has been accepted for inclusion in Open Access Dissertations by an authorized administrator of DigitalCommons@URI. For more information, please contact digitalcommons-group@uri.edu. For permission to reuse copyrighted content, contact the author directly.

DRY POWDER AEROSOL NANOCOMPOSITE MICROPARTICLES FOR THE
TREATMENT OF PULMONARY DISEASES

BY

ZIMENG WANG

A DISSERTATION SUBMITTED IN PARTIAL FULFILLMENT OF THE
REQUIREMENTS FOR THE DEGREE OF
DOCTOR OF PHILOSOPHY
IN
CHEMICAL ENGINEERING

UNIVERSITY OF RHODE ISLAND

2016

DOCTOR OF PHILOSOPHY DISSERTATION

OF

ZIMENG WANG

APPROVED:

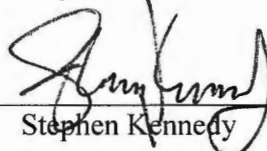
Dissertation Committee:

Major Professor


Samantha Meenach



Arijit Bose



Stephen Kennedy



Nasser H. Zawia

DEAN OF THE GRADUATE SCHOOL

UNIVERSITY OF RHODE ISLAND

2016

ABSTRACT

Dry powder aerosols have attracted increasing attention for the treatment of pulmonary diseases due to their capability of providing direct and efficient drug delivery to the lungs. Unfortunately, barriers exist in the implementation of dry powder pulmonary delivery systems, including: (1) dry powder aerosols with aerodynamic diameters smaller than 1 μm will often be exhaled; (2) particles with aerodynamic diameters above 5 μm tend to deposit in the mouth, throat or upper lung mucosa and will then be eliminated due to mucosal clearance mechanisms; and (3) particles larger than 1 μm that deposit in the deep lung area may be cleared from the alveoli via macrophages. Spray-dried nanocomposite microparticles (nCmP), combining the advantages of nanoscale and microscale carriers, can be employed to overcome these issues. Microscale powders facilitate effective deep lung deposition while the embedded nanoscale carriers can provide multiple functions such as the protection of active ingredients from degradation, enhancement of the solubility of drugs, controlled drug release, and reduction of systemic side effects. Several nCmP systems have been developed for various applications, but few comprehensive studies have been completed to illustrate how to effectively engineer optimal nCmP systems with desired properties including: targeted deposition in airways, controlled release of payloads, ability of overcoming physiological barriers, and favorable formulation stability.

This dissertation focuses on the development, characterization, and optimization of various dry powder aerosol nanocomposite microparticle systems for

the treatment of pulmonary diseases. In the production of nCmP, acetalated dextran (Ac-Dex) nanoparticles loaded with therapeutics are synthesized, suspended in an excipient solution or DI water, and transformed into microscale dry powder microparticles via spray drying. Upon pulmonary administration, the nCmP will deposit on the surface of the mucosal layer of the lungs and decompose into free NP, allowing the nanoparticles to reach the mucus and/or cell epithelium and then release drug(s) at sustained rate. Nanoparticles were prepared using Ac-Dex with different degradation rates to control the drug release profiles. In this work, various therapeutics were encapsulated in nanoparticles, and subsequently nCmP, for applications in the treatment of cystic fibrosis-related lung infections or pulmonary arterial hypertension. The physical properties of the nanoscale carriers in terms of size, size distribution, and surface properties were modified by manipulating the parameters of the nanoparticle preparation process. Dry powder aerosols embedded with nanoparticles were formulated using spray drying. The aerosol performance was optimized by manipulating the composition of feed solution and spray drying parameters. The optimal parameters to form nCmP with deep lung and whole lung deposition were studied. Furthermore, the favorable drying conditions necessary to achieve high therapeutic stability and formulation stability of the particles was also evaluated.

Overall, dry powder aerosol nanocomposite microparticles have the ability to provide pulmonary drug delivery systems with tunable properties to fit a wide variety of desired applications. These general-purpose systems exhibit promising potential in the improved treatment of pulmonary diseases through particle engineering and design.

ACKNOWLEDGMENTS

First of all, I would like to express my appreciation to my advisor, Professor Samantha Meenach, for her invaluable guidance and support through my Ph.D. studies at the University of Rhode Island. I still remember feeling a loss in the direction and confusion about my future in the first half of 2013. When summer began, Dr. Meenach, gave me the opportunity to join her research group, which rebuilt my faith to keep moving forward in my studies and career as an engineer. She taught me not only how to accomplish effective experimental work but also how to design a project from start to finish. Dr. Meenach showed me how to effectively give a presentation as well as helped me to learn to deliver my thoughts to others more effectively. With her tremendous help and encouragement, I was motivated to become an effective researcher, and more importantly, an independent thinker.

I would also like to thank my dissertation defense committee members, Professor Arijit Bose, Professor Stephen Kennedy, Professor Daniel Roxbury, and Professor Leon Thiem for their constructive comments and precious feedback on my dissertation and related research. I thank Dr. David Worthen for his kind help as a former dissertation defense committee member. I would like to express gratitude to Professor Peng Wang for his patient guidance when I first came to the United States and I also want to thank Dr. Stanley M. Barnett for his instruction in my second year of study. All of these individuals provided insightful ideas for my research from different points of view, which helped this dissertation to be in better shape.

I want to thank all my lab mates, but especially Qihua Sun, Sarah Brousseau, Elisa Torrico-Guzman, Sweta Gupta, Nishan Shah, and Julie Cuddigan for providing

me invaluable suggestions on my research and my life. I would also like to thank all the undergraduate students I have worked with for their feedback about my research as well as my training. I extend a special thanks to Anthony Brouillard, who has worked with me on four projects and helped me to set up several experiments.

I would like to thank Sheryl Girard, Brenda Moyer, Dr. Richard Brown, and Dr. Michael Greenfield for their kind help throughout my time at graduate school. I am also very grateful to Dr. Everett Crisman for his patient guidance on experimental operation of the SEM, to Dr. Geoffrey Bothun for his insightful advice on my research, and to Dr. Al Bach for his patient training and inspiring discussions.

Finally, my sincere gratitude goes to my mom, Li Li, and my dad Yuanfu Wang for their unconditional support and love. I want to thank my aunt Donghui Wang for her continuous encouragement in my life and studies. I would also like to thank my uncle, aunts, grandparents, cousins, and girlfriend, who have always had confidence in me. I would like to share this moment as well as every single achievement in future all together with them.

PREFACE

This thesis is written in manuscript format. The first chapter is an instruction of the entire dissertation. The second chapter, entitled “Nanocomposite Microparticles (nCmP) for Pulmonary Drug Delivery Applications,” was accepted as a chapter in the book, “In Strategies of Nanotechnology in Drug Delivery”. The third chapter, entitled “Synthesis and Characterization of Nanocomposite Microparticles (nCmP) for the Treatment of Cystic Fibrosis-Related Infections,” is published in *Pharmaceutical Research*. The third chapter entitled, “Nanocomposite Microparticles (nCmP) for the Delivery of Tacrolimus in the Treatment of Pulmonary Arterial Hypertension,” is published in the *International Journal of Pharmaceutics*. The fourth chapter, entitled “Optimization of Nanocomposite Microparticles (nCmP) for Deep Lung Delivery of Therapeutics via Spray Drying,” was submitted to *Powder Technology* in October 2016. The fifth chapter, entitled “Development and Physicochemical Characterization of Acetalated Dextran Aerosol Particle Systems for Deep Lung Delivery,” was submitted to *International Journal of Pharmaceutics* in October 2016. The seventh chapter includes the conclusions and future work related to this dissertation.

TABLE OF CONTENTS

ABSTRACT	ii
ACKNOWLEDGMENTS	iv
PREFACE	vi
TABLE OF CONTENTS	vii
LIST OF TABLES	xii
LIST OF FIGURES	xvi
CHAPTER 1	1
Introduction	1
1.1 Motivation	1
1.2 Significance of This Study	4
1.3 Objectives of This Research.....	5
1.4 Dissertation Organization.....	6
1.5 References	8
Nanocomposite Microparticles (nCmP) for Pulmonary Drug Delivery Applications. 10	
2.1. Introduction	11
2.1.1. Pulmonary delivery of dry powder particle-based therapeutics.....	11
2.1.2. Dry powder aerosol delivery devices.....	12
2.1.3. Overview of current dry powder aerosol therapeutics	14
2.1.4. Obstacles in pulmonary delivery of particle-based therapeutics.....	17
2.1.5. Design for pulmonary deposition of particles	20
2.1.6. Long-term storage considerations	21
2.2. Nanocomposite microparticles: a solution for overcoming the obstacles of particle-based pulmonary delivery	22
2.3. Preparation of nanocomposite microparticles (nCmP)	29
2.3.1. Techniques used to prepare drug-loaded nanoparticles	29
2.3.3. Materials and excipients used in the preparation of nCmP	35
2.4. Optimization of nCmP manufacturing via spray drying	37
2.4.1. How spray dryer settings influence dry powder formulations	38
2.4.2. A theoretical framework of nanocomposite microparticle (nCmP) formation	40
2.4.3. Influence of spray drying parameters on nCmP formation	42
2.5. Drug release behavior from nanocomposite microparticle (nCmP) systems.....	50

2.6. Therapeutic applications of nanocomposite microparticles: Impact in pulmonary and non-pulmonary diseases	52
2.5 References	53
CHAPTER 3	66
Synthesis and Characterization of Nanocomposite Microparticles (nCmP) for the Treatment of Cystic Fibrosis-Related Infections	66
3.1 Introduction	68
3.2 Materials and Methods	73
3.2.1 Materials	73
3.2.2 Synthesis of Acetalated Dextran (Ac-Dex)	73
3.2.3 Synthesis of Vitamin E Poly(ethylene glycol) (VP5k)	74
3.2.4 NMR Analysis of Ac-DEX and VP5k	74
3.2.5 Preparation of Drug-loaded Nanoparticles	75
3.2.6 Preparation of Nanocomposite Microparticles (nCmP)	75
3.2.7 Powder X-Ray Diffraction (PXRD)	76
3.2.8 Differential Scanning Calorimetry (DSC)	76
3.2.9 Scanning Electron Microscopy (SEM)	77
3.2.10 Particle Size, Size Distribution and Zeta Potential Analysis	77
3.2.11 Karl Fischer (KF) Titration	77
3.2.12 Aerosol Dispersion Analysis	78
3.2.13 Analysis of Nanoparticle Drug Loading and Nanoparticle Loading in nCmP	79
3.2.14 In Vitro Drug Release from Nanoparticles	80
3.2.15 Statistical analysis	81
3.3 Results and Discussion	81
3.3.1 NMR Analysis of Ac-Dex and VP5k	81
3.3.2 Characterization of Nanoparticles	82
3.3.3 Manufacturing of nCmP	83
3.3.4 nCmP Morphology, Sizing, and Size Distribution	83
3.3.5 Karl Fisher (KF) Titration	85
3.3.7 Powder X-ray Diffraction (PXRD)	86
3.3.8 Drug and Nanoparticles Loading in nCmP	87
3.3.9 Nanoparticle Redispersion from nCmP	87
3.3.10 In vitro Aerosol Performance of nCmP	89

3.4 Conclusions.....	92
3.5 Acknowledgements.....	93
3.6 References.....	93
CHAPTER 4	99
Nanocomposite Microparticles (nCmP) for the Delivery of Tacrolimus in the Treatment of Pulmonary Arterial Hypertension	99
4.1. Introduction.....	101
4.2 Materials and Methods.....	106
4.2.1 Materials	106
4.2.2 Synthesis and NMR Analysis of Acetalated Dextran (Ac-Dex).....	107
4.2.3 Formation of TAC-Loaded Ac-Dex Nanoparticles (TAC NP).....	107
4.2.4 Formulation of Nanocomposite Microparticles (nCmP) Via Spray Drying	108
4.2.5 Particle Morphology and Shape Analysis via Scanning Electron Microscopy (SEM)	108
4.2.6 Particle Size, Size Distribution, and Zeta Potential Analysis.....	109
4.2.7 Analysis of Nanoparticle Drug Loading and Nanoparticle Loading in nCmP.....	109
4.2.8 In Vitro Drug Release from Nanoparticles	110
4.2.9 Karl Fischer Coulometric Titration.....	111
4.2.10 Differential Scanning Calorimetry (DSC)	111
4.2.11 Powder X-Ray Diffraction (PXRD)	111
4.2.12 In Vitro Aerosol Dispersion Performance with the Next Generation Impactor (NGI)	112
4.2.13 Tapped Density and Theoretical Aerodynamic Diameter Analysis.....	113
4.2.14 In vitro cytotoxicity of TAC nCmP using resazurin assay	114
4.2.15 Statistical Analysis	115
4.3. Results and Discussion.....	115
4.3.1 Characterization of Ac-Dex.....	115
4.3.2 Characterization of Nanoparticles	116
4.3.3 Nanocomposite Microparticle Characterization	119
4.4 Conclusions.....	129
4.5 Acknowledgements.....	130
4.6 References.....	130
CHAPTER 5	136

Optimization of nanocomposite microparticles (nCmP) for deep lung delivery of therapeutics via spray drying	136
5.1. Introduction.....	138
5.2. Materials and Methods.....	143
5.2.1 Materials.....	143
5.2.2 Synthesis and NMR Analysis of Acetalated Dextran (Ac-Dex).....	144
5.2.3 Formation of CUR-Loaded Ac-Dex Nanoparticles (CUR NP)	144
5.2.4 Formulation of Nanocomposite Microparticles (nCmP) Via Spray Drying	145
5.2.5 Design of Experiment.....	145
5.2.6 Particle Morphology and Shape Analysis via Scanning Electron Microscopy (SEM)	148
5.2.7 Analysis of Nanoparticles Following Redispersion in Aqueous Solution	148
5.2.8 Analysis of Drug Loading of CUR NP and CUR nCmP	149
5.2.9 Karl Fischer Coulometric Titration.....	150
5.2.10 Differential Scanning Calorimetry (DSC)	150
5.2.11 In Vitro Aerosol Dispersion Performance with the Next Generation Impactor (NGI)	151
5.2.12 Statistical analysis.....	152
5.3. Results and Discussion.....	153
5.3.1 Preparation and Characterization of Curcumin-Loaded Nanoparticles (CUR NP).....	153
5.3.2 Design of Experiment and nCmP Characterization	154
5.4 Conclusions.....	165
5.5 Acknowledgements.....	166
5.6 References.....	168
CHAPTER 6	174
Development and Physicochemical Characterization of Acetalated Dextran Aerosol Particle Systems for Deep Lung Delivery.....	174
6.1 Introduction.....	176
6.2. Materials and Methods.....	180
6.2.1 Materials.....	180
6.2.2 Synthesis and NMR Analysis of Acetalated Dextran (Ac-Dex).....	181
6.2.3 Formation of CUR-Loaded Ac-Dex Nanoparticles (CUR NP)	182
6.2.4 Formulation of CUR Nanocomposite Microparticles (nCmP) Via Spray Drying	182
6.2.5 Formulation of CUR Microparticles (MP) Via Spray Drying	183

6.2.6 Particle Size, Size Distribution, and Zeta Potential Analysis.....	183
6.2.7 Particle Morphology and Shape Analysis via Scanning Electron Microscopy (SEM)	184
6.2.8 Tapped Density Evaluation.....	184
6.2.9 Drug Loading Analysis of CUR nCmP and CUR MP.....	185
6.2.10 In Vitro Drug Release from nCmP and MP.....	186
6.2.11 Differential Scanning Calorimetry (DSC).....	186
6.2.12 Powder X-Ray Diffraction (PXRD).....	187
6.2.13 Karl Fischer Coulometric Titration.....	187
6.2.14 In Vitro Aerosol Dispersion Performance with the Next Generation Impactor (NGI).....	187
6.2.15 Statistical analysis.....	189
6.3. Results and Discussion.....	189
6.3.1 Preparation and Characterization of Ac-Dex and Curcumin Nanoparticles	189
6.3.2 Preparation and Characterization of Nanocomposite Microparticles (nCmP) and Microparticles (MP)	192
6.4. Conclusions.....	206
6.5 Acknowledgements.....	206
6.6 References.....	207
CHAPTER 7	211
Conclusions and Future Work.....	211
7.1 Conclusions.....	211
7.2 Future Work.....	212
APPENDIX A.....	214
Supplementary Material for Chapter 3.....	214
APPENDIX B.....	222
Supplementary Material for Chapter 4.....	222
APPENDIX C.....	224
Supplementary Material for Chapter 5.....	224
APPENDIX D.....	230
Supplemental Material for Chapter 6.....	230
BIBLIOGRAPHY.....	236

LIST OF TABLES

2.1	Current dry powder inhaler (DPI) formulations approved by the FDA including the approval date, brand date, active pharmaceutical ingredient (API), disease, and company.....	16
2.2	Overview of nanocomposite microparticles (nCmP) systems used to deliver therapeutics for pulmonary applications with their active pharmaceutical ingredient (API), treatment application, and key findings.....	24
3.1	Size (as measured by dynamic light scattering), polydispersity index (PDI), zeta potential (ζ), drug loading, and encapsulation efficiency (EE) of nanoparticles.....	84
3.2	Size (as measured by SEM imaging and ImageJ analysis), water content, drug loading, nanoparticle (NP) loading in nanocomposite microparticles (nCmP), and NP loading efficacy in nCmP.....	87
3.3	<i>In vitro</i> aerosol dispersion performance properties including mass median aerodynamic diameter (MMAD), geometric standard deviation (GSD), fine particle dose (FPD), fine particle fraction (FPF), respirable fraction (RF), and emitted dose (ED) for nCmP.....	91
A.1	Characterization of nanoparticles after redispersion from nanocomposite microparticles in PBS including the size, polydispersity index (PDI), and zeta (ζ) potential.....	215
4.1	Diameter (as measured by dynamic light scattering), polydispersity index (PDI), zeta potential (ζ), TAC loading, and encapsulation efficiency (EE) of tacrolimus-loaded nanoparticles before spray drying (TAC NP) and after	

	spray drying and redispersion from nanocomposite microparticles (Redispersed TAC NP).....	117
4.2	Geometric diameter (as measured by SEM imaging and ImageJ analysis), water content, TAC loading, nanoparticle (NP) loading in nanocomposite microparticles (nCmP), and NP loading efficacy in nCmP.....	127
4.3	<i>In vitro</i> aerosol dispersion performance properties including theoretical mass median aerodynamic diameter (MMADT) from tapped density measurements, experimental mass median aerodynamic diameter (MMADE), geometric standard deviation (GSD), fine particle dose (FPD), fine particle fraction (FPF), respirable fraction (RF), and emitted dose (ED) for nCmP.....	143
5.1	Factors and levels for the Box-Behnken design of dry powder aerosol nanocomposite microparticle (nCmP) formulations corresponding to the spray drying parameters utilized.....	146
5.2	Spray drying formulation parameters of the nanocomposite microparticle (nCmP) system including the inlet temperature (T_{in}), nanoparticle loading in weight % (NP%), and feed concentration (F_c).....	147
5.3	Properties of curcumin nanoparticles (CUR NP) including their size (as measured by dynamic light scattering), polydispersity index (PDI), zeta potential, drug loading, and encapsulation efficiency (EE).....	154
5.4	Responses of the Box-Behnken design for the nanocomposite microparticle (nCmP) systems including drug loading, encapsulation efficiency (EE), water content, mass median aerodynamic diameter (MMAD), geometric standard	

	deviation (GSD), fine particle fraction (FPF), respirable fraction (RF), emitted dose (ED), percent size change, and percent polydispersity index (PDI) change.....	156
5.5	Statistical significance (p-value and coefficient estimation) of nanocomposite microparticle (nCmP) formulation parameters including drug loading (DL), encapsulation efficiency (EE), size change, polydispersity (PDI) change, mass median aerodynamic diameter (MMAD), fine particle fraction (FPF), respirable fraction (RF), emitted dose (ED), and water content (WC) with respect to the spray dryer inlet temperature (T_{in}), nanoparticle loading (NP%), and feed concentration (Fc).....	157
C.1	Summary of curcumin-loaded nanocomposite microparticle (nCmP) systems and their corresponding inlet temperature (T_{in}), nanoparticle loading (NP %), and feed concentration (Fc).....	225
C.2	Summary of the nCmP properties following spray drying.....	229
6.1	Average diameter (as measured by dynamic light scattering), polydispersity index (PDI), and zeta potential (ZP) of CUR-loaded nanoparticles before spray drying (NP) and after redispersion from nanocomposite microparticles (nCmP).....	206
6.2	Geometric diameter (as measured by SEM imaging and ImageJ analysis), water content, tapped density, theoretical mean mass aerodynamic diameter (MMADT), drug loading, and drug encapsulation efficiency of nCmP and MP.....	208

D.1	The drug release duration and total released fraction of each particle system at both pH.....	191
D.2	Summary of the coefficient of determinations (R^2) of all the models for all particle system. The model with relatively high R^2 for all particle systems was regarded as applicable.....	193

3.3	<i>In vitro</i> drug release profiles for azithromycin (AZI) and rapamycin (RAP) nanoparticle systems.....	84
3.4	Differential scanning calorimetry (DSC) thermograms of raw azithromycin (AZI), raw rapamycin (RAP), raw acetalated dextran (Ac-Dex), raw mannitol, AZI-nCmP, and RAP-nCmP.....	88
3.5	Powder X-ray (PXRD) diffractograms of raw azithromycin (AZI), raw rapamycin (RAP), raw acetalated dextran (Ac-Dex), raw mannitol, AZI-nCmP, and RAP-nCmP.....	89
3.6	Aerosol dispersion performance as % deposited on each stage of the Next Generation Impactor™ (NGI™) for AZI- and RAP-nCmP.....	90
A.1	Schematic of Ac-Dex synthesis	216
A.2	NMR spectra of VP5k where (top) indicates entire spectra and (bottom) is an enlarged portion.....	217
A.3	NMR spectrum of acetalated dextran degradation products.....	218
A.4	Structure of azithromycin.....	219
A.5	Structure of rapamycin.....	220
A.6	Next generation impactor.....	221
4.1	Schematic of an aerosol nanoparticle microparticle (nCmP) system interacting with the pulmonary mucosa.....	105
4.2	Representative SEM micrographs of tacrolimus (TAC) nanoparticles (NP) and nanocomposite microparticles (nCmP).....	116
4.3	<i>In vitro</i> drug release profile for tacrolimus (TAC) nanoparticle system...	118

LIST OF FIGURES

1.1	Figure 1.1. Schematic of nanoparticle formulation via nanoprecipitation...	3
1.2	Figure 1.2. Schematic of nanoparticle formulation via emulsion evaporation.....	3
1.3	Figure 1.3. Schematic of nanocomposite microparticle formulation via spray drying.....	4
2.1	Schematic of nanocomposite microparticle (nCmP) system used for pulmonary delivery applications.....	23
2.2	Representative nanocomposite microparticles (nCmP) systems imaged via scanning electron microscopy (SEM), transmission electron microscopy (TEM), and fluorescence imaging.....	30
2.3	Schematic of nanocomposite microparticle (nCmP) formation during spray drying from a droplet of feed solution of nanoparticles (NP) and excipients in a solvent.....	42
2.4	Schematic of processing parameters affecting the aerodynamic diameter of nanocomposite microparticles (nCmP).....	48
2.5	Schematic outlining the parameters that can influence the stability of nCmP.	49
2.6	Schematic of the parameters that affect the recovery of redispersed nanoparticles from nCmP.....	49
3.1	Schematic of an aerosol nanoparticle microparticle (nCmP) system interacting with the pulmonary mucosa.....	71
3.2	Representative SEM micrographs of azithromycin (AZI) nanoparticles (NP) and nanocomposite microparticles (nCmP).....	83

4.4	Representative differential scanning calorimetry (DSC) thermograms of raw tacrolimus (TAC), raw acetalated dextran (Ac-Dex), raw mannitol, TAC nanoparticles (TAC NP), and formulated TAC nanocomposite microparticles (TAC nCmP).....	122
4.5	Representative powder X-ray (PXRD) diffractograms of raw tacrolimus (TAC), raw acetalated dextran (Ac-Dex), raw mannitol, and formulated TAC nanocomposite microparticles (TAC nCmP).....	123
4.6	Aerosol dispersion performance of tacrolimus nanocomposite microparticles (TAC nCmP) as % particles deposited on each stage of the Next Generation Impactor™ (NGI™).....	126
4.7	A549 cell viability measured by resazurin assay after 48 h and 72 h exposure to (a) free TAC, and (b) TAC nanocomposite microparticles (nCmP).....	128
B.1	Structure of tacrolimus.....	223
5.1	Schematic of (A) the preparation of curcumin nanoparticles (CUR NP) via emulsion/solvent evaporation, (B) formation and collection of nanocomposite microparticles (nCmP) via spray drying, and (C and D) an aerosol nCmP system interacting with the pulmonary mucosa.....	141
5.2	Influence of spray dryer inlet temperature (T_{in}) on the size and polydispersity index (PDI) of nanoparticles redispersed from nanocomposite microparticles comprised of 100% NP loading.....	160
5.3	Representative differential scanning calorimetry (DSC) thermograms of raw Ac-Dex, PVA, curcumin, and mannitol.....	161

5.4	Representative SEM micrographs of curcumin-loaded nanocomposite microparticles (CUR nCmP) spray dried with varying conditions such as inlet temperature (T_{in}), nanoparticle loading (NP%), and feed concentration (Fc).....	163
5.5	Nanocomposite microparticle (nCmP) aerosol dispersion performance as % deposited on each stage of the Next Generation Impactor™ (NGI™) for representative CUR nCmP systems.....	165
5.6	Schematic outlining the influences of inlet temperature (T_{in}), weight ratio of NP (NP%), and feed concentration (Fc) on the properties of the resulting nanocomposite microparticles.....	167
C.1	Representative SEM micrographs of curcumin-loaded nanocomposite microparticle systems (CUR nCmP) corresponding to Table B.1.....	226
C.2	Representative SEM micrographs showing the crack generation caused by the high energy electron beam.....	227
C.3	Structure of curcumin.....	228
6.1	Schematic depicting the of synthesis of Ac-Dex (Left) and preparation of nanoparticles and formation of nanocomposite microparticles (nCmP) and microparticles (MP).....	180
6.2	SEM micrographs of curcumin-loaded nanocomposite microparticles (CUR nCmP) and microparticles (CUR MP).....	192
6.3	<i>In vitro</i> drug release profiles for curcumin (CUR) nanocomposite microparticle (nCmP) and microparticle (MP) systems.....	195

6.4	Representative differential scanning calorimetry (DSC) thermograms of raw curcumin (CUR), raw acetalated dextran-5min (Ac-Dex-5min), raw acetalated dextran-3h (Ac-Dex-3h), CUR nCmP-5min, CUR nCmP-h, CUR nCmP-3h, CUR MP-5min, CUR MP-h, and CUR MP-3h.....	200
6.5	Representative powder X-ray diffractograms (PXRD) of raw curcumin (CUR), raw acetalated dextran-5min (Ac-Dex-5min), raw acetalated dextran-3h (Ac-Dex-3h), CUR nCmP-5min, CUR nCmP-h, CUR nCmP-3h, CUR MP-5min, CUR MP-h, and CUR MP-3h.....	203
6.6	Aerosol dispersion performance of curcumin-loaded nanocomposite microparticles (CUR nCmP) and microparticles (CUR MP) as % particles deposited on each stage of the Next Generation Impactor™ (NGI™).....	204
6.7	<i>In vitro</i> aerosol dispersion performance properties including fine particle dose (FPD), fine particle fraction (FPF), respirable fraction (RF), and emitted dose (ED) for curcumin loaded nanocomposite microparticles (CUR nCmP) and microparticles (CUR MP).....	205
D.1	Original data and fitted curves of <i>in vitro</i> drug release profiles for curcumin (CUR) nCmP and MP systems including CUR nCmP-5min, CUR nCmP-h, CUR nCmP-3h, CUR MP-5min, CUR MP-h, and CUR MP-3h at pH = 5 (A, C) and pH = 7.4 (B, D).....	235

CHAPTER 1

Introduction

1.1 Motivation

Pulmonary drug delivery has exhibited promising potential in the effective treatment of lung diseases, as it allows for the delivery of a wide range of therapeutics directly and efficiently to the lungs, thereby increasing local drug concentration, reducing systemic side effects, providing a rapid onset of pharmaceutical action, and avoiding the first-pass metabolism associated with the liver (1-4). As a result, various therapeutics such as antibiotics, proteins, peptides, anti-cancer drugs (5), plasmid DNA (6), siRNA (7), and anti-tuberculosis (TB) drugs have been employed in inhalation formulations for the treatment of pulmonary diseases such as asthma, chronic obstructive pulmonary disease (COPD), cystic fibrosis (CF)-related pulmonary infections, and lung cancer (5, 8). In comparison to liquid aerosol formulations, aerosols based on dry powders offer additional benefits such as enhanced stability of the formulations, controllable particle size for targeting specific regions of the lung, and increased drug loading of hydrophobic or lipophilic payloads (9, 10). Unfortunately, barriers exist in the implementation of dry powder pulmonary delivery systems, including: (1) dry powder aerosols with aerodynamic diameters smaller than 1 μm will often be exhaled; (2) particles with aerodynamic diameters above 5 μm tend to deposit in the mouth, throat or upper lung mucosa and will then be eliminated due to mucosal clearance mechanisms; and (3) particles larger than 1 μm deposited in the deep lung area may be cleared from the alveoli via macrophages

(10-12). Spray-dried nanocomposite microparticles (nCmP) can be employed to overcome these issues, as the integration of nanoscale and microscale carriers combines the benefits of both types of systems. Microscale powders (1 - 5 μm) facilitate effective deep lung deposition (12) while the embedded nanoscale carriers can provide multiple functions such as the protection of drugs from degradation, enhancement of the solubility of drugs, provision of controlled drug release, and reduction of systemic side effects (2, 13, 14). Although many nCmP systems have been developed, few comprehensive studies have been completed to illustrate the effective engineering of optimal nCmP systems for the pulmonary delivery of therapeutics.

To this end, the purpose of this work was to develop and optimize several dry powder aerosol nanocomposite microparticle systems for the treatment of pulmonary diseases. In the production of nCmP, acetalated dextran (Ac-Dex) nanoparticles loaded with therapeutics were prepared using nanoprecipitation (**Figure 1.1**) or emulsion evaporation (**Figure 1.2**). The resulting nanoparticle were suspended in an excipient solution or DI water, and transformed into microscale dry powder microparticles via spray drying (**Figure 1.3**). Upon pulmonary administration, the nCmP will deposit on the surface of the mucosal layer of the lungs and decompose into free NP, allowing the nanoparticles to penetrate the mucus and then release drug at sustained rate. The polymer Ac-Dex was applied to form drug-loaded nanoscale carriers with simply tunable release profiles. Various drugs were encapsulated in the nanoparticle matrices for the treatment of different pulmonary diseases. Vitamin E poly(ethylene glycol) 5000 (VP5k) or polyvinyl alcohol (PVA) coating was used to

improve the surface properties of the nanoparticles. Mannitol was employed as excipient at various ratios to improve the particle properties in terms of aerosolization and storage. The spray drying process parameters were manipulated to optimize the aerosol performance of the resulting nCmP and to maintain the desirable properties of original nanoparticles.

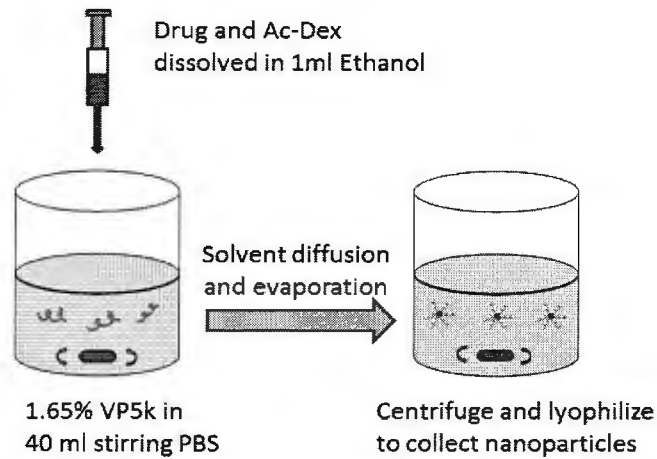


Figure 1.1. Schematic of nanoparticle formulation via nanoprecipitation.

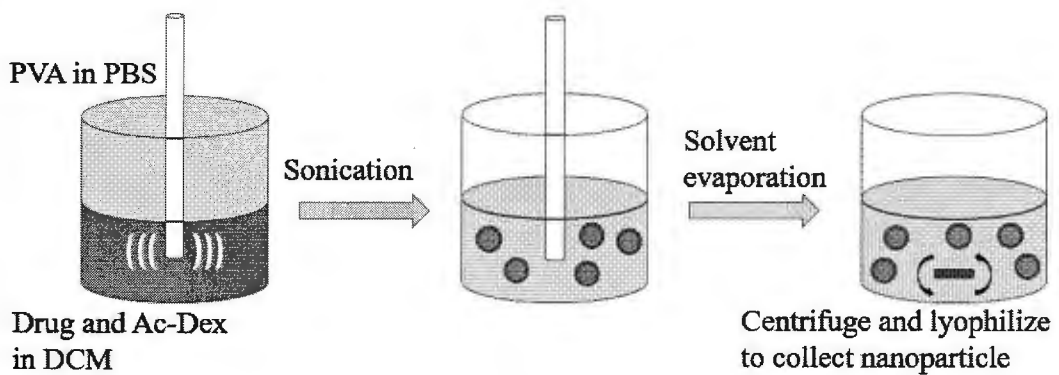


Figure 1.2. Schematic of nanoparticle formulation via emulsion evaporation.

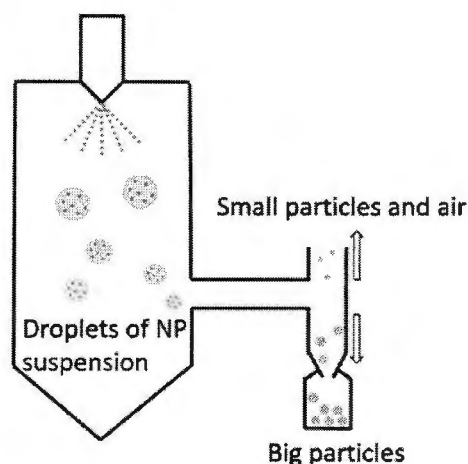


Figure 1.3. Schematic of nanocomposite microparticle formulation via spray drying.

1.2 Significance of This Study

This is a comprehensive study on the development, characterization, and optimization of nCmP systems for the treatment of pulmonary diseases. The significance of the research discussed in this dissertation is summarized as the following:

1. The nCmP system can provide a simply tailorable drug release profile of payloads by adjusting the synthesis of Ac-Dex polymer that is used for nanoparticle preparation.
2. The nCmP system can be design to primarily deposit at a targeted location in the airways by manipulating the nCmP formulation process parameters.
3. The nCmP system can overcome various physiological barriers by tuning the physical properties of nanoparticles, thus providing effective delivery of therapeutics for the treatment of pulmonary diseases.

1.3 Objectives of This Research

The overall objective of this dissertation was to develop, characterize, and optimize multipurpose dry powder aerosol nanocomposite microparticle systems for the treatment of pulmonary diseases. This involved four projects and the specific objectives of these are outlined as follows:

1. “Synthesis and characterization of nanocomposite microparticles (nCmP) for the treatment of cystic fibrosis-related infections”:
 - a) Prepare azithromycin or rapamycin-loaded nanoparticles with capable of mucus penetration and sustained release of therapeutics.
 - b) Formulate nanocomposite microparticles capable of delivering therapeutics to the deep lung.
 - c) Evaluate the physicochemical and aerosol dispersion properties of the particulate systems.
2. “Nanocomposite microparticles (nCmP) for the delivery of tacrolimus in the treatment of pulmonary arterial hypertension”:
 - a) Prepare tacrolimus-loaded nanoparticles capable sustained release.
 - b) Formulate nanocomposite microparticles capable of delivering therapeutics to the deep lung.
 - c) Evaluate the physicochemical and aerosol dispersion properties of the particulate systems.
3. “Optimization of nanocomposite microparticles (nCmP) for deep lung delivery of therapeutics via spray drying”:

- a) Identify the optimal spray drying condition in order to prepare nanocomposite microparticles with favorable properties including: ability of deep lung deposition, desirable nanoparticle re-dispersity, high drug loading, and low water content
4. “Development and Physicochemical Characterization of Acetalated Dextran Aerosol Particle Systems for Deep Lung Delivery”:
- a) Develop and characterize pulmonary delivery systems based on spray-dried Ac-Dex particles with the capability of delivering therapeutics to the deep lung, targeting to desired location, and releasing therapeutics in controlled rate.

1.4 Dissertation Organization

This dissertation will be organized as follows:

Chapter 2 provides the background information on nanocomposite microparticle systems for pulmonary drug delivery applications including an introduction of pulmonary delivery of dry powder particle-based therapeutics, a review of nanocomposite microparticles for pulmonary delivery, and a discussion of nanocomposite microparticles preparation, optimization, and applications.

Chapter 3 presents the project “Synthesis and characterization of nanocomposite microparticles (nCmP) for the treatment of cystic fibrosis-related infections,” which involves the development of nanocomposite microparticle systems for the delivery of antibiotics through viscous lung mucus caused by cystic fibrosis.

Chapter 4 includes the project “Nanocomposite microparticles (nCmP) for the delivery of tacrolimus in the treatment of pulmonary arterial hypertension (PAH),” which involves the development of nanocomposite microparticles for the deep lung delivery of tacrolimus, a novel treatment regime for PAH.

Chapter 5 includes the project “Optimization of nanocomposite microparticles (nCmP) for deep lung delivery of therapeutics via spray drying,” which discusses the optimization strategy necessary in order to prepare nanocomposite microparticles with favorable properties including: deep lung deposition, desirable nanoparticle re-dispersion, high drug loading, and low water content.

Chapter 6 focuses on the project “Development and Physicochemical Characterization of Acetalated Dextran Aerosol Particle Systems for Deep Lung Delivery,” which involves the development of Ac-Dex particles for targeted delivery and controlled release of therapeutics to the deep lung region.

Chapter 7 concludes the dissertation and also discusses the future directions in the development and optimization of multipurpose dry powder aerosol nanocomposite microparticle systems for the treatment of pulmonary diseases.

1.5 References

1. L. Cui, J.A. Cohen, K.E. Broaders, T.T. Beaudette, and J.M. Frechet. Mannosylated dextran nanoparticles: a pH-sensitive system engineered for immunomodulation through mannose targeting. *Bioconjugate chemistry*. 22:949-957 (2011).
2. H.M. Mansour, Y.-S. Rhee, and X. Wu. Nanomedicine in pulmonary delivery. *International Journal of Nanomedicine*. 4:299-319 (2009).
3. S. Belotti, A. Rossi, P. Colombo, R. Bettini, D. Rekkas, S. Politis, G. Colombo, A.G. Balducci, and F. Buttini. Spray-dried amikacin sulphate powder for inhalation in cystic fibrosis patients: The role of ethanol in particle formation. *European Journal of Pharmaceutics and Biopharmaceutics*. 93:165-172 (2015).
4. S.A. Meenach, Y.J. Kim, K.J. Kauffman, N. Kanthamneni, E.M. Bachelder, and K.M. Ainslie. Synthesis, Optimization, and Characterization of Camptothecin-Loaded Acetalated Dextran Porous Microparticles for Pulmonary Delivery. *Molecular Pharmaceutics*. 9:290-298 (2012).
5. L. Wu, X. Miao, Z. Shan, Y. Huang, L. Li, X. Pan, Q. Yao, G. Li, and C. Wu. Studies on the spray dried lactose as carrier for dry powder inhalation. *Asian Journal of Pharmaceutical Sciences*. 9:336-341 (2014).
6. Y. Takashima, R. Saito, A. Nakajima, M. Oda, A. Kimura, T. Kanazawa, and H. Okada. Spray-drying preparation of microparticles containing cationic PLGA nanospheres as gene carriers for avoiding aggregation of nanospheres. *Int J Pharm*. 343:262-269 (2007).
7. D.M.K. Jensen, D. Cun, M.J. Maltesen, S. Frokjaer, H.M. Nielsen, and C. Foged. Spray drying of siRNA-containing PLGA nanoparticles intended for inhalation. *J Control Release*. 142:138-145 (2010).
8. S.A. Meenach, K.W. Anderson, J. Zach Hilt, R.C. McGarry, and H.M. Mansour. Characterization and aerosol dispersion performance of advanced spray-dried chemotherapeutic PEGylated phospholipid particles for dry powder inhalation delivery in lung cancer. *European Journal of Pharmaceutical Sciences*. 49:699-711 (2013).
9. M.B. Dolovich, R.C. Ahrens, D.R. Hess, P. Anderson, R. Dhand, J.L. Rau, G.C. Smaldone, and G. Guyatt. Device selection and outcomes of aerosol therapy: Evidence-based guidelines*: american college of chest physicians/american college of asthma, allergy, and immunology. *Chest*. 127:335-371 (2005).
10. N.A. Stocke, S.A. Meenach, S.M. Arnold, H.M. Mansour, and J.Z. Hilt. Formulation and characterization of inhalable magnetic nanocomposite microparticles (MnMs) for targeted pulmonary delivery via spray drying. *International Journal of Pharmaceutics*. 479:320-328 (2015).

11. S. Stegemann, S. Kopp, G. Borchard, V.P. Shah, S. Senel, R. Dubey, N. Urbanetz, M. Cittero, A. Schoubben, C. Hippchen, D. Cade, A. Fuglsang, J. Morais, L. Borgström, F. Farshi, K.H. Seyfang, R. Hermann, A. van de Putte, I. Klebovich, and A. Hincal. Developing and advancing dry powder inhalation towards enhanced therapeutics. *European Journal of Pharmaceutical Sciences*. 48:181-194 (2013).
12. K. Kho, W.S. Cheow, R.H. Lie, and K. Hadinoto. Aqueous re-dispersibility of spray-dried antibiotic-loaded polycaprolactone nanoparticle aggregates for inhaled anti-biofilm therapy. *Powder Technology*. 203:432-439 (2010).
13. J.C. Sung, B.L. Pulliam, and D.A. Edwards. Nanoparticles for drug delivery to the lungs. *Trends in Biotechnology*. 25:563-570 (2007).
14. M.M. Bailey and C.J. Berkland. Nanoparticle formulations in pulmonary drug delivery. *Medicinal research reviews*. 29:196-212 (2009).

CHAPTER 2

Nanocomposite Microparticles (nCmP) for Pulmonary Drug Delivery Applications

Accepted for publication in the book “In Strategies of Nanotechnology in Drug Delivery” in 2016.

Zimeng Wang¹, Elisa A. Torrico-Guzmán¹, Sweta K. Gupta¹,
Samantha A. Meenach^{1,2,*}

¹Department of Chemical Engineering, ²Department of Biomedical and Pharmaceutical Sciences, University of Rhode Island, Kingston, RI 02881, USA

2.1. Introduction

2.1.1. Pulmonary delivery of dry powder particle-based therapeutics

Aerosols in their dry and wet forms, including steam, gas, and smoke, have been used for medical purposes for decades. In 1956, the first metered-dose inhaler became available and in 1970 the first dry powder inhaler reached the market (1). Such aerosol systems have been used for many therapeutic applications including local administration of chemopreventive agents (2), activators of the local immune system (3, 4), and antibiotics, among others. Aerosol delivery of therapeutics to the lungs offers an attractive way to deliver high drug concentrations directly to the site of disease, reducing toxicity while improving the therapeutic potential. Pulmonary delivery is also an attractive route for systemic administration with a more rapid onset of action than is traditionally seen when given orally. The rapid onset is due to fast absorption of the therapeutic by the massive surface area of the alveolar region, abundant pulmonary vasculature, thin air–blood barrier, high solute permeability, and the avoidance of first pass metabolism, which degrades many proteins that have shown promise for use as biotherapeutics (5, 6).

There is great promise for advances in pulmonary drug delivery using inhaled aerosols for the targeted treatment of respiratory diseases such as chronic obstructive pulmonary disease (COPD), asthma, cystic fibrosis, lung cancer, and infectious diseases (e.g. tuberculosis) (7). To date, several types of particle-based aerosol therapeutics have been developed including nanoparticulates suspended in aqueous form from inhalers and nebulizers as well as microparticle-based liquid and dry powder formulations. Both nanoparticle and microparticle-only formulations exhibit

limitations that will be discussed in detail later, leading to a need in the development of advanced formulations using particle engineering techniques. In particular, it has been shown that solid drug-loaded nanoparticles can be effectively delivered to the lungs when they are encapsulated in a carrier system that dissolves after coming in contact with the aqueous environment of the lung epithelium. These so-called nanocomposite microparticles (nCmP) can enhance the delivery of therapeutics via the aerosol route as described in the following sections. In this chapter, a general overview of pulmonary delivery and the current state-of-the-art related to nCmP will be followed by an overview of current nCmP systems and their design considerations.

2.1.2. Dry powder aerosol delivery devices

The most common inhaler devices are nebulizers, pressurized metered-dose inhalers (MDI), and dry powder inhalers (DPI). Nebulizers deliver liquid medication in a steady stream of tiny droplets, do not require patient coordination, and can deliver larger doses compared to the other devices (5). MDIs are the most popular devices used to treat local respiratory diseases and their mechanism utilizes a valve designed to deliver a precise aerosol amount each time the device is actuated (8, 9). DPIs are portable devices that deliver medication in the form of a dry powder directly to airways (10). Traditional dry powder blends are typically comprised of micronized drug particles with a mass median aerodynamic diameter (MMAD) less than 5 μm blended with inactive excipients of larger sizes (11-13). The drug is delivered when a patient inhales, pulling air through a punctured capsule, blister, or reservoir.

Advantages of DPIs are that they are portable, compact, and have multi-dose functionality. DPIs are breath-activated and unlike MDIs do not require any outside energy source or propellant, eliminating the need to coordinate actuation and inhalation (14). Another practical advantage of using a dry powder system is the far slower degradation of drugs in the dry state as compared to their suspension in a liquid form, resulting in higher long-term stability and sterility (6). Dry formulations of nanoparticles also reduce inter-particle attractive forces as does blending with larger carrier molecules, which improves aerodynamic performance (15). The use of biodegradable particles in DPIs may increase the bioavailability of therapeutic agents and change the pharmacokinetic plasma profile, making the agent more suitable for pulmonary delivery (16).

DPIs have many advantages with respect to medication delivery; however, they are not without their disadvantages. These disadvantages include poor deposition in the lower bronchioles and alveoli as well as the limited availability of drugs from the device itself. In many cases, DPIs are a relatively new technology still in the development stage, in comparison to the more established nebulizer and MDI technology. A more detailed overview of aerosol delivery devices can be found elsewhere (17-20). Overall, the ease of use and powder storage advantages discussed further in this chapter provide strong reasoning for the application of DPIs to deliver advanced dry powder formulations.

2.1.3. Overview of current dry powder aerosol therapeutics

As seen in **Table 2.1**, diseases that most commonly incorporate DPIs in treatment regimens are asthma and chronic obstructive pulmonary disease (COPD). COPD affects over 5% of the U.S. population and kills 120,000 individuals each year, ranking it as the third-leading cause of death. Management for asthma and COPD consists of short-acting bronchodilators for acute exacerbations and in more severe disease, daily maintenance therapy with bronchodilators and anti-inflammatory medications. Tiotropium bromide is an anticholinergic bronchodilator given to COPD patients via DPI in the U.S. A meta-analysis of various clinical trials found tiotropium to significantly improve mean quality of life and significantly reduce the number of participants suffering from exacerbations (21).

Combination therapy with an umeclidinium-vilanterol DPI is approved for once-daily use for COPD patients in the U.S. Compared to individual agents, this formulation results in greater increases in forced expiratory volume over 1-second (FEV1) at both trough and mean peak levels (22). In addition, a once-daily fluticasone-salmeterol DPI is FDA approved for COPD treatment (23). While not yet FDA-approved, a once-daily DPI containing glycopyrronium and indacaterol is approved for use in Europe and Japan (24). Also, a twice-daily combination DPI comprised of aclidinium-formoterol is approved for use in Europe, the United Kingdom, and Canada (25).

Asthma maintenance therapy is often similar to that seen in COPD with the goals of bronchodilation and reduction in inflammation. Some examples of these DPIs can be seen in Table 2.1. Recently, in April 2015, the FDA approved a new DPI

device for albuterol sulfate administration. Albuterol, traditionally delivered via MDI, is a short-acting beta-agonist (SABA) that is commonly used as a rapid and effective treatment for acute asthma exacerbations, in which the throat and airways can eventually close off if left untreated. In a news release, David I. Bernstein was quoted, "ProAir RespiClick is the first and only breath-actuated dry-powder rescue inhaler to be approved by the FDA for the treatment of acute asthma symptoms (26). In addition to the treatment of reactive airway diseases, DPIs can also be used in diagnostic applications. Aridol is a DPI that delivers mannitol, a sugar alcohol, to the lungs to assess for hyperresponsiveness, which indicates whether or not a patient has asthma. Research has been conducted to develop particles for DPIs including theophylline with sodium stearate and salmeterol xinafoate with lactose, both for the treatment of asthma.

Cystic Fibrosis (CF) is a genetic disorder caused by mutations in the cystic fibrosis transmembrane conductance regulator (CFTR) protein. Current U.S. guidelines suggest treating all CF patients older than 6 years with chronic pulmonary infections with inhaled antibiotics, first tobramycin, then aztreonam, and finally colistin. Aerosolized antibiotic therapy is traditionally given through a nebulizer; however, in March 2013 the TOBI Podhaler was approved as a DPI alternative for inhaled tobramycin. A trial comparing the tobramycin-inhaled powder (TIP) versus nebulized solution found that TIP was generally well tolerated, provided a significantly more convenient treatment option, and resulted in a higher discontinuation rate (27-29). Colistin, while considered third-line by U.S. guidelines,

is frequently used as first choice in Europe for CF patients (30). The DPI form of colistin (Colobreathe) is approved for use in Europe.

Antibiotic DPI formulations including vancomycin and clarithromycin with dipalmitoylphosphatidylcholine have been developed for the treatment of pulmonary infections (31). In addition, azithromycin microparticles have been developed successfully in an inhalable aerodynamic range ($< 10 \mu\text{m}$) (32).

Table 2.1. Current dry powder inhaler (DPI) formulations approved by the FDA including the approval date, brand name, active pharmaceutical ingredient (API), disease, and company.

Date	Brand Name	API	Disease	Company
2015	ProAir Respiclick	Albuterol sulfate	Asthma	Teva
2014	Arnuity Ellipta	Fluticasone furoate	Asthma	GlaxoSmithKline
2014	Incruse Ellipta	Umeclidinium	COPD	GlaxoSmithKline
2013	Tobi Podhaler	Tobramycin	Cystic fibrosis	Novartis
2013	Breo Ellipta	Fluticasone furoate, vilanterol	COPD	GlaxoSmithKline
2013	Anoro Ellipta	Umeclidinium, vilanterol	COPD	GlaxoSmithKline
2012	Tudorza	Acclidinium bromide	COPD	Forest Labs

	Pressair			
2011	Arcapta	Indacaterol	COPD	Novartis
2010	Aridol	Mannitol	Asthma (testing)	Pharmaxis
2006	Pulmicort Flexhaler	Budesonide	Asthma	Astrazeneca
2005	Asmanex Twisthaler	Mometasone furoate	Asthma	Merck
2004	Spiriva	Tiotropium	COPD	Boehringer Ingelheim
2001	Foradil Aerolizer	Formoterol fumarate	Asthma, COPD	Novartis
2000	Advair Diskus	Fluticasone propionate, salmeterol xinafoate	Asthma, COPD	Glaxo
2000	Flovent Diskus	Fluticasone	Asthma	GlaxoSmithKline
1999	Relenza	Zanamivir	Influenza	GlaxoSmithKline
1986	Provocholine	Methacholine Chloride	Diagnosis of bronchial airway hyperreactivity	Methapharm

2.1.4. Obstacles in pulmonary delivery of particle-based therapeutics

The human lungs have the innate ability to remove aerosolized particulates, which can decrease the delivered aerosol drug load. The natural removal mechanisms

include mucociliary clearance, phagocytosis, and enzymatic degradation. Mucociliary clearance is a critical host defense mechanism of the airways to clear locally produced debris, excessive secretions, or unwanted inhaled particles. It consists of ciliated epithelial cells present from the naso/oropharynx and the upper tracheobronchial regions down to the most peripheral terminal bronchioles (33). Effective mucociliary clearance requires appropriate mucus production and coordinated ciliary activity (34), including the “mucociliary escalator,” where ciliated epithelia sweep particles in the upper airways away from the lungs towards the mouth (35).

Phagocytosis occurs primarily in the deep lungs where alveolar sacs rich in macrophages play a key role in innate immune defense. Particles 1 – 5 μm in size are typical of bacteria and are readily engulfed via phagocytosis, thereby limiting the bioavailability of therapeutics (36). Phagocytic activity is maximized for particles 1-2 μm in diameter and less so for smaller or larger particles outside of this range (37). The contribution of pulmonary endocytosis to the overall lung clearance is determined by the particle size and shape, solubility, particle burden, and chemical nature of the inhaled aerosols.

Macromolecular drugs are also susceptible to enzymatic degradation. The contribution of drug breakdown along with other pulmonary clearance mechanisms is minimal in comparison with the gastrointestinal tract; however, it requires consideration in enzyme-sensitive compounds. Therefore, to protect from rapid clearance or degradation and achieve sustained release within the lung, encapsulation into nanoparticles or microparticles has been pursued.

Systemic diseases can be treated via pulmonary delivery as formulations and their released drugs can translocate from lung tissue to the cardiovascular endothelium. The mechanisms by which therapeutics are translocated from the lung occurs by either transcellular or paracellular transport. In transcellular transport, absorption of the therapeutic typically occurs through receptor/carrier-mediated endocytosis. This is a slow process (hours to days) and occurs for larger particles (>5-6 nm) having molecular weights of more than 40 kDa (36). Transcellular transport involves the internalization of caveolin-1, transcellular channels, and vesicular trafficking. Paracellular transport involves diffusion of drug through alveoli, which is a fast process (5 to 90 minutes) and happens in the case of smaller molecules (<5-6 nm). Several studies have evaluated the mechanisms of nanoparticle interaction with the lung and translocation of nanoparticles from nanocomposite microparticles through the epithelial barrier (38, 39).

Nanocomposite microparticles offer the ability to overcome many of the barriers associated with the aerosol delivery of therapeutics. First, nCmP are typically an appropriate size for effective pulmonary delivery (e.g. micrometer) and thereby can be delivered to all locations in the lungs. While micro-sized particles are usually removed from the lungs via mucociliary clearance and/or phagocytosis, nCmP can be designed to rapidly release nanoparticles from the nCmP bulk in a very quick fashion to avoid these clearance mechanisms. In addition to avoidance of pulmonary clearance, the nanoparticles released from nCmP offer their own advantages including the ability to translocate through mucus, penetrate into cells, and translocate across the

pulmonary epithelium/cardiovascular endothelium barrier (40, 41). At this point, the use of nCmP is the only effective way to delivery dry nanoparticle-based therapeutics.

2.1.5. Design for pulmonary deposition of particles

With respect to aerosol formulation and design, drug distribution and deposition along the respiratory tract depends on many characteristics of the inhaled formulation including the diameter, size distribution, shape, charge, density, and hygroscopicity of the particulate system. The mass median aerodynamic diameter (MMAD) and geometric standard deviation are what determine the site of deposition in the respiratory tract (42).

Dry powder particle formulations used in pulmonary applications must exhibit specific physical properties for successful implementation. Respirable particles with an MMAD between 0.5 and 5 μm undergo deposition in the alveolar region, which can facilitate systemic bioavailability (43, 44). Particles larger than this may potentially be deposited in the inhaler, oropharynx, and/or larynx, or they may not reach the desired site within the lung due to size constraints. For example, it was shown that decreasing the particle size from 5.4 μm to 2.7 μm reduced the total throat deposition by half and increased the total lung deposition by over two-fold for mannitol particles (45).

The process of particle deposition in human airways includes: a) inertial impaction, which is dominant in the upper airways where velocities are at a maximum and where many particles impact and stick to the pulmonary surface, b) sedimentation, which is predominant throughout the central and distal tract, where the particles settle

on the surface of the lung due to gravitational forces and air resistance, and c) diffusion, which is the most important for submicrometer-sized particles ($< 0.5 \mu\text{m}$), which are in random motion and deposit on the lung walls via Brownian motion (33, 42, 46). Previous studies have shown that the size and distribution site of particles inhaled in the lungs is as follows: particles smaller than $1 \mu\text{m}$ tend to diffuse, remaining suspended in the airways, and are typically exhaled; particles $1 - 3 \mu\text{m}$ in diameter deposit primarily in the alveolar region, $8 - 10 \mu\text{m}$ -sized particles undergo tracheobronchial deposition; and particle larger than $10 \mu\text{m}$ often exhibit deposition in the mouth (36).

2.1.6. Long-term storage considerations

Another major concern in the development of powder aerosols is in the storage of particles, which tend to agglomerate (16). In general, the more uniformly the particles are distributed, the more stable their shelf life is (47). Spray-drying, freeze-drying, and spray-freeze-drying often improve long-term particle stability during storage for dry formulations in comparison to aqueous formulations. For example, freeze-dried poly(methylidene malonate) nanoparticles were stored for twelve months at different temperatures and showed no significant variations in pH, size, turbidity and cytotoxicity (48). Suspensions of freeze-dried PLGA microspheres, either alone or loaded with cyclosporine, were stored at 8°C and room temperature (RT) for six months. The suspensions were substantially instable while the freeze-dried particles showed an alternative for long-term stability at low temperatures (49). In another study, a poorly soluble drug, celecoxib, was formulated into solid phospholipid

nanoparticles and showed that the amorphous matrix generated via spray-drying and freeze-drying significantly enhanced the dissolution rates and apparent solubility (50).

Another technique applied to enhance stability and solubility of particles is spray-drying. TIP used for the treatment of cystic fibrosis was designed and formulated considering the process parameters related to critical temperature transitions. A room temperature stable product was obtained that requires no refrigeration (51). Gentamicin particles for cystic fibrosis developed with L-leucine showed no significant degradation for up to 6 months of storage (52). Spray-freeze-drying is a relatively new method of producing biopharmaceutical powder preparations. It combines the advantages of freeze- and spray-drying techniques in order to get a stable product and increase the solubility of poorly water-soluble drugs. This technique was used to obtain a fine stable probiotic powder of *Lactobacillus casei* in mannose and CaCO₃ (53). Finally, re-aggregation of palygorskite nanofibers containing ofloxacin was successfully overcome by freeze-drying. Comparing with the traditional oven-dried sample, the freeze-dried sample showed enhanced dispersion stability of palygorskite in deionized water (54).

2.2. Nanocomposite microparticles: a solution for overcoming the obstacles of particle-based pulmonary delivery

Nanocomposites are an emerging class of materials utilized in pulmonary drug delivery. Such systems are typically multiphase structures, comprised of a single continuous phase or matrix (e.g. polymers) with one or more discontinuous or dispersed phases (e.g. drugs). A formulation of nanocomposite microparticles (nCmP)

utilizes a combination of phase or matrix components, active pharmaceutical ingredients (APIs), and inert components (excipients) as seen in **Figure 2.1**. Although the overall size of the nanocomposite microparticles can vary between 0.1 – 100 μm , a fraction of these particles having aerodynamic diameters 1-2 μm have been reported to be more effective in depositing into alveolar spaces (55). The properties of nanocomposite materials typically differ from conventional composite materials owing to the ‘critical size’ or ‘nanometer range’ of the dispersed drugs in the matrix, which enhances the properties of the nanocomposite particle.

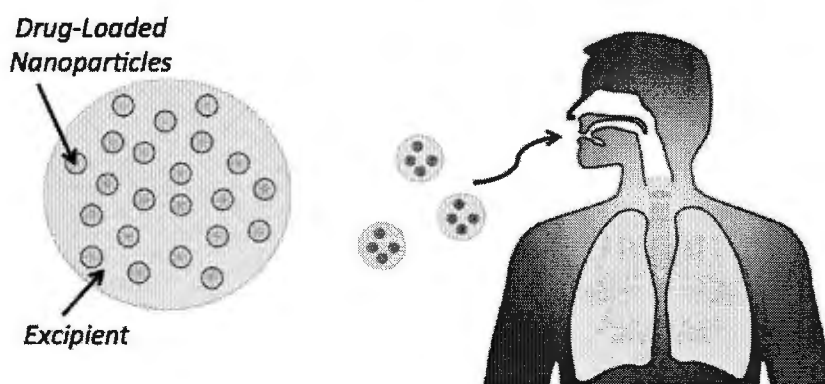


Figure 2.1. Schematic of nanocomposite microparticle (nCmP) system used for pulmonary delivery applications.

A list of nCmP developed for the treatment of pulmonary diseases is outlined in **Table 2.2**. The examples in this table not only cover a wide variety of pulmonary applications but also include different encapsulated nanoparticle (NP) systems, APIs, and carriers. The loaded NP are primarily polymer-based, however, systems with metals (iron oxide) and pure drug are also present. The table encompasses a comprehensive overview of the current pulmonary nCmP systems that have been

designed and evaluated and one significant conclusion is that the majority of the systems were fabricated via spray drying, which is a fairly straightforward, accessible, and high throughput synthesis method.

Table 2.2. Overview of nanocomposite microparticles (nCmP) systems used to deliver therapeutics for pulmonary applications with their active pharmaceutical ingredient (API), treatment application, and key findings.

Encapsulated NP	API/ Payload	Carrier/ Excipient	Synthesis Method	Application/ Disease Treated
Haloperidol-bovine serum albumin NP (56)	Doxorubicin	Trehalose, L-leucin, mannitol	Spray drying of NP suspension	Cancer
Iron oxide magnetic NP (57)	-	D-mannitol	Spray drying of NP suspension	Thermal treatment of the lung diseases
Poly(glycerol adipate-co-v-pentadecalacton) NP (58, 59)	Antigen PspA or BSA	L-leucine	Spray drying of NP suspension	Pneumonia, delivery of protein

Poly(ϵ -caprolactone) NP (60)	Hydrocortisone acetate	Poly(lactic-co-glycolic acid) (PLGA)	Double emulsion	Cancer
PLGA NP (61)	Salmon calcitonin	Chitosan	Spray drying fluidized bed granulation and dry powder coating techniques	Enhanced pulmonary absorption of drug
PLGA NP and alginate/PLGA NP (62)	Tobramycin	Lactose	Spray drying of NP suspension	Delivery of antibiotic
Chitosan/tripolyphosphate (TPP) NP (63)	Itraconazole	Lactose, mannitol, L-leucine	Spray drying of NP suspension	Delivery of antifungal drug
Itraconazole nanosuspension (64)	Itraconazole	Mannitol, sodium taurocholate	Spray drying of NP suspension	Invasive pulmonary aspergillosis

PLGA NP (65)	Coumarin 6	-	Spray drying of NP suspension	Alveolar tissue targeting
Chitosan/TPP NP (66)	Isoniazid	Lactose, mannitol, maltodext rin, leucine	Spray drying of NP suspension	Tuberculosis
PLGA NP (67)	Levofloxaci n	poly(vinyl alcohol) (PVA), leucine	Spray drying of NP suspension	Delivery of antibiotic
Glyceryl monostearate /soybean phosphatidylchol ine solid lipid NP (SLNs) (37)	Thymopenti n	Mannitol, leucine	Spray drying of SLN suspension	Delivery of peptide
PLGA NP (68)	siRNA	Trehalose, lactose, mannitol	Spray drying of NP suspension	Delivery of siRNA
PLGA NP (69)	Rifampicin	L-leucine	Spray drying of NP suspension	Tuberculosis

Tobramycin nanosuspension (70)	Tobramycin	-	Spray drying of NP suspension	Delivery of antibiotic
PLGA NP formed during spray drying (71)	Rifampicin	Mannitol	Four-fluid nozzle spray drying	Tuberculosis
PLGA NP (72)	Rifampicin	Trehalose, lactose	Spray drying of NP suspension	Tuberculosis
PLGA/Polyethyl enimine (PEI) nanospheres suspension (73)	Plasmid DNA (pCMV-Luc)	Mannitol	Spray drying of nanosphere suspension directly	Gene delivery, vaccination
Pranlukast hemihydrate particles formed during spray drying (74)	Pranlukast hemihydrate	Mannitol	Four-fluid nozzle spray drying	Asthma
Polyacrylate NP and silica NP (75-77)	-	Phospholipids	Spray drying of NP suspension	Pulmonary delivery

Chitosan/TPP NP (78)	FITC-BSA	Mannitol	Spray drying of NP suspension	Delivery of protein
Poly(butylcyano acrylate)(PBCA) NP (79)	FITC- dextran	Lactose	Spray drying of NP suspension	Pulmonary delivery
PBCA NP (80)	Doxorubicin	Lactose	Spray freeze- drying of NP suspension	Cancer
Chitosan/TPP NP (81)	Insulin	Mannitol, lactose	Spray drying of NP suspension	Delivery of protein
Terbutaline sulphate nanosuspension (82)	Terbutaline sulphate	Glyceryl behenate/ Tripalmiti n or Hydrogen ated palm oil	Spray drying of NP suspension	Delivery of drug with sustained release
Gelatin or PBCA NP (83)	Dextran	Lactose	Spray drying of NP suspension	Delivery of drugs and diagnostics

Polystyrene NP (84)	-	Phospholipids	Spray drying of NP suspension	Pulmonary drug delivery
------------------------	---	---------------	-------------------------------	-------------------------

As seen in **Figure 2.2**, nCmP formulations exhibit a variety of morphologies ranging from nanocomposite microcrystals, solid nanoparticle spheres, hollow nanoparticles spheroids, nanoparticle agglomerates, and nanoparticles dispersed in a carrier. The morphology can be tuned via synthesis parameters in order to ensure effective API delivery, stability, and and/or targeted pulmonary deposition.

2.3. Preparation of nanocomposite microparticles (nCmP)

Particle engineering is a key factor in the development of nCmP systems with desirable properties (85). In this section, we review techniques used in the preparation of nanoparticles that are used in nCmP formulations as well as techniques used to prepare the nCmP systems themselves.

2.3.1. Techniques used to prepare drug-loaded nanoparticles

2.3.1.1. Solvent evaporation

In this method, two main strategies are used to form emulsions including single emulsions with oil-in-water (o/w) and double emulsions with water-in-oil-in-water (w/o/w) phases. For single emulsion, drugs and polymers are dissolved in oil phase, while in double emulsion, drugs are usually in inner water phase. Volatile solvents such as dichloromethane, chloroform, and ethyl acetate are mostly used as oil phase. The emulsions are formulated using high-speed homogenization or

ultrasonication and converted into nanoparticle suspension by solvent evaporation in a spinning solution with surfactant (88).

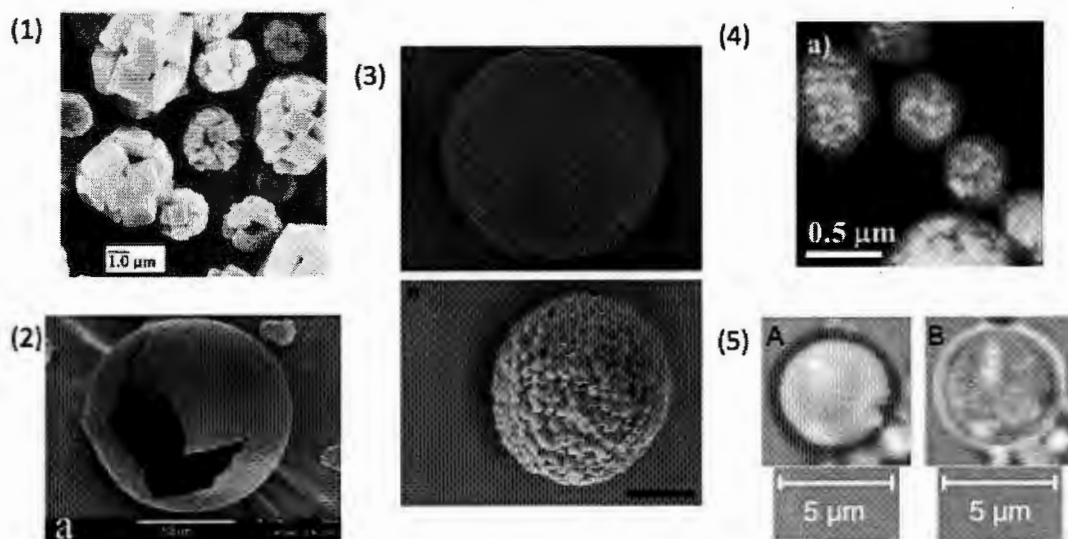


Figure 2.2. Representative nanocomposite microparticles (nCmP) systems imaged via scanning electron microscopy (SEM), transmission electron microscopy (TEM), and fluorescence imaging. The nCmP systems and imaging techniques are: (1) spray-dried NaCl particles (SEM), (2) hollow spherical LPNP (SEM), (3) poly(styrene) (top) and poly(lactide-co-glycolide) (bottom) where scale bar is 1 μm (SEM), (4) magnetic nCmP (TEM), and (5) hollow fluorescently-labeled polycyanoacrylate NP (fluorescence microscopy) (57, 83, 86, 87).

2.3.1.2. Nanoprecipitation

Nanoprecipitation, also called solvent displacement, is used to prepare nanoparticles by precipitating polymer at the interface between the water and the

organic solvent. The precipitation is driven by the diffusion of the organic solvent into the aqueous phase with or without surfactant. Therefore, water-miscible solvents like acetone, methanol, or ethanol are recommended. The nanoprecipitation method often results in high drug loading and encapsulation efficacy for hydrophobic drugs, however, it is not an efficient means to encapsulate water-soluble drugs because of the high diffusion rate of drug from organic solvent into water (88).

2.3.1.3. Emulsification/solvent diffusion

Emulsification/solvent diffusion is a modified version of the solvent evaporation method. In this method, an oil phase is formed by dissolving drug and polymer in a partially water soluble solvent such as propylene carbonate. This mixture is saturated with water to ensure the initial thermodynamic equilibrium of both liquids and then emulsified in an aqueous solution of surfactant. The solvent will diffuse into the aqueous phase leading to nanoparticle or nanocapsule formation and will then be eliminated by evaporation or filtration, according to its boiling point. This method also allows a high drug loading and encapsulation efficacy for hydrophobic drugs as well as for hydrophilic ones (88).

2.3.1.4. Salting out

Salting out, regarded as the modified version of emulsification/solvent diffusion, is based on the separation of a water-miscible solvent from aqueous solution caused by a salting out effect. In this method, drug and polymer are dissolved in a water-miscible solvent such as acetone. The mixture is emulsified in an aqueous gel

containing a salting-out agent such as magnesium chloride, calcium chloride, magnesium acetate, or sucrose as well as surfactant and is then diluted with a sufficient volume of aqueous solution to enhance the diffusion of solvent into the aqueous phase. Nanoparticles are formed as the result of solvent diffusion. The salting out agent is the key factor in the method influencing the efficacy of encapsulation but should be eliminated with solvent in the end. This method exhibits an advantage over others by avoiding high stress and increased temperature, which is suitable for protein encapsulation. Salting out is ineffective for hydrophobic drug and requires extensive washing steps (88-90).

2.3.1.5. Dialysis

Dialysis can be used as a simple and effective method for the preparation of nanoparticles of small size and narrow distribution (88). However, the mechanism of this method is not completely understood right now and is regarded as similar to that of nanoprecipitation (91). In dialysis, polymer and drug are dissolved in an organic solvent inside a dialysis tube with a proper molecular weight cut off. As the solvent displacement progresses, aggregation of polymer happens due to loss of solubility, thus forming a nanoparticle suspension. The properties of resulting nanoparticles are influenced by the type of solvent used in salting out.

2.3.1.6. Supercritical fluid (SCF) technology

A supercritical fluid is defined as any substance at a temperature and pressure above its critical point. Supercritical fluids are defined as compressed gases or liquids

above their critical pressures and temperatures, which exhibit several fundamental advantages as solvent or non-solvent. For pharmaceutical manufacturing, supercritical CO₂ is widely used due to its low critical temperature (31.1°C) and moderate pressure (73.8 bar), non-toxic inert nature, and low cost. Supercritical fluid technology offers an environmentally friendly way to make nanoparticles due to efficient extraction and separation of organic solvents in this process. The resulting nanoparticles are in pure dry form or as pure aqueous suspensions (92).

2.3.1.7. Preparation of nanoparticles from polymerization of monomers

Nanoparticles with desired properties can be prepared by polymerization of monomers. This method can be subdivided into emulsion polymerization, mini-emulsion polymerization, interfacial polymerization, and controlled/living radical polymerization. For this method, toxic organic solvents, surfactants, monomers and initiators must be removed from formed nanoparticles, which limit the use of the method (88).

2.3.2. Techniques used to prepare nCmP

The aerosol performance of nCmP is directly related to their preparation techniques. In this section, both traditional and more advanced methods used in the preparation of nCmP are discussed (93). These methods are classified into two categories, including top-down as milling larger particles to reduce size and bottom-up precipitation of nanoparticles out of solution. Techniques such as the modification of spray drying also show promise to prepare nCmP (94).

2.3.2.1. Milling

Milling is the traditional method of drug powder micronization, which has been intensively studied. The milling method can involve the use of ball mills, colloid mills, hammer mills, and jet or fluid energy mills, in which the jet mill is applied to prepare most inhalation powders. Jet milling is defined as a process of micronization by inter-particle collision and attrition. In this method, coarse particles carried by a high velocity gas as milling medium pass through a nozzle into the jet mill. The particles are then suspended in the turbulent gas stream where they break into smaller particles due to inter-particle collisions. The fine particles are then taken up by the gas stream out through the exit, while the larger ones remain in the mill for further micronization by more inter-particle collision. The application of jet milling is limited by lack of control over resulting particle properties and the high energy in the process increasing the risk of degradation of therapeutics (94, 95).

2.3.2.2. Supercritical fluid technology (SCF)

Supercritical fluid technology can also be used for preparation of micro-size inhalation as discussed previously. More specific discussion of SCF could be found in several review articles (85, 94, 95).

2.3.2.3. Spray drying

Spray drying is the most commonly used method to prepare dry powders for inhalation (96). In spray drying, nanoparticle suspensions with or without excipients are atomized at the nozzle. The droplets of the suspension go through the drying

chamber with heated gas, resulting in evaporation of solvent and generation of nCmP. The resulting nCmP are separated in a cyclone separator and collected in the collector (97). The spray drying method provides easily tunable process conditions and high reproducible properties of resulting particles. However, challenges exist to determine optimal processing conditions to achieve desirable properties, due to the fact that the drying process depends on complex parameters including the solvent used, solute concentration, inlet temperature, outlet temperature, atomizing pressure, feed properties, pump rate, drying gas type, and gas flow rate (81, 96, 98, 99).

2.3.2.4. Spray-freeze drying (SFD)

Spray freeze-drying is a modified version of spray-drying, in which the suspension or solution is atomized into a cryogenic liquid such as liquid nitrogen generating droplets (95). The droplets are then lyophilized, resulting in porous spherical particles suitable for inhalation. Application of SFD is limited by several disadvantages such as causing irreversible damage to the proteins by drying and freezing stress, time consumption, and high expense (100).

2.3.3. Materials and excipients used in the preparation of nCmP

2.3.3.1. Drug-loaded nanoparticle materials

The materials used in the polymer matrix of nanoparticles should exhibit biodegradable and biocompatible properties in themselves as well as their degradation products. These polymers could be natural polymers such as chitosan gelatin, sodium alginate, and albumin, or synthetic polymers including polylactides (PLA),

polyglycolides (PGA), poly(lactide-co-glycolides) (PLGA), poly(methylmethacrylate) (PMM), poly(cyanoacrylate) (PCA), poly(caprolactone) (PCL), and poly(ethylene glycol) (PEG)-conjugated- PLGA. To select a polymer as nanoparticle matrix, the nanoparticle formation techniques, the encapsulated drugs, the properties of polymers, and further nCmP preparation methods should be taken into consideration. In addition, the desired properties of nanoparticles are also an important concern when choosing polymers. Detailed discussion on the materials used for nanoparticle formation can be found in former reviews (6, 84, 88, 89, 101-109).

2.3.3.2 Excipients used in nCmP synthesis

The nCmP carriers and excipients are the inactive ingredients used to improve the delivery efficacy and stability of nCmP formulations for pulmonary delivery. The excipients have no therapeutic effects, but still have a significant role to form a desired delivery system of therapeutics by enhancing the mechanical properties of dry powder, physical or chemical stabilization of drug, and improving redispersion and dissolution properties of encapsulated nanoparticles (94). The Food and Drug Administration (FDA) recommends the use of excipients that are either commercially established or “generally recognized as safe” (GRAS). Hence, the choice of excipients used for nCmP formation is limited since the current excipients approved for pulmonary drug delivery are very limited in number (110). Detailed discussion on the excipients used for inhalation application can be found in other review and research articles (43, 94, 111, 112).

2.4. Optimization of nCmP manufacturing via spray drying

While there are obviously many methods available for the synthesis of nCmP, spray drying has been the primary method to date. Spray drying is a straightforward and high throughput method allowing for easy reproduction of nCmP and thus the remaining sections of this book chapter will focus on the optimization of nCmP via spray drying. In a spray drying process, several parameters can be optimized to achieve desirable properties for nCmP formulations. In this section, these parameters are classified into two major categories: 1) spray drying conditions and 2) feed solution composition. The spray drying conditions include the inlet temperature, aspirator, spray gas flow, feed speed (pump rate), which can be easily tuned through the control panel of spray dryer, and humidity of drying gas, which can be modified by incorporating a dehumidifier or using dry nitrogen or compressed air. The feed solution composition covers the ratio of nanoparticles to carriers (excipients), solid concentration (concentration of total dry materials), properties of carriers, properties of nanoparticles, and solvent composition (18, 113-115).

The relevant parameters for the spray process correlate with and depend on each other. Therefore, to design an optimal nCmP system with parameters suitable for desirable resulting particles, a comprehensive evaluation of all parameters should be taken. However, difficulties exist in the selection of the process conditions, lying in the facts that: 1) a single change in parameter may influence several other properties of spray drying products; 2) several parameters may influence one property of spray drying products and these parameters depend on each other; and 3) a parameter may have positive effects on products in one range and negative effects or no influence in

another range. In summary, there is no best spray drying condition for any given system, but only an optimal condition that is most suited for a product intended for a certain therapeutic application. This section aims at providing a strategy in the design of optimal process conditions and to aid in the understanding of the internal relationship between the process parameters and corresponding properties of resulting particles.

2.4.1. How spray dryer settings influence dry powder formulations

There are many spray dryer settings that influence the characteristics of dry powder formulations like nCmP (116, 117). These settings include the inlet temperature, aspiration rate, feed (pump) rate, spray-drying gas flow rate, composition of feed solution, and other external parameters discussed below.

The inlet temperature is directly proportional to outlet temperature, which is the actual temperature at which the spray-dried materials are exposed. A higher inlet temperature is able to reduce the relative humidity in the drying gas, resulting in dryer and less sticky powders, thus increasing the powder yield. Aspiration, which provides a gas flow depending on the pressure drop of the overall system, reflects the drying energy that the system exerts on the drying process. The aspiration rate leads to a positive effect on increasing outlet temperature, reducing the amount of residual moisture in the product, and thus improving the degree of product separation in the cyclone. The feed rate affects the amount of time that materials undergo the drying process. A higher feed rate results in larger droplet dispersion in the drying chamber, which decreases the outlet temperature. An increase in the feed rate also increases the

moisture content in the gas, resulting in more humid or moist products that could adhere to the glassware (cyclone or collector), thereby decreasing the yield. The spray-drying gas flow rate is another parameter that affects the products. Higher gas leads to a reduction in outlet temperature and reduces the droplet size, thus decreasing the size of resulting particles.

While the previous parameters can be tuned through the control panel of the spray dryer, the feed composition of the spray-dried solution can also affect the final powder product. A direct result of increasing the feed concentration is a decrease in the solvent amount, which results in less liquid evaporation, leading to higher outlet temperature. An increase in the feed concentration also reduces the partial pressure of solvent in the gas, leading to less water in the final product. The feed concentration exerts a positive influence on the particle size due to an increase of solid in droplets and a higher yield contributes to the ease in the collection of larger particles. The use of an organic solvent for the feed solution will result in smaller particles due to lower surface tension of these solvents. The organic solvent also requires less energy to vaporize, leading to higher outlet temperatures, thus resulting in dry products. Finally, the humidity of the drying gas can be reduced through the use of a dehumidifier or using ultra dry nitrogen, and this has a negative influence on the vapor uptake capability in the gas stream, resulting in positive effects on outlet temperature. As a result, higher drying gas humidity leads to higher humidity of the final products with lower yield.

2.4.2. A theoretical framework of nanocomposite microparticle (nCmP) formation

After a greater understanding of how spray dryer parameter settings influence the spray-drying process and resulting materials, we can move on to the more complicated spray-drying process with nanoparticles. Nanoparticles with various properties add complexity into the drying process in the droplet of feed solution dispersed in the drying chamber, while the formation process of droplet is affected by parameters such as the feed speed, aspirator speed, and drying gas flow rate. The engineering of nCmP formation requires an overall understanding of microbiology, chemistry, formulation science, colloid and interface science, heat and mass transfer, solid state physics, aerosol and powder science, and nanotechnology (18).

Figure 2.3 shows nCmP formation from a droplet of feed solution in the spray-drying process. Unlike traditional spray-dried formulations, where particle formation is due to the micronization and drying process of dry materials in feed solution, novel nCmP systems exhibit sophisticated inner attributes and substructures. During nCmP formation, the feed solution is atomized through the nozzle, forming droplets of the nanoparticle suspension in the carrier solution. In ideal conditions, the nanoparticle dispersion remains stable, where the carrier molecules and nanoparticles are dispersed uniformly in the solvent. Once the droplets come into contact with hot drying air, evaporation of the solvent at the droplet surface will occur. Accompanied by the shrinkage of the droplets, two driving forces are generated, which in combination are responsible for the separation of the components in the droplets. The first driving force is the local temperature gradient created at the droplet surface contributed by the flux

of heat caused by water evaporation from the surface of the droplet into the gas stream. As a result, thermophoresis of the nanoparticles occurs, leading to their movement towards the surface of the droplets (18, 118, 119). A detailed mathematical model of this phenomenon can be found in Ferry Iskandar's research (118, 120).

The other driving force is caused by the concentration gradients in the droplet. The evaporation of solvent at the droplet surface increases the concentration of components in the same plane, causing diffusion of the solute and nanoparticles towards the droplet center (shown in **Figure 2.3**) (18, 121, 122). For the solute or nanoparticles that diffuse fast enough compared to the shrinkage of droplet caused by evaporation, their concentration gradient along the droplet radius will be insignificant, resulting in relatively uniform distribution of the dry materials in the nanoparticles. However, if the diffusion is slower than the surface shrinkage, there will be a higher concentration of solute or nanoparticles at the droplet surface compared to the droplet center, resulting in a shell of particles. The ratio of evaporation rate to diffusion rate can be described by the dimensionless Péclet number, which is an important factor influencing the size, shape, surface morphology, and component distribution of resulting particles. The Péclet number is well discussed in other review and research articles (18, 121, 123) and can be used to explain how the inlet temperature influences the properties nCmP. In the final step during nCmP formation, solvent evaporation finalizes, and the particles undergo changes in morphology and thermal states. Crystallization or re-crystallization may occur, resulting in crystals with different sizes located inside or at the surface of resulting particles. Whether nCmP exhibit spherical or wrinkled morphology is also determined in this final step (18, 123, 124).

2.4.3. Influence of spray drying parameters on nCmP formation

After covering the basics on how spray drying parameters influence the properties of nCmP and an overall theoretical framework of nCmP formation, we can continue with a detailed discussion of these parameters. As previously mentioned, the parameters relevant to the spray process correlate with and depend on each other. In this section we discuss the influences of these parameters in terms of primary parameters, secondary parameters, physicochemical properties, and application properties (desirable properties). It is assumed that while discussing a given parameter, that the others remain constant.

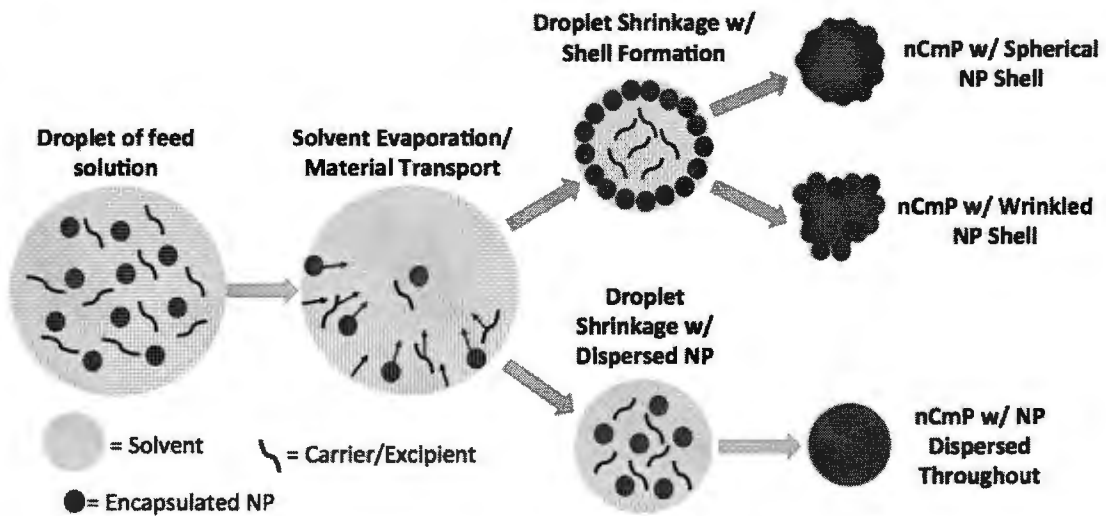


Figure 2.3. Schematic of nanocomposite microparticle (nCmP) formation during spray drying from a droplet of feed solution of nanoparticles (NP) and excipients in a solvent.

2.4.3.1. Influence of inlet temperature

The inlet temperature proportionally determines the outlet temperature, which is close to the actual temperatures that spray-dried materials are exposed to. At high spray drying temperatures evaporation is rapid, resulting in a higher Péclet number thus indicating a fast increase of the solute or nanoparticle concentration at the droplet surface. Once a critical concentration is reached at the surface, precipitation will take place. Early precipitation results in smaller differences between the solid particle shell and the initial droplet size, producing larger shells. In the preparation of nCmP, suspended nanoparticles will form a composite shell in early processes and insufficient solids remain to fill the internal space of the shell, thus forming large and hollow nCmP. On the contrary, lower temperatures lead to slower evaporation that may lag behind the solid diffusion rate, causing delayed shell formation and smaller nCmP. In general, higher inlet temperature leads to higher processing temperature, improving the formation of larger and hollow particles, which tend to exhibit favorable aerosol performance. However, exceptions have been reported indicating that temperature may not influence the particle size (125). In that case, a wider temperature range could be applied for study on influence of temperature (123). In another study, temperature firstly has a negative effect on size of nCmP, then presents a positive effect (72). In that case, an optimal inlet temperature should be chosen based on comprehensive consideration on other parameters.

The inlet temperature also influences the crystallization of carrier molecules during solvent evaporation at the droplet surface, thereby changing the surface roughness of the resulting particles. At very high temperatures, carriers may not have

enough time to crystallize during the precipitation process, thus forming into an amorphous state. Given enough time for crystallization, lower temperatures ensure larger crystals due to low nucleation rates from the solution, resulting in more roughness at particle surfaces. On the contrary, spray drying at higher temperatures leads to higher nucleation rates with more nuclei, resulting in smaller crystals and smooth surfaces. However, converse results have also been reported, in which higher temperature leads to larger crystals, while at lower temperature smaller crystals are produced. This latter case usually happens in the spray drying of small droplets at lab scale, where high temperature results in higher possibility of supersaturation at the surface than in large droplets. Therefore, delayed crystallization from a highly supersaturated viscous liquid or even water-free melt may occur, leading to larger crystals and rougher surfaces. In summary, temperature is able to influence the crystalline states of carrier molecules, which may further affect the performance of pulmonary delivery (126, 127). More detailed discussions on the influence of temperature on crystalline states of spray-dried particles can be found elsewhere (115, 125, 128, 129).

Another consideration with process temperature is its influence on the bioactivity of the powder products. Although therapeutics are encapsulated and protected by nanoparticles and microcarriers, the process temperature should be run at a safe range to keep bioactivity of the payloads (68, 73, 113, 114). In addition, temperature can impact the redispersion of the nanoparticles from the dissolved nCmP. At high temperatures, the melting of dry materials can occur, which will lead to the fusion of nanoparticles when they diffuse towards the droplet center and form a

nanocomposite shell. Poor redispersion can cause nanoparticles to lose their favorable properties as drug delivery systems and impair the efficacy of nCmP.

2.4.3.2. Influence of ratio and properties of nanoparticles

In the absence of other driving forces, the freely soluble carrier molecules driven by diffusion exhibit even distribution in the droplet during the evaporation. The initial saturation of carriers is small and the characteristic time for precipitation at the droplet surface is close to the droplet lifetime. Given that no nanoparticles are included, solid particles with a density close to the true density of the dry materials tend to form (115, 116, 123, 125, 126, 130-134). In the case of when a system with lower ratio of nanoparticles to carrier molecules mixture is spray-dried, nanoparticles in the droplet may not be able to form a shell (135). When the nanoparticles account for a larger part in the dry materials, a nanocomposite shell is able to form and this determines the shape and size of resulting nCmP. Although the formation of nCmP is initiated from the same initial droplet solidification at surface, the morphology varies significantly. For nanoparticles capable of building rigid shells quickly, solid hollow spherical nCmP are formed. Otherwise, dimpled or wrinkled particles are formed. This difference may be caused by the properties of the suspended nanoparticles and thus it varies significantly in different spray drying conditions and feed solutions. No universal conclusion can be elucidated from this conclusion, yet optimization should be performed based on specific conditions by referring to former studies. Extensive studies have been done reporting or discussing the variety in the morphology of spray-dried nCmP (68, 76, 84, 136-140) or particles based on other colloids (114, 135, 141-

145). The ratio of nanoparticles to carriers also influences the redispersion of the nanoparticles from nCmP, as well as the particle size (72). Properties of nanoparticles including particle size and surface properties can influence the properties of resulting nCmP. No overall review of this field has been performed and thus further studies may be warranted (6, 17, 57, 62, 68, 72, 103, 105, 106, 109, 146, 147).

2.4.3.3. Influence of excipients

Carriers (excipients) are inactive materials that are applied in spray drying to enhance the physical or chemical stability of the active pharmaceutical ingredient. Sugars are widely used as excipients of nCmP, as they provide advantages such as rapid dissolution in aqueous environment, leading to the immediate release of encapsulated nanoparticles. These excipients have been well studied in aerosol manufacturing processes with highly reproducible products (94, 148, 149). Safety should be a primary consideration in choosing the carrier excipient for nCmP. Many excipients that can be used in drug formulations for delivery in non-pulmonary routes may not be suitable for pulmonary delivery due to their potential to injure the lungs (149). Excipients approved for pulmonary delivery or presented as interesting alternatives for DPI formulations should be considered in high priority. Carriers also have significant impact on properties of nCmP, including the size, surface morphology, water content, and redispersion potential of nanoparticles. Comparisons of the influence of different excipients on dry powder formulation that can provide insight into how the excipient properties will affect nCmP have been studied (43, 94, 111).

2.4.3.4. Summary

Several parameters in the spray drying process can be tuned to achieve desirable properties of nCmP. These parameters, which correlate with and depend on each other, should be considered comprehensively to design optimized particles. Some parameters may have variable effects on the nCmP systems, and not all will be regarded as favorable. In this case, some of the properties may be abandoned in an overall consideration.

2.4.4. Optimization of nCmP formation process

Pulmonary delivery of therapeutics using nCmP is increasingly recommended for the treatment of lung disease due to their high efficacy of delivery, more convenient administration, and more flexible storage conditions. These advantages are a result of effective particle engineering of the delivery system, which includes optimal aerodynamic size, stability, and recovery of primary nanoparticles. In this section, strategies to achieve these favorable properties are discussed.

2.4.4.1. Optimization of aerodynamic size and morphology

A schematic showing the parameters involved in optimization of aerodynamic size of nCmP is shown in **Figure 2.4**. The proper aerodynamic diameter will be dependent on the delivery strategy and final particle location for a given application. Since higher temperatures may impair the redispersion of nanoparticles and bioactivity of encapsulated therapeutics, relatively lower temperature should be given priority if possible. A way to prepare nCmP with small aerodynamic sizing is to prepare particles

with small geometric sizing, since these sizes are positively proportional to one another. This goal can be achieved by reducing the feed speed and feed solution concentration during spray drying. The former way results in smaller droplet size with lower dry material content, while the latter one decreases the dry materials in droplet directly, thus leading to smaller particles. nCmP can be designed with rough surface morphology and low water content to allow for high aerosol dispersion and low cohesion of the resulting nCmP. Overall, the aerodynamic diameter can be influenced by the geometric diameter, structure, processing conditions, and materials used in the preparation of nCmP.

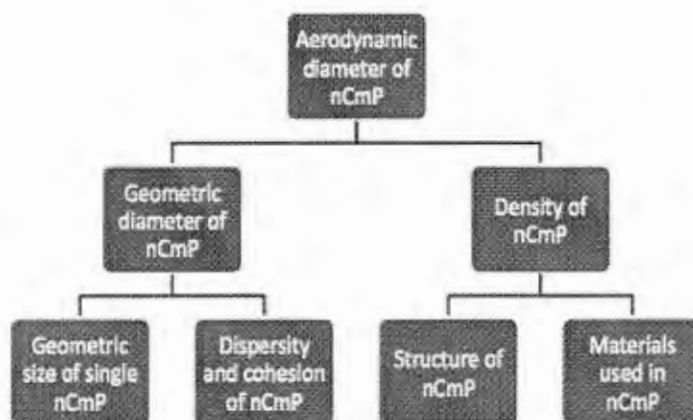


Figure 2.4. Schematic of processing parameters affecting the aerodynamic diameter of nanocomposite microparticles (nCmP).

2.4.4.2. Optimization of stability

Figure 2.5 is a schematic outlining the factors important in the stability of nCmP. The stability of pulmonary delivery systems based on nCmP includes not only activity of encapsulated therapeutics, but also the integrated structure of the delivery

system. The drying temperature should be set to maintain the activity of therapeutic(s). Minimum water content should be a target to enhance stability of the structure of nCmP so that the favorable amorphous state of the nCmP is maintained.

2.4.4.3. Optimization of primary nanoparticle recovery

A schematic outlining the optimization of nanoparticle recovery from nCmP is shown in **Figure 2.6**. To combine the advantages of both nanoparticle and microparticle systems, recovery of primary nanoparticles plays a significant role. An increase in the amount of nanoparticles released from nCmP can be achieved by increasing the ratio of nanoparticles to carrier (excipient). Meanwhile, the high redispersion of nanoparticles can be achieved by applying a suitable coating on the nanoparticles and by using a lower drying temperature. At last, improvement of overall nCmP yield may be regarded as an indirect way to obtain higher primary nanoparticle recovery.

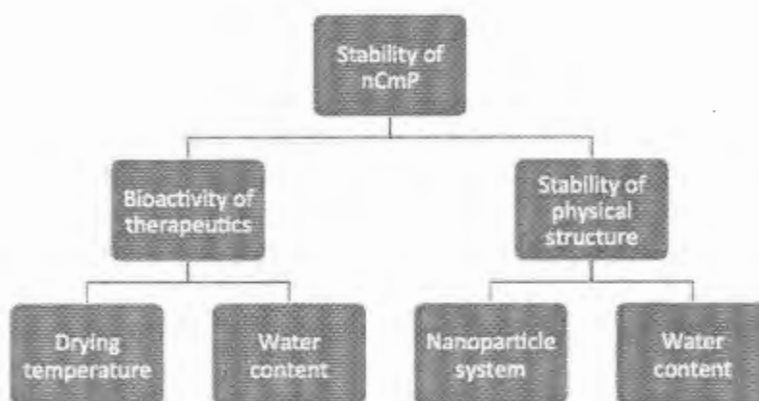


Figure 2.5. Schematic outlining the parameters that can influence the stability of nCmP.

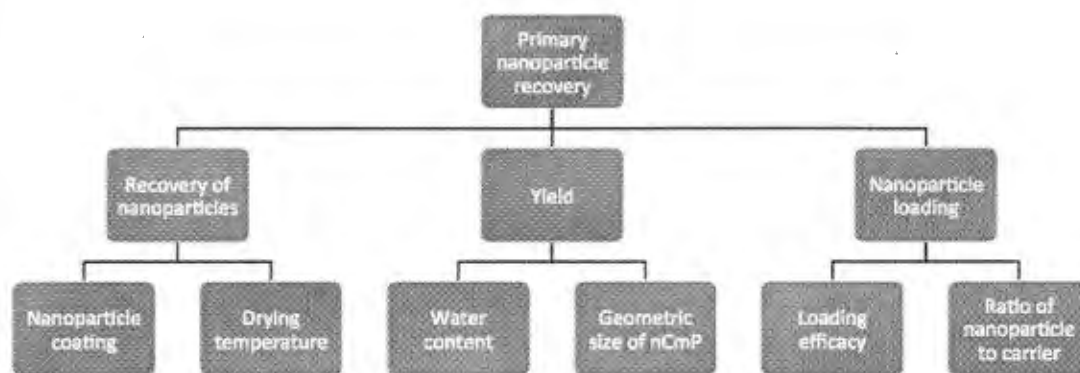


Figure 2.6. Schematic of the parameters that affect the recovery of redispersed nanoparticles from nCmP.

2.5. Drug release behavior from nanocomposite microparticle (nCmP) systems

As with many other drug delivery systems, nCmP is comprised of mainly carriers and API. The carrier often serves as the most important component for successful and targeted drug delivery. Significant amounts of research has been underway to explore the potential of nanoparticles as drug delivery carriers as they offer several advantages including enhanced cellular uptake, increased drug stability, decreased side-effects and prolonged drug release (150). Drugs encapsulated in a carrier are released from the nanoparticles by various physicochemical processes such as diffusion, dissolution, osmosis, magnetically controlled and targeted delivery, and the mechanism of drug release depends on the selection of carrier system and the solubility of the drug. The general physicochemical process for drug release from NP in nCmP are discussed as follows:

1. Diffusion: As a result of hydration, polymeric NP swell and release drugs through diffusion. The rate of drug release from the inner core of the water insoluble polymeric material follows Fick's law of diffusion (151-153). The diffusion of drug from the nanoparticle depends on the type of polymer, thickness of polymer coating, solution-diffusion membrane, and rate of permeation.
2. Dissolution: NP dissolution is a process that involves three steps: 1) release of drugs from the surface, 2) slight degradation of the polymer entrapping the remaining drugs, and 3) complete disintegration of polymer membrane, resulting in the rapid release of the entrapped drug. The degradation of the polymer membrane can be achieved using chemical or enzymatic reaction (154).
3. Solvent controlled (osmosis): When semipermeable polymers are used to encapsulate drug molecules, water crosses the polymer membrane and dissolves the encapsulated drug since the osmotic pressure builds up in the NP interior and drugs are forced to dissociate from the polymer and release outside of the particles (154).
4. Magnetically controlled: If a component of the nCmP is comprised of superparamagnetic nanoparticles (Fe_3O_4), a high frequency alternating magnetic field can be used to release the encapsulated drugs. Stocke et al. demonstrated the incorporation of iron oxide magnetic nanoparticles in magnetic nCmP (MnMs), which could enhance drug release with the presence of an alternating magnetic field (57).

2.6. Therapeutic applications of nanocomposite microparticles: Impact in pulmonary and non-pulmonary diseases

Over the past few years, research in the field of pulmonary drug delivery has gained momentum for treatment of pulmonary and non-pulmonary diseases. Pulmonary route for drug delivery is an attractive target, yet it poses serious challenges for investigation. Particles are being engineered in such a way to overcome the lung clearance mechanism, targeting specific regions of the lungs and being retained in the lung for longer time period. The nCmP formulations form an attractive interdisciplinary area that brings together polymer/material science, nanotechnology and biology for a multitude of biomedical applications. These are ‘intelligent’ systems widely used to deliver small molecules, genes, protein/peptides or drug nanoparticles to various targeted locations in the body. nCmP help in protecting them from degradation during delivery, targeting them to specific sites and regulating their release properties with respect to time. There are various nCmP that have been used to deliver therapeutic agents to the lungs (pulmonary drug delivery) and other body parts (non-pulmonary drug delivery) with their key findings discussed in **Table 2.1** and **Table 2.2**.

2.5 References

1. J.H. Bell, P.S. Hartley, and J.S. Cox. Dry powder aerosols. I. A new powder inhalation device. *J Pharm Sci.* 60:1559-1564 (1971).
2. R.A. Lubet, Z. Zhang, Y. Wang, and M. You. Chemoprevention of lung cancer in transgenic mice. *Chest.* 125:144S-147S (2004).
3. K.M. Skubitz and P.M. Anderson. Inhalational interleukin-2 liposomes for pulmonary metastases: a phase I clinical trial. *Anticancer Drugs.* 11:555-563 (2000).
4. M.E. Wylam, R. Ten, U.B. Prakash, H.F. Nadrous, M.L. Clawson, and P.M. Anderson. Aerosol granulocyte-macrophage colony-stimulating factor for pulmonary alveolar proteinosis. *Eur Respir J.* 27:585-593 (2006).
5. D.R. Hess. Aerosol delivery devices in the treatment of asthma. *Respir Care.* 53:699-723; discussion 723-695 (2008).
6. J.C. Sung, B.L. Pulliam, and D.A. Edwards. Nanoparticles for drug delivery to the lungs. *Trends in Biotechnology.* 25:563-570 (2007).
7. H.M. Mansour, Y.S. Rhee, C.W. Park, and P.P. DeLuca. Lipid Nanoparticulate Drug Delivery and Nanomedicine. In A. Moghis (ed.), *Lipids in Nanotechnology*, American Oil Chemists Society (AOCS) Press, Urbana, Illinois, 2011, pp. 221-268.
8. S.K. Vaswani and P.S. Creticos. Metered dose inhaler: past, present, and future. *Ann Allergy Asthma Immunol.* 80:11-19; quiz 19-20 (1998).
9. R.H. Cummings. Pressurized metered dose inhalers: chlorofluorocarbon to hydrofluoroalkane transition-valve performance. *J Allergy Clin Immunol.* 104:S230-236 (1999).
10. J. Sanchis, C. Corrigan, M.L. Levy, J.L. Viejo, and A. Group. Inhaler devices - from theory to practice. *Respir Med.* 107:495-502 (2013).
11. M. Lippmann, D.B. Yeates, and R.E. Albert. Deposition, retention, and clearance of inhaled particles. *Br J Ind Med.* 37:337-362 (1980).
12. S.P. Newman and W.W. Busse. Evolution of dry powder inhaler design, formulation, and performance. *Respir Med.* 96:293-304 (2002).
13. N. Islam and E. Gladki. Dry powder inhalers (DPIs)--a review of device reliability and innovation. *Int J Pharm.* 360:1-11 (2008).
14. B.L. Laube, H.M. Janssens, F.H.C. de Jongh, S.G. Devadason, R. Dhand, P. Diot, M.L. Everard, I. Horvath, P. Navalesi, T. Voshaar, and H. Chrystyn. What the pulmonary specialist should know about inhalation therapies. *European Respiratory Journal.* 37:1308-1331 (2011).

15. L. Willis, D. Hayes, and H.M. Mansour. Therapeutic Liposomal Dry Powder Inhalation Aerosols for Targeted Lung Delivery. *Lung*. 190:251-262 (2012).
16. D.A. Edwards, A. Ben-Jebria, and R. Langer. Recent advances in pulmonary drug delivery using large, porous inhaled particles. *Journal of Applied Physiology*. 85:379-385 (1998).
17. M.H. Al-Hallak, M.K. Sarfraz, S. Azarmi, W.H. Roa, W.H. Finlay, and R. Lobenberg. Pulmonary delivery of inhalable nanoparticles: dry powder inhalers. *Ther Deliv*. 2:1313-1324 (2011).
18. R. Vehring. Pharmaceutical particle engineering via spray drying. *Pharmaceutical Research*. 25:999-1022 (2008).
19. Z. Xu, H.M. Mansour, and A.J. Hickey. Particle Interactions in Dry Powder Inhaler Unit Processes. *Journal of Adhesion Science and Technology*. 25:451-482 (2011).
20. S. Ziffels, N.L. Bemelmans, P.G. Durham, and A.J. Hickey. *In vitro* dry powder inhaler formulation performance considerations. *Journal of Controlled Release*. 199:45-52 (2015).
21. C. Karner, J. Chong, and P. Poole. Tiotropium versus placebo for chronic obstructive pulmonary disease. *Cochrane Database Syst Rev*. 7:CD009285 (2014).
22. J.F. Donohue, M.R. Maleki-Yazdi, S. Kilbride, R. Mehta, C. Kalberg, and A. Church. Efficacy and safety of once-daily umeclidinium/vilanterol 62.5/25 mcg in COPD. *Respiratory Medicine*. 107:1538-1546 (2013).
23. F.J. Martinez, J. Boscia, G. Feldman, C. Scott-Wilson, S. Kilbride, L. Fabbri, C. Crim, and P.M. Calverley. Fluticasone furoate/vilanterol (100/25; 200/25 mug) improves lung function in COPD: a randomised trial. *Respir Med*. 107:550-559 (2013).
24. J.E. Frampton. QVA149 (indacaterol/glycopyrronium fixed-dose combination): a review of its use in patients with chronic obstructive pulmonary disease. *Drugs*. 74:465-488 (2014).
25. E.D. Bateman, K.R. Chapman, D. Singh, A.D. D'Urzo, E. Molins, A. Leselbaum, and E.G. Gil. Acclidinium bromide and formoterol fumarate as a fixed-dose combination in COPD: pooled analysis of symptoms and exacerbations from two six-month, multicentre, randomised studies (ACLIFORM and AUGMENT). *Respir Res*. 16:92 (2015).
26. K.C. Mannix and R. Meir. Teva Announces FDA Approval of ProAir® RespiClick.
http://www.tevapharm.com/news/teva_announces_fda_approval_of_proair_respiclick_04_15.aspx.

27. M.D. Parkins and J.S. Elborn. Tobramycin Inhalation Powder: a novel drug delivery system for treating chronic *Pseudomonas aeruginosa* infection in cystic fibrosis. *Expert Rev Respir Med.* 5:609-622 (2011).
28. M.W. Konstan, D.E. Geller, P. Minic, F. Brockhaus, J. Zhang, and G. Angyalosi. Tobramycin Inhalation Powder for *P. aeruginosa* Infection in Cystic Fibrosis: The EVOLVE Trial. *Pediatric Pulmonology.* 46:230-238 (2011).
29. M.W. Konstan, P.A. Flume, M. Kappler, R. Chiron, M. Higgins, F. Brockhaus, J. Zhang, G. Angyalosi, E. He, and D.E. Geller. Safety, efficacy and convenience of tobramycin inhalation powder in cystic fibrosis patients: The EAGER trial. *J Cyst Fibros.* 10:54-61 (2011).
30. A.R. Smyth, S.C. Bell, S. Bojcin, M. Bryon, A. Duff, P. Flume, N. Kashirskaya, A. Munck, F. Ratjen, S.J. Schwarzenberg, I. Sermet-Gaudelus, K.W. Southern, G. Taccetti, G. Ullrich, S. Wolfe, and S. European Cystic Fibrosis Society. European Cystic Fibrosis Society Standards of Care: Best Practice guidelines. *J Cyst Fibros.* 13 Suppl 1:S23-42 (2014).
31. C.W. Park, X. Li, F.G. Vogt, D. Hayes, Jr., J.B. Zwischenberger, E.S. Park, and H.M. Mansour. Advanced spray-dried design, physicochemical characterization, and aerosol dispersion performance of vancomycin and clarithromycin multifunctional controlled release particles for targeted respiratory delivery as dry powder inhalation aerosols. *Int J Pharm.* 455:374-392 (2013).
32. X. Li, F.G. Vogt, D. Hayes Jr, and H.M. Mansour. Physicochemical characterization and aerosol dispersion performance of organic solution advanced spray-dried microparticulate/nanoparticulate antibiotic dry powders of tobramycin and azithromycin for pulmonary inhalation aerosol delivery. *European Journal of Pharmaceutical Sciences.* 52:191-205 (2014).
33. S. Suarez and A.J. Hickey. Drug properties affecting aerosol behavior. *Respiratory Care.* 45:652-666 (2000).
34. M.B. Antunes and N.A. Cohen. Mucociliary clearance--a critical upper airway host defense mechanism and methods of assessment. *Curr Opin Allergy Clin Immunol.* 7:5-10 (2007).
35. D. Pavia. Aerosols and the Lung: Clinical and Experimental Aspects. In S.W. Clarke and D. Pavia (eds.), Butterworths, London, 1984, pp. 200-229.
36. A. Mahmud and D.E. Discher. Lung Vascular Targeting Through Inhalation Delivery: Insight from Filamentous Viruses and Other Shapes. *Iubmb Life.* 63:607-612 (2011).
37. Y.-Z. Li, X. Sun, T. Gong, J. Liu, J. Zuo, and Z.-R. Zhang. Inhalable microparticles as carriers for pulmonary delivery of thymopentin-loaded solid lipid nanoparticles. *Pharmaceutical Research.* 27:1977-1986 (2010).

38. N.R. Yacobi, N. Malmstadt, F. Fazlollahi, L. DeMaio, R. Marchelletta, S.F. Hamm-Alvarez, Z. Borok, K.-J. Kim, and E.D. Crandall. Mechanisms of Alveolar Epithelial Translocation of a Defined Population of Nanoparticles. *American Journal of Respiratory Cell and Molecular Biology*. 42:604-614 (2010).
39. D.P. McIntosh, X.Y. Tan, P. Oh, and J.E. Schnitzer. Targeting endothelium and its dynamic caveolae for tissue-specific transcytosis in vivo: a pathway to overcome cell barriers to drug and gene delivery. *Proc Natl Acad Sci U S A*. 99:1996-2001 (2002).
40. B.C. Tang, M. Dawson, S.K. Lai, Y.Y. Wang, J.S. Suk, M. Yang, P. Zeitlin, M.P. Boyle, J. Fu, and J. Hanes. Biodegradable polymer nanoparticles that rapidly penetrate the human mucus barrier. *Proceedings of the National Academy of Sciences of the United States of America*. 106:19268-19273 (2009).
41. J.M. Chen, M.G. Tan, A. Nemmar, W.M. Song, M. Dong, G.L. Zhang, and Y. Li. Quantification of extrapulmonary translocation of intratracheal-instilled particles in vivo in rats: Effect of lipopolysaccharide. *Toxicology*. 222:195-201 (2006).
42. R. Vanbever, J.D. Mintzes, J. Wang, J. Nice, D. Chen, R. Batycky, R. Langer, and D.A. Edwards. Formulation and physical characterization of large porous particles for inhalation. *Pharmaceutical Research*. 16:1735-1742 (1999).
43. C. Bosquillon, C. Lombry, V. Preat, and R. Vanbever. Influence of formulation excipients and physical characteristics of inhalation dry powders on their aerosolization performance. *Journal of Controlled Release*. 70:329-339 (2001).
44. A.L. Coates and C. O'Callaghan. *Drug administration by aerosol in children*, Saunders-Elsevier, Philadelphia, PA, 2006.
45. W. Glover, H.K. Chan, S. Eberl, E. Daviskas, and J. Verschuer. Effect of particle size of dry powder mannitol on the lung deposition in healthy volunteers. *Int J Pharm*. 349:314-322 (2008).
46. W.C. Hinds. *Aerosol technology: properties, behavior, and measurement of airborne particles*, Wiley-Interscience 1999.
47. R.H. Muller, K. Mader, and S. Gohla. Solid lipid nanoparticles (SLN) for controlled drug delivery - a review of the state of the art. *Eur J Pharm Biopharm*. 50:161-177 (2000).
48. D. Roy, X. Guillon, F. Lescure, P. Couvreur, N. Bru, and P. Breton. On shelf stability of freeze-dried poly(methylidene malonate 2.1.2) nanoparticles. *International Journal of Pharmaceutics*. 148:165-175 (1997).
49. M. Chacón, L. Berges, J. Molpeceres, M.R. Aberturas, and M. Guzman. Optimized preparation of poly d,l (lactic-glycolic) microspheres and nanoparticles for oral administration. *International Journal of Pharmaceutics*. 141:81-91 (1996).

50. S.Y.K. Fong, A. Ibisogly, and A. Bauer-Brandl. Solubility enhancement of BCS Class II drug by solid phospholipid dispersions: Spray drying versus freeze-drying. *International Journal of Pharmaceutics*.
51. D.P. Miller, T. Tan, T.E. Tarara, J. Nakamura, R.J. Malcolmson, and J.G. Weers. Physical Characterization of Tobramycin Inhalation Powder: I. Rational Design of a Stable Engineered-Particle Formulation for Delivery to the Lungs. *Mol Pharm*. 12:2582-2593 (2015).
52. R.P. Aquino, L. Prota, G. Auriemma, A. Santoro, T. Mencherini, G. Colombo, and P. Russo. Dry powder inhalers of gentamicin and leucine: formulation parameters, aerosol performance and *in vitro* toxicity on CuFil cells. *Int J Pharm*. 426:100-107 (2012).
53. J.Y. Her, M.S. Kim, and K.G. Lee. Preparation of probiotic powder by the spray freeze-drying method. *Journal of Food Engineering*. 150:70-74 (2015).
54. Q. Wang, J. Zhang, and A. Wang. Freeze-drying: A versatile method to overcome re-aggregation and improve dispersion stability of palygorskite for sustained release of ofloxacin. *Applied Clay Science*. 87:7-13 (2014).
55. F. Ungaro, I. d'Angelo, A. Miro, M.I. La Rotonda, and F. Quaglia. Engineered PLGA nano- and micro-carriers for pulmonary delivery: challenges and promises. *J Pharm Pharmacol*. 64:1217-1235 (2012).
56. J. Varshosaz, F. Hassanzadeh, A. Mardani, and M. Rostami. Feasibility of haloperidol-anchored albumin nanoparticles loaded with doxorubicin as dry powder inhaler for pulmonary delivery. *Pharmaceutical development and technology*. 20:183-196 (2015).
57. N.A. Stocke, S.A. Meenach, S.M. Arnold, H.M. Mansour, and J.Z. Hilt. Formulation and characterization of inhalable magnetic nanocomposite microparticles (MnMs) for targeted pulmonary delivery via spray drying. *International Journal of Pharmaceutics*. 479:320-328 (2015).
58. N.K. Kunda, I.M. Alfagih, E.N. Miyaji, D.B. Figueiredo, V.M. Goncalves, D.M. Ferreira, S.R. Dennison, S. Somavarapu, G.A. Hutcheon, and I.Y. Saleem. Pulmonary Dry Powder Vaccine of Pneumococcal Antigen Loaded Nanoparticles. *Int J Pharm*(2015).
59. N.K. Kunda, I.M. Alfagih, S.R. Dennison, S. Somavarapu, Z. Merchant, G.A. Hutcheon, and I.Y. Saleem. Dry powder pulmonary delivery of cationic PGA-co-PDL nanoparticles with surface adsorbed model protein. *International Journal of Pharmaceutics*. 492:213-222 (2015).
60. Y.S. Lee, P.J. Johnson, P.T. Robbins, and R.H. Bridson. Production of nanoparticles-in-microparticles by a double emulsion method: A comprehensive study. *European Journal of Pharmaceutics and Biopharmaceutics*. 83:168-173 (2013).

61. M.S. Yang, H. Yamamoto, H. Kurashima, H. Takeuchi, T. Yokoyama, H. Tsujimoto, and Y. Kawashima. Design and evaluation of inhalable chitosan-modified poly (DL-lactic-co-glycolic acid) nanocomposite particles. *European Journal of Pharmaceutical Sciences*. 47:235-243 (2012).
62. F. Ungaro, I. d'Angelo, C. Coletta, R. d'Emmanuele di Villa Bianca, R. Sorrentino, B. Perfetto, M.A. Tufano, A. Miro, M.I. La Rotonda, and F. Quaglia. Dry powders based on PLGA nanoparticles for pulmonary delivery of antibiotics: Modulation of encapsulation efficiency, release rate and lung deposition pattern by hydrophilic polymers. *Journal of Controlled Release*. 157:149-159 (2012).
63. S. Jafarinejad, K. Gilani, E. Moazeni, M. Ghazi-Khansari, A.R. Najafabadi, and N. Mohajel. Development of chitosan-based nanoparticles for pulmonary delivery of itraconazole as dry powder formulation. *Powder Technology*. 222:65-70 (2012).
64. C. Duret, N. Wauthoz, T. Sebti, F. Vanderbist, and K. Amighi. New inhalation-optimized itraconazole nanoparticle-based dry powders for the treatment of invasive pulmonary aspergillosis. *Int J Nanomedicine*. 7:5475-5489 (2012).
65. M. Beck-Broichsitter, C. Schweiger, T. Schmehl, T. Gessler, W. Seeger, and T. Kissel. Characterization of novel spray-dried polymeric particles for controlled pulmonary drug delivery. *Journal of Controlled Release*. 158:329-335 (2012).
66. P.S. Pourshahab, K. Gilani, E. Moazeni, H. Eslahi, M.R. Fazeli, and H. Jamalifar. Preparation and characterization of spray dried inhalable powders containing chitosan nanoparticles for pulmonary delivery of isoniazid. *J Microencapsul*. 28:605-613 (2011).
67. W.S. Cheow, M.W. Chang, and K. Hadinoto. The roles of lipid in anti-biofilm efficacy of lipid-polymer hybrid nanoparticles encapsulating antibiotics. *Colloids and Surfaces A: Physicochemical and Engineering Aspects*. 389:158-165 (2011).
68. D.M.K. Jensen, D. Cun, M.J. Maltesen, S. Frokjaer, H.M. Nielsen, and C. Foged. Spray drying of siRNA-containing PLGA nanoparticles intended for inhalation. *J Control Release*. 142:138-145 (2010).
69. J.C. Sung, D.J. Padilla, L. Garcia-Contreras, J.L. Verberkmoes, D. Durbin, C.A. Peloquin, K.J. Elbert, A.J. Hickey, and D.A. Edwards. Formulation and pharmacokinetics of self-assembled rifampicin nanoparticle systems for pulmonary delivery. *Pharm Res*. 26:1847-1855 (2009).
70. G. Pilcer, F. Vanderbist, and K. Amighi. Preparation and characterization of spray-dried tobramycin powders containing nanoparticles for pulmonary delivery. *International Journal of Pharmaceutics*. 365:162-169 (2009).
71. K. Ohashi, T. Kabasawa, T. Ozeki, and H. Okada. One-step preparation of rifampicin/poly(lactic-co-glycolic acid) nanoparticle-containing mannitol

microspheres using a four-fluid nozzle spray drier for inhalation therapy of tuberculosis. *Journal of Controlled Release*. 135:19-24 (2009).

72. K. Tomoda, T. Ohkoshi, Y. Kawai, M. Nishiwaki, T. Nakajima, and K. Makino. Preparation and properties of inhalable nanocomposite particles: Effects of the temperature at a spray-dryer inlet upon the properties of particles. *Colloids and Surfaces B: Biointerfaces*. 61:138-144 (2008).

73. Y. Takashima, R. Saito, A. Nakajima, M. Oda, A. Kimura, T. Kanazawa, and H. Okada. Spray-drying preparation of microparticles containing cationic PLGA nanospheres as gene carriers for avoiding aggregation of nanospheres. *International Journal of Pharmaceutics*. 343:262-269 (2007).

74. T. Mizoe, T. Ozeki, and H. Okada. Preparation of drug nanoparticle-containing microparticles using a 4-fluid nozzle spray drier for oral, pulmonary, and injection dosage forms. *Journal of Controlled Release*. 122:10-15 (2007).

75. K. Hadinoto, P. Phanapavudhikul, Z. Kewu, and R.B.H. Tan. Novel Formulation of Large Hollow Nanoparticles Aggregates as Potential Carriers in Inhaled Delivery of Nanoparticulate Drugs. *Industrial & Engineering Chemistry Research*. 45:3697-3706 (2006).

76. K. Hadinoto, P. Phanapavudhikul, Z. Kewu, and R.B.H. Tan. Dry powder aerosol delivery of large hollow nanoparticulate aggregates as prospective carriers of nanoparticulate drugs: Effects of phospholipids. *International Journal of Pharmaceutics*. 333:187-198 (2007).

77. K. Hadinoto, K. Zhu, and R.B.H. Tan. Drug release study of large hollow nanoparticulate aggregates carrier particles for pulmonary delivery. *International Journal of Pharmaceutics*. 341:195-206 (2007).

78. A. Grenha, C.I. Grainger, L.A. Dailey, B. Seijo, G.P. Martin, C. Remuñán-López, and B. Forbes. Chitosan nanoparticles are compatible with respiratory epithelial cells *in vitro*. *European Journal of Pharmaceutical Sciences*. 31:73-84 (2007).

79. L. Ely, W. Roa, W.H. Finlay, and R. Löbenberg. Effervescent dry powder for respiratory drug delivery. *European Journal of Pharmaceutics and Biopharmaceutics*. 65:346-353 (2007).

80. S. Azarmi, X. Tao, H. Chen, Z. Wang, W.H. Finlay, R. Löbenberg, and W.H. Roa. Formulation and cytotoxicity of doxorubicin nanoparticles carried by dry powder aerosol particles. *International Journal of Pharmaceutics*. 319:155-161 (2006).

81. A. Grenha, B. Seijo, and C. Remuñán-López. Microencapsulated chitosan nanoparticles for lung protein delivery. *European Journal of Pharmaceutical Sciences*. 25:427-437 (2005).

82. R.O. Cook, R.K. Pannu, and I.W. Kellaway. Novel sustained release microspheres for pulmonary drug delivery. *Journal of Controlled Release*. 104:79-90 (2005).
83. J.O.H. Sham, Y. Zhang, W.H. Finlay, W.H. Roa, and R. Löbenberg. Formulation and characterization of spray-dried powders containing nanoparticles for aerosol delivery to the lung. *International Journal of Pharmaceutics*. 269:457-467 (2004).
84. N. Tsapis, D. Bennett, B. Jackson, D.A. Weitz, and D.A. Edwards. Trojan particles: Large porous carriers of nanoparticles for drug delivery. *Proceedings of the National Academy of Sciences*. 99:12001-12005 (2002).
85. P. Muralidharan, M. Malapit, E. Mallory, D. Hayes Jr, and H.M. Mansour. Inhalable nanoparticulate powders for respiratory delivery. *Nanomedicine: Nanotechnology, Biology and Medicine*. 11:1189-1199 (2015).
86. M. Beck-Broichsitter, O.M. Merkel, and T. Kissel. Controlled pulmonary drug and gene delivery using polymeric nano-carriers. *Journal of Controlled Release*. 161:214-224 (2012).
87. N. Schafroth, C. Arpagaus, U.Y. Jadhav, S. Makne, and D. Douroumis. Nano and microparticle engineering of water insoluble drugs using a novel spray-drying process. *Colloids and Surfaces B: Biointerfaces*. 90:8-15 (2012).
88. B.V.N.Y. Nagavarma, Hemant K. S.; Ayaz, A.; Vasudha, L. S.; Shivakumar, H. G. DIFFERENT TECHNIQUES FOR PREPARATION OF POLYMERIC NANOPARTICLES- A REVIEW. *Asian Journal of Pharmaceutical & Clinical Research*. 5:(2012).
89. T. Jung, W. Kamm, A. Breitenbach, E. Kaiserling, J.X. Xiao, and T. Kissel. Biodegradable nanoparticles for oral delivery of peptides: is there a role for polymers to affect mucosal uptake? *European Journal of Pharmaceutics and Biopharmaceutics*. 50:147-160 (2000).
90. G. Lambert, E. Fattal, and P. Couvreur. Nanoparticulate systems for the delivery of antisense oligonucleotides. *Adv Drug Deliv Rev*. 47:99-112 (2001).
91. H. Fessi, F. Puisieux, J.P. Devissaguet, N. Ammoury, and S. Benita. Nanocapsule formation by interfacial polymer deposition following solvent displacement. *International Journal of Pharmaceutics*. 55:R1-R4 (1989).
92. P. York. Strategies for particle design using supercritical fluid technologies. *Pharmaceutical Science & Technology Today*. 2:430-440 (1999).
93. M.M. Bailey and C.J. Berkland. Nanoparticle formulations in pulmonary drug delivery. *Medicinal research reviews*. 29:196-212 (2009).

94. G. Pilcer and K. Amighi. Formulation strategy and use of excipients in pulmonary drug delivery. *Int J Pharm.* 392:1-19 (2010).
95. S.A. Shoyele and S. Cawthorne. Particle engineering techniques for inhaled biopharmaceuticals. *Advanced Drug Delivery Reviews.* 58:1009-1029 (2006).
96. X. Wu, D. Hayes, Jr., J.B. Zwischenberger, R.J. Kuhn, and H.M. Mansour. Design and physicochemical characterization of advanced spray-dried tacrolimus multifunctional particles for inhalation. *Drug Des Devel Ther.* 7:59-72 (2013).
97. M. Irngartinger, V. Camuglia, M. Damm, J. Goede, and H.W. Frijlink. Pulmonary delivery of therapeutic peptides via dry powder inhalation: effects of micronisation and manufacturing. *European Journal of Pharmaceutics and Biopharmaceutics.* 58:7-14 (2004).
98. P. Calvo, C. Remuñán-López, J.L. Vila-Jato, and M.J. Alonso. Novel hydrophilic chitosan-polyethylene oxide nanoparticles as protein carriers. *Journal of Applied Polymer Science.* 63:125-132 (1997).
99. K. Corkery. Inhalable drugs for systemic therapy. *Respiratory Care.* 45:831-835 (2000).
100. V. Codrons, F. Vanderbist, R.K. Verbeeck, M. Arras, D. Lison, V. Preat, and R. Vanbever. Systemic delivery of parathyroid hormone (1-34) using inhalation dry powders in rats. *J Pharm Sci.* 92:938-950 (2003).
101. W.H. De Jong and P.J.A. Borm. Drug delivery and nanoparticles: Applications and hazards. *International Journal of Nanomedicine.* 3:133-149 (2008).
102. T. Sun, Y.S. Zhang, B. Pang, D.C. Hyun, M. Yang, and Y. Xia. Engineered Nanoparticles for Drug Delivery in Cancer Therapy. *Angewandte Chemie International Edition.* 53:12320-12364 (2014).
103. J. Zhang, L. Wu, H.-K. Chan, and W. Watanabe. Formation, characterization, and fate of inhaled drug nanoparticles. *Advanced Drug Delivery Reviews.* 63:441-455 (2011).
104. A.Z. Wilczewska, K. Niemirowicz, K.H. Markiewicz, and H. Car. Nanoparticles as drug delivery systems. *Pharmacol Rep.* 64:1020-1037 (2012).
105. B. Pulliam, J.C. Sung, and D.A. Edwards. Design of nanoparticle-based dry powder pulmonary vaccines. *Expert Opinion on Drug Delivery.* 4:651-663 (2007).
106. W.S. Shim, J.-H. Kim, K. Kim, Y.-S. Kim, R.-W. Park, I.-S. Kim, I.C. Kwon, and D.S. Lee. pH- and temperature-sensitive, injectable, biodegradable block copolymer hydrogels as carriers for paclitaxel. *International Journal of Pharmaceutics.* 331:11-18 (2007).

107. S. Parveen, R. Misra, and S.K. Sahoo. Nanoparticles: a boon to drug delivery, therapeutics, diagnostics and imaging. *Nanomedicine: Nanotechnology, Biology and Medicine*. 8:147-166 (2012).
108. S.R. Mudshinge, A.B. Deore, S. Patil, and C.M. Bhalgat. Nanoparticles: Emerging carriers for drug delivery. *Saudi Pharmaceutical Journal*. 19:129-141 (2011).
109. S. Azarmi, W.H. Roa, and R. Löbenberg. Targeted delivery of nanoparticles for the treatment of lung diseases. *Advanced Drug Delivery Reviews*. 60:863-875 (2008).
110. P. Baldrick. Pharmaceutical excipient development: the need for preclinical guidance. *Regul Toxicol Pharmacol*. 32:210-218 (2000).
111. A. Minne, H. Boireau, M.J. Horta, and R. Vanbever. Optimization of the aerosolization properties of an inhalation dry powder based on selection of excipients. *European Journal of Pharmaceutics and Biopharmaceutics*. 70:839-844 (2008).
112. S.S. Razavi Rohani, K. Abnous, and M. Tafaghodi. Preparation and characterization of spray-dried powders intended for pulmonary delivery of Insulin with regard to the selection of excipients. *International Journal of Pharmaceutics*. 465:464-478 (2014).
113. P. Kaur, S.K. Singh, V. Garg, M. Gulati, and Y. Vaidya. Optimization of spray drying process for formulation of solid dispersion containing polypeptide-k powder through quality by design approach. *Powder Technology*. 284:1-11 (2015).
114. M. Ameriand Y.F. Maa. Spray Drying of Biopharmaceuticals: Stability and Process Considerations. *Drying Technology*. 24:763-768 (2006).
115. E.M. Littringer, A. Mescher, S. Eckhard, H. Schröttner, C. Langes, M. Fries, U. Griesser, P. Walzel, and N.A. Urbanetz. Spray Drying of Mannitol as a Drug Carrier—The Impact of Process Parameters on Product Properties. *Drying Technology*. 30:114-124 (2011).
116. D. Das, E. Wang, and T.A.G. Langrish. Solid-phase crystallization of spray-dried glucose powders: A perspective and comparison with lactose and sucrose. *Advanced Powder Technology*. 25:1234-1239 (2014).
117. Y.F. Maa, P.A. Nguyen, J.D. Andya, N. Dasovich, T.D. Sweeney, S.J. Shire, and C.C. Hsu. Effect of spray drying and subsequent processing conditions on residual moisture content and physical/biochemical stability of protein inhalation powders. *Pharmaceutical Research*. 15:768-775 (1998).
118. F. Iskandar, H.W. Chang, and K. Okuyama. Preparation of microencapsulated powders by an aerosol spray method and their optical properties. *Advanced Powder Technology*. 14:349-367 (2003).

119. E.H.J. Kim. Surface composition of industrial spray-dried dairy powders and its formation mechanisms, *Chemical and Materials Engineering*, Vol. PhD, University of Auckland 2008.
120. F. Iskandar, L. Gradon, and K. Okuyama. Control of the morphology of nanostructured particles prepared by the spray drying of a nanoparticle sol. *Journal of Colloid and Interface Science*. 265:296-303 (2003).
121. R. Vehring, W.R. Foss, and D. Lechuga-Ballesteros. Particle formation in spray drying. *Journal of Aerosol Science*. 38:728-746 (2007).
122. A.S. Verkman, Y.L. Song, and J.R. Thiagarajah. Role of airway surface liquid and submucosal glands in cystic fibrosis lung disease. *American Journal of Physiology-Cell Physiology*. 284:C2-C15 (2003).
123. E.M. Littringer, R. Paus, A. Mescher, H. Schroettner, P. Walzel, and N.A. Urbanetz. The morphology of spray dried mannitol particles — The vital importance of droplet size. *Powder Technology*. 239:162-174 (2013).
124. P. Tewa-Tagne, S. Briançon, and H. Fessi. Preparation of redispersible dry nanocapsules by means of spray-drying: Development and characterisation. *European Journal of Pharmaceutical Sciences*. 30:124-135 (2007).
125. S.G. Maas, G. Schaldach, E.M. Littringer, A. Mescher, U.J. Griesser, D.E. Braun, P.E. Walzel, and N.A. Urbanetz. The impact of spray drying outlet temperature on the particle morphology of mannitol. *Powder Technology*. 213:27-35 (2011).
126. E.M. Littringer, A. Mescher, H. Schroettner, L. Achelis, P. Walzel, and N.A. Urbanetz. Spray dried mannitol carrier particles with tailored surface properties – The influence of carrier surface roughness and shape. *European Journal of Pharmaceutics and Biopharmaceutics*. 82:194-204 (2012).
127. S.G. Maas, G. Schaldach, P. Walzel, and N.A. Urbanetz. Tailoring dry powder inhaler performance by modifying carrier surface topography by spray drying. 20:763-774 (2010).
128. K. Ståhl, M. Claesson, P. Lilliehorn, H. Lindén, and K. Bäckström. The effect of process variables on the degradation and physical properties of spray dried insulin intended for inhalation. *International Journal of Pharmaceutics*. 233:227-237 (2002).
129. J. Raula, H. Eerikäinen, and E.I. Kauppinen. Influence of the solvent composition on the aerosol synthesis of pharmaceutical polymer nanoparticles. *International Journal of Pharmaceutics*. 284:13-21 (2004).
130. T.M. Ho, T. Howes, and B.R. Bhandari. Characterization of crystalline and spray-dried amorphous α -cyclodextrin powders. *Powder Technology*. 284:585-594 (2015).

131. X. Shian and Q. Zhong. Crystallinity and quality of spray-dried lactose powder improved by soluble soybean polysaccharide. *LWT - Food Science and Technology*. 62:89-96 (2015).
132. M. Maury, K. Murphy, S. Kumar, L. Shi, and G. Lee. Effects of process variables on the powder yield of spray-dried trehalose on a laboratory spray-dryer. *European Journal of Pharmaceutics and Biopharmaceutics*. 59:565-573 (2005).
133. A. Burger, J.O. Henck, S. Hetz, J.M. Rollinger, A.A. Weissnicht, and H. Stöttner. Energy/temperature diagram and compression behavior of the polymorphs of D-mannitol. *Journal of Pharmaceutical Sciences*. 89:457-468 (2000).
134. L. Wu, X. Miao, Z. Shan, Y. Huang, L. Li, X. Pan, Q. Yao, G. Li, and C. Wu. Studies on the spray dried lactose as carrier for dry powder inhalation. *Asian Journal of Pharmaceutical Sciences*. 9:336-341 (2014).
135. E.H.J. Kim, X.D. Chen, and D. Pearce. On the Mechanisms of Surface Formation and the Surface Compositions of Industrial Milk Powders. *Drying Technology*. 21:265-278 (2003).
136. F.L. Fu, T.B. Mi, S.S. Wong, and Y.J. Shyu. Characteristic and controlled release of anticancer drug loaded poly (D,L-lactide) microparticles prepared by spray drying technique. *Journal of Microencapsulation*. 18:733-747 (2001).
137. H.-Y. Li and J. Birchall. Chitosan-Modified Dry Powder Formulations for Pulmonary Gene Delivery. *Pharmaceutical Research*. 23:941-950 (2006).
138. L. Mu and S.S. Feng. Fabrication, characterization and *in vitro* release of paclitaxel (Taxol®) loaded poly (lactic-co-glycolic acid) microspheres prepared by spray drying technique with lipid/cholesterol emulsifiers. *Journal of Controlled Release*. 76:239-254 (2001).
139. T.-Y. Ting, I. Gonda, and E. Gipps. Microparticles of Polyvinyl Alcohol for Nasal Delivery. I. Generation by Spray-Drying and Spray-Desolvation. *Pharmaceutical Research*. 9:1330-1335 (1992).
140. B. Baras, M.A. Benoit, and J. Gillard. Parameters influencing the antigen release from spray-dried poly(dl-lactide) microparticles. *International Journal of Pharmaceutics*. 200:133-145 (2000).
141. Y.-F. Maa, H.R. Costantino, P.-A. Nguyen, and C.C. Hsu. The Effect of Operating and Formulation Variables on the Morphology of Spray-Dried Protein Particles. *Pharmaceutical Development and Technology*. 2:213-223 (1997).
142. G.S. Zijlstra, W.L.J. Hinrichs, A.H.d. Boer, and H.W. Frijlink. The role of particle engineering in relation to formulation and de-agglomeration principle in the development of a dry powder formulation for inhalation of cetorelix. *European Journal of Pharmaceutical Sciences*. 23:139-149 (2004).

143. Y.-F. Maa, P.-A.T. Nguyen, and S.W. Hsu. Spray-drying of air-liquid interface sensitive recombinant human growth hormone. *Journal of Pharmaceutical Sciences*. 87:152-159 (1998).
144. M. Maury, K. Murphy, S. Kumar, A. Mauerer, and G. Lee. Spray-drying of proteins: effects of sorbitol and trehalose on aggregation and FT-IR amide I spectrum of an immunoglobulin G. *European Journal of Pharmaceutics and Biopharmaceutics*. 59:251-261 (2005).
145. N.Y. Chewand H.K. Chan. Use of solid corrugated particles to enhance powder aerosol performance. *Pharm Res*. 18:1570-1577 (2001).
146. J.U. Menon, P. Ravikumar, A. Pise, D. Gyawali, C.C.W. Hsia, and K.T. Nguyen. Polymeric nanoparticles for pulmonary protein and DNA delivery. *Acta Biomaterialia*. 10:2643-2652 (2014).
147. D.K. Jensen, L.B. Jensen, S. Koocheki, L. Bengtson, D. Cun, H.M. Nielsen, and C. Foged. Design of an inhalable dry powder formulation of DOTAP-modified PLGA nanoparticles loaded with siRNA. *Journal of Controlled Release*. 157:141-148 (2012).
148. H.C. Smythand A.J. Hickey. Carriers in drug powder delivery. *American Journal of Drug Delivery*. 3:117-132 (2005).
149. M.J. Telkoand A.J. Hickey. Dry Powder Inhaler Formulation. *Respiratory Care*. 50:1209-1227 (2005).
150. H.M. Mansour, Y.S. Rhee, and X. Wu. Nanomedicine in pulmonary delivery. *International Journal of Nanomedicine*. 4:299-319 (2009).
151. C.A. Wolfe, P.S. James, A.R. Mackie, S. Ladha, and R. Jones. Regionalized lipid diffusion in the plasma membrane of mammalian spermatozoa. *Biol Reprod*. 59:1506-1514 (1998).
152. H.C. Gaedeand K. Gawrisch. Lateral diffusion rates of lipid, water, and a hydrophobic drug in a multilamellar liposome. *Biophys J*. 85:1734-1740 (2003).
153. S. Guenneauand T.M. Puvirajesinghe. Fick's second law transformed: one path to cloaking in mass diffusion. *J R Soc Interface*. 10:20130106 (2013).
154. A.M. Hillery. *Advanced Drug Delivery and targeting: An Introduction*, CRC Press2002.

CHAPTER 3

Synthesis and Characterization of Nanocomposite Microparticles (nCmP) for the Treatment of Cystic Fibrosis-Related Infections

Published in Pharmaceutical Research in 2016.

Zimeng Wang¹, Samantha A. Meenach^{1,2}

¹Department of Chemical Engineering, ²Department of Biomedical and Pharmaceutical Sciences, University of Rhode Island, Kingston, RI 02881, USA

ABSTRACT

Purpose: Pulmonary antibiotic delivery is recommended as maintenance therapy for cystic fibrosis (CF) patients who experience chronic infections. However, abnormally thick and sticky mucus present in the respiratory tract of CF patients impairs mucus penetration and limits the efficacy of inhaled antibiotics. To overcome the obstacles of pulmonary antibiotic delivery, we have developed nanocomposite microparticles (nCmP) for the inhalation application of antibiotics in the form of dry powder aerosols.

Methods: Azithromycin-loaded and rapamycin-loaded polymeric nanoparticles (NP) were prepared via nanoprecipitation and nCmP were prepared by spray drying and the physicochemical characteristics were evaluated.

Results: The nanoparticles were 200 nm in diameter both before loading into and after redispersion from nCmP. The NP exhibited smooth, spherical morphology and the nCmP were corrugated spheres about 1 μm in diameter. Both drugs were successfully encapsulated into the NP and were released in a sustained manner. The NP were successfully loaded into nCmP with favorable encapsulation efficacy. All materials were stable at manufacturing and storage conditions and nCmP were in an amorphous state after spray drying. nCmP demonstrated desirable aerosol dispersion characteristics, allowing them to deposit into the deep lung regions for effective drug delivery.

Conclusions: The described nCmP have the potential to overcome mucus-limited pulmonary delivery of antibiotics.

KEYWORDS

Nanocomposite microparticles, pulmonary delivery, cystic fibrosis, spray drying

3.1 Introduction

Cystic fibrosis (CF) is a progressive, incurable, autosomal recessive disease that affects around 70,000 people worldwide (1, 2). It is caused by mutations in the cystic fibrosis transmembrane conductance regulator (CFTR) gene, which leads to defective or insufficient amounts of functional CFTR proteins. The dysfunctional proteins result in an absence or decrease of chloride in secretions, leading to increased sodium and water absorption and airway surface liquid depletion (3). CF affects various organ systems of patients including the sweat glands, reproductive tract, intestine, liver, pancreas, and respiratory tract (4), in which lung disease is the primary cause of mortality (4, 5). The dysfunction of the respiratory tract results in frequent pulmonary infections, inflammation, bronchiectasis, and eventually respiratory failure, which causes over 90% of deaths in CF patients (6). Pulmonary infection is one of the primary complications among patients with CF and these patients tend to develop chronic infections within a year if no treatment is implemented, which will accelerate the decline in lung function, resulting in earlier mortality (7, 8).

Pseudomonas aeruginosa (*P. aeruginosa*) is regarded as the most prevalent pathogen in CF patients' lungs (7, 9). Azithromycin (AZI) is a macrolide antibiotic with a broad gram-negative antibacterial spectrum and is highly effective against planktonic, actively growing bacteria (10). AZI has been extensively studied for the treatment of CF-related infections due to its ability to decrease *P. aeruginosa* accumulation (10-15) as well as its pharmacokinetic advantages including high bioavailability, distribution, and extended half-life (13, 14).

Burkholderia cenocepacia (*B. cepacia*) infection is also considered to be a lethal threat to CF patients because it causes severe and persistent lung inflammation and it is resistant to nearly all available antibiotics (16). Rapamycin (RAP), also known as sirolimus, is an immunosuppressive macrolide that is the most commonly used chemical to induce autophagy (17). It has been shown that RAP can markedly decrease *B. cepacia* infection *in vitro* by enhancing the clearance of this bacterium via induced autophagy. RAP has been shown to reduce bacterial burden and decrease inflammation in the lungs of CF infected mice (16).

Acetalated dextran (Ac-Dex) is an acid sensitive, biodegradable, biocompatible polymer that can be prepared in a one-step reaction by reversibly modifying dextran with acetal groups (18). This modification reverses the solubility properties of dextran from hydrophilic to hydrophobic, making it possible to form polymeric particles using standard emulsion or nanoprecipitation techniques. Drug loaded Ac-Dex nanoparticles exhibit sustained release profile, with the advantages of extended duration of action, decreased drug use, improved management of therapy, enhanced compliance and reduced side effects. (19, 20) In comparison to other commonly used polymers in drug delivery such as poly(lactic-co-glycolic acid) (PLGA) and polyesters, Ac-Dex offers several advantages. Most notably, the degradation rate of Ac-Dex can be tuned from minutes to months by modifying the ratio of cyclic and acyclic acetal groups, which have different rates of hydrolysis. Also, Ac-Dex degrades into dextran, a biocompatible, biodegradable, FDA-approved by-product, and very low levels of methanol and acetone (20-22).

Mannitol, an FDA approved, non-toxic, readily degradable sugar alcohol commonly used in pharmaceutical products, was applied as the excipient of nCmP due to its beneficial properties.(23) First, mannitol can be rapidly dissolved into an aqueous environment, leading to a burst release of encapsulated nanoparticles. In addition, mannitol can improve the fluidity of mucus, thus enhancing the mucus penetration rate of nanoparticles (24). Mannitol has been extensively studied as a carrier in spray-dried powder aerosols for pulmonary drug administration and the resulting particles have been shown to exhibit desirable water content, size, and surface morphology for successful aerosol delivery (25, 26).

Pulmonary antibiotic delivery is increasingly recommended as maintenance therapy to prolong the interval between pulmonary exacerbations and to slow the progression of lung disease of CF patients due to the capability of these systems to achieve high drug concentrations at the site of infection and to minimize the risk of systemic toxicity and drug resistance (31-34). Extensive studies have been devoted to the development of new inhalation devices and advanced drug delivery formulations for the treatment of CF-related infections (35-38). Despite these advances, there has only been incremental improvement in the treatment of pulmonary infections. This is partly due to the presence of mucus in the lung airways that can trap and remove foreign particles. Also, the abnormally thick and viscous mucus in the respiratory tract of CF patients impairs efficient mucus penetration and limits the efficacy of antibiotics delivered via inhalation. Polyethylene glycol (PEG)-coated nanoparticles have been shown to significantly improve the mucus penetration of various therapeutics encapsulated in NP due to the formulation size, PEG coating, and protection of active pharmaceutical

ingredients (39). Unfortunately, aerosolized nanoparticles will be exhaled owing to their small size and mass and while aerosolized particles with aerodynamic diameters of 1-5 μm can deposit into the deep lung region, which limits their efficacy for targeting the infection site in mucus as aerosol drug delivery vehicles (40, 41).

To overcome the aforementioned obstacles of pulmonary antibiotic delivery, we developed nanocomposite microparticles (nCmP) in the form of dry powder aerosols (**Figure 1**). This system is comprised of drug-loaded nanoparticles (NP) entrapped in microparticle carriers with the excipient mannitol to allow for the delivery of mucus-penetrating NP to the lungs. The drug-loaded nanoparticles contain azithromycin or rapamycin as model drugs and are coated by a vitamin E poly(ethylene glycol) (MW 5000) layer, which has shown to improve the stability and mucus penetration rate of nanoparticles (39). Upon pulmonary administration, the nCmP will deposit on the mucus in the respiratory tract, dissociate into free NP and mannitol, and allow the nanoparticles to penetrate the mucus and then release drug to the targeted site at sustained rate. This nCmP system exhibits features favorable for dry powder-based antibiotic delivery including targeted delivery, rapid mucus penetration, and controlled drug release. The goal of the described research was the initial development and physicochemical characterization of the nCmP systems via particle engineering.

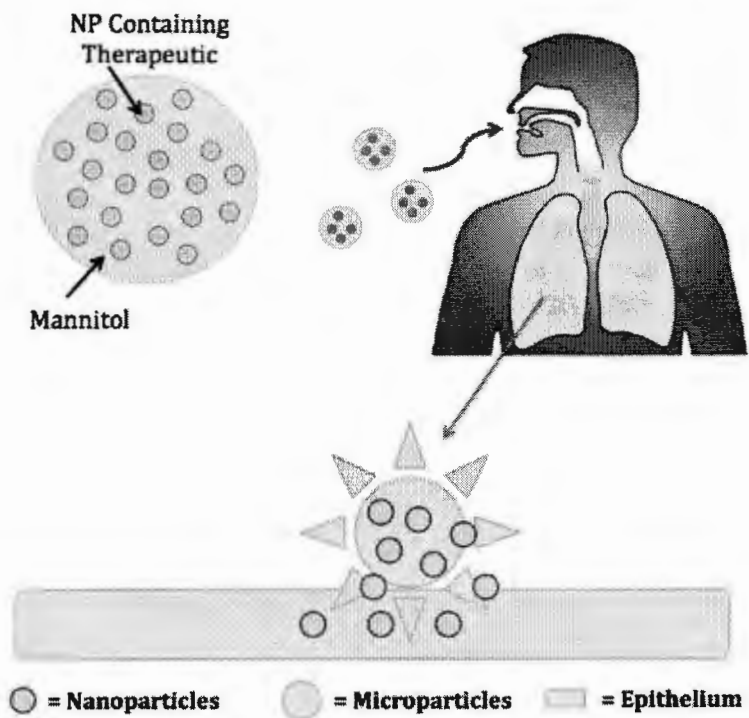


Figure 3.1. Schematic of an aerosol nanoparticle microparticle (nCmP) system interacting with the pulmonary mucosa. Once the nCmP impact the surface of the mucus coating the pulmonary epithelium they immediately degrade to release nanoparticles.

3.2 Materials and Methods

3.2.1 Materials

Dextran from *Leuconostoc mesenteroides* (9000 - 11000 MW), pyridinium p-toluenesulfonate (PPTS, 98%), poly(ethylene glycol) methyl ether (mPEG, Mn 5000), D- α -tocopherol succinate (vitamin E succinate, 1210 IU/g), N,N'-dicyclohexylcarbodiimide (DCC, 99%), 4-(dimethylamino) pyridine (DMAP, $\geq 99\%$), potassium phosphate dibasic, potassium phosphate monobasic, D-mannitol ($\geq 98\%$), 2-methoxypropene (2-MOP, 97%), triethylamine (TEA, $\geq 99\%$), anhydrous dimethyl sulfoxide (DMSO, $\geq 99.9\%$), deuterium chloride (DCl, 35 weight % in D₂O, 99 atom % D), deuterated chloroform (CDCl₃, 100%, 99.96 atom % D), TWEEN® 80, methanol (HPLC grade, $\geq 99.9\%$), and acetonitrile (HPLC grade, $\geq 99.9\%$) were obtained from Sigma-Aldrich (St. Louis, MO). Ethanol (anhydrous, ASC/USP grade) was obtained from Pharmco-AAPER (Brookfield, CT). Deuterium oxide (D₂O, 99.8% atom D) was obtained from Acros Organics (Geel, Belgium). Phosphate buffered saline (PBS) was obtained from Fisher Scientific. Hydranal® KF reagent was obtained from Fluka Analytical. Rapamycin was obtained from LC Laboratories (Woburn, MA). Azithromycin was obtained from AstaTech Inc. (Bristol, PA).

3.2.2 Synthesis of Acetalated Dextran (Ac-Dex)

Ac-Dex was synthesized as described previously (22) with minor modifications. Briefly, 1 g of lyophilized dextran and 25 mg of PPTS were dissolved in 10 mL anhydrous DMSO. The resulting solution was reacted with 5 mL of 2-MOP

under nitrogen gas for 5 minutes and was quenched with 1 mL of TEA. The reaction mixture was then precipitated in basic water (water and TEA, pH 9), vacuum filtered, and lyophilized ($-50\text{ }^{\circ}\text{C}$, 0.023 mbar) for 24 hours to yield a solid product.

3.2.3 Synthesis of Vitamin E Poly(ethylene glycol) (VP5k)

VP5k was prepared with some modifications to a previously described method (42). 0.65 g of vitamin E succinate and 7.334 g of mPEG were dissolved in 20 mL of DCM. 0.278 g of DCC and 15 mg of DMAP were added to the solution. The reaction mixture was stirred at room temperature overnight, vacuum filtered ($0.45\text{ }\mu\text{m}$), and concentrated under reduced pressure via a rotor evaporator (IKA-RV, Wilmington, NC) to obtain a crude product. The resulting crude product was dissolved at 5% (w/v) in DI water and centrifuged at 12000 rpm for 30 minutes. The filtrate was vacuum filtered ($0.22\text{ }\mu\text{m}$) and lyophilized ($-50\text{ }^{\circ}\text{C}$, 0.023 mbar) for 72 hours to yield the final product.

3.2.4 NMR Analysis of Ac-DEX and VP5k

The cyclic-to-acyclic (CAC) ratio of acetal coverage and degrees of total acetal coverage per 100 glucose molecules was confirmed by ^1H NMR spectroscopy (Bruker 300 MHz NMR, MA). 10 mg of Ac-Dex was added to 700 μL of D_2O and was hydrolyzed with 30 μL of DCl prior to analysis. The hydrolysis of one cyclic acetal group produces one acetone whereas one acyclic acetal produces one acetone and one methanol. Consequently, from the normalized integrations of peaks related to acetone,

methanol, and the carbon ring of dextran, the CAC ratio of acetal coverage and degrees of total acetal coverage per 100 glucoses were determined.

Conjugation of mPEG to Vitamin E succinate was also confirmed by NMR spectroscopy. 20 mg of VP5k was dissolved in 600 μL of CDCl_3 . The resulting solution was analyzed by 2D ^1H - ^{13}C HMBC-GP NMR spectroscopy. Shift of the signal at 2.8 ppm and 178.8 ppm related to the $-\text{COOH}$ group of vitamin E succinate and 2.7 ppm and 172.2 ppm related to the ester group indicated conjugation of mPEG to vitamin E succinate for the successful formation of VP5k.

3.2.5 Preparation of Drug-loaded Nanoparticles

Azithromycin (AZI)-loaded nanoparticles and rapamycin (RAP)-loaded nanoparticles were prepared via nanoprecipitation. 40 mg of Ac-Dex and 12 mg of AZI or 4 mg of RAP were dissolved in 1 mL of ethanol and injected into 40 mL of 1.5 % (w/v) VP5k solution. The resulting suspension was stirred for 3 hours for removal of ethanol and hardening of the particles and the final solution was centrifuged at 12000 rpm for 20 minutes to collect the NP. The NP were washed once with basic water and lyophilized for 24 hours to give the final AZI-NP and RAP-NP systems.

3.2.6 Preparation of Nanocomposite Microparticles (nCmP)

nCmP were prepared via the spray drying of a AZI NP or RAP NP suspensions and mannitol in an aqueous solution using a Büchi B-290 spray dryer (Büchi Labortechnik, AG, Switzerland) in open mode. The spray drying conditions were as

follows: 1:1 (w:w) ratio of NP to mannitol in DI water; feed solution concentration of 1% (w/v); 1.4 mm nozzle diameter; atomization gas flow rate of 414 L/h (UHP dry nitrogen); aspiration rate of 28 m³/h, inlet temperature of 50 °C; pump rate of 0.6 mL/min; and nozzle cleaner rate of 4. The resulting nCmP were separated in a high-performance cyclone, collected in a sample collector, and stored in amber glass vials in desiccators at -20°C.

3.2.7 Powder X-Ray Diffraction (PXRD)

Crystalline states of the nCmP were examined by PXRD using a Rigaku Multiflex X-ray diffractometer (The Woodlands, TX) with a Cu K α radiation source (40 kV, 44 mA). The samples were placed on a horizontal quartz glass sample holder (3 mm). The scan range was 5 – 65° in 2 θ with a step width of 0.02 and scan rate of 2°/min.

3.2.8 Differential Scanning Calorimetry (DSC)

The thermal phase transitions of the nCmP were determined by DSC using a TA Q200 DSC system (TA Instruments, New Castle, DE, USA) equipped with an automated computer-controlled RSC-90 cooling accessory. 1 - 3 mg of sample was weighed into Tzero™ alodined aluminum pans that were hermetically sealed. The sealed pans were placed into the DSC furnace along with an empty sealed reference pan. The heating range was 0 – 250 °C at a heating rate of 10 °C/min.

3.2.9 Scanning Electron Microscopy (SEM)

The shape and surface morphology of the NP and nCmP were evaluated by SEM using a Hitachi S-4300 microscope (Tokyo, Japan). nCmP samples were placed on aluminum SEM stubs (TedPella, Inc., Redding, CA, USA) with double-sided adhesive carbon tabs. Nanoparticles were dispersed in basic water (pH = 9, 10 mg/mL) and this suspension was dropped onto aluminum SEM stubs and then dried at room temperature. Both the NP and nCmP samples were coated with a thin film of a gold/palladium alloy using an Emscope SC400 sputter coating system at 20 μ A for 75 seconds under argon gas. Images were captured at 5 kV.

3.2.10 Particle Size, Size Distribution and Zeta Potential Analysis

The size, size distribution, and zeta potential of the NP systems were measured by dynamic light scattering (DLS) using a Malvern Nano Zetasizer (Malvern Instruments, Worcestershire, UK). The NP were dispersed in basic water (pH = 9, 0.3 mg/mL). All experiments were performed in triplicate with a scattering angle of 173° at 25 °C. The mean size and standard deviation of the nCmP were measured digitally from SEM images using ImageJ software (Sysstat, San Jose, CA, USA). Representative micrographs (5k magnification) for each sample were analyzed by measuring the diameter of at least 100 particles.

3.2.11 Karl Fischer (KF) Titration

The water content of the nCmP was quantified by Karl Fischer (KF) titration using a 737 KF coulometer (Metrohm, Riverview, FL). Approximately 10 mg of

powder was dissolved in anhydrous methanol. The resulting solution was injected into the KF reaction cell filled with Hydranal® KF reagent and then the amount of water was analyzed. Pure solvent was also injected for use as a background sample.

3.2.12 Aerosol Dispersion Analysis

In vitro aerosol dispersion performance of the nCmP was evaluated using a Next Generation Impactor™ (NGI™, MSP Corporation, Shoreview, MN) equipped with a stainless steel induction port (USP throat adaptor) attachment and stainless steel NGI™ gravimetric insert cups. The NGI™ was coupled with a Copley TPK 2000 critical flow controller, which was connected to a Copley HCP5 vacuum pump (Copley Scientific, United Kingdom). The airflow rate (Q) was measured and adjusted to 60 L/min in order to model the flow rate in a healthy adult lung before each experiment. Glass fiber filters (55 mm, Type A/E, Pall Life Sciences, PA) were placed in the gravimetric insert cups for stages 1 through 7 to minimize bounce or re-entrapment (43) and these filters were weighed before and after the experiment to determine the particle mass deposited on each stage. Approximately 10 mg of powder was loaded into a hydroxypropyl methylcellulose (HPMC, size 3, Quali-V®, Qualicaps® Inc., Whitsett, NC, USA) capsule and the capsule was placed into a human dry powder inhaler device (HandiHaler, Boehringer Ingelheim Pharmaceuticals, CT) attached to a customized rubber mouthpiece connected to the NGI™. Three HPMC capsules were loaded and released in each measurement and experiments were performed in triplicate. The NGI™ was run with a delay time of 10 s and running time of 10 s. For Q = 60 L/min, the effective cutoff diameters for each stage of the impactor

were given from the manufacturer as: stage 1 (8.06 μm); stage 2 (4.46 μm); stage 3 (2.82 μm); stage 4 (1.66 μm); stage 5 (0.94 μm); stage 6 (0.55 μm); and stage 7 (0.34 μm). The fine particle dose (FPD), fine particle fraction (FPF), respirable fraction (RF), and emitted dose (ED) were calculated as follows:

Fine particles dose (FPD) = mass of particles on Stages 2 through 7

$$\text{Fine particles fraction (FPF)} = \frac{\text{fine particles dose}}{\text{initial particle mass loaded into capsules}} \times 100\%$$

$$\text{Respirable fraction (RF)} = \frac{\text{mass of particles on Stages 2 through 7}}{\text{total particle mass on all stages}} \times 100\%$$

$$\text{Emitted dose (ED)} = \frac{\text{initial mass in capsules} - \text{final mass remaining in capsules}}{\text{initial mass in capsules}} \times 100\%$$

The mass median aerodynamic diameter (MMAD) and geometric standard deviation (GSD) for the particles were determined using a Mathematica® program written by Dr. Warren Finlay (43, 44).

3.2.13 Analysis of Nanoparticle Drug Loading and Nanoparticle Loading in nCmP

Drug loading and encapsulation efficacy of AZI and RAP NP and nCmP were determined using high performance liquid chromatograph (HPLC) (Hitachi Elite LaChrom, Japan). Detection of AZI was performed using the following conditions: C₁₈, 5 μm \times 150 mm \times 4.6 mm column (XTerra™, Waters); 1.5 mL/min pump rate; 6 minute retention time; mobile phase of 70% methanol and 30% PBS (0.03 M, pH =

7.4); absorbance of 215 nm; and ambient temperature. Detection of RAP was performed using following conditions: C₁₈, 5 μm × 150 mm × 4.6 mm column (Supelco, Sigma-Aldrich, St. Louis, MO); 1 mL/min pump rate; 6 minute retention time; mobile phase of 65% acetonitrile and 35% DI water; absorbance of 278 nm; and temperature of 50°C. Drug-loaded NP and nCmP were fully dissolved in their respective mobile phases. The experimental drug concentration in each sample was quantified by comparison with a standard curve of drug in its mobile phase. The drug loading of NP, drug loading of nCmP, NP loading in nCmP, drug encapsulation efficiency of NP, and NP encapsulation efficacy in nCmP were determined by the following equations:

$$\text{Drug loading} = \frac{\text{mass of drug loaded in nanoparticles}}{\text{mass of particles}} \times 100\%$$

$$\text{Drug encapsulation efficacy (EE)} = \frac{\text{mass of drug loaded in nanoparticles}}{\text{initial mass of drug in particle formulation}} \times 100\%$$

$$\text{Nanoparticles loading} = \frac{\text{mass of NPs loaded in nCmPs}}{\text{mass of nCmPs}} \times 100\%$$

$$\text{NP loading efficacy} = \frac{\text{mass of NPs loaded in nCmPs}}{\text{initial mass of NPs in nCmPs formulation}} \times 100\%$$

3.2.14 *In Vitro* Drug Release from Nanoparticles

The *in vitro* release profiles of AZI or RAP from nanoparticles was determined via a release study of NP suspended (1 mg/mL) in modified phosphate buffer (0.1 M, pH = 7.4) with 0.2% (w/v) of Tween® 80. The suspension was incubated at 37 °C and

100 rpm. At various time points (0 to 48 h), NP samples were centrifuged at 14000 rpm for 5 minutes at 4 °C to isolate the NP. 200 µL of supernatant was withdrawn and replaced by the same amount of fresh modified PBS in each sample. The withdrawn solutions were analyzed for drug content via HPLC using the same methods described in the previous section.

3.2.15 Statistical analysis

All measurements were performed in at least triplicate. Values are given in the form of means \pm SD. The statistical significance of the results was determined using t-Test. A p-value of <0.05 was considered statistically significant.

3.3 Results and Discussion

3.3.1 NMR Analysis of Ac-Dex and VP5k

Successful synthesis of Ac-Dex and VP5k was confirmed by NMR (**Figure A.1** in Supplemental Information). Ac-Dex exhibited 68.7% cyclic acetal coverage (CAC) and 79.1% total acetal coverage (conversion of -OH groups). A yield of approximately 95% was obtained for this Ac-Dex. An increase in CAC is known to slow drug release due to slower degradation.(21, 22) A high total acetal coverage (higher than 75% according to our research) is required to stabilize the VP5k coating of nanoparticles, which ensures small particles size and narrow size distribution. The signals for ester groups were detected via NMR, indicating successful conjugation of

mPEG to vitamin E succinate for the successful formation of VP5k (45). The yield of VP5k was approximately 30%.

3.3.2 Characterization of Nanoparticles

The azithromycin-loaded nanoparticles (AZI-NP), shown in **Figure 3.2A**, appear as uniform spheres with smooth surface morphology. NP size, size distribution, and zeta potential are shown in **Table 3.1**. The resulting sizes of the NP analyzed via DLS (approximately 200 nm) were larger than those observed from SEM micrographs and ImageJ analysis (approximately 100 nm) due to shrinking of the particles during freeze-drying from the collapse of hydrated PEGylated chains (46). Both drug-loaded NP systems exhibited desirable size (less than 200 nm) with narrow size distribution to allow for potential mucus penetration. The relative surface charge of the NP systems were nearly neutral, confirming PEG coverage on their surfaces (45). Similar results were obtained for drug-loaded and blank nanoparticles with respect to their size, size distribution, and surface charge, indicating that drug encapsulation did not affect the formation of the NP.

Both AZI and RAP were successfully encapsulated into the described NP systems. 13.0 % of initial AZI and 25.8 % of initial RAP were effectively entrapped within the NP prepared using nanoprecipitation of Ac-Dex and drugs in VP5k solution. The low encapsulation of the drugs may be due to the improved solubility of the drugs in the spinning solution by VP5K micelles. RAP-NP exhibited a higher encapsulation efficacy as a result of the lower solubility of RAP than AZI in the aqueous spinning solution.

Results of the *in vitro* release of AZI-NP and RAP-NP at physiological pH and temperature are reported in **Figure 3.3** as the percentage of drug released over time. Both NP systems displayed sustained release for approximately 12 hours, which matched the degradation profile of other Ac-Dex particle systems (43). Based on previous research, Ac-Dex made of 10kDa dextran and reacted for 5 minutes showed a maximum of degradation at 6 hours and negligible degradation after that (47). A possible explanation of the release profiles could be that the first release stage corresponds to Ac-Dex degradation as well as nanoparticle dissociation, whereas after 6 hours the rate of drug release is controlled by drugs passively diffuse out of the dissociated matrix of nanoparticles following the partial degradation of Ac-Dex.

3.3.3 Manufacturing of nCmP

With respect to nCmP manufacturing, the outlet temperatures of AZI- and RAP-nCmP were 30 - 31 °C and 30 - 33 °C, respectively, while the yields were 62.4% and 60.6%, respectively.

3.3.4 nCmP Morphology, Sizing, and Size Distribution

As seen in the SEM images, the AZI-nCmP were mostly spherical with a corrugated surface (**Figure 3.2B**) and encapsulated nanoparticles were visible on the surface of the nCmP as seen in **Figure 3.2C**. Both RAP-NP and RAP-nCmP exhibited the same morphology as the AZI loaded systems (data not shown). The number average geometric diameters were 1.03 ± 0.46 and 1.12 ± 0.43 μm for AZI-nCmP and

RAP-nCmP, respectively, as determined by ImageJ analysis. Both nCmP systems exhibited similar morphology, geometric size, and size distribution due to the similarities in spray drying conditions.

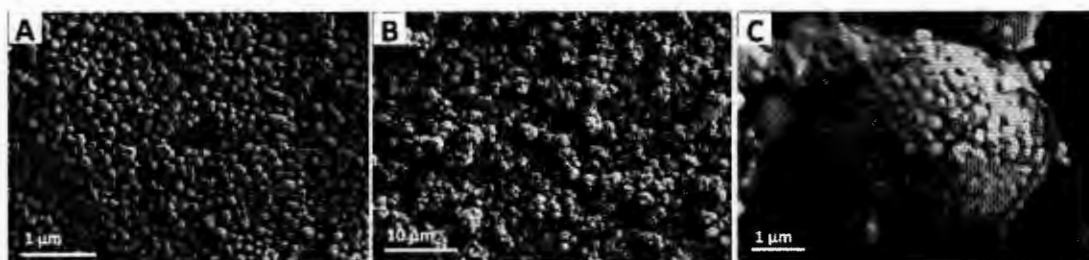


Figure 3.2. Representative SEM micrographs of azithromycin (AZI) nanoparticles (NP) and nanocomposite microparticles (nCmP) including: (A) AZI-NP, (B) AZI-nCmP, (C) Representative zoomed in image of AZI-nCmP.

Table 3.1. Size (as measured by dynamic light scattering), polydispersity index (PDI), zeta potential (ζ), drug loading, and encapsulation efficiency (EE) of nanoparticles (mean \pm standard deviation, $n = 3$).

NP System	Diameter (nm)	PDI	ζ Potential (mV)	Drug Loading (mg drug/100mg NP)	EE (%)
AZI-NP	204.7 \pm 0.4	0.11 \pm 0.01	-4.62 \pm 0.19	3.89 \pm 2.67	13.0 \pm 0.9
RAP-NP	189.1 \pm 1.1	0.16 \pm 0.02	-2.26 \pm 0.14	2.58 \pm 0.04	25.8 \pm 0.4
Blank	211.4 \pm 3.2	0.18 \pm 0.03	-6.13 \pm 0.62	n/a	n/a

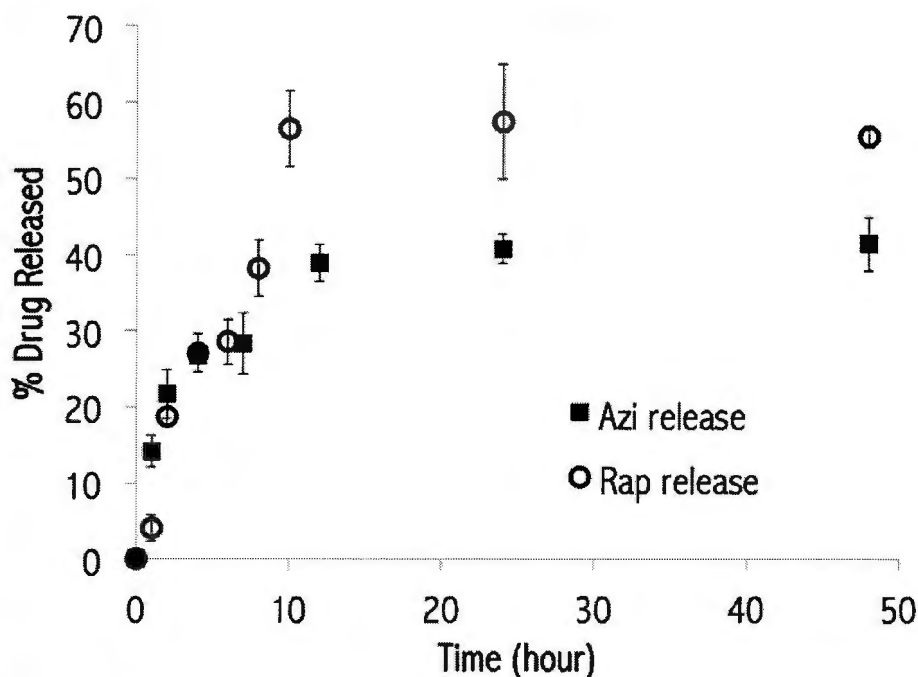


Figure 3.3. *In vitro* drug release profiles for azithromycin (AZI) and rapamycin (RAP) nanoparticle systems.

3.3.5 Karl Fisher (KF) Titration

The residual water contents of AZI-nCmP and RAP-nCmP were approximately 6% (Table 3.2). This is within the range of other nCmP in our group (results not published) and that of previously reported inhalable dry powder formulations prepared by other groups (25, 48-51). Water in inhalable powders can significantly reduce their dispersion properties during aerosolization due to the interparticulate capillary forces acting at the solid–solid interface between particles (52) and also have a negative effect on the stability of the powders (50). Correspondingly, low water content in the powder is highly favorable for efficient dry powder aerosolization and effective particle delivery (52, 53).

3.3.6 Differential Scanning Calorimetry (DSC)

Figure 3.4 shows DSC thermograms of the raw materials used in particle preparation and the final drug-loaded nCmP. Raw Ac-Dex, AZI, RAP, and mannitol displayed endothermic main phase transition peaks (T_m) near 170, 140, 180, and 170 °C respectively, which are in accordance with previously reported values (54-56). The drug-loaded nCmP systems exhibited similar thermal behaviors with a main phase transition peak near 165 °C corresponding to the melting of Ac-Dex and mannitol. This melting point was lower than those of raw Ac-Dex and mannitol, indicating an increase in the amorphous state of these raw materials in nCmP. No glass transition or other phase transitions were present under 120 °C, which indicated that all the materials will be stable during manufacturing and storage.

3.3.7 Powder X-ray Diffraction (PXRD)

X-ray diffraction diffractograms of the raw materials and drug-loaded nCmP are shown in **Figure 3.5**. Strong peaks were present for raw AZI, RAP, and mannitol powders. These strong peaks indicate that the raw materials are in their crystalline forms prior to spray drying, which is in accordance with previous research (54-56). No strong peaks were present for raw Ac-Dex, indicating that it is non-crystalline. This is quite different from commercialized polymers such as PLGA, which exhibits strong XRD characterization peaks (54-57). The absence of diffraction peaks in Ac-Dex is likely because the Ac-Dex is collected by rapid precipitation in water. XRD patterns of AZI-nCmP and RAP-nCmP showed the absence of any diffraction peaks, suggesting amorphization of raw AZI and RAP in the particle matrix. Also, the peaks

characterizing mannitol were significantly reduced, indicating that mannitol is primarily in an amorphous state in the nCmP. The results obtained from the XRD diffractograms confirmed those from DSC thermograms, where raw AZI, RAP, and mannitol were converted into amorphous form in the nCmP manufacturing process.

3.3.8 Drug and Nanoparticles Loading in nCmP

HPLC was used to determine the amount of drug loading in nCmP, which can be used to calculate the resulting nanoparticles loading and nanoparticle encapsulation efficacy in nCmP. These results are shown in **Table 3.2**. Both AZI- and RAP-nCmP exhibited desirable drug loading, high nanoparticle loading, and nanoparticle encapsulation efficacy. In addition, standard deviations of these three values were very low, which indicated reproducible drug loading of the nCmP can be achieved.

3.3.9 Nanoparticle Redispersion from nCmP

The properties of NP redispersed from nCmP were evaluated using DLS (**Table A.1** in Supplementary Material). The size and size distribution of the NP increased after redispersion, which is likely a result of agglomeration that occurred during spray drying. The NP surface charges remained neutral due to the presence of PEG on the surface of the NP. These parameters were all within the desirable ranges for effective mucus penetration.

Table 3.2. Size (as measured by SEM imaging and ImageJ analysis), water content, drug loading, nanoparticle (NP) loading in nanocomposite microparticles (nCmP), and NP loading efficacy in nCmP (mean \pm standard deviation, n = 3).

nCmP System	Diameter (μm)	Water Content (%)	Drug Loading (mg drug/100 mg nCmP)	NP Loading (%)	NP Loading Efficacy (%)
AZI-nCmP	1.03 ± 0.46	5.7 ± 1.25	0.77 ± 0.08	20.47 ± 1.80	40.94 ± 3.60
RAP-nCmP	1.12 ± 0.43	6.1 ± 1.05	0.56 ± 0.02	20.14 ± 0.68	44.28 ± 1.34

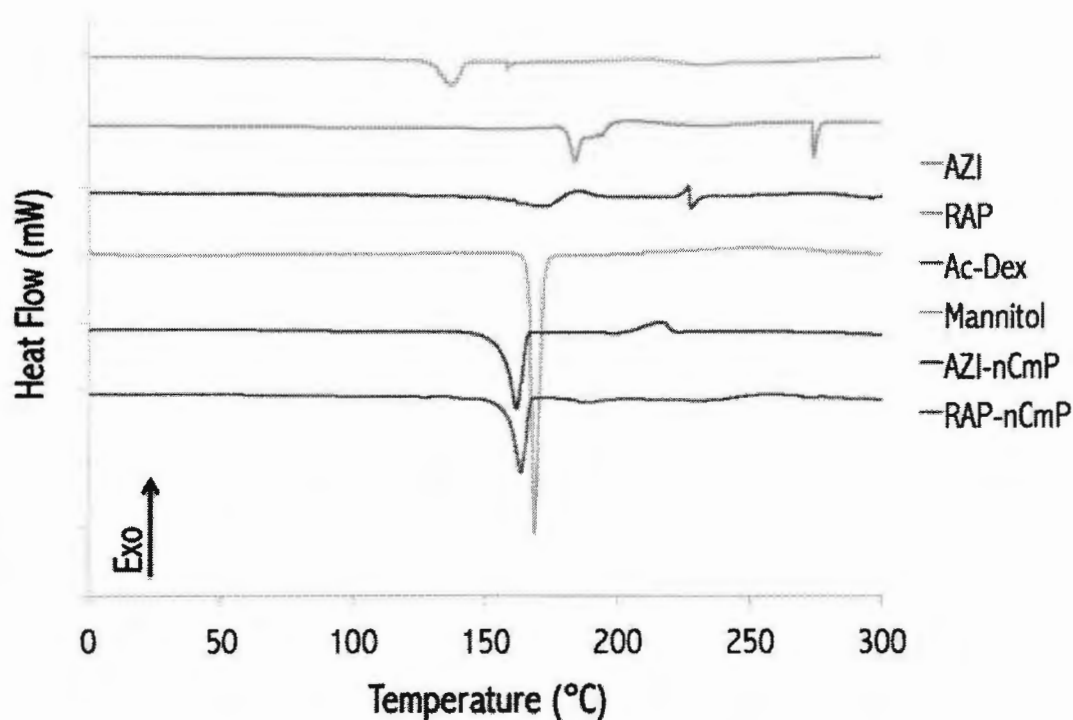


Figure 3.4. Differential scanning calorimetry (DSC) thermograms of raw azithromycin (AZI), raw rapamycin (RAP), raw acetalated dextran (Ac-Dex), raw mannitol, AZI-nCmP, and RAP-nCmP.

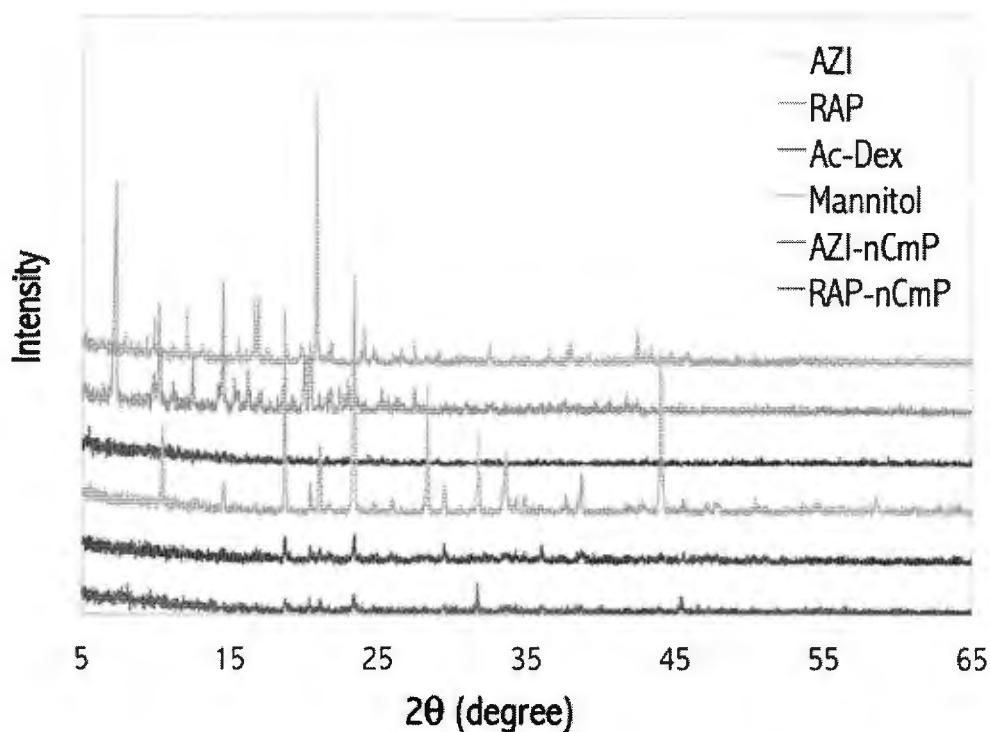


Figure 3.5. Powder X-ray (PXRD) diffractograms of raw azithromycin (AZI), raw rapamycin (RAP), raw acetalated dextran (Ac-Dex), raw mannitol, AZI-nCmP, and RAP-nCmP.

3.3.10 *In vitro* Aerosol Performance of nCmP

In vitro aerosol dispersion performance properties (**Figure 3.6** and **Table 3.3**) of the nCmP were evaluated using a Next Generation Impactor™ coupled with a human DPI device. The results indicated that the formulated nCmP are favorable for efficient dry powder aerosolization and effective targeted delivery. The MMAD values of AZI-nCmP and RAP-nCmP were 3.93 ± 0.09 and 3.86 ± 0.07 μm , while the GSD values were 1.73 ± 0.06 and 1.78 ± 0.06 μm , respectively. The MMAD values were within the range of 1 - 5 μm , which is required for predominant deposition of nCmP

into the deep lung region where infection persists (49). The GSD values were within those previously reported and the RF, FPF, and ED values were all higher (43, 49, 58). Assuming that nCmP drug loading is homogenous, fine particle doses in terms of drug mass of AZI-nCmP and RAP-nCmP are $110.42 \pm 0.22 \mu\text{g}$ and $100.97 \pm 9.19 \mu\text{g}$. There is no research on the therapeutic level of rapamycin for the treatment of CF-related infection. Oral delivery of azithromycin requires 500 mg/week to 1500 mg/ week, but the bioavailability is limited.(13) The nCmP system is expected to achieve therapeutic effect using a low drug amount by improving the delivery efficacy. 8.1% and 9.4% of AZI-nCmP and RAP-nCmP deposited on stages 5 - 7, respectively, and are predicted to deposit in the deep lung alveolar region due to diffusion mechanisms (59) of deposition, while approximate 84% of both the nCmP deposited on stages 2 - 4, and are predicted to deposit predominantly in the deep lung regions by sedimentation due to gravitational settling (60-62). Overall, the nCmP exhibited desirable aerosol dispersion characteristics allowing them to deposit in deep lung regions for drug delivery.

Summary

Both nCmP systems exhibited similar morphology, geometric size, size distribution, water content, drug loading, nanoparticles loading, and nanoparticle encapsulation efficacy as well as outlet temperature and yield due to the fact that they were prepared with nanoparticles with the same spray drying conditions.

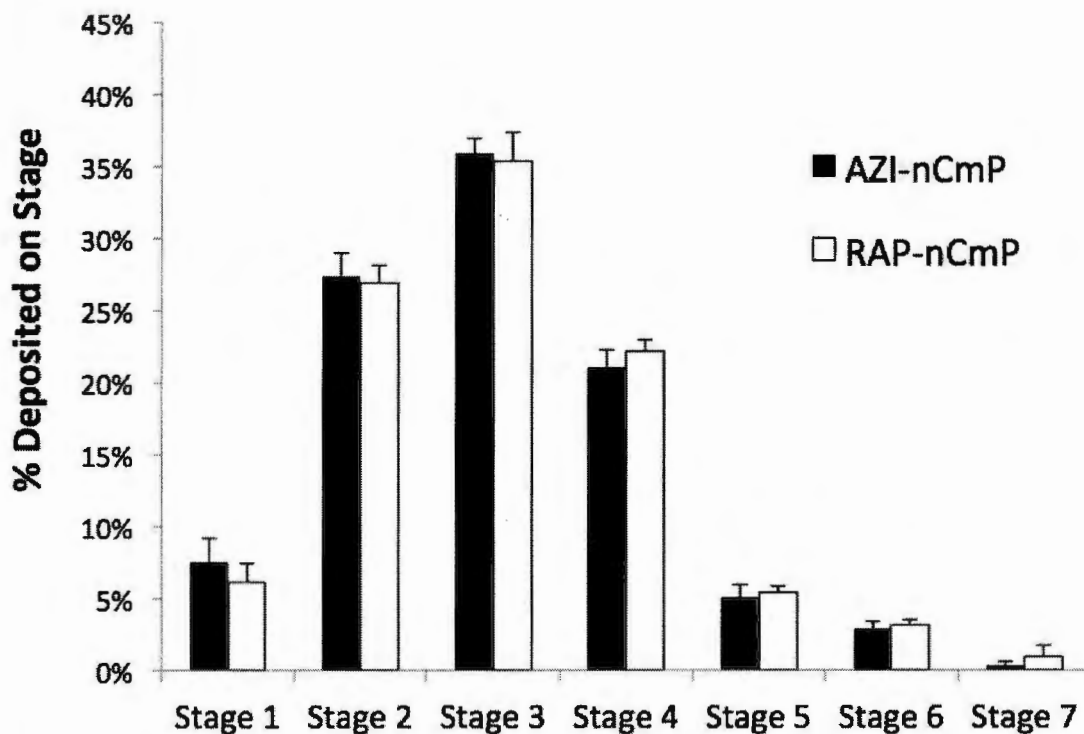


Figure 3.6. Aerosol dispersion performance as % deposited on each stage of the Next Generation Impactor™ (NGI™) for AZI- and RAP-nCmP.

Table 3.3. *In vitro* aerosol dispersion performance properties including mass median aerodynamic diameter (MMAD), geometric standard deviation (GSD), fine particle dose (FPD), fine particle fraction (FPF), respirable fraction (RF), and emitted dose (ED) for nCmP (mean ± standard deviation, n = 3).

nCmP system	MMAD (µm)	GSD (µm)	FPD (mg)	FPF (%)	RF (%)	ED (%)
AZI-nCmP	3.93 ± 0.09	1.73 ± 0.06	19.63 ± 0.59	93.9 ± 1.3	79.7 ± 0.8	98.9 ± 0.4
RAP-nCmP	3.86 ± 0.07	1.78 ± 0.06	20.90 ± 0.62	92.5 ± 1.7	73.6 ± 2.1	99.7 ± 0.3

3.4 Conclusions

Both azithromycin and rapamycin were successfully encapsulated in Ac-Dex nanoparticles and can be released in a sustained rate. The drug-loaded nanoparticles were smooth spheres 200 nm in diameter with narrow size distribution and slightly negative surface charge, which is desirable for mucus penetration. Most nanoparticles maintained these properties during the nCmP manufacturing process as shown in redispersion testing. The nCmP systems were corrugated spheres of 1 μm with observable nanoparticles present on their surfaces. The water content of the nCmP systems was relatively low, which can enable efficient dry powder aerosolization and particle delivery. None of the raw materials underwent degradation during nCmP manufacturing, indicating the stability of the therapeutics during formation. No crystalline structures of AZI and RAP were observed in the nCmP, which confirmed that both drugs in the nCmP were in their amorphous form. *In vitro* aerosol performance testing demonstrated desirable aerosol dispersion characteristics of nCmP, allowing them to deposit in deep lung regions for drug delivery.

This nCmP system sheds a light on dry powder-based antibiotic delivery due to its novel features including targeted pulmonary delivery, rapid mucus penetration potential, and controlled drug release. It can be applied as a promising alternative of the traditional antibiotic treatment by providing effective delivery of therapeutics, more convenient administration, more flexible storage conditions, and lower risk of contamination in the device.

3.5 Acknowledgements

The authors gratefully acknowledge financial support from an Institutional Development Award (IDeA) from the National Institute of General Medical Sciences of the National Institutes of Health under grant number P20GM103430. The content is solely the responsibility of the authors and does not necessarily represent the official views of the National Institutes of Health. The authors thank RI-INBRE for HPLC access and RIN2 for SEM, DLS, PXRD, and DSC access.

3.6 References

1. S.-J. Bowen and J. Hull. The basic science of cystic fibrosis. *Paediatrics and Child Health*. 25:159-164 (2015).
2. N.A. Bradbury. *Cystic Fibrosis*, Academic Press 2016.
3. R.M. Thursfield and J.C. Davies. Cystic Fibrosis: therapies targeting specific gene defects. *Paediatric Respiratory Reviews*. 13:215-219 (2012).
4. A. Chuchalin, E. Amelina, and F. Bianco. Tobramycin for inhalation in cystic fibrosis: Beyond respiratory improvements. *Pulmonary Pharmacology & Therapeutics*. 22:526-532 (2009).
5. C.E. Milla. Nutrition and Lung Disease in Cystic Fibrosis. *Clinics in Chest Medicine*. 28:319-330 (2007).
6. C. Fibrosis Foundation. *Patient Registry 2005 Annual Report*, Bethesda, Maryland, 2005.
7. H. Heijerman, E. Westerman, S. Conway, and D. Touw. Inhaled medication and inhalation devices for lung disease in patients with cystic fibrosis: A European consensus. *Journal of Cystic Fibrosis*. 8:295-315 (2009).
8. R. Sand S. L. Pulmonary infections in patients with cystic fibrosis. *Seminars in Respiratory Infections* 17:47-56 (2002).
9. W.E. Regelman, G.R. Elliott, W.J. Warwick, and C.C. Clawson. Reduction of Sputum *Pseudomonas aeruginosa* Density by Antibiotics Improves Lung Function in Cystic Fibrosis More than Do Bronchodilators and Chest Physiotherapy Alone. *American Review of Respiratory Disease*. 141:914-921 (1990).

10. T. Wagner, G. Soong, S. Sokol, L. Saiman, and A. Prince. Effects of azithromycin on clinical isolates of *Pseudomonas aeruginosa* from cystic fibrosis patients*. *Chest*. 128:912-919 (2005).
11. K.W. Southern and P.M. Barker. Azithromycin for cystic fibrosis. *European Respiratory Journal*. 24:834-838 (2004).
12. L. Saiman, B.C. Marshall, N. Mayer-Hamblett, and et al. Azithromycin in patients with cystic fibrosis chronically infected with *Pseudomonas aeruginosa*: A randomized controlled trial. *JAMA*. 290:1749-1756 (2003).
13. E.B. Wilms, D.J. Touw, H.G.M. Heijerman, and C.K. van der Ent. Azithromycin maintenance therapy in patients with cystic fibrosis: A dose advice based on a review of pharmacokinetics, efficacy, and side effects. *Pediatric Pulmonology*. 47:658-665 (2012).
14. P. SC, D. LH, and R. KA. Clarithromycin and azithromycin: new macrolide antibiotics. *Clinical Pharmacology*. 11:137-152 (1992).
15. M. Zhao, Y. You, Y. Ren, Y. Zhang, and X. Tang. Formulation, characteristics and aerosolization performance of azithromycin DPI prepared by spray-drying. *Powder Technology*. 187:214-221 (2008).
16. B.A. Abdulrahman, A.A. Khweek, A. Akhter, K. Caution, S. Kotrange, D.H.A. Abdelaziz, C. Newland, R. Rosales-Reyes, B. Kopp, K. McCoy, R. Montione, L.S. Schlesinger, M.A. Gavrilin, M.D. Wewers, M.A. Valvano, and A.O. Amer. Autophagy stimulation by rapamycin suppresses lung inflammation and infection by *Burkholderia cenocepacia* in a model of cystic fibrosis. *Autophagy*. 7:1359-1370 (2011).
17. Y.-C. Chen, C.-L. Lo, Y.-F. Lin, and G.-H. Hsiue. Rapamycin encapsulated in dual-responsive micelles for cancer therapy. *Biomaterials*. 34:1115-1127 (2013).
18. K.E. Broaders, J.A. Cohen, T.T. Beaudette, E.M. Bachelder, and J.M.J. Fréchet. Acetalated dextran is a chemically and biologically tunable material for particulate immunotherapy. *Proceedings of the National Academy of Sciences of the United States of America*. 106:5497-5502 (2009).
19. R.O. Cook, R.K. Pannu, and I.W. Kellaway. Novel sustained release microspheres for pulmonary drug delivery. *J Control Release*. 104:79-90 (2005).
20. K.J. Kauffman, N. Kanthamneni, S.A. Meenach, B.C. Pierson, E.M. Bachelder, and K.M. Ainslie. Optimization of rapamycin-loaded acetalated dextran microparticles for immunosuppression. *International Journal of Pharmaceutics*. 422:356-363 (2012).
21. K.E. Broaders, J.A. Cohen, T.T. Beaudette, E.M. Bachelder, and J.M.J. Fréchet. Acetalated dextran is a chemically and biologically tunable material for

particulate immunotherapy. *Proceedings of the National Academy of Sciences*. 106:5497-5502 (2009).

22. E.M. Bachelder, T.T. Beaudette, K.E. Broaders, J. Dashe, and J.M.J. Fréchet. Acetal-Derivatized Dextran: An Acid-Responsive Biodegradable Material for Therapeutic Applications. *Journal of the American Chemical Society*. 130:10494-10495 (2008).

23. J.O.H. Sham, Y. Zhang, W.H. Finlay, W.H. Roa, and R. Löbenberg. Formulation and characterization of spray-dried powders containing nanoparticles for aerosol delivery to the lung. *International Journal of Pharmaceutics*. 269:457-467 (2004).

24. H.X. Ong, D. Traini, G. Ballerin, L. Morgan, L. Buddle, S. Scalia, and P.M. Young. Combined Inhaled Salbutamol and Mannitol Therapy for Mucus Hypersecretion in Pulmonary Diseases. *Aaps J*. 16:269-280 (2014).

25. D.M.K. Jensen, D. Cun, M.J. Maltesen, S. Frokjaer, H.M. Nielsen, and C. Foged. Spray drying of siRNA-containing PLGA nanoparticles intended for inhalation. *J Control Release*. 142:138-145 (2010).

26. E.M. Littringer, A. Mescher, H. Schroettner, L. Achelis, P. Walzel, and N.A. Urbanetz. Spray dried mannitol carrier particles with tailored surface properties – The influence of carrier surface roughness and shape. *European Journal of Pharmaceutics and Biopharmaceutics*. 82:194-204 (2012).

27. W. Kaialy, H. Larhrib, G. Martin, and A. Nokhodchi. The Effect of Engineered Mannitol-Lactose Mixture on Dry Powder Inhaler Performance. *Pharm Res*. 29:2139-2156 (2012).

28. K. Kramek-Romanowska, M. Odziomek, T.R. Sosnowski, and L. Gradoń. Effects of Process Variables on the Properties of Spray-Dried Mannitol and Mannitol/Disodium Cromoglycate Powders Suitable for Drug Delivery by Inhalation. *Industrial & Engineering Chemistry Research*. 50:13922-13931 (2011).

29. E.M. Littringer, R. Paus, A. Mescher, H. Schroettner, P. Walzel, and N.A. Urbanetz. The morphology of spray dried mannitol particles — The vital importance of droplet size. *Powder Technology*. 239:162-174 (2013).

30. T.F. Guimarães, A.D. Lanchote, J.S. da Costa, A.L. Viçosa, and L.A.P. de Freitas. A multivariate approach applied to quality on particle engineering of spray-dried mannitol. *Advanced Powder Technology*. 26:1094-1101 (2015).

31. G.F. Cooney, B.L. Lum, M. Tomaselli, and S.B. Fiel. Absolute Bioavailability and Absorption Characteristics of Aerosolized Tobramycin in Adults with Cystic Fibrosis. *The Journal of Clinical Pharmacology*. 34:255-259 (1994).

32. M. Hoppentocht, P. Hagedoorn, H.W. Frijlink, and A.H. de Boer. Developments and strategies for inhaled antibiotic drugs in tuberculosis therapy: A critical evaluation. *European Journal of Pharmaceutics and Biopharmaceutics*. 86:23-30 (2014).
33. S. Stanojevic, V. Waters, J.L. Mathew, L. Taylor, and F. Ratjen. Effectiveness of inhaled tobramycin in eradicating *Pseudomonas aeruginosa* in children with cystic fibrosis. *Journal of Cystic Fibrosis*. 13:172-178 (2014).
34. D.E. Geller, W.H. Pitlick, P.A. Nardella, W.G. Tracewell, and B.W. Ramsey. Pharmacokinetics and bioavailability of aerosolized tobramycin in cystic fibrosis. *Chest*. 122:219-226 (2002).
35. M.B. Dolovich and R. Dhand. Aerosol drug delivery: developments in device design and clinical use. *The Lancet*. 377:1032-1045.
36. B.M. Ibrahim, M.D. Tsifansky, Y. Yang, and Y. Yeo. Challenges and advances in the development of inhalable drug formulations for cystic fibrosis lung disease. *Expert Opinion on Drug Delivery*. 8:451-466 (2011).
37. A. Kuzmov and T. Minko. Nanotechnology approaches for inhalation treatment of lung diseases. *J Control Release*.
38. D. T, M. N, and W. P. Nebuliser systems for drug delivery in cystic fibrosis. *Cochrane Database of Systematic Reviews*(2013).
39. B.C. Tang, M. Dawson, S.K. Lai, Y.-Y. Wang, J.S. Suk, M. Yang, P. Zeitlin, M.P. Boyle, J. Fu, and J. Hanes. Biodegradable polymer nanoparticles that rapidly penetrate the human mucus barrier. *Proceedings of the National Academy of Sciences*. 106:19268-19273 (2009).
40. S. Stegemann, S. Kopp, G. Borchard, V.P. Shah, S. Senel, R. Dubey, N. Urbanetz, M. Cittero, A. Schoubben, C. Hippchen, D. Cade, A. Fuglsang, J. Morais, L. Borgström, F. Farshi, K.H. Seyfang, R. Hermann, A. van de Putte, I. Klebovich, and A. Hincal. Developing and advancing dry powder inhalation towards enhanced therapeutics. *European Journal of Pharmaceutical Sciences*. 48:181-194 (2013).
41. A.B. Watts and R.O. Williams. Nanoparticles for Pulmonary Delivery. In D.C.H. Smyth and J.A. Hickey (eds.), *Controlled Pulmonary Drug Delivery*, Springer New York, New York, NY, 2011, pp. 335-366.
42. E.-M. Collnot, C. Baldes, M.F. Wempe, J. Hyatt, L. Navarro, K.J. Edgar, U.F. Schaefer, and C.-M. Lehr. Influence of vitamin E TPGS poly(ethylene glycol) chain length on apical efflux transporters in Caco-2 cell monolayers. *J Control Release*. 111:35-40 (2006).
43. S.A. Meenach, K.W. Anderson, J. Zach Hilt, R.C. McGarry, and H.M. Mansour. Characterization and aerosol dispersion performance of advanced spray-

dried chemotherapeutic PEGylated phospholipid particles for dry powder inhalation delivery in lung cancer. *European Journal of Pharmaceutical Sciences*. 49:699-711 (2013).

44. F. W. The ARLA Respiratory Deposition Calculator 2008.

45. O. Mert, S.K. Lai, L. Ensign, M. Yang, Y.-Y. Wang, J. Wood, and J. Hanes. A poly(ethylene glycol)-based surfactant for formulation of drug-loaded mucus penetrating particles. *J Control Release*. 157:455-460 (2012).

46. A. Bootz, V. Vogel, D. Schubert, and J. Kreuter. Comparison of scanning electron microscopy, dynamic light scattering and analytical ultracentrifugation for the sizing of poly(butyl cyanoacrylate) nanoparticles. *European Journal of Pharmaceutics and Biopharmaceutics*. 57:369-375 (2004).

47. S.A. Meenach, Y.J. Kim, K.J. Kauffman, N. Kanthamneni, E.M. Bachelder, and K.M. Ainslie. Synthesis, Optimization, and Characterization of Camptothecin-Loaded Acetalated Dextran Porous Microparticles for Pulmonary Delivery. *Molecular Pharmaceutics*. 9:290-298 (2012).

48. X. Wu, D. Hayes, J.B. Zwischenberger, R.J. Kuhn, and H.M. Mansour. Design and physicochemical characterization of advanced spray-dried tacrolimus multifunctional particles for inhalation. *Drug Design, Development and Therapy*. 7:59-72 (2013).

49. S.A. Meenach, F.G. Vogt, K.W. Anderson, J.Z. Hilt, R.C. McGarry, and H.M. Mansour. Design, physicochemical characterization, and optimization of organic solution advanced spray-dried inhalable dipalmitoylphosphatidylcholine (DPPC) and dipalmitoylphosphatidylethanolamine poly(ethylene glycol) (DPPE-PEG) microparticles and nanoparticles for targeted respiratory nanomedicine delivery as dry powder inhalation aerosols. *International Journal of Nanomedicine*. 8:275-293 (2013).

50. X. Wu, W. Zhang, D. Hayes, and H.M. Mansour. Physicochemical characterization and aerosol dispersion performance of organic solution advanced spray-dried cyclosporine A multifunctional particles for dry powder inhalation aerosol delivery. *International Journal of Nanomedicine*. 8:1269-1283 (2013).

51. X. Li and H.M. Mansour. Physicochemical Characterization and Water Vapor Sorption of Organic Solution Advanced Spray-Dried Inhalable Trehalose Microparticles and Nanoparticles for Targeted Dry Powder Pulmonary Inhalation Delivery. *AAPS PharmSciTech*. 12:1420-1430 (2011).

52. A.J. Hickey, H.M. Mansour, M.J. Telko, Z. Xu, H.D.C. Smyth, T. Mulder, R. McLean, J. Langridge, and D. Papadopoulos. Physical characterization of component particles included in dry powder inhalers. I. Strategy review and static characteristics. *Journal of Pharmaceutical Sciences*. 96:1282-1301 (2007).

53. C. Nora Y.K. , Hak-Kim Chan. The Role of Particle Properties in Pharmaceutical Powder Inhalation Formulations. *Journal of Aerosol Medicine*. 15:325-330 (2002).
54. G. Mohammadi, H. Valizadeh, M. Barzegar-Jalali, F. Lotfipour, K. Adibkia, M. Milani, M. Azhdarzadeh, F. Kiafar, and A. Nokhodchi. Development of azithromycin-PLGA nanoparticles: Physicochemical characterization and antibacterial effect against *Salmonella typhi*. *Colloids and Surfaces B: Biointerfaces*. 80:34-39 (2010).
55. W. Kaialyand A. Nokhodchi. Dry powder inhalers: Physicochemical and aerosolization properties of several size-fractions of a promising alterative carrier, freeze-dried mannitol. *European Journal of Pharmaceutical Sciences*. 68:56-67 (2015).
56. Z. Zhang, L. Xu, H. Chen, and X. Li. Rapamycin-loaded poly(ϵ -caprolactone)-poly(ethylene glycol)-poly(ϵ -caprolactone) nanoparticles: preparation, characterization and potential application in corneal transplantation. *Journal of Pharmacy and Pharmacology*. 66:557-563 (2014).
57. X. Li, S. Chang, G. Du, Y. Li, J. Gong, M. Yang, and Z. Wei. Encapsulation of azithromycin into polymeric microspheres by reduced pressure-solvent evaporation method. *International Journal of Pharmaceutics*. 433:79-88 (2012).
58. F. Ungaro, G. De Rosa, A. Miro, F. Quaglia, and M.I. La Rotonda. Cyclodextrins in the production of large porous particles: Development of dry powders for the sustained release of insulin to the lungs. *European Journal of Pharmaceutical Sciences*. 28:423-432 (2006).
59. S. Sand H. AJ. Drug properties affecting aerosol behavior. *Respiratory Care*. 45:652-666 (2000).
60. H. AJand M. HM. Delivery of drugs by the pulmonary route, Taylor and Francis, New York, 2009.
61. A.J. Hickeyand H.M. Mansour. Formulation challenges of powders for the delivery of small molecular weight molecules as aerosols, Informa Healthcare, New York, 2008.
62. D.A. Edwards. The macrotransport of aerosol particles in the lung: Aerosol deposition phenomena. *Journal of Aerosol Science*. 26:293-317 (1995).

CHAPTER 4

Nanocomposite Microparticles (nCmP) for the Delivery of Tacrolimus in the Treatment of Pulmonary Arterial Hypertension

Published in the International Journal of Pharmaceutics in 2016

Zimeng Wang¹, Julie L. Cuddigan¹, Sweta K. Gupta¹, Samantha A. Meenach^{1,2}

¹University of Rhode Island, College of Engineering, Department of Chemical Engineering, Kingston, RI 02881, USA

²University of Rhode Island, College of Pharmacy, Department of Biomedical and Pharmaceutical Sciences, Kingston, RI 02881, USA

ABSTRACT

Tacrolimus (TAC) has exhibited promising therapeutic potential in the treatment of pulmonary arterial hypertension (PAH); however, its application is prevented by its poor solubility, instability, poor bioavailability, and negative systemic side effects. To overcome the obstacles of using TAC for the treatment of PAH, we developed nanocomposite microparticles (nCmP) for the pulmonary delivery of tacrolimus in the form of dry powder aerosols. These particles can provide targeted pulmonary delivery, improved solubility of tacrolimus, the potential of permeation through mucus barrier, and controlled drug release. In this system, tacrolimus-loaded polymeric nanoparticles (NP) were prepared via emulsion solvent evaporation and nCmP were prepared by spray drying these NP with mannitol.

The NP were approximately 200 nm in diameter with narrow size distribution both before loading into and after redispersion from nCmP. The NP exhibited smooth, spherical morphology and the nCmP were raisin-like spheres. High encapsulation efficacy was achieved both in the encapsulation of tacrolimus in NP and that of NP in nCmP. nCmP exhibited desirable aerosol dispersion properties, allowing them to deposit into the deep lung regions for effective drug delivery. A549 cells were used as *in vitro* models to demonstrate the non-cytotoxic behavior of TAC nCmP. Overall, the designed nCmP have the potential to aid in the delivery of tacrolimus for improved treatment of PAH.

KEYWORDS:

Nanocomposite microparticles, pulmonary delivery, pulmonary arterial hypertension, spray drying, tacrolimus

4.1. Introduction

Pulmonary arterial hypertension (PAH) is a progressive cardiovascular disease that leads to limited exercise capacity, right ventricular heart failure, and ultimately death (1). It is hemo-dynamically defined as an increased mean pulmonary arterial pressure higher than 25 mmHg with a pulmonary capillary wedge pressure lower than 15 mmHg at rest (2, 3). Patients often develop PAH because of genetic and/or environmental insult, resulting in endothelial cell apoptosis, loss of distal vessels, and occlusive vascular remodeling, which causes elevated pulmonary arterial pressures.

The primary treatment options currently available for patients with PAH are based on drugs with vasodilatory properties that improve cardiopulmonary function. Unfortunately, these drugs show no effect on prohibiting the progress of obliterative vascular pathology. Because of this, the only option for many patients to improve their health and quality of life is heart-lung transplantation. Therefore, new approaches to utilize compounds that focus on activating cellular mechanisms to reverse vascular remodeling are under investigation (4). Improving the function of the bone morphogenetic protein receptor-2 (BMPR2) signaling pathway is a potential direction in the development of improved PAH therapies, as the mutations of BMPR2 have been identified as the main cause of inherited PAH, accounting for 60 to 80% of

familial cases. BMPR2 mutations are also the main cause of 10 to 25% in sporadic PAH and 9% of PAH associated with fenfluramine use (4-8).

Since challenges exist in the clinical application of BMPR2 gene therapy, tacrolimus can be applied instead, as it increases signaling through the BMPR2 pathway. Tacrolimus (TAC) is an FDA-approved immunosuppressive drug with a known pharmacokinetic and toxicity profile. Previous research on the use of TAC to treat PAH has shown that: 1) low-dose TAC can reverse dysfunctional BMPR2 signaling in pulmonary artery endothelial cells (ECs) from patients with idiopathic PAH, 2) low-dose TAC can prevent exaggerated chronic hypoxic PAH in mice with conditional BMPR2 deletion in ECs, and 3) low-dose TAC can reverse severe PAH in rats with medial hypertrophy following monocrotaline exposure and in rats with neointima formation following vascular endothelial growth factor receptor blockade and chronic hypoxia (4).

Although TAC shows promising potential in the treatment of PAH, its application is hindered by its poor solubility (water solubility of 1.3 $\mu\text{g/mL}$), instability, and limited bioavailability (9-11). In addition to these limiting pharmacokinetic properties, systemic side effects such as neurotoxicity and nephrotoxicity also complicate the clinical use of TAC (12). To overcome this problem, biodegradable polymeric acetalated dextran (Ac-Dex) nanoparticles (NP) can be applied to more safely and effectively deliver TAC. Ac-Dex NP can improve hydrophobic agent solubility, promote drug penetration into cell membranes to obtain higher plasma concentration, provide sustained drug release, and provide reduced systemic side effects.

Ac-Dex is an acid-sensitive, biodegradable, and biocompatible polymer that can be prepared in a one-step reaction by reversibly modifying dextran with acetal groups (13). This modification reverses the solubility properties of dextran from hydrophilic to hydrophobic, making it possible to form polymeric particles using standard emulsion or nanoprecipitation techniques. In contrast to poly(lactic-co-glycolic acid) (PLGA) and other polyesters, which are widely applied as excipients in drug delivery applications, Ac-Dex shows additional advantages. Most notably, the degradation rate of Ac-Dex can be tuned from minutes to months to suit various applications. Tunable degradation rates result from the adjustment of the ratio of cyclic acetal groups with a slower degradation rate to acyclic acetal groups with a faster degradation rate, which can be easily completed by controlling the reaction time during the formation of Ac-Dex. Furthermore, Ac-Dex particulates show no burst release at physiological conditions (pH 7.4), which is necessary to maintain a steady drug level in the body. Finally, Ac-Dex degrades into biocompatible, biodegradable, FDA-approved by-products of dextran and very low levels of methanol and acetone (13-16).

Pulmonary aerosols have attracted increasing attention for the treatment of lung diseases, as they are capable of delivering a wide range of therapeutics directly and efficiently to the lungs. Pulmonary delivery systems offer several advantages including increased local drug concentration in the lungs, reduced systemic side effects, rapid onset of action due to the enormous surface area and plentiful capillary vessels in the lung, and avoidance of the first-pass metabolism associated with the liver (17-22). While dry powder aerosolized nanoparticles (less than 500 nm) will be

exhaled owing to their small size and mass, aerosolized particles with aerodynamic diameters of 1-5 μm can effectively deposit into the lungs. However, this larger microparticle size range is also the size at which particles are commonly phagocytosed by alveolar macrophages, which limits their efficacy as aerosol drug delivery vehicles (23). To overcome these aforementioned obstacles for pulmonary TAC delivery, we developed nanocomposite microparticles (nCmP) in the form of dry powder aerosols (**Figure 4.1**). This system is comprised of TAC-loaded Ac-Dex NP entrapped in microparticle carriers comprised using the excipient mannitol to allow for the delivery of TAC NP to the lungs.

Mannitol was used as the excipient of nCmP due to its beneficial properties in aerosol formulations. First, mannitol is highly water-soluble, which ensures rapid decomposition of nCmP in the aqueous environment of mucus and pulmonary surfactant in the lungs, leading to a burst release of NP from the nCmP system. Furthermore, mannitol is able to enhance mucus penetration of nanoparticles by increasing fluidity of mucus in the lung (24). Finally, mannitol has been extensively studied as a carrier in spray-dried powder aerosols for pulmonary drug administration and the resulting particles have been shown to exhibit desirable water content, size, and surface morphology for successful aerosol delivery (25-30).

In the present nCmP system, the drug-loaded nanoparticles contain TAC as a therapeutic and these NP are coated by polyvinyl alcohol (PVA). Upon pulmonary administration, the nCmP will deposit on the mucus in the respiratory tract, decompose into free NP and mannitol, and allow the nanoparticles to penetrate the mucus barrier and then release drug to the targeted site. The goal of the described

research was the initial development and physicochemical characterization of the nCmP systems with ability of targeted delivery, improved drug solubility, and potential of efficient penetration of mucus barrier and of controlled release via particle engineering.

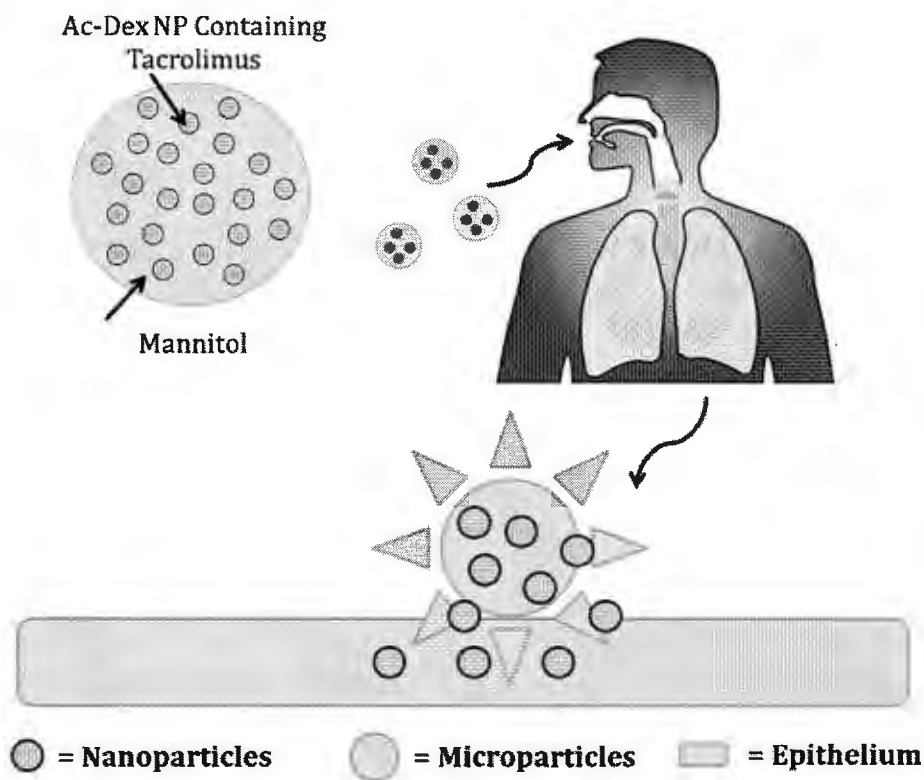


Figure 4.1. Schematic of an aerosol nanoparticle microparticle (nCmP) system interacting with the pulmonary mucosa. Once the nCmP impact the surface of the mucus coating the pulmonary epithelium they immediately degrade to release nanoparticles.

4.2 Materials and Methods

4.2.1 Materials

Dextran from *Leuconostoc mesenteroides* (9000-11000 MW), pyridinium p-toluenesulfonate (PPTS, 98%), D-mannitol ($\geq 98\%$), 2-methoxypropene (2-MOP, 97%), triethylamine (TEA, $\geq 99\%$), anhydrous dimethyl sulfoxide (DMSO, $\geq 99.9\%$), poly(vinyl alcohol) (PVA, MW 13,000-23,000, 87-89% hydrolyzed), dichloromethane (DCM, anhydrous, $\geq 99.8\%$), deuterium chloride (DCl, 35 weight % in D₂O, 99 atom % D), Tween® 80, potassium phosphate dibasic, potassium phosphate monobasic, and acetonitrile (HPLC grade, $\geq 99.9\%$) were obtained from Sigma-Aldrich (St. Louis, MO). Deuterium oxide (D₂O, 99.8% atom D) was obtained from Acros Organics (Geel, Belgium). Phosphate buffered saline (PBS) and phosphoric acid (extra pure, 85% solution in water) were obtained from Fisher Scientific (Somerville, NJ). Hydranal® KF reagent was obtained from Fluka Analytical. Tacrolimus (FK-506) was purchased from LC Laboratories (Woburn, MA). A549 cells were obtained from American Type Culture Collection (Manassas, VA, USA). Dulbecco's Modified Eagle Medium (DMEM), pen-strep, and fungizone® were obtained from Life Technologies (Norwalk, CT, USA). Sodium pyruvate was obtained from Fisher Scientific. Dimethyl sulfoxide (DMSO) was obtained from Wilkem Scientific (Pawtucket, RI, USA). Fetal bovine serum (FBS) was obtained from Atlanta Biologics (Flowery Branch, GA, USA) and Resazurin was obtained from Acros Organics.

4.2.2 Synthesis and NMR Analysis of Acetalated Dextran (Ac-Dex)

Ac-Dex was synthesized as described previously (14) with minor modifications. Briefly, 1 g of lyophilized dextran and 25 mg of PPTS were dissolved in 10 mL anhydrous DMSO. The resulting solution was reacted with 5 mL of 2-MOP under nitrogen gas for 5 minutes and was quenched with 1 mL of TEA. The reaction mixture was then precipitated in basic water (water and TEA, pH 9), vacuum filtered, and lyophilized ($-50\text{ }^{\circ}\text{C}$, 0.023 mbar) for 24 hours to yield a solid product.

The cyclic-to-acyclic (CAC) ratio of acetal coverage and degrees of total acetal coverage per 100 glucose molecules was confirmed by ^1H NMR spectroscopy (Bruker 300 MHz NMR, MA). 10 mg of Ac-Dex was added to 700 μL of D_2O and was hydrolyzed with 30 μL of DCl prior to analysis. The hydrolysis of one cyclic acetal group produces one acetone whereas one acyclic acetal produces one acetone and one methanol. Consequently, from the normalized integrations of peaks related to acetone, methanol, and the carbon ring of dextran, the CAC ratio of acetal coverage and degrees of total acetal coverage per 100 glucoses was determined.

4.2.3 Formation of TAC-Loaded Ac-Dex Nanoparticles (TAC NP)

Tacrolimus-loaded nanoparticles (TAC NP) were prepared via oil/water emulsion and solvent evaporation. 90 mg of Ac-Dex and 10 mg of TAC were dissolved in 1 mL of DCM over an ice bath, establishing the organic phase. 3% PVA in PBS, the aqueous phase, was added to the organic phase and the resulting solution was sonicated (Q500 Sonicator, Qsonica, Newtown, CT) for 30 seconds with a 1 second on/off pulse at 70% amplitude. The emulsion was transferred to a spinning

solution of 0.3% PVA in PBS and stirred for 4 hours for evaporation of the organic solvent and particle hardening. The solution was then centrifuged at 12000 rpm for 20 minutes to collect the nanoparticles. Nanoparticles were washed once with basic water, redispersed in 0.1% PVA, and lyophilized ($-50\text{ }^{\circ}\text{C}$, 0.023 mbar) for 48 hours.

4.2.4 Formulation of Nanocomposite Microparticles (nCmP) Via Spray Drying

nCmP were prepared via the spray drying of TAC NP suspensions and mannitol in an aqueous solution using a Büchi B-290 spray dryer (Büchi Labortechnik, AG, Switzerland) in open mode. The spray drying conditions were as follows: 1:1 (weight) ratio of TAC NP to mannitol in DI water, feed solution concentration of 1% (w/v), 0.7 mm nozzle diameter, atomization gas flow rate of 414 L/h using UHP dry nitrogen, aspiration rate of $28\text{ m}^3/\text{h}$, inlet temperature of $50\text{ }^{\circ}\text{C}$, pump rate of 0.6 mL/min, and nozzle cleaner rate of 4. The resulting nCmP were separated in a high-performance cyclone, collected in a sample collector, and stored in amber glass vials in desiccators at $-20\text{ }^{\circ}\text{C}$.

4.2.5 Particle Morphology and Shape Analysis via Scanning Electron Microscopy (SEM)

The shape and surface morphology of the NP and nCmP were evaluated by SEM using a Zeiss SIGMA VP Field Emission-Scanning Electron Microscope (FE-SEM) (Germany). nCmP samples were placed on aluminum SEM stubs with double-sided adhesive carbon tabs. Nanoparticles were dispersed in basic water (pH = 9, 10 mg/mL) and this suspension was dropped onto aluminum SEM stubs and then dried at

room temperature. Both the NP and nCmP samples were coated with a thin film of a gold/palladium alloy using a BIO-RAD sputter coating system at 20 μ A for 60 seconds under argon gas. Images were captured at 5 kV at various magnifications.

4.2.6 Particle Size, Size Distribution, and Zeta Potential Analysis

The size, size distribution, and zeta potential of the NP systems were measured by dynamic light scattering (DLS) using a Malvern Nano Zetasizer (Malvern Instruments, Worcestershire, UK). The NP were dispersed in basic water (pH = 9, 0.3 mg/mL). All experiments were performed in triplicate with a scattering angle of 173° at 25 °C. The mean size (geometric diameter) of the nCmP was measured digitally from SEM images using ImageJ software (Systat, San Jose, CA, USA). Representative micrographs (5000x magnification) for each sample were analyzed by measuring the diameter of at least 100 particles.

4.2.7 Analysis of Nanoparticle Drug Loading and Nanoparticle Loading in nCmP

Drug loading and encapsulation efficacy of TAC NP and nCmP were determined via Ultra-Performance Liquid Chromatography (UPLC) (LaChrom, Hitachi, Japan). Detection of TAC was performed using following conditions: C₁₈, 5 μ m \times 150 mm \times 4.6 mm column (Ascentis, Sigma-Aldrich, St. Louis, MO), 1 mL/min pump rate, 6 minute retention time, mobile phase of 70% acetonitrile and 30% phosphoric acid aqueous solution (0.1%), absorbance of 215 nm, and temperature of 50 °C. Drug-loaded NP and nCmP were fully dissolved in the mobile phase prior to analysis. The drug concentration in each sample was quantified by comparison with a

standard curve of TAC in its mobile phase. The TAC loading of NP, TAC loading of nCmP, NP loading in nCmP, drug encapsulation efficiency (EE) of NP, and NP encapsulation efficacy in nCmP were determined by the following equations:

$$\text{Drug loading} = \frac{\text{mass of drug loaded in NP}}{\text{mass of NP}} \times 100\%$$

$$\text{Drug encapsulation efficacy (EE)} = \frac{\text{mass of drug loaded in NP}}{\text{initial mass of drug in NP formulation}} \times 100\%$$

$$\text{Nanoparticles loading} = \frac{\text{mass of NP loaded in nCmP}}{\text{mass of nCmP}} \times 100\%$$

$$\text{NP loading efficacy} = \frac{\text{mass of NP loaded in nCmP}}{\text{initial mass of NP in nCmP formulation}} \times 100\%$$

4.2.8 *In Vitro* Drug Release from Nanoparticles

The *in vitro* release profiles of TAC from nanoparticles were determined via the release of NP (1 mg/mL) in modified phosphate buffer (PB, 0.1 M, pH = 7.4) with 0.5% (w/v) of Tween® 80. The NP suspension was incubated at 37 °C and 100 rpm. At various time points (0 to 24 h), NP samples were centrifuged at 12000 rpm for 5 minutes at 4 °C to isolate the NP. 200 µL of supernatant was withdrawn and replaced by the same amount of fresh modified PB in each sample. The withdrawn solutions were analyzed for drug content via UPLC using the same methods described previously.

4.2.9 Karl Fischer Coulometric Titration

The water content of the nCmP was quantified by Karl Fischer (KF) titration using a 737 KF coulometer (Metrohm, Riverview, FL). 10 mg of powder was dissolved in anhydrous methanol. The resulting solution was injected into the KF reaction cell filled with Hydranal® KF reagent and then the amount of water was analyzed.

4.2.10 Differential Scanning Calorimetry (DSC)

The thermal phase transitions of the nCmP, NP, and their raw components were determined via DSC using a TA Q10 DSC system (TA Instruments, New Castle, DE, USA) equipped with an automated computer-controlled TA instruments DSC refrigerated cooling system. 1 - 3 mg of sample was weighed into Tzero™ alodined aluminum pans that were hermetically sealed. The sealed pans were placed into the DSC furnace along with an empty sealed reference pan. The heating range used was 0 – 300 °C at a heating rate of 10 °C/min.

4.2.11 Powder X-Ray Diffraction (PXRD)

Crystalline states of the nCmP and its raw components were examined by PXRD using a Rigaku Multiflex X-ray diffractometer (The Woodlands, TX) with a Cu K α radiation source (40 kV, 44 mA). The samples were placed on a horizontal quartz glass sample holder (3 mm). The scan range was 5 – 80° in 2 Θ with a step width of 0.02 and scan rate of 2 °/min.

4.2.12 *In Vitro* Aerosol Dispersion Performance with the Next Generation

Impactor (NGI)

In vitro aerosol dispersion performance of the nCmP was evaluated using a Next Generation Impactor™ (NGI™, MSP Corporation, Shoreview, MN) equipped with a stainless steel induction port (USP throat adaptor) attachment and stainless steel gravimetric insert cups. The NGI™ was coupled with a Copley TPK 2000 critical flow controller, which was connected to a Copley HCP5 vacuum pump (Copley Scientific, United Kingdom). The airflow rate (Q) was measured and adjusted to 60 L/min in order to model the flow rate in a healthy adult lung before each experiment. Glass fiber filters (55 mm, Type A/E, Pall Life Sciences, PA) were placed in the gravimetric insert cups for stages 1 through 7 to minimize bounce or re-entrapment (31) and these filters were weighed before and after the experiment to determine the particle mass deposited on each stage. Approximately 10 mg of powder was loaded into a hydroxypropyl methylcellulose (HPMC, size 3, Quali-V®, Qualicaps® Inc., Whitsett, NC, USA) capsule and the capsule was placed into a human dry powder inhaler device (HandiHaler, Boehringer Ingelheim Pharmaceuticals, CT) attached to a customized rubber mouthpiece connected to the NGI™. Three HPMC capsules were loaded and released in each measurement and experiments were performed in triplicate. The NGI™ was run with a delay time of 10 s and running time of 10 s. For Q = 60 L/min, the effective cutoff diameters for each stage of the impactor were given from the manufacturer as: stage 1 (8.06 µm); stage 2 (4.46 µm); stage 3 (2.82 µm); stage 4 (1.66 µm); stage 5 (0.94 µm); stage 6 (0.55 µm); and stage 7 (0.34 µm). The

fine particle dose (FPD), fine particle fraction (FPF), respirable fraction (RF), and emitted dose (ED) were calculated as follows:

Fine particles dose (FPD) = mass of particles on Stages 2 through 7

$$\text{Fine particles fraction (FPF)} = \frac{\text{fine particles dose}}{\text{initial particle mass loaded into capsules}} \times 100\%$$

$$\text{Respirable fraction (RF)} = \frac{\text{mass of particles on Stages 2 through 7}}{\text{total particle mass on all stages}} \times 100\%$$

$$\text{Emitted dose (ED)} = \frac{\text{initial mass in capsules} - \text{final mass remaining in capsules}}{\text{initial mass in capsules}} \times 100\%$$

The experimental mass median aerodynamic diameter (MMAD_E) and geometric standard deviation (GSD) for the particles were determined using a Mathematica® program written by Dr. Warren Finlay (31, 32).

4.2.13 Tapped Density and Theoretical Aerodynamic Diameter Analysis

The density of the nCmP was evaluated via tapped density measurements as described previously with minor modifications (33). 30 - 35 mg nCmP was weighed in a glass tube. The tube was tapped 200 times to ensure efficient packing of the nCmP and then the volume occupied by the particles was measured. The density was determined by the following equation:

$$\rho = \frac{m}{V}$$

where ρ is the density of the nCmP, m is the nCmP mass, and V is the nCmP volume determined by measuring the height of the particles in a tube with a known diameter (5 mm). The theoretical MMAD ($MMAD_T$) of the nCmP was calculated using the following equation:

$$MMAD_T = d \sqrt{\frac{\rho}{\rho^*}}$$

where d is the geometric diameter of the nCmP determined by ImageJ, ρ is the density of the TAC nCmP, and $\rho^* = 1 \text{ g/cm}^3$ (polymer reference density).

4.2.14 *In vitro* cytotoxicity of TAC nCmP using resazurin assay

The *in vitro* cytotoxicity of TAC nCmP as well as free TAC were evaluated using the resazurin assay. Human adenocarcinomic alveolar basal epithelial cell line (A549, passage 6) was used as *in vitro* model to evaluate the effect of various TAC nCmP concentrations at different time intervals on their viability. A549 cells were maintained in DMEM supplemented with 10% (v/v) fetal bovine serum, 100 U/ml penicillin, 100 $\mu\text{g/ml}$ streptomycin, fungizone® (0.5 μg amphotericin, B, 0.41 $\mu\text{g/mL}$ sodium deoxycholate) and 1 mM sodium pyruvate at 37°C in CO₂ incubator. The cells were trypsinized and plated at density 5×10^4 cells/ml (100 $\mu\text{l/well}$) in flat-bottomed 96-well plate and incubated overnight at 37°C in CO₂ incubator. On the following day, the A549 cells were exposed to various sets of concentration of free TAC and TAC nCmP (0.00001 to 10 μM) in hexaplets for 48 h and 72 h. After respective time period of 48 h and 72 h exposure, 20 μl of resazurin solution (60 μM) was added to each well

and the plate was incubated for another 3 h, allowing the viable cells to convert resazurin to resorufin, and the fluorescence intensity of the resorufin produced by viable cells was detected at 520 nm (excitation) and 590 nm (emission) using Cytation 3 plate reader (BioTek, Winooski, VT, USA). The wells containing complete medium and resazurin, without cells, were taken as blank and the wells containing cells and resazurin, without particles, served as control. The relative viability of each sample was calculated by:

$$\text{Relative Viability (\%)} = \frac{\text{(Sample Fluorescence Intensity)}}{\text{(Control Fluorescence Intensity)}} \times 100\%$$

4.2.15 Statistical Analysis

All measurements were performed in at least triplicate. Values are given in the form of means \pm SD. The statistical significance of the results was determined using t-tests where a p-value of <0.05 was considered statistically significant.

4.3. Results and Discussion

4.3.1 Characterization of Ac-Dex

Successful synthesis of Ac-Dex was confirmed by NMR. Ac-Dex exhibited 71.5% cyclic acetal coverage and 79.2% total conversion of -OH groups. An increase in CAC is known to decrease the drug release rate due to slower degradation of Ac-Dex (13, 14). A high total acetal coverage (higher than 75% according to our research)

is required to stabilize the PVA coating of nanoparticles, which ensures small particles size and narrow size distribution

4.3.2 Characterization of Nanoparticles

4.3.2.1 NP Size, Distribution, and Surface Charge

The tacrolimus-loaded nanoparticles (TAC NP) shown in **Figure 4.2A**, appear as uniform spheres with smooth surface morphology. NP size, size distribution (PDI), and zeta potential are shown in **Table 4.1**. The resulting sizes of the NP analyzed via DLS (approximately 200 nm) were larger than those observed from SEM micrographs and ImageJ analysis (approximately 100 nm) due to shrinking of the particles during freeze-drying or sputter coating and agglomeration of particles during resuspension into aqueous solutions (34, 35). The TAC NP system exhibited desirable size (less than 200 nm) with narrow size distribution to potentially allow for mucus penetration and pulmonary epithelial targeting. The surface charge of the NP system was slightly negative, which is suitable to reduce interactions with negatively charged mucin fibers, enhancing the particle permeation through the mucus barrier (35).

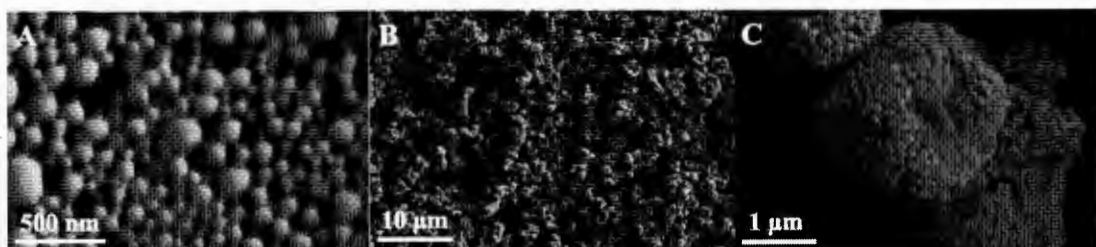


Figure 4.2. Representative SEM micrographs of tacrolimus (TAC) nanoparticles (NP) and nanocomposite microparticles (nCmP) including: (A) TAC NP, (B) TAC nCmP, (C) representative zoomed in image of TAC nCmP.

Table 4.1. Diameter (as measured by dynamic light scattering), polydispersity index (PDI), zeta potential (ζ), TAC loading, and encapsulation efficiency (EE) of tacrolimus-loaded nanoparticles before spray drying (TAC NP) and after spray drying and redispersion from nanocomposite microparticles (Redispersed TAC NP) (mean \pm standard deviation, n = 3).

System	Diameter (nm)	PDI	ζ Potential (mV)	TAC Loading (mg drug/100mg NP)	EE (%)
TAC NP	199.7 \pm 3.2	0.07 \pm 0.00	-6.33 \pm 1.27	7.04 \pm 0.45	69.25 \pm 4.38
Redispersed TAC NP	227.5 \pm 6.3	0.16 \pm 0.03	-9.42 \pm 3.83	N/A	N/A

4.3.2.2 TAC Loading and in Vitro Release

TAC was successfully encapsulated into the described TAC NP system. 69.25% of the initially loaded TAC was effectively encapsulated within the NP prepared using emulsion solvent evaporation of Ac-Dex and drug in PVA solution. The high encapsulation efficacy of the drug is due to the low solubility of TAC in the aqueous spinning solution.

Results of the *in vitro* release of TAC NP at physiological pH and temperature are reported in **Figure 4.3** as the percentage of drug released over time. The TAC NP system displayed a sustained release of 40% of its payload after 12 hours, in which 30% of TAC was released in the first 6 hours and 10% was released in the next 6 hours. Previous research showed that Ac-Dex NP made of 10kDa dextran and reacted for 5

minutes exhibited a maximum of degradation at 6 hours and negligible degradation after that (15). Based on these results, the TAC release profiles in this study can likely be explained as follows: the first release stage (up to 6 hours) corresponds to Ac-Dex degradation as well as nanoparticle dissociation, whereas after 6 hours the rate of TAC release is controlled by drugs passively diffusing out of the dissociated matrix of nanoparticles following the partial degradation of Ac-Dex. This two-stage release profile of Ac-Dex based particles matches that of other drug-loaded Ac-Dex nanoparticle systems in our group and other previous studies (33).

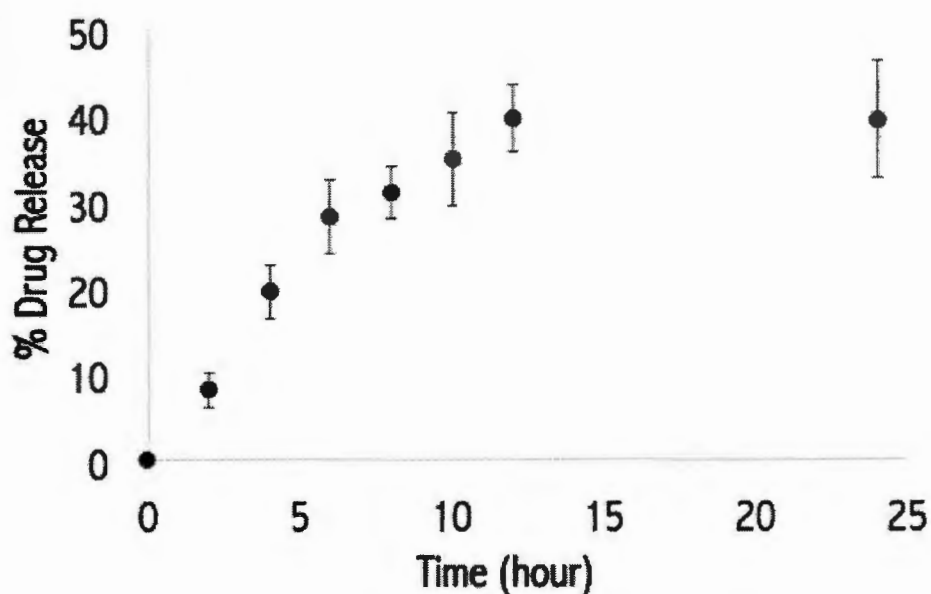


Figure 4.3. *In vitro* drug release profile for tacrolimus (TAC) nanoparticle system.

4.3.3 Nanocomposite Microparticle Characterization

4.3.3.1 nCmP Morphology, Size, and Size Distribution

TAC nCmP displayed a wrinkled and raisin-like surface with visibly encapsulated NP as seen in **Figures 4.2B and 4.2C**. The corrugated surface of the nCmP reduces their contact area, which prevents the particles from aggregating upon aerosolization, thus improving aerosol performance and the dispersion of the NP from the dry powder nCmP formulation. The cause of the raisin-like morphology of the nCmP may be attributed to the early formation of nanoparticle shells in droplets during spray drying. The formation of nanoparticle shells during spray drying determines the geometric size of nCmP. As the drying proceeds, the remaining water keeps evaporating from the droplet center, resulting in hollow particles that tend to shrink (36, 37). The number average geometric diameter of the TAC nCmP system was $2.13 \pm 0.52 \mu\text{m}$, as determined by ImageJ analysis.

4.3.3.2 Karl Fischer Titration

The residual water content of TAC nCmP was approximately 8% (**Table 4.2**), which is acceptable in this dry powder formulation. Water in inhalable dry powders can significantly reduce their dispersion properties during aerosolization due to the interparticulate capillary forces acting at the solid–solid interface between particles (38) and the presence of water is also responsible for the instability of the powders during storage (39). Correspondingly, low water content in inhalable dry powders is highly favorable for efficient dry powder aerosolization and effective particle delivery (38, 40).

Table 4.2. Geometric diameter (as measured by SEM imaging and ImageJ analysis), water content, TAC loading, nanoparticle (NP) loading in nanocomposite microparticles (nCmP), and NP loading efficacy in nCmP (mean \pm standard deviation, n = 3).

System	Geometric Diameter (μm)	Water Content (weight %)	Drug Loading (mg drug/100 mg nCmP)	NP Loading (%)	NP Loading Efficacy (%)
TAC nCmP	2.13 \pm 0.52	7.99 \pm 0.31	3.19 \pm 0.31	45.29 \pm 4.42	90.59 \pm 8.85

4.3.3.3 Differential Scanning Calorimetry

Figure 4.4 shows DSC thermograms of the raw materials used in particle preparation and the final drug-loaded nCmP. Raw Ac-Dex, TAC, and mannitol displayed endothermic main phase transition peaks (T_m) near 170, 135, and 167 °C, respectively, which are in accordance with previously reported values (41, 42). The TAC nCmP system exhibited a main phase transition peak (T_m) near 142 °C, corresponding to the melting of mannitol. This melting point was lower than those of raw mannitol, indicating an increase in the amorphous state of these raw materials in nCmP. No glass transitions or other phase transitions were evident under 120 °C, which indicated that all the materials are stable during manufacturing and storage conditions.

4.3.3.4 Powder X-ray Diffraction (PXRD)

X-ray diffraction diffractograms of the raw materials and TAC nCmP are shown in **Figure 4.5**. Strong peaks were present for raw TAC and mannitol powders. These strong peaks indicate that the raw materials are in their crystalline forms prior to spray drying, which is in accordance with previous studies (41, 42). No strong peaks were present for raw Ac-Dex, indicating that it is non-crystalline. The non-crystallinity of Ac-Dex is quite different from commercialized polymers such as PLGA, which exhibits strong XRD characterization peaks (43-45). The absence of diffraction peaks in Ac-Dex is likely because the Ac-Dex was collected by rapid precipitation in water. XRD patterns of TAC nCmP displayed the absence of any diffraction peaks of raw TAC, suggesting amorphization of raw TAC in the particle matrix, which is suitable for the improvement of tacrolimus solubility in physiological conditions. Also, the peaks characterizing mannitol were significantly reduced, indicating that mannitol is reduced to its amorphous state in the nCmP. The results obtained from the XRD diffractograms confirmed those from DSC thermograms, where raw TAC and mannitol were converted into amorphous forms in the nCmP manufacturing process.

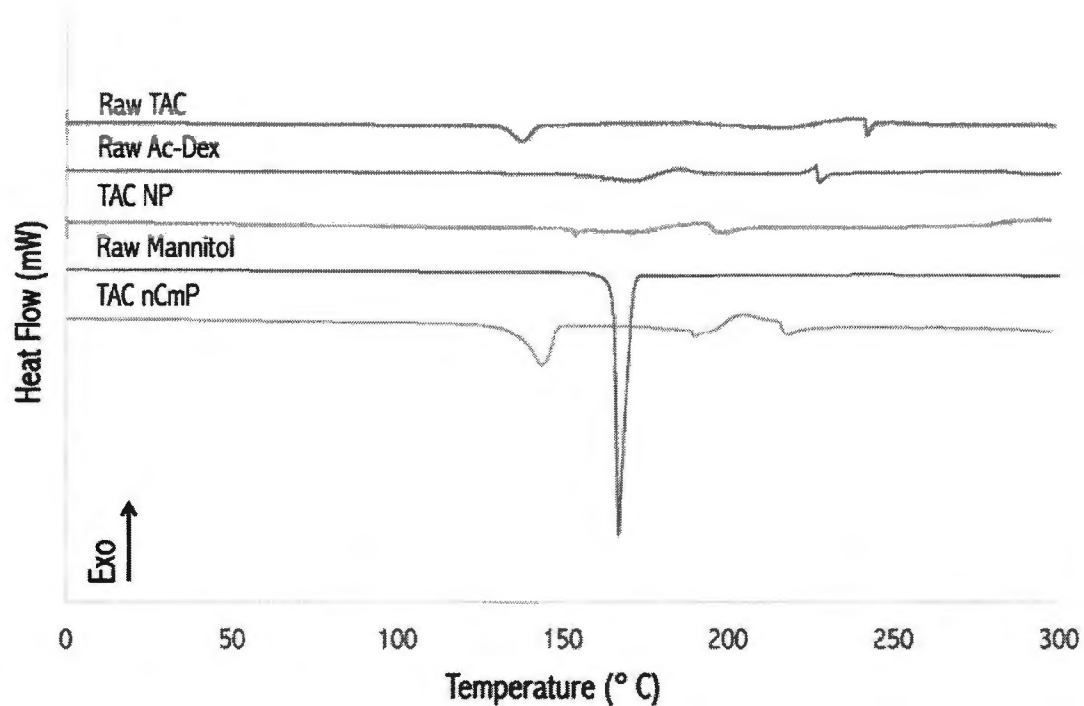


Figure 4.4. Representative differential scanning calorimetry (DSC) thermograms of raw tacrolimus (TAC), raw acetalated dextran (Ac-Dex), raw mannitol, TAC nanoparticles (TAC NP), and formulated TAC nanocomposite microparticles (TAC nCmP).

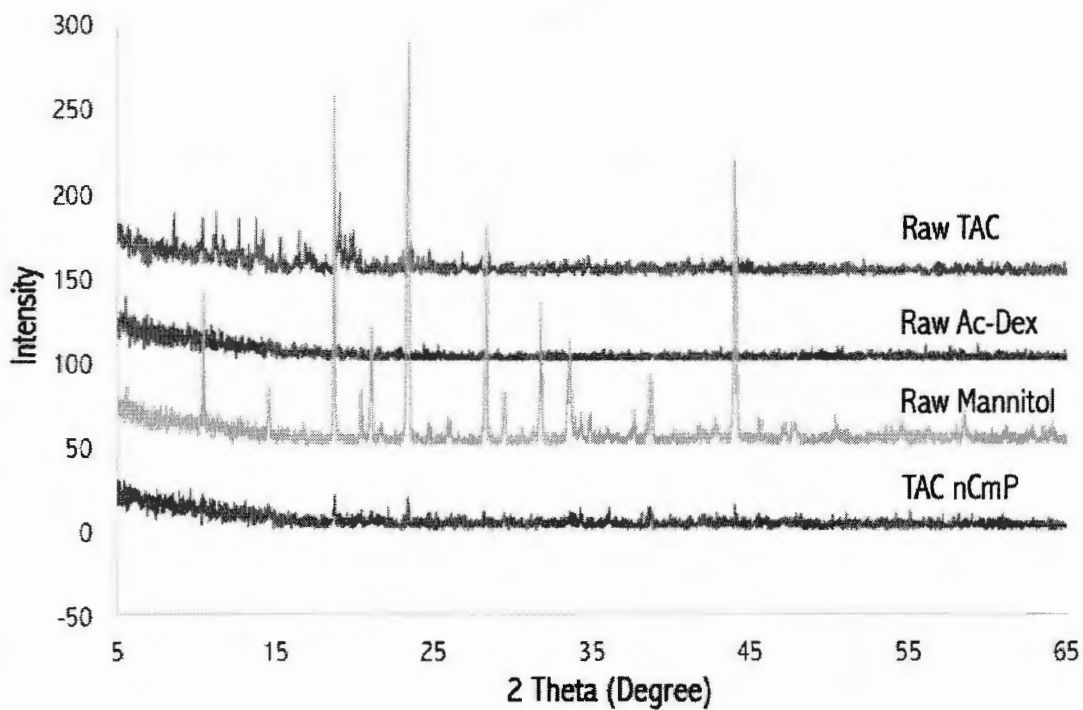


Figure 4.5. Representative powder X-ray (PXRD) diffractograms of raw tacrolimus (TAC), raw acetalated dextran (Ac-Dex), raw mannitol, and formulated TAC nanocomposite microparticles (TAC nCmP).

4.3.3.5 Drug and Nanoparticles Loading in nCmP

UPLC was used to determine the amount of TAC loading in the nCmP and this data was used to calculate the resulting NP loading and NP encapsulation efficacy in the nCmP formulation as seen in **Tables 4.1 and 4.2**. The TAC NP exhibited desirable drug loading (more than 69% encapsulation efficiency), which is a result of the poor water solubility of tacrolimus. The TAC nCmP showed high NP loading (> 45%), and very high NP encapsulation efficacy (> 90%). The high drug loading in the nCmP formulation is favorable to reduce the amount of particles administered to achieve target therapeutic effect.

4.3.3.6 Nanoparticle Redispersion from nCmP

The properties of NP redispersed from nCmP dissolved in water were evaluated using DLS (**Table 4.1**). The size and PDI of the redispersed NP exhibited slight increases after redispersion from nCmP, which is likely a result of agglomeration that occurred during the spray drying process. The NP surface charge remained slightly negative. These parameters were all within the desirable ranges for effective penetration of NP through the mucus barrier, demonstrating the favorable properties of nanoparticles remain intact after spray drying.

4.3.3.7 In Vitro Aerosol Dispersion Performance Using Next Generation Impactor (NGI)

In vitro aerosol dispersion performance properties of the nCmP were evaluated using a Next Generation Impactor™ coupled with a human DPI device (**Figure 4.6**

and Table 4.3). The results indicated that the formulated nCmP aerosol properties are favorable for efficient dry powder aerosolization and effective targeted pulmonary delivery. The experimental mass mean aerodynamic diameter ($MMAD_E$) value of TAC-nCmP was $3.57 \pm 0.17 \mu\text{m}$, while the geometric standard deviation (GSD) value was $1.78 \pm 0.02 \mu\text{m}$. The $MMAD_E$ value is within the range of 1 - 5 μm that is required for predominant deposition of nCmP into the deep lung regions (46), which would be desirable for the delivery of TAC to the periphery of the lungs. The GSD values were within the range of those previously reported and the respirable fraction (RF), fine particle fraction (FPF), and emitted dose (ED) values were all higher than reports from similar systems (31, 46, 47). In clinical research, PAH patients are treated with TAC with a target blood level of 1.5 - 5 ng/mL (48-50). The present nCmP system is expected to achieve a therapeutic effect using a low amount of TAC through its improved delivery efficacy over current systemic methods. 9.8% of TAC nCmP deposited on stages 5 - 7 and it is predicted that these particles will deposit in the deep lung alveolar region due to diffusion mechanisms of deposition (51). Subsequently, 71.2% of nCmP deposited on stages 2 - 4 and are thus predicted to deposit predominantly in the lungs by sedimentation due to gravitational settling (18, 52, 53). Overall, the nCmP exhibited desirable aerosol dispersion characteristics allowing them to deposit in deep lung regions for effective drug delivery of TAC.

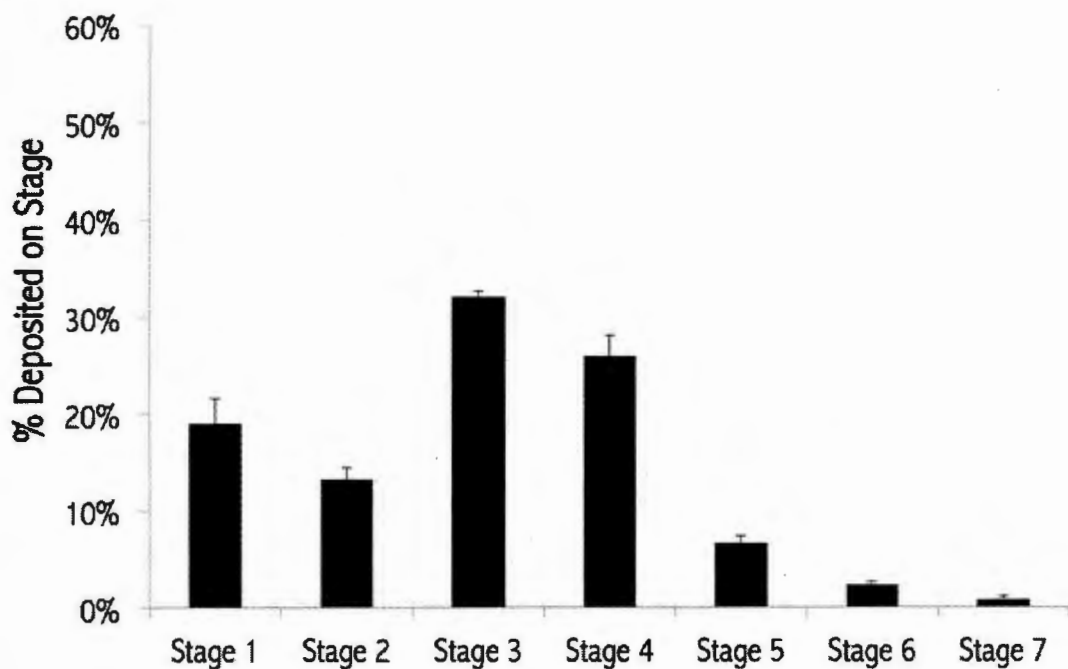


Figure 4.6. Aerosol dispersion performance of tacrolimus nanocomposite microparticles (TAC nCmP) as % particles deposited on each stage of the Next Generation Impactor™ (NGI™). For $Q = 60$ L/min, the effective cutoff diameters (D_{50}) for each impaction stage are as follows: stage 1 ($8.06 \mu\text{m}$), stage 2 ($4.46 \mu\text{m}$), stage 3 ($2.82 \mu\text{m}$), stage 4 ($1.66 \mu\text{m}$), stage 5 ($0.94 \mu\text{m}$), stage 6 ($0.55 \mu\text{m}$), and stage 7 ($0.34 \mu\text{m}$) (mean \pm standard deviation, $n = 3$).

Table 4.3. *In vitro* aerosol dispersion performance properties including theoretical mass median aerodynamic diameter (MMAD_T) from tapped density measurements, experimental mass median aerodynamic diameter (MMAD_E), geometric standard deviation (GSD), fine particle dose (FPD), fine particle fraction (FPF), respirable fraction (RF), and emitted dose (ED) for nCmP (mean ± standard deviation, n = 3).

System	MMAD _T (μm)	MMAD _E (μm)	GSD (μm)	FPF (%)	RF (%)	ED (%)
TAC	0.79 ±	3.57 ±	1.78 ±	81.0 ±	67.6 ±	96.3 ±
nCmP	0.79	0.17	0.02	2.6	3.0	1.37

4.3.3.8 Analysis of nCmP Density and Theoretical Aerodynamic Diameter

The density of the particles was determined via tapped density measurements. The TAC nCmP exhibited a relative low density value of $0.138 \pm 0.001 \text{ g/cm}^3$ compared with the raw materials (1.5 g/cm^3), which can be attributed to the raisin-like surface morphology and hollow structure of the nCmP. The theoretical MMAD calculated with the geometric diameter and tapped density was $0.79 \pm 0.19 \mu\text{m}$, which was lower than the experimental result. The lower MMAD_T in comparison to MMAD_E can be attributed to nCmP agglomeration during aerosolization, which increased the geometric size (and thus aerodynamic diameter) of the dry powder formulation.

4.3.3.9 *In vitro* cytotoxicity of TAC nCmP microparticles using resazurin assay

To evaluate the response of particles on cell viability, *in vitro* cytotoxicity of TAC nCmP as well as free TAC against A549 cells were conducted. TAC nCmP and free

TAC were exposed to A549 cells at different concentrations for 48 h and 72 h, and the cell viability was analyzed using resazurin assay (**Figure 4.7**). For free TAC, the relative viability of the A549 cells remains constant for increasing drug concentrations at 48 h and 72 h, demonstrating that TAC is non-toxic to lung cells up to 10 μ M concentration (**Figure 4.7 (a)**). TAC nCmP does not exhibit significant cytotoxic effect at various TAC concentrations (0.00001 – 10 μ M) until 72 h, and there is no significant decrease in the viability of A549 cells at 48 h and 72 h (**Figure 4.7 (b)**). However, for TAC nCmP, a slight increase in cell viability was observed at 72 h as compared to 48 h. This might be due to the presence of mannitol in TAC nCmP. Previous study suggests that an increase in glucose (mannitol) concentration can lead to increase in the cell proliferation by upregulating heme oxygenase-1 via reactive oxygen species or the TGF- β 1/PI3K/Akt signaling pathway. Thus, TAC nCmP was not cytotoxic and could be used for the treatment of PAH, hence minimizing the potential negative side effects.

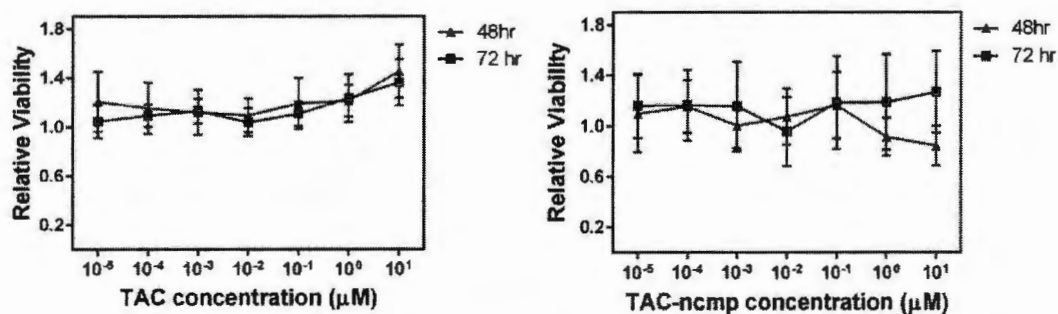


Figure 4.7. A549 cell viability measured by resazurin assay after 48 h and 72 h exposure to (a) free TAC, and (b) TAC nanocomposite microparticles (nCmP) (mean \pm standard deviation, n = 3).

4.4 Conclusions

Tacrolimus was successfully encapsulated in Ac-Dex nanoparticles with a high encapsulation efficacy. The drug-loaded nanoparticles were 200 nm smooth spheres with narrow size distribution and slightly negative surface charge, which is desirable to overcome the mucus barrier in the lung. These favorable properties were maintained during the nCmP manufacturing process as shown in redispersion testing. The nCmP systems were 2 μm , raisin-like spheres with observable nanoparticles present on their surface. The water content of the nCmP systems was relatively low, which can enable efficient dry powder aerosolization and particle delivery. None of the raw materials underwent degradation during nCmP manufacturing, indicating the stability of the therapeutics during formation. No crystalline structures of TAC was observed in the nCmP, which confirmed that the drug in the nCmP were in their amorphous form. *In vitro* aerosol performance testing demonstrated desirable aerosol dispersion characteristics of nCmP, allowing them to deposit in deep lung regions for drug delivery. There was no significant effect in the viability of A549 cells, which confirmed the non-cytotoxic behavior of TAC nCmP.

This nCmP system exhibits promising application in pulmonary TAC delivery for the treatment of PAH due to its novel features including targeted pulmonary delivery, improved solubility of tacrolimus, potential of permeation through mucus barrier, and of controlled drug release. In contrast to other delivery methods, this dry powder formulation also provides more convenient administration, more flexible storage conditions, and lower risk of contamination in the device.

4.5 Acknowledgements

The authors gratefully acknowledge financial support from an Institutional Development Award (IDeA) from the National Institute of General Medical Sciences of the National Institutes of Health under grant number P20GM103430. The content is solely the responsibility of the authors and does not necessarily represent the official views of the National Institutes of Health. This material is based upon work conducted at a Rhode Island NSF EPSCoR research facility, supported in part by the National Science Foundation EPSCoR Cooperative Agreement #EPS-1004057. Finally, the authors thank RI-INBRE for UPLC access and RIN2 for SEM, DLS, PXRD, and DSC access.

4.6 References

1. B. Badiani and A. Messori. Targeted Treatments for Pulmonary Arterial Hypertension: Interpreting Outcomes by Network Meta-analysis. *Heart, lung & circulation*. 25:46-52 (2016).
2. K.M. Chin and L.J. Rubin. Pulmonary Arterial Hypertension. *Journal of the American College of Cardiology*. 51:1527-1538 (2008).
3. D. Montani, M.-C. Chaumais, C. Guignabert, S. Günther, B. Girerd, X. Jaïs, V. Algalarrondo, L.C. Price, L. Savale, O. Sitbon, G. Simonneau, and M. Humbert. Targeted therapies in pulmonary arterial hypertension. *Pharmacology & Therapeutics*. 141:172-191 (2014).
4. E. Spiekerkoetter, X. Tian, J. Cai, R.K. Hopper, D. Sudheendra, C.G. Li, N. El-Bizri, H. Sawada, R. Haghghat, R. Chan, L. Haghghat, V. de Jesus Perez, L. Wang, S. Reddy, M. Zhao, D. Bernstein, D.E. Solow-Cordero, P.A. Beachy, T.J. Wandless, P. ten Dijke, and M. Rabinovitch. FK506 activates BMPR2, rescues endothelial dysfunction, and reverses pulmonary hypertension. *The Journal of Clinical Investigation*. 123:3600-3613 (2013).
5. J.D.W. Evans, B. Girerd, D. Montani, X.-J. Wang, N. Galiè, E.D. Austin, G. Elliott, K. Asano, E. Grünig, Y. Yan, Z.-C. Jing, A. Manes, M. Palazzini, L.A. Wheeler, I. Nakayama, T. Satoh, C. Eichstaedt, K. Hinderhofer, M. Wolf, E.B. Rosenzweig, W.K. Chung, F. Soubrier, G. Simonneau, O. Sitbon, S. Gräf, S. Kaptoge,

E. Di Angelantonio, M. Humbert, and N.W. Morrell. BMPR2 mutations and survival in pulmonary arterial hypertension: an individual participant data meta-analysis. *The Lancet Respiratory Medicine*.

6. F. Soubrier, W.K. Chung, R. Machado, E. Grünig, M. Aldred, M. Geraci, J.E. Loyd, C.G. Elliott, R.C. Trembath, J.H. Newman, and M. Humbert. Genetics and Genomics of Pulmonary Arterial Hypertension. *Journal of the American College of Cardiology*. 62:D13-D21 (2013).

7. L.J. Rubin and N. Galiè. Pulmonary arterial hypertension: a look to the future. *Journal of the American College of Cardiology*. 43:S89-S90 (2004).

8. J. West, E. Austin, J.P. Fessel, J. Loyd, and R. Hamid. Rescuing the BMPR2 signaling axis in pulmonary arterial hypertension. *Drug Discovery Today*. 19:1241-1245 (2014).

9. M. Vicari-Christensen, S. Repper, S. Basile, and D. Young. Tacrolimus: review of pharmacokinetics, pharmacodynamics, and pharmacogenetics to facilitate practitioners' understanding and offer strategies for educating patients and promoting adherence. *Prog Transplant*. 19:277-284 (2009).

10. W. Xu, P. Ling, and T. Zhang. Toward immunosuppressive effects on liver transplantation in rat model: Tacrolimus loaded poly(ethylene glycol)-poly(D,L-lactide) nanoparticle with longer survival time. *International Journal of Pharmaceutics*. 460:173-180 (2014).

11. H. Arima, K. Yunomae, K. Miyake, T. Irie, F. Hirayama, and K. Uekama. Comparative studies of the enhancing effects of cyclodextrins on the solubility and oral bioavailability of tacrolimus in rats. *J Pharm Sci*. 90:690-701 (2001).

12. F. Kur, H. Reichenspurner, B.M. Meiser, A. Welz, H. Furst, C. Muller, C. Vogelmeier, M. Schwaiblmaier, J. Briegel, and B. Reichart. Tacrolimus (FK506) as primary immunosuppressant after lung transplantation. *The Thoracic and Cardiovascular Surgeon*. 47:174-178 (1999).

13. K.E. Broaders, J.A. Cohen, T.T. Beaudette, E.M. Bachelder, and J.M.J. Fréchet. Acetalated dextran is a chemically and biologically tunable material for particulate immunotherapy. *Proceedings of the National Academy of Sciences*. 106:5497-5502 (2009).

14. E.M. Bachelder, T.T. Beaudette, K.E. Broaders, J. Dashe, and J.M.J. Fréchet. Acetal-Derivatized Dextran: An Acid-Responsive Biodegradable Material for Therapeutic Applications. *Journal of the American Chemical Society*. 130:10494-10495 (2008).

15. K.J. Kauffman, N. Kanthamneni, S.A. Meenach, B.C. Pierson, E.M. Bachelder, and K.M. Ainslie. Optimization of rapamycin-loaded acetalated dextran

microparticles for immunosuppression. *International Journal of Pharmaceutics*. 422:356-363 (2012).

16. J.F. Coelho, P.C. Ferreira, P. Alves, R. Cordeiro, A.C. Fonseca, J.R. Góis, and M.H. Gil. Drug delivery systems: Advanced technologies potentially applicable in personalized treatments. *The EPMA Journal*. 1:164-209 (2010).

17. C.W.M. Park, Heidi M.; Hayes, Don Pulmonary inhalation aerosols for targeted antibiotics drug delivery. *European Pharmaceutical Review*. 1:(2011).

18. A.J. Hickey, Mansour, Heidi M. Delivery of Drugs by the Pulmonary Route. In J.S. A. T. Florence (ed.), *Modern Pharmaceutics: Applications and Advances*, Vol. 2, Informa Healthcare, New York, NY, 2009, pp. 191-219.

19. D. Hayes, Jr., J.B. Zwischenberger, and H.M. Mansour. Aerosolized tacrolimus: a case report in a lung transplant recipient. *Transplantation proceedings*. 42:3876-3879 (2010).

20. J.S. Patton and P.R. Byron. Inhaling medicines: delivering drugs to the body through the lungs. *Nat Rev Drug Discov*. 6:67-74 (2007).

21. X.-F. Yang, Y. Xu, D.-S. Qu, and H.-Y. Li. The influence of amino acids on aztreonam spray-dried powders for inhalation. *Asian Journal of Pharmaceutical Sciences*. 10:541-548 (2015).

22. L. Wu, X. Miao, Z. Shan, Y. Huang, L. Li, X. Pan, Q. Yao, G. Li, and C. Wu. Studies on the spray dried lactose as carrier for dry powder inhalation. *Asian Journal of Pharmaceutical Sciences*. 9:336-341 (2014).

23. S. Stegemann, S. Kopp, G. Borchard, V.P. Shah, S. Senel, R. Dubey, N. Urbanetz, M. Cittero, A. Schoubben, C. Hippchen, D. Cade, A. Fuglsang, J. Morais, L. Borgstrom, F. Farshi, K.H. Seyfang, R. Hermann, A. van de Putte, I. Klebovich, and A. Hincal. Developing and advancing dry powder inhalation towards enhanced therapeutics. *European journal of pharmaceutical sciences : official journal of the European Federation for Pharmaceutical Sciences*. 48:181-194 (2013).

24. H.X. Ong, D. Traini, G. Ballerin, L. Morgan, L. Buddle, S. Scalia, and P.M. Young. Combined Inhaled Salbutamol and Mannitol Therapy for Mucus Hypersecretion in Pulmonary Diseases. *Aaps J*. 16:269-280 (2014).

25. W. Kaiyaly, H. Larhrib, G. Martin, and A. Nokhodchi. The Effect of Engineered Mannitol-Lactose Mixture on Dry Powder Inhaler Performance. *Pharm Res*. 29:2139-2156 (2012).

26. K. Kramek-Romanowska, M. Odziomek, T.R. Sosnowski, and L. Gradoń. Effects of Process Variables on the Properties of Spray-Dried Mannitol and Mannitol/Disodium Cromoglycate Powders Suitable for Drug Delivery by Inhalation. *Industrial & Engineering Chemistry Research*. 50:13922-13931 (2011).

27. E.M. Littringer, R. Paus, A. Mescher, H. Schroettner, P. Walzel, and N.A. Urbanetz. The morphology of spray dried mannitol particles — The vital importance of droplet size. *Powder Technology*. 239:162-174 (2013).
28. T.F. Guimarães, A.D. Lanchote, J.S. da Costa, A.L. Viçosa, and L.A.P. de Freitas. A multivariate approach applied to quality on particle engineering of spray-dried mannitol. *Advanced Powder Technology*. 26:1094-1101 (2015).
29. E.M. Littringer, A. Mescher, H. Schroettner, L. Achelis, P. Walzel, and N.A. Urbanetz. Spray dried mannitol carrier particles with tailored surface properties – The influence of carrier surface roughness and shape. *European Journal of Pharmaceutics and Biopharmaceutics*. 82:194-204 (2012).
30. D.M.K. Jensen, D. Cun, M.J. Maltesen, S. Frokjaer, H.M. Nielsen, and C. Foged. Spray drying of siRNA-containing PLGA nanoparticles intended for inhalation. *J Control Release*. 142:138-145 (2010).
31. S.A. Meenach, K.W. Anderson, J. Zach Hilt, R.C. McGarry, and H.M. Mansour. Characterization and aerosol dispersion performance of advanced spray-dried chemotherapeutic PEGylated phospholipid particles for dry powder inhalation delivery in lung cancer. *European Journal of Pharmaceutical Sciences*. 49:699-711 (2013).
32. F. W. The ARLA Respiratory Deposition Calculator2008.
33. S.A. Meenach, Y.J. Kim, K.J. Kauffman, N. Kanthamneni, E.M. Bachelder, and K.M. Ainslie. Synthesis, Optimization, and Characterization of Camptothecin-Loaded Acetalated Dextran Porous Microparticles for Pulmonary Delivery. *Molecular Pharmaceutics*. 9:290-298 (2012).
34. A. Bootz, V. Vogel, D. Schubert, and J. Kreuter. Comparison of scanning electron microscopy, dynamic light scattering and analytical ultracentrifugation for the sizing of poly(butyl cyanoacrylate) nanoparticles. *European Journal of Pharmaceutics and Biopharmaceutics*. 57:369-375 (2004).
35. K.T. Householder, D.M. DiPerna, E.P. Chung, G.M. Wohlleb, H.D. Dhruv, M.E. Berens, and R.W. Sirianni. Intravenous delivery of camptothecin-loaded PLGA nanoparticles for the treatment of intracranial glioma. *Int J Pharm*. 479:374-380 (2015).
36. Y. You, M. Zhao, G. Liu, and X. Tang. Physical characteristics and aerosolization performance of insulin dry powders for inhalation prepared by a spray drying method. *The Journal of pharmacy and pharmacology*. 59:927-934 (2007).
37. R. Vehring. *Pharmaceutical Particle Engineering via Spray Drying*. *Pharm Res*. 25:999-1022 (2008).

38. A.J. Hickey, H.M. Mansour, M.J. Telko, Z. Xu, H.D. Smyth, T. Mulder, R. McLean, J. Langridge, and D. Papadopoulos. Physical characterization of component particles included in dry powder inhalers. I. Strategy review and static characteristics. *J Pharm Sci.* 96:1282-1301 (2007).
39. X. Wu, W. Zhang, D. Hayes, and H.M. Mansour. Physicochemical characterization and aerosol dispersion performance of organic solution advanced spray-dried cyclosporine A multifunctional particles for dry powder inhalation aerosol delivery. *International Journal of Nanomedicine.* 8:1269-1283 (2013).
40. C. Nora Y.K. , Hak-Kim Chan. The Role of Particle Properties in Pharmaceutical Powder Inhalation Formulations. *Journal of Aerosol Medicine.* 15:325-330 (2002).
41. W. Kaialyand A. Nokhodchi. Dry powder inhalers: Physicochemical and aerosolization properties of several size-fractions of a promising alternative carrier, freeze-dried mannitol. *European Journal of Pharmaceutical Sciences.* 68:56-67 (2015).
42. X. Wu, D. Hayes, J.B. Zwischenberger, R.J. Kuhn, and H.M. Mansour. Design and physicochemical characterization of advanced spray-dried tacrolimus multifunctional particles for inhalation. *Drug Design, Development and Therapy.* 7:59-72 (2013).
43. G. Mohammadi, H. Valizadeh, M. Barzegar-Jalali, F. Lotfipour, K. Adibkia, M. Milani, M. Azhdarzadeh, F. Kiafar, and A. Nokhodchi. Development of azithromycin-PLGA nanoparticles: Physicochemical characterization and antibacterial effect against *Salmonella typhi*. *Colloids and Surfaces B: Biointerfaces.* 80:34-39 (2010).
44. Z. Zhang, L. Xu, H. Chen, and X. Li. Rapamycin-loaded poly(ϵ -caprolactone)-poly(ethylene glycol)-poly(ϵ -caprolactone) nanoparticles: preparation, characterization and potential application in corneal transplantation. *Journal of Pharmacy and Pharmacology.* 66:557-563 (2014).
45. X. Li, S. Chang, G. Du, Y. Li, J. Gong, M. Yang, and Z. Wei. Encapsulation of azithromycin into polymeric microspheres by reduced pressure-solvent evaporation method. *International Journal of Pharmaceutics.* 433:79-88 (2012).
46. S.A. Meenach, F.G. Vogt, K.W. Anderson, J.Z. Hilt, R.C. McGarry, and H.M. Mansour. Design, physicochemical characterization, and optimization of organic solution advanced spray-dried inhalable dipalmitoylphosphatidylcholine (DPPC) and dipalmitoylphosphatidylethanolamine poly(ethylene glycol) (DPPE-PEG) microparticles and nanoparticles for targeted respiratory nanomedicine delivery as dry powder inhalation aerosols. *International Journal of Nanomedicine.* 8:275-293 (2013).
47. F. Ungaro, G. De Rosa, A. Miro, F. Quaglia, and M.I. La Rotonda. Cyclodextrins in the production of large porous particles: Development of dry

powders for the sustained release of insulin to the lungs. *European Journal of Pharmaceutical Sciences*. 28:423-432 (2006).

48. S. Edda. FK506 (Tacrolimus) in Pulmonary Arterial Hypertension (TransformPAH)2012.

49. E. Spiekerkoetter, Y.K. Sung, D. Sudheendra, M. Bill, M.A. Aldred, M.C. van de Veerdonk, A. Vonk Noordegraaf, J. Long-Boyle, R. Dash, P.C. Yang, A. Lawrie, A.J. Swift, M. Rabinovitch, and R.T. Zamanian. Low-Dose FK506 (Tacrolimus) in End-Stage Pulmonary Arterial Hypertension. *American journal of respiratory and critical care medicine*. 192:254-257 (2015).

50. T.Z. Roham, S. Yon, S. Val, L. Yuwen, L.-B. Janel, and S. Edda. TrANsFoRM PAH: Phase II Study of safety and efficacy of fk-506 (tacrolimus) in pulmonary arterial hypertension. b64 management of pulmonary hypertension, *American Thoracic Society*2013, pp. A3275-A3275.

51. S. Sand H. AJ. Drug properties affecting aerosol behavior. *Respiratory Care*. 45:652-666 (2000).

52. A.J. Hickey and H.M. Mansour. Formulation challenges of powders for the delivery of small molecular weight molecules as aerosols. In R. MJ, H. J, R. MS, and L. ME (eds.), *Modified-Release Drug Delivery Technology*, Vol. 2, Informa Healthcare, New York, 2008.

53. D.A. Edwards. The macrotransport of aerosol particles in the lung: Aerosol deposition phenomena. *Journal of Aerosol Science*. 26:293-317 (1995).

CHAPTER 5

Optimization of nanocomposite microparticles (nCmP) for deep lung delivery of therapeutics via spray drying

Submitted to Powder Technology

Zimeng Wang¹, Samantha A. Meenach^{1,2}

¹University of Rhode Island, College of Engineering, Department of Chemical Engineering, Kingston, RI 02881, USA

²University of Rhode Island, College of Pharmacy, Department of Biomedical and Pharmaceutical Sciences, Kingston, RI 02881, USA

ABSTRACT

Dry powder aerosols have attracted increasing attention for the treatment of pulmonary diseases, as they are capable of delivering therapeutics directly and efficiently to the lungs. Nanocomposite microparticle (nCmP) systems, combining the advantages of nanoscale and microscale carriers, exhibit promising potential in the application of therapeutics for deep and whole lung drug delivery. Several nCmP systems have been developed for various applications, but few comprehensive studies have been completed to illustrate how to effectively engineer an optimal nCmP system for delivery of therapeutics to the deep (alveolar) region of the lungs. In the present research, we aimed to identify the optimal spray drying condition(s) to prepare nCmP with desirable drug delivery properties including: (a) small aerodynamic diameter, (b) effective nanoparticle redispersion upon nCmP exposure to an aqueous solution, (c) high drug loading, (d) and low water content. Acetalated dextran (Ac-Dex) was used as the polymer to form the nanoparticles, curcumin was used as a model drug, and mannitol was applied as an excipient in the nCmP formulation. Box–Behnken design was applied using Design-Expert software for nCmP parameter optimization. The results indicated that the nanoparticle ratio (NP%) and feed concentration (Fc) are significant parameters that affect the aerodynamic diameters of nCmP systems. NP% is also a significant parameter that affects the drug loading. Fc is the only parameter that influenced the water content of the particles significantly. All prepared nCmP systems could be completely redispersed into the parent nanoparticles, indicating that none of the factors have an influence on the redispersion of the nanoparticles within the design range. Overall, the optimal spray drying condition to prepare nCmP with a small aerodynamic diameter, complete

redispersion of the nanoparticles, low water content, and high drug loading is that with an 80% nanoparticle ratio, 0.5% feed concentration, and an inlet temperature lower than 130 °C.

KEYWORDS:

Nanocomposite microparticles, pulmonary delivery, design of experiment, spray drying, particle engineering

5.1. Introduction

The deep lung (alveolar) region has attracted increasing attention as a target for drug delivery for several reasons (1). First, the alveolar surface area of the adult human ranges between 97 and 194 m², providing a large surface for drug absorption. Second, the liquid layer over the alveoli is very thin (approximately 0.1 μm), ensuring rapid and unhindered drug absorption. Third, the plentiful capillary vessels situated beneath the thin alveolar epithelium provide efficient passive drug transport from the lungs to the bloodstream. Finally, the enzymatic activity in the lung is comparatively low, which enhances drug absorption (2, 3). As a result of the direct delivery of therapeutics to the lungs, aerosol drug delivery systems can provide several advantages including increased local drug concentration, reduced side effects, rapid onset of pharmaceutical action, and avoidance of the first-pass metabolism associated with the liver (4-6). These systems have been widely applied in the delivery of therapeutics such as antibiotics, proteins, peptides, and chemotherapeutics (7) for the treatment of diseases such as asthma, chronic

obstructive pulmonary disease (COPD), cystic fibrosis (CF)-related pulmonary infections (8), pulmonary hypertension (9) and lung cancer (10, 11).

In comparison to liquid aerosol formulations, inhalation aerosols based on dry powders offer additional benefits such as enhanced stability of formulations, controllable particle size for targeting specific regions of the lung, and increased drug loading of hydrophobic or lipophilic payloads (10, 12). Unfortunately, barriers exist in the implementation of dry powder pulmonary delivery systems, including: (1) dry powder aerosols with aerodynamic diameters smaller than 1 μm will often be exhaled; (2) particles with aerodynamic diameters above 5 μm tend to deposit in the mouth, throat or upper lung mucosa and will then be eliminated due to mucus clearance; and (3) particles larger than 1 μm deposited in the deep lung area may be cleared from the alveoli via macrophages (10, 13, 14).

The application of traditional dry powder aerosols comprised of a mixture of drugs and excipients may be limited by the aforementioned barriers, but fortunately spray-dried nanocomposite microparticles (nCmP) can be employed to solve these issues. In the production of nCmP (**Figure 5.1A and 5.1B**), polymeric nanoparticles (NP) loaded with a therapeutic are prepared, suspended in an excipient solution, and transformed into micro-scale dry powder microparticles via spray drying. Upon pulmonary administration (**Figure 5.1C and 5.1D**), the nCmP will deposit on the surface of the mucosal layer of the lungs and decompose into free NP and excipient, allowing the nanoparticles to penetrate the mucus and then release drug at sustained rate. The integration of nanoscale and microscale carriers combines the benefits of both types of systems. Microscale powders (1 - 5 μm) facilitate effective deep lung deposition (14) while the embedded

nanoscale carriers can provide multiple functions such as the protection of drugs from degradation, enhancement of the solubility of drugs, provision of controlled drug release, and reduction of side effects (15-17).

nCmP systems have been widely applied in the pulmonary delivery of therapeutics including proteins (18-20), plasmid DNA (21), siRNA (22), antibiotics (23-25), anti-tuberculosis (TB) drugs (26-28), anti-cancer drugs (29-31), and antifungal drugs (30). Small molecules such as mannitol (19, 20, 22, 26, 28, 30-37), lactose (20, 22, 25, 26, 29, 30, 38-41), trehalose (22, 31, 38, 39), and L-leucine (18, 27, 30, 31, 42) have been applied as excipients to form nCmP. Biocompatible and biodegradable polymers such as poly(lactic-co-glycolic acid) (PLGA) (22, 25, 27, 28, 36, 38, 39), poly(butylcyanoacrylate) (PBCA) (29, 40, 41), and poly- ϵ -caprolactone (PCL) (6) have been commonly used for nanoparticle formulations in nCmP systems.

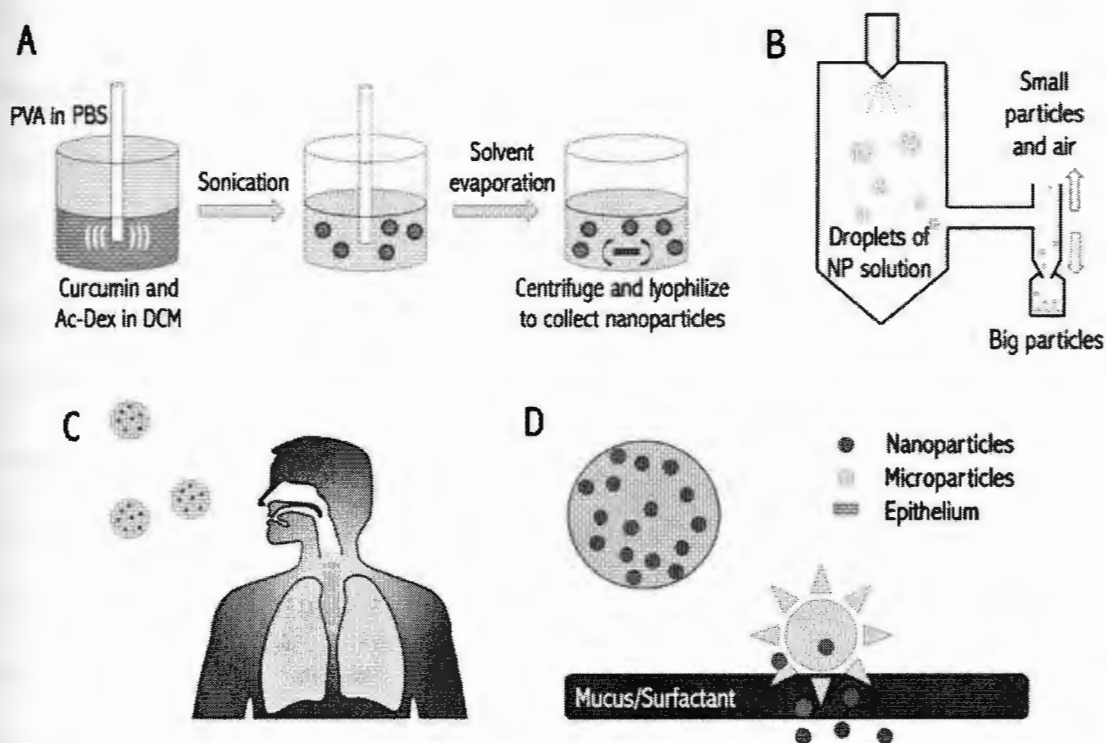


Figure 5.1. Schematic of (A) the preparation of curcumin nanoparticles (CUR NP) via emulsion/solvent evaporation, (B) formation and collection of nanocomposite microparticles (nCmP) via spray drying, and (C and D) an aerosol nCmP system interacting with the pulmonary mucosa where (C) a patient breathes the nCmP into their lungs and (D) once the nCmP impact on the surface of the mucus coating the pulmonary epithelium they degrade to release the nanoparticles.

Although many nCmP systems have been developed, few comprehensive studies have been completed to illustrate the effective engineering an optimal nCmP system for deep lung delivery of therapeutics. To date, the influence of parameters such as the spray drying inlet temperature, nanoparticle size, or the mass ratio of nanoparticles within the nCmP system have been studied using one-factor-at-a-time optimization methods (38,

39). In one study, a factorial $2 \times 2 \times 3$ experimental design was applied to evaluate the influence of the type of carbohydrate excipient, ratio of nanoparticles, and total concentration of carbohydrate excipient to NP in the feed solution on the produced nCmP (22). As the type of carbohydrate excipient is a categorical factor, limitations exist in the statistical analysis of the overall influence of the three factors. Since the parameters relevant for the nCmP preparation correlate with and depend on each other, a comprehensive consideration of the parameters should be taken. Design of experiment (DOE) has been widely used to screen relevant factors and study their influence on products, thus allowing for the determination of optimal manufacturing conditions (43, 44). Response surface methodologies (RSM) such as central composite design (CCD) or Box-Behnken design (BBD) have been applied as optimization methods in the development and improvement of pharmaceutical formulations (45, 46).

In the current study, Box-Behnken design was used to investigate the influence of the spray drying parameters: (1) weight ratio of NP (NP%), (2) total feed concentration of mannitol and NP (Fc), (3) and spray drying inlet temperature (T_{in}) in order to optimize the nCmP systems. These factors were selected as they have been proven to be significant in the successful formation of nCmP in previous research (22, 38, 39). Mannitol was used as excipient due to its ability to enhance the mucus penetration of nanoparticles by increasing the fluidity of mucus in the lungs (46). Acetalated dextran (Ac-Dex) was applied as the polymer to form nanoparticles as Ac-Dex is a novel, acid-sensitive, biodegradable, and biocompatible polymer that has attracted increasing attention in nanoparticle drug delivery applications. Compared to PLGA or other polyesters, Ac-Dex shows advantages including easily tunable degradation, minimal burst release at

physiological conditions (pH 7.4), degradation into neutral by-products avoiding undesirable changes of micro-environmental pH, and acid-sensitivity, facilitating the targeted delivery of therapeutics (47-49). Curcumin (CUR) was used as model drug owing to its hydrophobic nature and fluorescent properties. The goal of this research was to identify the optimal spray drying condition(s) in order to prepare nCmP systems comprised of CUR-loaded Ac-Dex nanoparticles. The optimal nCmP should show favorable properties including: small aerodynamic diameter, effective nanoparticle redispersion, high drug loading, and low water content.

5.2. Materials and Methods

5.2.1 Materials

Dextran from *Leuconostoc mesenteroides* (9000-11000 MW), pyridinium p-toluenesulfonate (PPTS, 98%), D-mannitol ($\geq 98\%$), 2-methoxypropene (2-MOP, 97%), triethylamine (TEA, $\geq 99\%$), anhydrous dimethyl sulfoxide (DMSO, $\geq 99.9\%$), poly(vinyl alcohol) (PVA, MW 13,000-23,000, 87-89% hydrolyzed), dichloromethane (DCM, anhydrous, $\geq 99.8\%$), deuterium chloride (DCl, 35 weight % in D₂O, 99 atom % D), Tween® 80, curcumin, and methanol (anhydrous, $\geq 99.9\%$) were obtained from Sigma-Aldrich (St. Louis, MO). Deuterium oxide (D₂O, 99.8% atom D) was obtained from Acros Organics (Geel, Belgium). Phosphate buffered saline (PBS) was obtained from Fisher Scientific (Somerville, NJ). Hydranal® KF reagent was obtained from Fluka Analytical.

5.2.2 Synthesis and NMR Analysis of Acetalated Dextran (Ac-Dex)

Ac-Dex was synthesized as described previously (49) with minor modifications. Briefly, 1 g of lyophilized dextran and 25 mg of PPTS were dissolved in 10 mL anhydrous DMSO. 5 mL of 2-MOP was added into the solution to initiate the reaction and 1 mL of TEA was added after 5 minutes to quench the reaction. The resulting mixture was then precipitated in basic water (water and TEA, pH 9), vacuum filtered, and lyophilized ($-50\text{ }^{\circ}\text{C}$, 0.023 mbar) for 24 hours to yield a solid product.

The cyclic-to-acyclic (CAC) ratio of acetal coverage and the total acetal coverage was confirmed by ^1H NMR spectroscopy (Bruker 300 MHz NMR, MA). 10 mg of Ac-Dex was added to 700 μL of D_2O and was hydrolyzed with 30 μL of DCl prior to analysis. The hydrolysis of one cyclic acetal group produces one acetone whereas one acyclic acetal produces one acetone and one methanol. Consequently, from the normalized integrations of peaks related to acetone, methanol, and the carbon ring of dextran, the CAC ratio of acetal coverage and total acetal coverage per 100 glucoses were determined.

5.2.3 Formation of CUR-Loaded Ac-Dex Nanoparticles (CUR NP)

Curcumin-loaded nanoparticles (CUR NP) were prepared via oil-in-water emulsion solvent evaporation. 49 mg of Ac-Dex and 1 mg of CUR were dissolved in 1 mL of DCM over an ice bath, establishing the organic phase. The aqueous phase, comprised of 6 ml of 3% PVA in PBS, was added to the organic phase. The resulting mixture was sonicated (Q500 Sonicator, Qsonica, Newtown, CT) for 30 seconds with a 1 second on/off pulse at 70% amplitude. The emulsion was transferred to a spinning

solution of 0.3% PVA in PBS and stirred for 3 hours to allow for evaporation of the organic solvent and particle hardening. The solution was then centrifuged at 19802 ×g for 20 minutes to collect the nanoparticles. The nanoparticles were then washed once with DI water, redispersed in 0.1% PVA, and lyophilized (−50 °C, 0.023 mbar) for 48 hours.

5.2.4 Formulation of Nanocomposite Microparticles (nCmP) Via Spray Drying

nCmP were prepared via the spray drying an aqueous suspension of a CUR NP and mannitol using a Büchi B-290 spray dryer (Büchi Labortechnik, AG, Switzerland) in open mode. The CUR NP/mannitol suspension was sonicated for 10 minutes before spray drying. The spray drying conditions were as follows: 0.7 mm nozzle diameter, atomization gas flow rate of 414 L/h using UHP dry nitrogen, aspiration rate of 28 m³/h, pump rate of 0.9 mL/min, and nozzle cleaner rate of 3. The spray dryer inlet temperature, feed concentration, and nanoparticle loading were varied as seen in **Table 1**. The resulting nCmP were separated in a high-performance cyclone, dried for 15 minutes in the spray dryer, collected in a sample collector, and stored in amber glass vials in desiccators at −20°C.

5.2.5 Design of Experiment

The spray drying parameters evaluated by design of experiment (DOE) were: the weight ratio of NP (NP%), total feed concentration of excipient and NP (Fc), and spray dryer inlet temperature (T_{in}) (**Table 1**). BBD was applied to determine the experimental conditions using Design Expert (Version 8 Stat-Ease, Inc.). The DOE responses including the aerodynamic diameter, properties of the nanoparticles following redispersion

(characterized by particle size and PDI), drug loading, and water content were analyzed in Design Expert software using an analysis of variance (ANOVA) approach. The complete design and formulation parameters that were varied are shown in **Table 2**.

Table 5.1. Factors and levels for the Box-Behnken design of dry powder aerosol nanocomposite microparticle (nCmP) formulations corresponding to the spray drying parameters utilized.

Factors	Level		
	Low	Center	High
Inlet Temperature, T_{in} (°C)	50	90	130
NP ratio, NP% (% w/w)	20	50	80
Total Feed Concentration, T_c (% w/v)	0.5	1.5	2.5

Table 5.2. Spray drying formulation parameters of the nanocomposite microparticle (nCmP) system including the inlet temperature (T_{in}), nanoparticle loading in weight % (NP%), and feed concentration (Fc).

Run	Factors		
	T_{in} (°C)	NP (%)	Fc (%)
1	130	80	1.5
2	50	50	0.5
3	50	50	2.5
4	90	50	1.5
5	90	80	0.5
6	90	50	1.5
7	50	20	1.5
8	90	80	2.5
9	130	50	0.5
10	90	20	2.5
11	130	50	2.5
12	90	50	1.5
13	50	80	1.5
14	90	20	0.5
15	130	20	1.5

5.2.6 Particle Morphology and Shape Analysis via Scanning Electron Microscopy (SEM)

The shape and surface morphology of the NP and nCmP were evaluated by SEM using a Zeiss SIGMA VP Field Emission Scanning Electron Microscope (FE-SEM) (Germany). nCmP samples were placed on aluminum SEM stubs (Ted Pella, Inc., Redding, CA) with double-sided adhesive carbon tabs. Nanoparticles were dispersed in DI water (pH 7, 10 mg/mL) and the suspensions were dropped onto aluminum SEM stubs and then dried at room temperature. The samples were coated with a thin film of a gold/palladium alloy using a BIO-RAD sputter coating system at 20 μ A for 60 seconds under argon gas. Images were captured at 5 kV at various magnifications.

5.2.7 Analysis of Nanoparticles Following Redispersion in Aqueous Solution

Following nCmP formation, the properties of the NP entrapped in and subsequently released from the nCmP were analyzed. The nCmP were dispersed in DI water (pH 7, 0.3 mg/mL) and the size, PDI, and zeta potential of the particles were measured by dynamic light scattering (DLS) using a Malvern Nano Zetasizer (Malvern Instruments, Worcestershire, UK). All experiments were performed in triplicate with a scattering angle of 173° at 25 °C. This study characterized the ability of the nCmP systems to be redispersed back to individual nanoparticles in an aqueous environment. Two values were applied to quantify the redispersion potential of the particles: (1) the ratio of nanoparticle size change after redispersion to the original nanoparticle size to denote the increase of nanoparticle average size, and (2) the ratio of PDI change after

redispersion to the original nanoparticle PDI to denote the change of nanoparticle size distribution. These values were determined by the following equations:

$$\text{Size change \%} = \frac{\text{Final NP size} - \text{Original NP size}}{\text{Original NP size}} \times 100\%$$

$$\text{PDI change \%} = \frac{\text{Final NP PDI} - \text{Original NP PDI}}{\text{Original NP PDI}} \times 100\%$$

In addition, the influence of the spray dryer inlet temperature on size and PDI at higher spray drying temperatures was evaluated by spray drying CUR NP without mannitol (100 nCmP) at 50, 90, 130, 160, 190, and 220 °C. The resulting particle samples were sonicated for 1, 2, and 15 minutes prior to DLS measurement.

5.2.8 Analysis of Drug Loading of CUR NP and CUR nCmP

Drug loading and encapsulation efficiency of CUR NP and CUR nCmP were determined via fluorescence spectroscopy (Biotek Cytation 3, Winooski, VT). The particle samples were dissolved in DMSO and evaluated at 420 nm (excitation) and 540 nm (emission). The CUR loading of NP, CUR loading of nCmP, NP loading in nCmP, CUR encapsulation efficiency (EE) of NP, and NP encapsulation efficiency of nCmP were determined by the following equations:

$$\text{Drug loading of NP} = \frac{\text{mass of drug loaded in NP}}{\text{mass of NP}} \times 100\%$$

$$\text{Drug loading of nCmP} = \frac{\text{mass of drug loaded in nCmP}}{\text{mass of nCmP}} \times 100\%$$

$$\text{Encapsulation efficiency (EE)} = \frac{\text{mass of drug loaded in NP}}{\text{initial mass of drug in NP formulation}} \times 100\%$$

$$\text{Nanoparticle loading} = \frac{\text{mass of NP loaded in nCmP}}{\text{mass of nCmP}} \times 100\%$$

$$\text{NP loading efficiency} = \frac{\text{mass of NP loaded in nCmP}}{\text{initial mass of NP in nCmP formulation}} \times 100\%$$

5.2.9 Karl Fischer Coulometric Titration

The water content of the nCmP was quantified by Karl Fischer (KF) titration using a 737 KF coulometer (Metrohm, Riverview, FL). 3 mg of powder was dissolved in anhydrous methanol. The resulting solution was injected into the KF reaction cell filled with Hydranal® KF reagent and then the amount of water was analyzed. Pure solvent was also injected for use as a background sample.

5.2.10 Differential Scanning Calorimetry (DSC)

The thermal phase transitions of the raw particle components were determined via DSC using a TA Q10 DSC system (TA Instruments, New Castle, DE, USA) equipped with an automated computer-controlled TA instruments DSC refrigerated cooling system. 1 - 3 mg of sample was weighed into Tzero™ alodined aluminum pans that were hermetically sealed. The sealed pans were placed into the DSC furnace along with an

empty sealed reference pan. The samples were analyzed at a heating range of 0 – 250 °C and heating rate of 10 °C/min.

5.2.11 *In Vitro* Aerosol Dispersion Performance with the Next Generation Impactor (NGI)

The *in vitro* aerosol dispersion performance of nCmP was evaluated using a Next Generation Impactor™ (NGI™, MSP Corporation, Shoreview, MN) equipped with a stainless steel induction port (USP throat adaptor) attachment and stainless steel gravimetric insert cups. The NGI™ was coupled with a Copley TPK 2000 critical flow controller, which was connected to a Copley HCP5 vacuum pump (Copley Scientific, United Kingdom). The airflow rate (Q) was measured and adjusted to 60 L/min in order to model the flow rate in a healthy adult lung before each experiment. Glass fiber filters (55 mm, Type A/E, Pall Life Sciences, PA) were placed in the gravimetric insert cups for stages 1 through 7 to minimize bounce or re-entrapment (50) and these filters were weighed before and after the experiment to determine the particle mass deposited on each stage. Approximately 10 mg of powder was loaded into a hydroxypropyl methylcellulose (HPMC, size 3, Quali-V®, Qualicaps® Inc., Whitsett, NC, USA) capsule and the capsule was placed in a human dry powder inhaler device (HandiHaler, Boehringer Ingelheim Pharmaceuticals, CT) attached to a customized rubber mouthpiece connected to the NGI™. Three HPMC capsules were loaded and released in each measurement and experiments were performed in triplicate. The NGI™ was run with a delay time of 10 s and running time of 10 s. For Q = 60 L/min, the effective cutoff diameters for each stage of the impactor were given from the manufacturer as: stage 1 (8.06 µm); stage 2 (4.46

μm); stage 3 (2.82 μm); stage 4 (1.66 μm); stage 5 (0.94 μm); stage 6 (0.55 μm); and stage 7 (0.34 μm). The fine particle dose (FPD), fine particle fraction (FPF), respirable fraction (RF), and emitted dose (ED) were calculated as follows:

$$\text{Fine particles fraction (FPF)} = \frac{\text{mass of particles on Stages 2 through 7}}{\text{initial particle mass loaded into capsules}} \times 100\%$$

$$\text{Respirable fraction (RF)} = \frac{\text{mass of particles on Stages 2 through 7}}{\text{total particle mass on all stages}} \times 100\%$$

$$\text{Emitted Dose (ED)} = \frac{\text{initial mass in capsules} - \text{final mass remaining in capsules}}{\text{initial mass in capsules}} \times 100\%$$

The mass median aerodynamic diameter (MMAD) and geometric standard deviation (GSD) for the particles were determined using a Mathematica® program written by Dr. Warren Finlay (50, 51).

5.2.12 Statistical analysis

All measurements were performed in at least triplicate. Values are given in the form of mean \pm standard deviation. The statistical significance of the results was determined using analysis of variance (ANOVA). A p-value less than 0.05 was considered statistically significant.

5.3. Results and Discussion

5.3.1 Preparation and Characterization of Curcumin-Loaded Nanoparticles (CUR NP)

5.3.1.1 Preparation and Characterization of Acetalated Dextran (Ac-Dex)

Successful synthesis of Ac-Dex was confirmed by ¹H NMR where the polymer exhibited 61.3% cyclic acetal coverage and 77.1% total conversion of -OH groups. A high CAC is known to decrease the degradation rate of Ac-Dex (50), and a high total acetal coverage is required to stabilize the PVA coating of nanoparticles, which ensures small particle size and narrow particle size distribution.

5.3.1.2 Preparation and Characterization of Original CUR NP

The average nanoparticle size, size distribution/polydispersion index (PDI), zeta potential, drug loading, and encapsulation efficiency of curcumin-loaded nanoparticles (CUR NP) are shown in **Table 5.3**. The original CUR NP exhibited an average diameter of approximately 200 nm, which is in the desirable range to avoid macrophage clearance and mucus entrapment (14). The low PDI value denotes a narrow size distribution of nanoparticles. The surface of nanoparticles was slightly negative, which is suitable to reduce the interaction of the NP with negatively charged mucin fibers present in airway mucus (52). Curcumin was successfully encapsulated into the CUR NP and the amount of the drug in CUR NP was sufficient for the quantification of CUR and NP in nCmP samples.

Table 5.3. Properties of curcumin nanoparticles (CUR NP) including their size (as measured by dynamic light scattering), polydispersity index (PDI), zeta potential, drug loading, and encapsulation efficiency (EE) (mean \pm standard deviation, n = 3).

System	Diameter (nm)	PDI	Zeta Potential (mV)	Drug Loading (mg drug/100mg NP)	EE (%)
CUR NP	204.1 \pm 4.4	0.07 \pm 0.02	-6.98 \pm 0.73	0.64 \pm 0.04	31.99 \pm 3.69

5.3.2 Design of Experiment and nCmP Characterization

5.3.2.1 Box-Behnken Design

The results of the Box-Behnken design are shown in **Table 5.4**. Analysis of variance (ANOVA) was performed to evaluate the influence of the factors on the responses. The statistical significance and the magnitude of the exerted effects (coefficient estimates) of each factor are shown in **Table 5.5**. The interaction of parameters was not included, as its effect on the results was negligible. The sign of the coefficient estimates signifies a positive or negative influence of the factor on the corresponding response. Since this study was designed to qualify the effects of the formulation parameters on particle properties and the final model will not be used for prediction purposes at this point, a lack of fit test was not a major consideration in model selection.

5.3.2.2 Drug Loading and Encapsulation Efficiency (EE)

The drug loading of CUR nCmP was only affected by the nanoparticle loading (NP%, $p < 0.0001$) and no other factors had a significant influence on this parameter. Since the drug loading of the CUR NP was constant in this study, the NP% was the only parameter that should definitively affect the drug loading of nCmP. Therefore, either increasing the NP% in the nCmP formulation or using original NP with higher drug loading can be applied to achieve higher drug loading in the nCmP system. Unlike the formation of traditional spray-dried particles (53, 54) composed of a mixture of drug and excipient, the drug loading capacity of nCmP can be optimized beforehand during nanoparticle preparation. By providing an optimal nanoparticle system, drug loading optimization during spray drying can be remarkably simplified.

Table 5.4. Responses of the Box-Behnken design for the nanocomposite microparticle (nCmP) systems including drug loading, encapsulation efficiency (EE), water content, mass median aerodynamic diameter (MMAD), geometric standard deviation (GSD), fine particle fraction (FPF), respirable fraction (RF), emitted dose (ED), percent size change, and percent polydispersity index (PDI) change. The corresponding particle conditions can be seen in Table 2.

Run	Responses									
	Drug Loading (%)	EE (%)	Water Content (%)	MMAD (μm)	GSD (μm)	FPF (%)	RF (%)	EF (%)	Size Change (%)	PDI Change (%)
1	0.372	72.74	4.51%	2.44	2.34	98.6%	76.0%	97.7%	0.2%	-2.9%
2	0.201	62.78	5.71%	1.69	2.79	99.4%	77.2%	98.0%	5.6%	20.0%
3	0.192	60.14	3.82%	4.49	1.95	85.0%	57.9%	99.0%	0.0%	31.4%
4	0.201	62.83	2.95%	4.28	1.70	84.4%	60.9%	99.6%	2.5%	14.3%
5	0.357	69.79	5.94%	1.50	2.57	98.8%	86.0%	96.3%	9.7%	17.1%
6	0.087	58.45	3.41%	4.05	2.34	86.1%	67.4%	99.6%	4.9%	14.3%
7	0.074	58.12	5.43%	7.44	2.34	54.2%	48.4%	99.8%	1.0%	-21.4%
8	0.402	78.70	4.69%	2.48	2.77	97.5%	70.0%	94.6%	4.9%	57.1%
9	0.195	61.09	5.66%	3.69	2.81	83.6%	73.0%	98.8%	7.5%	30.0%
10	0.083	65.33	2.63%	7.20	2.81	62.2%	38.0%	100.1%	4.8%	20.0%
11	0.172	53.71	3.84%	5.78	2.50	66.2%	55.8%	99.2%	1.1%	-20.0%
12	0.193	60.34	3.23%	4.11	1.88	85.3%	61.6%	99.9%	2.3%	-1.4%
13	0.288	56.43	4.68%	2.38	2.71	98.1%	82.2%	95.7%	4.2%	15.7%
14	0.093	72.93	6.72%	3.24	3.00	83.3%	64.4%	97.1%	-0.2%	32.9%
15	0.113	88.07	4.13%	5.46	1.88	68.8%	46.2%	100.0%	8.3%	22.9%

Table 5.5. Statistical significance (p-value and coefficient estimation) of nanocomposite microparticle (nCmP) formulation parameters including drug loading (DL), encapsulation efficiency (EE), size change, polydispersity (PDI) change, mass median aerodynamic diameter (MMAD), fine particle fraction (FPF), respirable fraction (RF), emitted dose (ED), and water content (WC) with respect to the spray dryer inlet temperature (T_{in}), nanoparticle loading (NP%), and feed concentration (Fc).

Factors	Drug Loading Capacity		Re-dispersity					
	DL (%)		EE (%)		Size change (%)		PDI change (%)	
	p-Value	Coef. Est.	p-Value	Coef. Est.	p-Value	Coef. Est.	p-Value	Coef. Est.
T_{in}	-	-	-	-	-	-	-	-
NP%	< 0.0001	0.13	-	-	-	-	-	-
Fc%	-	-	-	-	-	-	-	-

Factors	<i>In Vitro</i> Aerosol Performance								Water Content	
	MMAD (μm)		FPF (%)		RF (%)		ED (%)		WC (%)	
	p-Value	Coef. Est.	p-Value	Coef. Est.	p-Value	Coef. Est.	p-Value	Coef. Est.	p-Value	Coef. Est.
T_{in}	-	-	-	-	-	-	< 0.0001	4.07E-03	-	-
NP%	0.0002	-1.82	0.0001	0.16	< 0.0001	0.15	0.0036	-0.016	-	-
Fc%	0.0026	1.23	0.0258	-0.068	< 0.0001	-0.099	< 0.0001	3.26E-03	0.0009	-0.011

5.3.2.3 Analysis of Properties Following Redispersion of CUR NP from CUR nCmP

The average size and PDI of CUR NP before and after spray drying (and subsequent redispersion in water) were measured by DLS. No significant differences were found in the NP properties before and after nCmP formation ($p < 0.05$), which indicates that the NP from the nCmP systems can be fully redispersed with no adverse effects. The ANOVA analysis of the DOE results showed that T_{in} , NP%, and Fc had no effect on the redispersion properties of CUR NP. In previous studies, NP%, Fc, and the type of excipient have been reported to have no impact on the redispersion of PLGA NP from prepared at a low spray drying inlet temperature (50 °C). However, in a study by Tomoda et al., the inlet temperature was an important factor affecting the redispersion of NP from nCmP comprised of PLGA NP and trehalose or lactose (20, 55). In that study, a higher T_{in} (100 °C) resulted in poor NP redispersion due to the aggregation or fusion of the primary nanoparticles during spray drying. The authors claimed that the aggregation of the NP could be attributed to the low melting temperature of PLGA ($T_m = 45$ °C). Since Ac-Dex has a higher melting point (170 °C) and no thermal transitions before melting, we hypothesize that the nCmP comprised of Ac-Dex NP can be completely redispersed when the outlet temperature during spray drying is lower than the melting point of Ac-Dex. The spray drying outlet temperatures were approximately half of the inlet temperatures in the present study (**Table B.1**), so even the maximum T_{in} (220 °C) capable by a Büchi B-290 spray dryer should be within an acceptable temperature range to allow for effective nCmP formation and NP redispersion.

nCmP systems with 100% NP loading were formulated to evaluate the influence of higher T_{in} values on NP redispersion, since the NP% showed no influence on the

redispersion of NP in the initial formulations. The influence of the spray dryer inlet temperature on the redispersed nanoparticles is shown in **Figure 5.2**. NP from 100% nCmP manufactured at 50, 90, and 130°C were fully redispersed upon dissolving in DI water. NP from 100% nCmP manufactured at 160, 190, and 220 °C exhibited an increase in both size and PDI due to NP agglomeration. By sonicating the nCmP samples prior to DLS measurement, both the average size and PDI can be reduced and higher manufacturing temperatures required more sonication to effectively redisperse the NP.

DSC analysis was performed on the raw NP and nCmP materials (**Figure 5.3**). The melting points of PVA, Ac-Dex, curcumin, and mannitol were 175, 170, 172, and 167 °C, respectively, which were all higher than the spray drying outlet temperature (112 °C). PVA exhibited a glass transition temperature at 49 °C, which should have no effect on nanoparticle agglomeration, as NP from 100% NP-loaded nCmP prepared at 90 and 130 °C could be completely redispersed. The aforementioned results failed to support our initial hypothesis. In summary, manufacturing nCmP at temperatures lower than the melting point of the raw materials cannot necessarily ensure the avoidance of nanoparticle fusion and agglomeration. A reasonable explanation is that the high pressure during the quick drying process at high temperatures may cause nanoparticle agglomeration. Further studies will be carried out to determine the influence of the drying rate on nanoparticle redispersion.

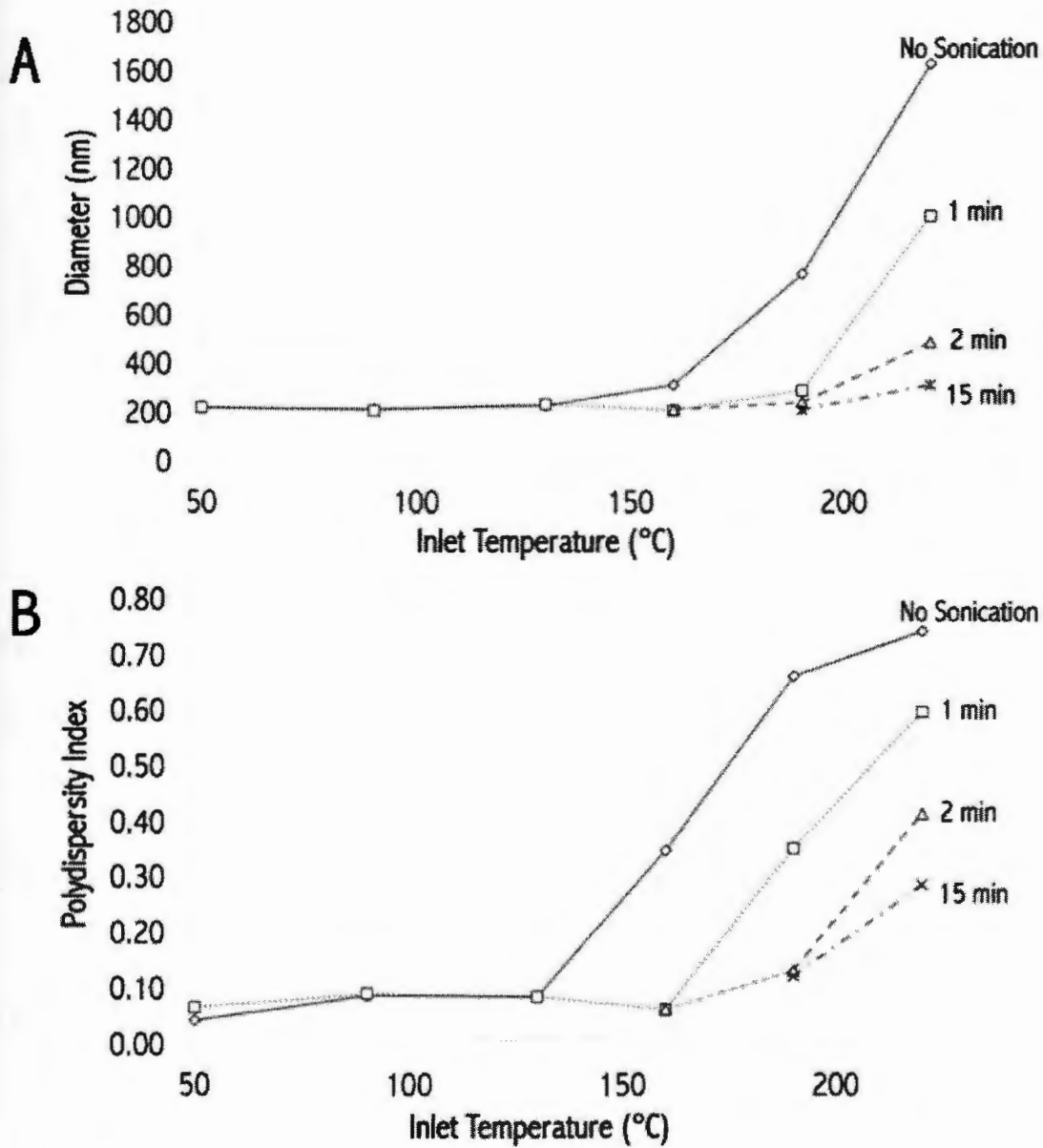


Figure 5.2. Influence of spray dryer inlet temperature (T_{in}) on the size and polydispersity index (PDI) of nanoparticles redispersed from nanocomposite microparticles comprised of 100% NP loading.

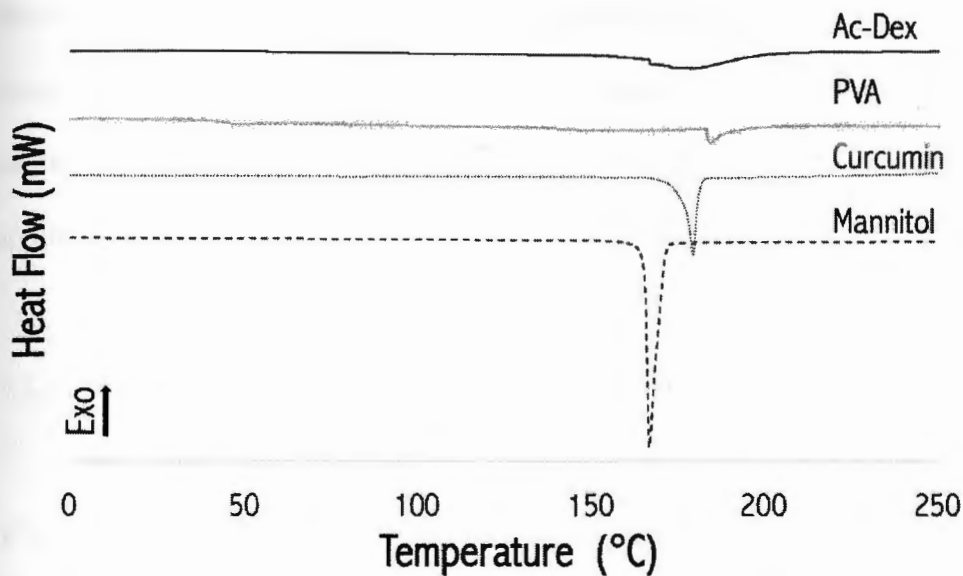


Figure 5.3. Representative differential scanning calorimetry (DSC) thermograms of raw Ac-Dex, PVA, curcumin, and mannitol.

5.3.2.4 Water Content of CUR nCmP

The CUR nCmP samples exhibited water content in the range of 2.6 - 6.7% (**Table 5.4**). The water content of the nCmP was affected only by the feed solution concentration ($p = 0.0009$). Higher feed solution concentration resulted in lower water content in the particles, which corresponds to previous research on nCmP systems (22) and traditional spray-dried particles (56). However, unlike previous studies (22, 56), T_{in} and NP% showed no effect on water content. The reason for this is likely the post drying process, which further removed water from the nCmP, thus reducing the difference in water content among the samples. Low water content is highly favorable in inhalable dry powders to allow for efficient aerosolization and particle delivery as it improves particle dispersion properties during aerosolization by reducing the interparticulate capillary

forces acting at the solid–solid interface between particles (53, 57). Furthermore, low water content enhances the stability of dry powders during storage (58). Since the water content of all of the samples were acceptable in this study, the post drying process can be applied to simplify optimization in future studies.

5.3.2.5 Morphology of CUR nCmP

As seen in the representative SEM images in **Figure 5.4** (SEM images of all nCmP systems are available in **Figure B.1**), nCmP showed two kinds of morphology: (1) raisin-like particles with wrinkled surfaces and (2) spherical particles with cracks on the surface. nCmP with 80% NP (**Figure 5.4C**) exhibited raisin-like morphology, while nCmP with 20% NP (**Figure 5.4A**) were cracked spheres. Particles with surface morphology of both types can be seen in the 50% NP sample (**Figure 5.4B**). The corrugated surface of the nCmP systems facilitate aerosol performance by reducing the contact area between particles during aerosolization. As a result, aggregation of the nCmP can be reduced, thus improving the redispersion of NP from nCmP formulations. The raisin-like morphology of nCmP may be attributed to the early formation of nanoparticle shells in droplets during the spray drying process, during which the geometric size of nCmP is determined. As the drying process proceeds, the remaining water evaporates from the droplet center and the newly precipitated dry materials cannot fill the hollow interior of the nCmP, which results in shrinkage of the particles (59, 60). The spherical particle systems with cracks in their surface are the typical morphology of particles with mannitol shells. The cracks evident on these types of particles were not

caused by the spray drying process but instead were generated during SEM imaging due to the high energy of the electron beam (**Figure B.2**).



Figure 5.4. Representative SEM micrographs of curcumin-loaded nanocomposite microparticles (CUR nCmP) spray dried with varying conditions such as inlet temperature (T_{in}), nanoparticle loading (NP%), and feed concentration (Fc), including: (A) $T_{in} = 50\text{ }^{\circ}\text{C}$, NP% = 20%, Fc = 1.5%, (B) $T_{in} = 90\text{ }^{\circ}\text{C}$, NP% = 50%, Fc = 1.5%, and (C) $T_{in} = 90\text{ }^{\circ}\text{C}$, NP% = 80%, Fc = 0.5%. Scale bar = 5 μm .

5.3.2.6 In Vitro Aerosol Dispersion Performance Using the Next Generation Impactor (NGI)

In vitro aerosol dispersion performance properties of the nCmP were evaluated using a Next Generation Impactor™ coupled with a human DPI device. Mass mean aerodynamic diameter (MMAD), geometric standard deviation (GSD), respirable fraction (RF), fine particle fraction (FPF), and emitted dose (ED) were calculated (**Table 5.4**). None of the spray drying parameters exhibited a significant influence on the GSD values ($p > 0.05$). Both NP% and Fc showed a significant effect on the MMAD, RF, FPF, and ED. Higher NP% resulted in smaller MMAD, higher RF, and higher FPF, which are all beneficial for effective delivery of payloads into the lungs by nCmP. A MMAD in the

range of 1 - 5 μm is required for predominant deposition of nCmP into the deep lung (alveolar) region, and particles with higher MMAD tend to deposit in the upper airways and throat. NP% had a negative influence on the ED, however, the ED of all of the samples was within a high range of 94.6% - 100%, which makes it acceptable to apply high NP% in the optimization of aerosol dispersion properties.

The feed solution concentration (F_c) showed a negative influence on the RF and FPF but positive influence on the MMAD. As a result, low F_c should be applied to achieve an optimal nCmP system. F_c and T_{in} had a negligible positive influence on ED (**Table 5.5**), which was not taken into consideration. The aerosol distribution performance of a representative nCmP system is shown in **Figure 5.5**. The three nCmP samples analyzed correspond to the three SEM micrographs in **Figure 5.4**. The nCmP sample with more wrinkled particles deposited in the lower NGI stages, indicating the potential for predominant particle deposition into the lower airways. This phenomenon was in accordance with the negative influence of NP% on the MMAD. As the increased NP% can result in more wrinkled and hollow particles with low density and favorable aerosol dispersion, the MMAD was thus reduced. F_c had positive influence on the MMAD, as more dry material exists in the droplets during spray drying, which increases the density of resulting particles.

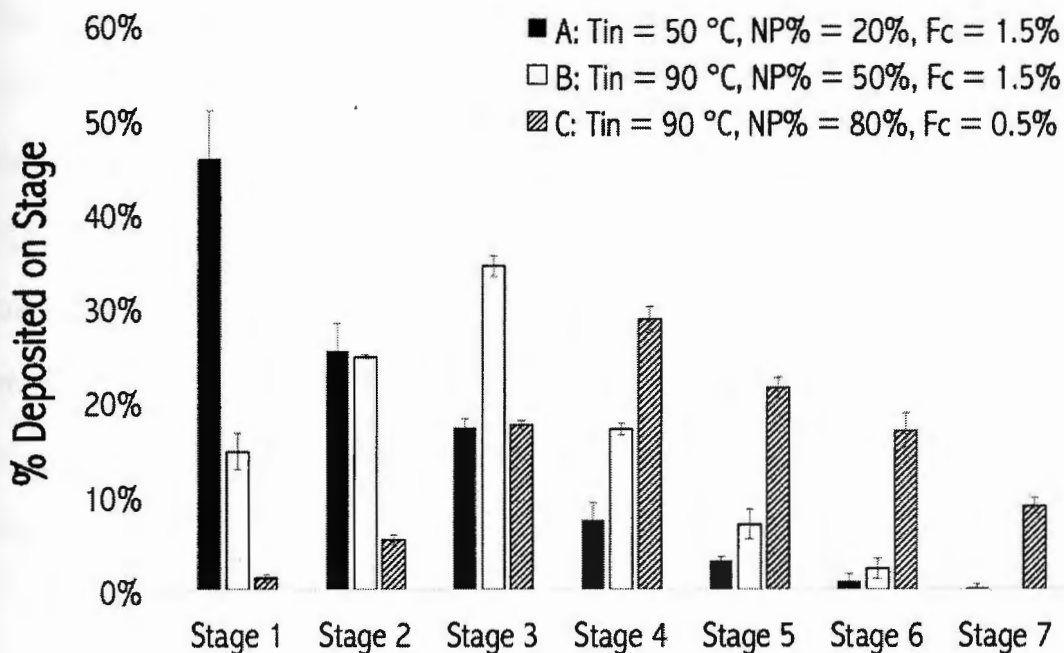


Figure 5.5. Nanocomposite microparticle (nCmP) aerosol dispersion performance as % deposited on each stage of the Next Generation Impactor™ (NGI™) for representative CUR nCmP systems. For $Q = 60$ L/min, the effective cutoff diameters (D_{50}) for each impaction stage are as follows: stage 1 ($8.06 \mu\text{m}$), stage 2 ($4.46 \mu\text{m}$), stage 3 ($2.82 \mu\text{m}$), stage 4 ($1.66 \mu\text{m}$), stage 5 ($0.94 \mu\text{m}$), stage 6 ($0.55 \mu\text{m}$), and stage 7 ($0.34 \mu\text{m}$). (mean \pm standard deviation, $n = 3$).

5.4 Conclusions

The current study identified the optimal spray drying conditions to prepare Ac-Dex nanoparticles-based nCmP systems with favorable properties including: small aerodynamic diameter, effective nanoparticle redispersion, high drug loading, and low water content. Higher NP% resulted in nCmP systems with smaller MMAD, high FPF,

higher RF, and higher drug loading. Lower F_c lead to smaller MMAD, higher FPF, and high RF, while higher F_c was beneficial for lower water content. T_{in} had a negligible influence on the nCmP properties in the design range, while in higher range it will hinder the redispersion of NP from the nCmP. The drug loading was only affected by the NP% of nCmP, which simplifies the optimization of spray drying nCmP given that high drug loading of NP can be achieved. The influence of each spray drying parameter on the properties of the resulting particles is summarized in **Figure 5.6**. The optimal condition to prepare nCmP with a small aerodynamic diameter, desirable nanoparticle redispersion, high drug loading, and low water content is via high NP%, low F_c , and a T_{in} under 130 °C.

5.5 Acknowledgements

The authors gratefully acknowledge financial support from an Institutional Development Award (IDeA) from the National Institute of General Medical Sciences of the National Institutes of Health under grant number P20GM103430. The content is solely the responsibility of the authors and does not necessarily represent the official views of the National Institutes of Health. This material is based upon work conducted at a Rhode Island NSF EPSCoR research facility, supported in part by the National Science Foundation EPSCoR Cooperative Agreement #EPS-1004057. In addition, this material is based in part upon work supported by the National Science Foundation under grant number #1508868. Any opinions, findings, and conclusions or recommendations expressed in this material are those of the authors and do not necessarily reflect the view

of the National Science Foundation. Finally, the authors thank RI-INBRE for UPLC access and RIN2 for SEM, DLS, PXRD, and DSC access.

Response	Factor		
	Inlet Temperature	Weight ratio of NP	Feed Concentration
Drug loading	✗	↑	✗
Encapsulation efficiency	✗	✗	✗
NP size change	✗↑ *	✗	✗
NP PDI change	✗↑ *	✗	✗
MMAD	✗	↓	↑
Fine particle fraction	✗	↑	↓
Respirable fraction	✗	↑	↓
Emitted dose	↑	↓	↑
Water content	✗	✗	↑

✗ No influence ↑ Major influence ↑ Minor influence

Figure 5.6. Schematic outlining the influences of inlet temperature (T_{in}), weight ratio of NP (NP%), and feed concentration (F_c) on the properties of the resulting nanocomposite microparticles. * indicates that the inlet temperature exhibited no influence on the NP size change and NP PDI change when T_{in} was lower than 130 °C and that it showed a positive influence when T_{in} was higher than 130 °C.

5.6 References

1. Agu RU, Ugwoke MI, Armand M, Kinget R, Verbeke N. The lung as a route for systemic delivery of therapeutic proteins and peptides. *Respiratory research*. 2001;2(4):198-209.
2. Matthias Ochs PHB, Joan Gil, and Ewald R, Weibel. Anatomy of the Chest Wall and Lungs. In: Thomas W. Shields JLI, Carolyn E. Reed, and Richard H. Feins, editor. *General Thoracic Surgery*. Philadelphia: Wolters Kluwer/ Lippincott Williams and Wilkins Health; 2009. p. 47.
3. Labiris NR, Dolovich MB. Pulmonary drug delivery. Part I: Physiological factors affecting therapeutic effectiveness of aerosolized medications. *British Journal of Clinical Pharmacology*. 2003;56(6):588-599.
4. Park CWM, Heidi M.; Hayes, Don Pulmonary inhalation aerosols for targeted antibiotics drug delivery. *European Pharmaceutical Review*. 2011;1.
5. Patton JS, Byron PR. Inhaling medicines: delivering drugs to the body through the lungs. *Nat Rev Drug Discov*. 2007;6(1):67-74.
6. AJ H, HM M. Delivery of drugs by the pulmonary route. New York: Taylor and Francis; 2009.
7. Muralidharan P, Malapit M, Mallory E, Hayes Jr D, Mansour HM. Inhalable nanoparticulate powders for respiratory delivery. *Nanomedicine: Nanotechnology, Biology and Medicine*. 2015;11(5):1189-1199.
8. Wang Z, Meenach SA. Synthesis and Characterization of Nanocomposite Microparticles (nCmP) for the Treatment of Cystic Fibrosis-Related Infections. *Pharmaceutical Research*. 2016;33(8):1862-1872.
9. Wang Z, Cuddigan JL, Gupta SK, Meenach SA. Nanocomposite Microparticles (nCmP) for the Delivery of Tacrolimus in the Treatment of Pulmonary Arterial Hypertension. *International Journal of Pharmaceutics*. 2016;512(1):305-313.
10. Stocke NA, Meenach SA, Arnold SM, Mansour HM, Hilt JZ. Formulation and characterization of inhalable magnetic nanocomposite microparticles (MnMs) for targeted pulmonary delivery via spray drying. *International Journal of Pharmaceutics*. 2015;479(2):320-328.
11. Lee W-H, Loo C-Y, Traini D, Young PM. Inhalation of nanoparticle-based drug for lung cancer treatment: Advantages and challenges. *Asian Journal of Pharmaceutical Sciences*. 2015;10(6):481-489.
12. Dolovich MB, Ahrens RC, Hess DR, Anderson P, Dhand R, Rau JL, Smaldone GC, Guyatt G. Device selection and outcomes of aerosol therapy: Evidence-based

guidelines*: american college of chest physicians/american college of asthma, allergy, and immunology. *Chest*. 2005;127(1):335-371.

13. Stegemann S, Kopp S, Borchard G, Shah VP, Senel S, Dubey R, Urbanetz N, Cittero M, Schoubben A, Hippchen C, Cade D, Fuglsang A, Morais J, Borgström L, Farshi F, Seyfang KH, Hermann R, van de Putte A, Klebovich I, Hincal A. Developing and advancing dry powder inhalation towards enhanced therapeutics. *European Journal of Pharmaceutical Sciences*. 2013;48(1-2):181-194.

14. Kho K, Cheow WS, Lie RH, Hadinoto K. Aqueous re-dispersibility of spray-dried antibiotic-loaded polycaprolactone nanoparticle aggregates for inhaled anti-biofilm therapy. *Powder Technology*. 2010;203(3):432-439.

15. Mansour HM, Rhee Y-S, Wu X. Nanomedicine in pulmonary delivery. *International Journal of Nanomedicine*. 2009;4:299-319.

16. Sung JC, Pulliam BL, Edwards DA. Nanoparticles for drug delivery to the lungs. *Trends in Biotechnology*. 2007;25(12):563-570.

17. Bailey MM, Berkland CJ. Nanoparticle formulations in pulmonary drug delivery. *Medicinal research reviews*. 2009;29(1):196-212.

18. Kunda NK, Alfaqih IM, Dennison SR, Somavarapu S, Merchant Z, Hutcheon GA, Saleem IY. Dry powder pulmonary delivery of cationic PGA-co-PDL nanoparticles with surface adsorbed model protein. *Int J Pharm*. 2015;492(1-2):213-222.

19. Grenha A, Grainger CI, Dailey LA, Seijo B, Martin GP, Remuñán-López C, Forbes B. Chitosan nanoparticles are compatible with respiratory epithelial cells *in vitro*. *European Journal of Pharmaceutical Sciences*. 2007;31(2):73-84.

20. Grenha A, Seijo B, Remunan-Lopez C. Microencapsulated chitosan nanoparticles for lung protein delivery. *European journal of pharmaceutical sciences : official journal of the European Federation for Pharmaceutical Sciences*. 2005;25(4-5):427-437.

21. Capan Y, Woo BH, Gebrekidan S, Ahmed S, DeLuca PP. Influence of formulation parameters on the characteristics of poly(d,l-lactide-co-glycolide) microspheres containing poly(l-lysine) complexed plasmid DNA. *J Control Release*. 1999;60(2-3):279-286.

22. Jensen DM, Cun D, Maltesen MJ, Frokjaer S, Nielsen HM, Foged C. Spray drying of siRNA-containing PLGA nanoparticles intended for inhalation. *Journal of controlled release : official journal of the Controlled Release Society*. 2010;142(1):138-145.

23. Cheow WS, Chang MW, Hadinoto K. The roles of lipid in anti-biofilm efficacy of lipid-polymer hybrid nanoparticles encapsulating antibiotics. *Colloids and Surfaces A: Physicochemical and Engineering Aspects*. 2011;389(1-3):158-165.

24. Pilcer G, Vanderbist F, Amighi K. Preparation and characterization of spray-dried tobramycin powders containing nanoparticles for pulmonary delivery. *Int J Pharm.* 2009;365(1-2):162-169.
25. Ungaro F, d'Angelo I, Coletta C, d'Emmanuele di Villa Bianca R, Sorrentino R, Perfetto B, Tufano MA, Miro A, La Rotonda MI, Quaglia F. Dry powders based on PLGA nanoparticles for pulmonary delivery of antibiotics: modulation of encapsulation efficiency, release rate and lung deposition pattern by hydrophilic polymers. *Journal of controlled release : official journal of the Controlled Release Society.* 2012;157(1):149-159.
26. Pourshahab PS, Gilani K, Moazeni E, Eslahi H, Fazeli MR, Jamalifar H. Preparation and characterization of spray dried inhalable powders containing chitosan nanoparticles for pulmonary delivery of isoniazid. *Journal of microencapsulation.* 2011;28(7):605-613.
27. Sung JC, Padilla DJ, Garcia-Contreras L, Verberkmoes JL, Durbin D, Peloquin CA, Elbert KJ, Hickey AJ, Edwards DA. Formulation and pharmacokinetics of self-assembled rifampicin nanoparticle systems for pulmonary delivery. *Pharm Res.* 2009;26(8):1847-1855.
28. Ohashi K, Kabasawa T, Ozeki T, Okada H. One-step preparation of rifampicin/poly(lactic-co-glycolic acid) nanoparticle-containing mannitol microspheres using a four-fluid nozzle spray drier for inhalation therapy of tuberculosis. *Journal of controlled release : official journal of the Controlled Release Society.* 2009;135(1):19-24.
29. Azarmi S, Tao X, Chen H, Wang Z, Finlay WH, Löbenberg R, Roa WH. Formulation and cytotoxicity of doxorubicin nanoparticles carried by dry powder aerosol particles. *International Journal of Pharmaceutics.* 2006;319(1-2):155-161.
30. Jafarinejad S, Gilani K, Moazeni E, Ghazi-Khansari M, Najafabadi AR, Mohajel N. Development of chitosan-based nanoparticles for pulmonary delivery of itraconazole as dry powder formulation. *Powder Technology.* 2012;222:65-70.
31. Varshosaz J, Hassanzadeh F, Mardani A, Rostami M. Feasibility of haloperidol-anchored albumin nanoparticles loaded with doxorubicin as dry powder inhaler for pulmonary delivery. *Pharmaceutical development and technology.* 2015;20(2):183-196.
32. Stocke NA, Meenach SA, Arnold SM, Mansour HM, Hilt JZ. Formulation and characterization of inhalable magnetic nanocomposite microparticles (MnMs) for targeted pulmonary delivery via spray drying. *Int J Pharm.* 2015;479(2):320-328.
33. Duret C, Wauthoz N, Sebti T, Vanderbist F, Amighi K. New inhalation-optimized itraconazole nanoparticle-based dry powders for the treatment of invasive pulmonary aspergillosis. *Int J Nanomedicine.* 2012;7:5475-5489.

34. Beck-Broichsitter M, Schweiger C, Schmehl T, Gessler T, Seeger W, Kissel T. Characterization of novel spray-dried polymeric particles for controlled pulmonary drug delivery. *Journal of Controlled Release*. 2012;158(2):329-335.
35. Li YZ, Sun X, Gong T, Liu J, Zuo J, Zhang ZR. Inhalable microparticles as carriers for pulmonary delivery of thymopentin-loaded solid lipid nanoparticles. *Pharm Res*. 2010;27(9):1977-1986.
36. Takashima Y, Saito R, Nakajima A, Oda M, Kimura A, Kanazawa T, Okada H. Spray-drying preparation of microparticles containing cationic PLGA nanospheres as gene carriers for avoiding aggregation of nanospheres. *Int J Pharm*. 2007;343(1-2):262-269.
37. Mizoe T, Ozeki T, Okada H. Preparation of drug nanoparticle-containing microparticles using a 4-fluid nozzle spray drier for oral, pulmonary, and injection dosage forms. *Journal of controlled release : official journal of the Controlled Release Society*. 2007;122(1):10-15.
38. Tomoda K, Ohkoshi T, Nakajima T, Makino K. Preparation and properties of inhalable nanocomposite particles: Effects of the size, weight ratio of the primary nanoparticles in nanocomposite particles and temperature at a spray-dryer inlet upon properties of nanocomposite particles. *Colloids and Surfaces B: Biointerfaces*. 2008;64(1):70-76.
39. Tomoda K, Ohkoshi T, Kawai Y, Nishiwaki M, Nakajima T, Makino K. Preparation and properties of inhalable nanocomposite particles: effects of the temperature at a spray-dryer inlet upon the properties of particles. *Colloids and surfaces B, Biointerfaces*. 2008;61(2):138-144.
40. Ely L, Roa W, Finlay WH, Löbenberg R. Effervescent dry powder for respiratory drug delivery. *European Journal of Pharmaceutics and Biopharmaceutics*. 2007;65(3):346-353.
41. Sham JOH, Zhang Y, Finlay WH, Roa WH, Löbenberg R. Formulation and characterization of spray-dried powders containing nanoparticles for aerosol delivery to the lung. *International Journal of Pharmaceutics*. 2004;269(2):457-467.
42. Kunda NK, Alfagih IM, Miyaji EN, Figueiredo DB, Goncalves VM, Ferreira DM, Dennison SR, Somavarapu S, Hutcheon GA, Saleem IY. Pulmonary dry powder vaccine of pneumococcal antigen loaded nanoparticles. *Int J Pharm*. 2015;495(2):903-912.
43. Atalar I, Dervisoglu M. Optimization of spray drying process parameters for kefir powder using response surface methodology. *LWT - Food Science and Technology*. 2015;60(2, Part 1):751-757.
44. Gu B, Linehan B, Tseng YC. Optimization of the Buchi B-90 spray drying process using central composite design for preparation of solid dispersions. *Int J Pharm*. 2015;491(1-2):208-217.

45. Muzaffar K, Kumar P. Parameter optimization for spray drying of tamarind pulp using response surface methodology. *Powder Technology*. 2015;279:179-184.
46. Ong HX, Traini D, Ballerin G, Morgan L, Buddle L, Scalia S, Young PM. Combined inhaled salbutamol and mannitol therapy for mucus hyper-secretion in pulmonary diseases. *The AAPS journal*. 2014;16(2):269-280.
47. Kauffman KJ, Kanthamneni N, Meenach SA, Pierson BC, Bachelder EM, Ainslie KM. Optimization of rapamycin-loaded acetalated dextran microparticles for immunosuppression. *International Journal of Pharmaceutics*. 2012;422(1-2):356-363.
48. Broaders KE, Cohen JA, Beaudette TT, Bachelder EM, Fréchet JMJ. Acetalated dextran is a chemically and biologically tunable material for particulate immunotherapy. *Proceedings of the National Academy of Sciences*. 2009;106(14):5497-5502.
49. Bachelder EM, Beaudette TT, Broaders KE, Dashe J, Fréchet JMJ. Acetal-Derivatized Dextran: An Acid-Responsive Biodegradable Material for Therapeutic Applications. *Journal of the American Chemical Society*. 2008;130(32):10494-10495.
50. Meenach SA, Anderson KW, Zach Hilt J, McGarry RC, Mansour HM. Characterization and aerosol dispersion performance of advanced spray-dried chemotherapeutic PEGylated phospholipid particles for dry powder inhalation delivery in lung cancer. *European Journal of Pharmaceutical Sciences*. 2013;49(4):699-711.
51. W F. The ARLA Respiratory Deposition Calculator. In.; 2008.
52. Lai SK, Wang Y-Y, Hanes J. Mucus-penetrating nanoparticles for drug and gene delivery to mucosal tissues. *Advanced Drug Delivery Reviews*. 2009;61(2):158-171.
53. Kilicarslan M, Gumustas M, Yildiz S, Baykara T. Preparation and characterization of chitosan-based spray-dried microparticles for the delivery of clindamycin phosphate to periodontal pockets. *Current drug delivery*. 2014;11(1):98-111.
54. Durrigl M, Kwokal A, Hafner A, Segvic Klaric M, Dumcic A, Cetina-Cizmek B, Filipovic-Grcic J. Spray dried microparticles for controlled delivery of mupirocin calcium: process-tailored modulation of drug release. *Journal of microencapsulation*. 2011;28(2):108-121.
55. Cook RO, Pannu RK, Kellaway IW. Novel sustained release microspheres for pulmonary drug delivery. *Journal of Controlled Release*. 2005;104(1):79-90.
56. BUCHI. Mini Spray Dryer B-290 operation manual.
57. Wu X, Zhang W, Hayes D, Jr., Mansour HM. Physicochemical characterization and aerosol dispersion performance of organic solution advanced spray-dried cyclosporine A multifunctional particle for dry powder inhalation aerosol delivery. *Int J Nanomedicine*. 2013; 8:1269-1283.

58. Hickey AJ, Mansour HM, Telko MJ, Xu Z, Smyth HD, Mulder T, McLean R, Langridge J, Papadopoulos D. Physical characterization of component particles included in dry powder inhalers. I. Strategy review and static characteristics. *J Pharm Sci.* 2007;96(5):1282-1301.
59. You Y, Zhao M, Liu G, Tang X. Physical characteristics and aerosolization performance of insulin dry powders for inhalation prepared by a spray drying method. *The Journal of pharmacy and pharmacology.* 2007;59(7):927-934.
60. Vehring R. Pharmaceutical Particle Engineering via Spray Drying. *Pharm Res.* 2008;25(5):999-1022.

CHAPTER 6

Development and Physicochemical Characterization of Acetalated Dextran Aerosol Particle Systems for Deep Lung Delivery

Submitted to International Journal of Pharmaceutics

Zimeng Wang¹, Sweta K. Gupta¹, Samantha A. Meenach^{1,2}

¹University of Rhode Island, College of Engineering, Department of Chemical Engineering, Kingston, RI 02881, USA

²University of Rhode Island, College of Pharmacy, Department of Biomedical and Pharmaceutical Sciences, Kingston, RI 02881, USA

ABSTRACT

Biocompatible, biodegradable polymers are commonly used as excipients to improve the drug delivery properties of aerosol formulations, in which acetalated dextran (Ac-Dex) exhibits promising potential as a polymer in various therapeutic applications. Despite this promise, there is no comprehensive study on the use of Ac-Dex as an excipient for dry powder aerosol formulations. In this study, we developed and characterized pulmonary drug delivery aerosol microparticle systems based on spray-dried Ac-Dex with capabilities of (1) delivering therapeutics to the deep lung, (2) targeting the particles to a desired location, and (3) releasing the therapeutics in a controlled fashion. Two types of Ac-Dex, with either rapid or slow degradation rates, were synthesized. Nanocomposite microparticle (nCmP) and microparticle (MP) systems were successfully formulated using both kinds of Ac-Dex as an excipient and curcumin as a model drug. The resulting MP were collapsed spheres approximately 1 μm in diameter, while the nCmP were similar in size, with wrinkled surfaces, and these systems dissociated into 200 nm nanoparticles upon reconstitution in water. The drug release rates of the Ac-Dex particles were tuned by modifying the Ac-Dex reaction time, particle size, and ratio of fast to slow degrading Ac-Dex. The pH of the environment was also a significant factor that influenced the drug release rate. All nCmP and MP systems exhibited desirable aerodynamic diameters that are suitable for deep lung delivery (e.g. below 5 μm). Overall, the engineered Ac-Dex aerosol particle systems have the potential to provide targeted and effective delivery of therapeutics into the deep lung.

KEYWORDS: Acetalated dextran, nanocomposite microparticles, microparticles, pulmonary delivery, spray drying, controlled release

6.1 Introduction

Pulmonary drug delivery has exhibited promising potential in the treatment of lung diseases, as it allows for the delivery of a wide range of therapeutics directly and efficiently to the lungs, thereby increasing local drug concentration, reducing systemic side effects, providing a rapid onset of pharmaceutical action, and avoiding the first-pass metabolism associated with the liver (1-4). The deep lung (alveolar) region can be utilized as a route for systematic drug delivery due to the enormous surface area available and nearby plentiful capillary vessels that facilitate drug absorption, the very thin (approximately 0.1 μm) liquid layer over the alveoli that ensures rapid and unhindered drug absorption, and low enzymatic activity, which enhances drug availability (1, 5, 6). As a result, various therapeutics such as antibiotics, proteins, peptides, anti-cancer drugs (7), plasmid DNA (8), siRNA (9), and anti-tuberculosis (TB) drugs have been employed in the inhalation forms for the treatment of pulmonary diseases such as asthma, chronic obstructive pulmonary disease (COPD), cystic fibrosis (CF)-related pulmonary infections, and lung cancer (7, 10).

Dry powders is a dosage form that delivers therapeutics to the lung, in the form of particles, using a dry powder inhaler (7). Compared with liquid aerosols, these formulations offer additional benefits such as enhanced stability of the formulation, controllable particle size for targeting different regions of the lung, and increased drug loading of hydrophobic payloads (10, 11). Spray drying has proven to be a suitable

technology in the preparation of dry powder therapeutics (10), as it is capable of producing respirable microparticles for deep lung delivery with acceptable aerosol dispersion properties (4). The properties of dry powder particles such as particle size, particle shape, and surface morphology can be modified by controlling the production process, thus providing desirable particle characteristics (4, 7).

Biocompatible, biodegradable polymers such as poly(ϵ -caprolactone) (PCL) and poly(lactic-co-glycolic acid) (PLGA) have been used as dry powder formulation excipients to carry drug molecules, protect drugs from degradation, and impart sustained release to aerosol formulations (3). However, the PLGA and PCL delivery systems show significant bolus release of their payloads due to bulk erosion of the polymers, and it is difficult to control the polymer degradation rate and modulate their release profiles (12) (Acetalated dextran (Ac-Dex) is an acid-sensitive, biodegradable, biocompatible polymer prepared via a one-step reaction by reversibly modifying dextran with acetal groups. This modification reverses the solubility properties of dextran from hydrophilic to hydrophobic, making it possible to form polymeric particles using standard emulsion or nanoprecipitation techniques. In contrast to other commonly used polymers such as PLGA, polylactic acid, and PCL, Ac-Dex exhibits attractive properties suitable for the controlled release of the payloads. By controlling the reaction time during the formation of Ac-Dex, the ratio of cyclic acetal groups with a slower degradation rate to acyclic acetal groups with a faster degradation rate can be adjusted. As a result, the degradation rate of the resulting Ac-Dex can be tuned from hours to months to suit various applications. Moreover, the acid-sensitivity of Ac-Dex enables it to degrade faster in lower pH environments, such as lysosomes in macrophage or tumor cells, allowing for

controlled release of drug. Furthermore, Ac-Dex degrades into neutral by-products, which avoids undesirable changes in the micro-environmental pH in the body. Finally, Ac-Dex offers the potential of targeted delivery, due to the dextran chains present that can be further modified with a variety of functional moieties, which can enhance the efficacy of therapeutic delivery to a targeted site (13-15).

Owing to aforementioned advantages, Ac-Dex has been widely applied in the formation of polymeric carriers for drug delivery. Porous Ac-Dex microparticles loaded with the chemotherapeutic camptothecin for pulmonary delivery were developed using emulsion techniques, which exhibited in a respirable fraction of 37% and experimental mass mean aerodynamic diameters from 5.3 - 11.9 μm (2). Ac-Dex nanoparticle systems have also been investigated in the application of protein delivery for immunotherapy (13), gene delivery to phagocytic and non-phagocytic cells (11), tandem delivery of peptide and chemotherapeutic for controlled combination chemotherapy (1), delivery of the host-mediated compound AR-12 (Arno Therapeutics; formerly known as OSU-03012) for the treatment of *Leishmania donovani* (6), and the control of *Salmonella* infection (6). Both Ac-Dex nanoparticles and microparticles loaded with horseradish peroxidase have been evaluated to improve vaccine stability outside cold chain conditions (16).

Despite this work, there is no comprehensive study on using Ac-Dex as an excipient for dry powder aerosol formulations. In this study, we aimed to develop and characterize pulmonary delivery systems based on spray-dried Ac-Dex particles with capabilities of (a) delivering therapeutics to the deep lung, (b) targeting the particles to a particular location in the lungs, and (c) releasing therapeutics in controlled rate. Previous

studies have shown that: (a) aerodynamic diameter (d_a) determines the region of the lungs where particles will deposit, where particles with an d_a of 1 - 5 μm tend to deposit in the deep lung region (10); (b) geometric size plays an important role in the cellular uptake of particles, where nanoscale particles (approximately 150 nm) tend to escape phagocytic uptake (17), while particles larger than 1 μm will suffer from macrophage clearance in the alveoli (18); and (c) the drug release rate of Ac-Dex particles can be tuned by modifying the synthesis time of the Ac-Dex polymer (2, 15).

To prepare the engineered particle systems, two types of Ac-Dex with rapid or slow degradation rates were synthesized. Nanocomposite microparticle (nCmP) and microparticle (MP) systems were successfully formulated using both kinds of Ac-Dex as the excipient and curcumin (CUR) as the model drug. The nCmP were prepared by spray drying an aqueous suspension of CUR-loaded Ac-Dex nanoparticles (200 nm) and the MP were formulated by spray drying a solution of Ac-Dex and CUR in a solution of tetrahydrofuran (THF) and acetone. We hypothesize that upon pulmonary administration, the nCmP will deposit in the deep lung, decompose into free NP, and will facilitate the sustained release of drug to the targeted site, while the MP will remain the original size after deposition in the deep lung region. A schematic of particle preparation and design is shown in **Figure 6.1**. Overall, the goal of the described research was the initial development and physicochemical characterization of dry powder Ac-Dex aerosol particle systems with the potential for effective delivery of therapeutics in to the deep lung, targeting at desired pulmonary location, and continuous controlled release of a drug.

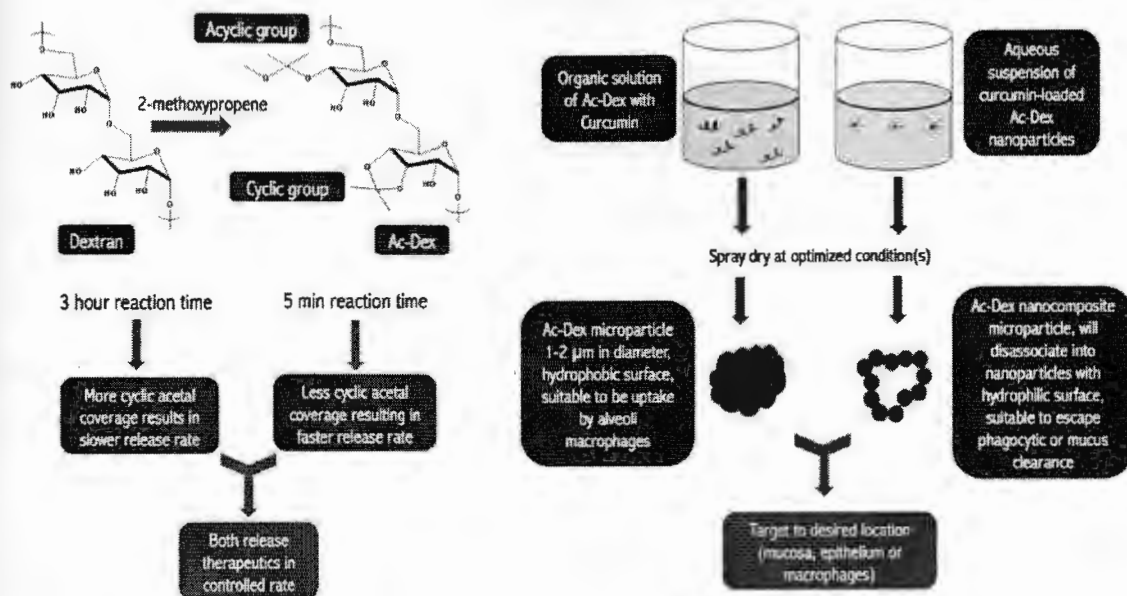


Figure 6.1. Schematic depicting the of synthesis of Ac-Dex (Left) and preparation of nanoparticles and formation of nanocomposite microparticles (nCmP) and microparticles (MP) (Right).

6.2. Materials and Methods

6.2.1 Materials

Dextran from *Leuconostoc mesenteroides* (9000-11000 MW), pyridinium p-toluenesulfonate (PPTS, 98%), 2-methoxypropene (2-MOP, 97%), triethylamine (TEA, $\geq 99\%$), anhydrous dimethyl sulfoxide (DMSO, $\geq 99.9\%$), poly(vinyl alcohol) (PVA, MW 13,000-23,000, 87-89% hydrolyzed), dichloromethane (DCM, anhydrous, $\geq 99.8\%$), deuterium chloride (DCl, 35 weight % in D₂O, 99 atom % D), Tween® 80, curcumin,

sodium acetate ($\geq 99\%$), acetic acid solution (1.0 N), acetone ($\geq 99.8\%$), tetrahydrofuran (THF, $\geq 99\%$), and methanol (anhydrous, $\geq 99.9\%$) were obtained from Sigma–Aldrich (St. Louis, MO). Deuterium oxide (D_2O , 99.8% atom D) was obtained from Acros Organics (Geel, Belgium). Phosphate buffered saline (PBS) was obtained from Fisher Scientific (Somerville, NJ). Hydranal® KF reagent was obtained from Fluka Analytical.

6.2.2 Synthesis and NMR Analysis of Acetalated Dextran (Ac-Dex)

Ac-Dex was synthesized as described previously (14) with minor modifications. 1 g of lyophilized dextran and 25 mg of PPTS were dissolved in 10 mL of anhydrous DMSO. The resulting solution was reacted with 5 mL of 2-MOP under nitrogen gas for 5 minutes to prepare Ac-Dex with a rapid degradation rate (Ac-Dex-5min) or for 3 hours to prepare Ac-Dex with a slower degradation rate (Ac-Dex-3h). The reaction was quenched with 1 mL of TEA. The reaction mixture was then precipitated in basic water (water and TEA, pH 9), vacuum filtered, and lyophilized ($-50\text{ }^\circ\text{C}$, 0.023 mbar) for 24 hours to yield a solid product.

The cyclic-to-acyclic (CAC) ratio of acetal coverage and degrees of total acetal coverage per 100 glucose molecules was confirmed by ^1H NMR spectroscopy (Bruker 300 MHz NMR, MA). 10 mg of Ac-Dex was added to 700 μL of D_2O and was hydrolyzed with 30 μL of DCl prior to analysis. The hydrolysis of one cyclic acetal group produces one acetone molecule whereas one acyclic acetal produces one acetone and one methanol molecule each. Consequently, from the normalized integration of peaks related to acetone, methanol, and the carbon ring of dextran, the CAC ratio of acetal coverage and degrees of total acetal coverage per 100 glucoses were determined.

6.2.3 Formation of CUR-Loaded Ac-Dex Nanoparticles (CUR NP)

Curcumin-loaded nanoparticles (CUR NP) were prepared via an oil/water emulsion solvent evaporation using Ac-Dex-5min, Ac-Dex-3h, or a mixture of both types of Ac-Dex (50 % w/w). 49 mg of Ac-Dex and 1 mg of CUR were dissolved in 1 mL of DCM over an ice bath, establishing the organic phase. The aqueous phase was comprised of 6 ml of 3% PVA in PBS and was added to the organic phase. The resulting mixture was sonicated (Q500 Sonicator, Qsonica, Newtown, CT) for 30 seconds with a 1 second on/off pulse at 70% amplitude. The emulsion was transferred to a spinning solution of 0.3% PVA in PBS and was stirred for 3 hours to allow for evaporation of the organic solvent and particle hardening. The solution was then centrifuged at 19802 \times g for 20 minutes to collect the nanoparticles. Nanoparticles were washed once with DI water, redispersed in 0.1% PVA, and lyophilized (-50 °C, 0.023 mbar) for 48 hours. The resulting NP systems were: CUR NP-5min (made of Ac-Dex-5min), CUR NP-3h (made of Ac-Dex-3h), and CUR NP-h (50 wt% Ac-Dex-5min and 50 wt% Ac-Dex-3h).

6.2.4 Formulation of CUR Nanocomposite Microparticles (nCmP) Via Spray Drying

CUR nCmP were prepared via the spray drying of an aqueous suspension of each type of CUR NP (0.5%, w/v) using a Büchi B-290 spray dryer (Büchi Labortechnik, AG, Switzerland) in open mode. The CUR-NP suspension was sonicated for 10 minutes before spray drying. The spray drying conditions were as follows: 0.7 mm nozzle diameter, atomization gas flow rate of 414 L/h using dry nitrogen, aspiration rate of 28 m^3/h , pump rate of 0.9 mL/min, and nozzle cleaner rate of 3. The resulting nCmP were separated in a high-performance cyclone, dried for 15 minutes in the spray dryer,

collected in a sample collector, and stored in amber glass vials in a desiccator at -20°C . nCmP comprised of each kind of NP described previously were produced: nCmP-5min, nCmP-3h, and nCmP-h, correspondingly.

6.2.5 Formulation of CUR Microparticles (MP) Via Spray Drying

CUR MP were prepared via the spray drying of an organic solution of a mixture of Ac-Dex and CUR (2 %, w/v) using a Büchi B-290 spray dryer in closed mode. The organic solutions were prepared by dissolving CUR and Ac-Dex (2:98 w/w) in an organic solvent comprised of 85% acetone and 15% THF (v/v) at a solids concentration of 2% (w/v). The spray drying conditions were as follows: 0.7 mm nozzle diameter, atomization gas flow rate of 414 L/h using UHP dry nitrogen, aspiration rate of $40\text{ m}^3/\text{h}$, pump rate of 3 mL/min, and nozzle cleaner rate of 0. The resulting MP were separated in a high-performance cyclone, dried for 15 minutes in the spray dryer, collected in a sample collector, and stored in amber glass vials in a desiccator at -20°C . The resulting MP were: MP-5min (from Ac-Dex-5min), MP-3h (from Ac-Dex-3h), and MP-h (from 50 wt% Ac-Dex-5min and 50 wt% Ac-Dex-3h).

6.2.6 Particle Size, Size Distribution, and Zeta Potential Analysis

The average diameter, size distribution, and zeta potential of the original NP and the NP entrapped in the nCmP were measured by dynamic light scattering (DLS) using a Malvern Nano Zetasizer (Malvern Instruments, Worcestershire, UK). Original NP were dispersed in DI water (pH = 7, 0.3 mg/mL), and nCmP were dispersed in DI water as well

to recover the entrapped NP. All experiments were performed in triplicate with a scattering angle of 173° at 25°C .

6.2.7 Particle Morphology and Shape Analysis via Scanning Electron Microscopy (SEM)

The shape and surface morphology of the nCmP and MP were evaluated by SEM using a Zeiss SIGMA VP Field Emission-Scanning Electron Microscope (FE-SEM) (Germany). Particle samples were placed on aluminum SEM stubs (Ted Pella, Inc., Redding, CA) with double-sided adhesive carbon tabs. Both the nCmP and MP samples were coated with a thin film of a gold/palladium alloy using a BIO-RAD sputter coating system at $20\ \mu\text{A}$ for 60 seconds under argon gas. Images were captured at 8 kV at various magnifications. The geometric mean diameter and standard deviation of the MP were measured digitally from SEM images using ImageJ software (19). Representative micrographs (5000x magnification) for each sample were analyzed by measuring the diameter of at least 100 particles.

6.2.8 Tapped Density Evaluation

The tapped density of the particles was measured as described previously with minor modifications (20). 35 - 40 mg of nCmP or MP was weighed into a glass tube. The tube was tapped 200 times to ensure efficient packing of the nCmP and then the volume occupied by the particles was measured using calipers. The density was determined by the following equation:

$$\rho = \frac{m}{V}$$

where ρ is the tapped density, m is the particles mass, and V is the volume occupies by the particles as determined by measuring the height of the particles in the tube with a known diameter (5 mm). The theoretical MMAD ($MMAD_T$) of the particles was then calculated using the following equation:

$$MMAD_T = d \sqrt{\frac{\rho}{\rho^*}}$$

where d is the geometric diameter determined by ImageJ, ρ is the tapped density of the particles, and $\rho^* = 1 \text{ g/cm}^3$, which is the reference density of solid polymer.

6.2.9 Drug Loading Analysis of CUR nCmP and CUR MP

Drug loading and encapsulation efficiency of CUR nCmP and CUR MP were determined via fluorescence spectroscopy (Biotek Cytation 3, Winooski, VT). All particle samples were dissolved in DMSO and were evaluated at 420 nm (excitation) and 520 nm (emission). The CUR drug loading and encapsulation efficiency (EE) of the particles were determined by the following equations:

$$\text{Drug loading} = \frac{\text{mass of CUR loaded in particles}}{\text{mass of particles}}$$

$$\text{Encapsulation efficiency (EE)} = \frac{\text{mass of CUR loaded in particles}}{\text{initial mass of CUR in particles}} \times 100\%$$

6.2.10 *In Vitro* Drug Release from nCmP and MP

The *in vitro* release profiles of CUR from nCmP and MP were determined via the release of suspended particles (0.5 mg/mL, 1.5 mL) in modified phosphate buffer (0.1 M, pH = 7.4, 0.5 wt% Tween® 80) and modified acetate buffer (0.1 M, pH = 5, 0.5 wt% Tween® 80). The particle suspension was incubated at 37 °C and 100 rpm. At various time points, particle samples were centrifuged at 23102 ×g for 5 minutes at 4 °C to isolate the NP. 200 µL of supernatant was withdrawn and replaced by the same amount of fresh modified buffer in each sample. The withdrawn solutions were mixed with same volume of DMSO and analyzed for CUR content via fluorescence spectroscopy using the same method described for drug loading. The release data was fitted to several commonly utilized drug release models (S.6.1) to study the mechanism of drug release of Ac-Dex particles. The coefficient of determination (R^2) was applied to test the applicability of the release models.

6.2.11 Differential Scanning Calorimetry (DSC)

The thermal phase transitions of the nCmP, MP, and their raw components were determined via DSC using a TA Q10 DSC system (TA Instruments, New Castle, DE, USA) equipped with an automated computer-controlled TA instruments DSC refrigerated cooling system. 1 - 3 mg of sample was weighed into Tzero™ alodine-coated aluminum

pans that were hermetically sealed. The sealed pans were placed into the DSC furnace along with an empty sealed reference pan. The heating range was 0 – 200 °C at a heating rate of 10 °C/min.

6.2.12 Powder X-Ray Diffraction (PXRD)

The crystalline states of the nCmP, MP, and its raw components were examined by PXRD using a Rigaku Multiflex X-ray diffractometer (The Woodlands, TX) with a Cu K α radiation source (40 kV, 44 mA). The samples were placed on a horizontal quartz glass sample holder (3 mm) prior to analysis. The scan range was 5 – 60° in 2 θ with a step width of 0.1 and scan rate of 1 °/min.

6.2.13 Karl Fischer Coulometric Titration

The water content of the nCmP and MP was quantified by Karl Fischer (KF) titration using a 737 KF coulometer (Metrohm, Riverview, FL). 5 mg of powder was dissolved in anhydrous methanol. The resulting solution was injected into the KF reaction cell filled with Hydranal® KF reagent and then the amount of water was analyzed. Pure solvent was also injected for use as a background sample.

6.2.14 *In Vitro* Aerosol Dispersion Performance with the Next Generation Impactor (NGI)

In vitro aerosol dispersion performance of the nCmP and MP was evaluated using a Next Generation Impactor™ (NGI™, MSP Corporation, Shoreview, MN) equipped with a stainless steel induction port (USP throat adaptor) attachment and stainless steel

gravimetric insert cups. The NGI™ was coupled with a Copley TPK 2000 critical flow controller, which was connected to a Copley HCP5 vacuum pump (Copley Scientific, United Kingdom). The air flow rate (Q) was measured and adjusted to 60 L/min in order to model the flow rate in a healthy adult lung before each experiment. Glass fiber filters (55 mm, Type A/E, Pall Life Sciences, PA) were placed in the gravimetric insert cups for stages 1 through 7 to minimize particle bounce or re-entrapment (10) and these filters were weighed before and after the experiment to determine the particle mass deposited on each stage. Approximately 10 mg of powder was loaded into a hydroxypropyl methylcellulose (HPMC, size 3, Quali-V®, Qualicaps® Inc., Whitsett, NC, USA) capsule and the capsule was placed into a human dry powder inhaler device (HandiHaler, Boehringer Ingelheim Pharmaceuticals, CT) attached to a customized rubber mouthpiece connected to the NGI™. Three HPMC capsules were loaded and released in each measurement and experiments were performed in triplicate. The NGI™ was run with a delay time of 10 s and running time of 10 s. For Q = 60 L/min, the effective cutoff diameters for each stage of the impactor were given from the manufacturer as: stage 1 (8.06 μm); stage 2 (4.46 μm); stage 3 (2.82 μm); stage 4 (1.66 μm); stage 5 (0.94 μm); stage 6 (0.55 μm); and stage 7 (0.34 μm). The fine particle dose (FPD), fine particle fraction (FPF), respirable fraction (RF), and emitted dose (ED) were calculated as follows:

$$\text{Fine particles fraction (FPF)} = \frac{\text{mass of particles on Stages 2 through 7}}{\text{initial particle mass loaded into capsules}} \times 100\%$$

$$\text{Respirable fraction (RF)} = \frac{\text{mass of particles on Stages 2 through 7}}{\text{total particle mass on all stages}} \times 100\%$$

$$\text{Emitted Dose (ED)} = \frac{\text{initial mass in capsules} - \text{final mass remaining in capsules}}{\text{initial mass in capsules}} \times 100\%$$

The experimental mass median aerodynamic diameter (MMAD_T) and geometric standard deviation (GSD) for the particles were determined using a Mathematica® program written by Dr. Warren Finlay (10, 21).

6.2.15 Statistical analysis

All measurements were performed in at least triplicate. Values are given in the form of mean \pm standard deviation. The statistical significance of the results was determined using analysis of variance (ANOVA) and student's t-test. A p-value of <0.05 was considered statistically significant.

6.3. Results and Discussion

6.3.1 Preparation and Characterization of Ac-Dex and Curcumin Nanoparticles

6.3.1.1 NMR Analysis of Ac-Dex

Successful synthesis of Ac-Dex was confirmed by ^1H NMR. Ac-Dex-5min exhibited 61.2% cyclic acetal coverage (CAC) and 71.6% total conversion of -OH

groups, while Ac-Dex-3h exhibited 82.5% CAC and 80.0% total conversion of -OH groups. The Ac-Dex with longer synthesis time (Ac-Dex-3h) exhibited a higher CAC, which was in accordance with previous studies. An increase in CAC is known to decrease polymer degradation and ultimately, the drug release rate, due to the slower degradation of the cyclic acetal groups on the Ac-Dex backbone (13, 14). Ac-Dex-3h also showed a higher total conversion of -OH groups, which could be a result of elongated reaction time. This higher total acetal coverage is favorable in the enhancement of the stability of the PVA coating of nanoparticles (data not shown), thus ensuring small particle size and narrow size distribution.

6.3.1.2 Dynamic Light Scattering (DLS) Analysis of Original and Redispersed CUR NP

Average nanoparticle (NP) size, size distribution/polydispersion index (PDI), and zeta potential are shown in **Table 6.1**. No significant changes in NP size, PDI, or zeta potential was found between the original and redispersed NP ($p < 0.05$), indicating that the CUR NP maintained their desirable properties after redispersion. The original and redispersed NP exhibited an average diameter of approximately 200 nm, which is in the desirable range to avoid macrophage clearance and mucus entrapment (18). The low PDI value denotes a narrow size distribution of the NP, and the slightly negatively charged surface of nanoparticles, as measured by zeta potential, is desirable in order to reduce the interactions with negatively charged mucin fibers in the airway mucus (22). According to our preliminary experiments (data not shown), a low total conversion of -OH groups on the Ac-Dex results in NP with larger sizes and PDI due to NP agglomeration. This phenomenon could be a result of the lessened hydrophobicity of Ac-Dex with fewer -OH

groups converted to acetal groups, which leads to insufficient absorption of PVA on the NP surface. However, the Ac-Dex in this study was prepared to produce NP with small sizes and low PDI, as the total conversion of -OH groups was kept in a higher range to prevent NP agglomeration.

Table 6.1. Average diameter (as measured by dynamic light scattering), polydispersity index (PDI), and zeta potential (ZP) of CUR-loaded nanoparticles before spray drying (NP) and after redispersion from nanocomposite microparticles (nCmP) (mean \pm standard deviation, n = 3).

	Average Diameter (nm)	PDI	ZP (mV)
NP-5min	192.2 \pm 2.7	0.07 \pm 0.03	-8.4 \pm 4.1
NP-h	201.1 \pm 1.5	0.02 \pm 0.01	-8.0 \pm 3.7
NP-3h	206.1 \pm 1.3	0.03 \pm 0.03	-7.0 \pm 1.6
nCmP-5min	199.3 \pm 1.3	0.09 \pm 0.02	-14.5 \pm 1.0
nCmP-h	210.2 \pm 2.5	0.07 \pm 0.01	-13.3 \pm 1.9
nCmP-3h	213.5 \pm 2.4	0.02 \pm 0.00	-11.2 \pm 1.6

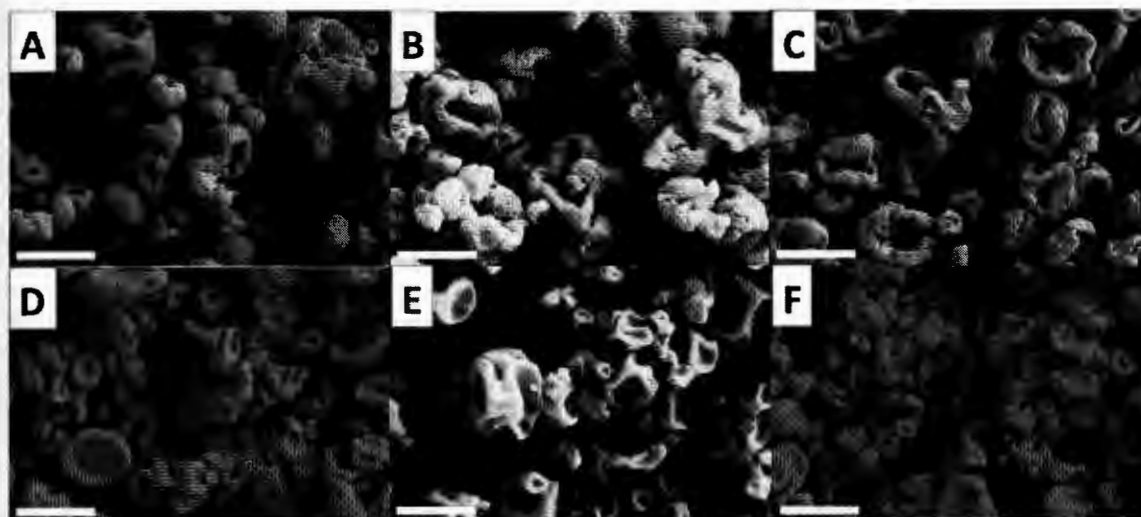


Figure 6.2. SEM micrographs of curcumin-loaded nanocomposite microparticles (CUR nCmP) and microparticles (CUR MP) including: (A) CUR nCmP-5min, (B) CUR nCmP-h, (C) CUR nCmP-3h, (D) CUR MP-5min, (E) CUR MP-h, and (F) CUR MP-3h systems. Scale bar = 2 μm .

6.3.2 Preparation and Characterization of Nanocomposite Microparticles (nCmP) and Microparticles (MP)

6.3.2.1 Morphology, Sizing, and Size Distribution

CUR nCmP displayed a wrinkled and raisin-like surface with visibly encapsulated NP as seen in **Figures 6.2A-C**. The raisin-like morphology of the nCmP can be attributed to the early formation of nanoparticle shells in the solution droplets during spray drying, which determines the geometric size of nCmP during spray drying. As the drying process proceeds, the remaining solvent evaporates from the droplet center, resulting in hollow particles that tend to shrink (23, 24).

CUR MP were collapsed spheres with smooth surfaces as seen in **Figures 6.2D-F**. Differing the Ac-Dex composition of particles had no impact on particle morphology. The geometric diameters (d_g) of the CUR nCmP and MP system are shown in **Table 6.2**. All of the MP d_g were approximately 1 μm in size, which is reported to make the particles vulnerable to macrophage uptake (25). On the contrary, the nCmP system can escape macrophage clearance as they dissociate into NP upon reaching the deep lung.

Table 6.2. Geometric diameter (as measured by SEM imaging and ImageJ analysis), water content, tapped density, theoretical mean mass aerodynamic diameter (MMAD_T), drug loading, and drug encapsulation efficiency of nCmP and MP (mean \pm standard deviation, $n = 3$).

Particle System	Geometric Diameter (μm)	Water Content (%)	Tapped Density (g/cm^3)	MMAD_T (μm)	Drug Loading (mg/100 mg particle)	Encapsulation Efficiency (%)
nCmP-5min	1.50 ± 0.52	7.69 ± 0.76	0.122 ± 0.001	0.52 ± 0.09	0.57 ± 0.006	28.7 ± 0.32
nCmP-h	1.78 ± 0.67	7.89 ± 1.56	0.115 ± 0.004	0.60 ± 0.09	0.58 ± 0.008	28.4 ± 0.42
nCmP-3h	1.77 ± 0.87	7.86 ± 0.43	0.133 ± 0.002	0.64 ± 0.12	0.62 ± 0.013	31.2 ± 0.63
MP-5min	0.93 ± 0.34	6.12 ± 1.33	0.050 ± 0.001	0.21 ± 0.03	1.33 ± 0.092	66.3 ± 4.62
MP-h	1.29 ± 0.42	5.87 ± 1.85	0.050 ± 0.001	0.29 ± 0.32	1.03 ± 0.030	51.6 ± 1.48
MP-3h	1.03 ± 0.45	5.23 ± 1.13	0.052 ± 0.001	0.23 ± 0.03	1.12 ± 0.012	55.8 ± 0.61

6.3.2.2 Analysis of Particle Density

The density of the particles was determined via tapped density measurements, as shown in **Table 6.2**. CUR nCmP exhibited tapped density values around 0.12 g/cm^3 , while the MP system showed values around 0.05 g/cm^3 . These density values are relatively low compared with the raw materials ($\sim 1 \text{ g/cm}^3$), which can be attributed to the wrinkled morphology and hollow structures of the particle systems. It has been reported that particles $> 1 \text{ }\mu\text{m}$ in diameter and having greater density will get deposited in the lung by sedimentation (26). Therefore, the increased density of CUR nCmP system as compared to MP will enhance their rate of deposition into the deep lung.

6.3.2.3 CUR Loading and in Vitro Release of CUR

CUR was successfully encapsulated into both the nCmP and MP systems as seen in **Table 6.2**. The MP systems prepared via closed mode, organic spray drying exhibited higher encapsulation efficiency (EE, $> 50\%$) than the nCmP systems (approximately 30%) prepared in open mode in aqueous solutions. The lower EE of the nCmP can be attributed to the low EE of the original CUR-loaded NP, which was also approximately 30%. The spray drying process had no influence on the CUR loading and EE for the nCmP systems ($p < 0.05$), which indicates that the drug loading of nCmP systems can be determined during NP preparation.

Results of the *in vitro* release of CUR from nCmP and MP systems in modified phosphate (pH 7.4) and acetate (pH 5) buffers at physiological temperature (37°C) are reported in **Figure 6.3** as the percentage of cumulative drug released over time. As shown in **Table C.1**, all particle systems exhibited shorter release duration and increased release

of CUR ($p < 0.05$) at acidic pH (except nCmP-5min), which is in accordance with previous studies (2, 27). The pH-sensitive release profiles suggest that the drug will be released at significantly higher rates once the carrier particles reaches an acidic environment. This can allow the Ac-Dex particles the ability to provide the controlled release of a therapeutic payload in cells and tissue with lower pH values, such as tumor cells and macrophages. On the contrary, if the carrier particles remain in the extracellular or neutral pH environments, the release rate can be reduced, which will minimize systemic and local cytotoxicity (2).

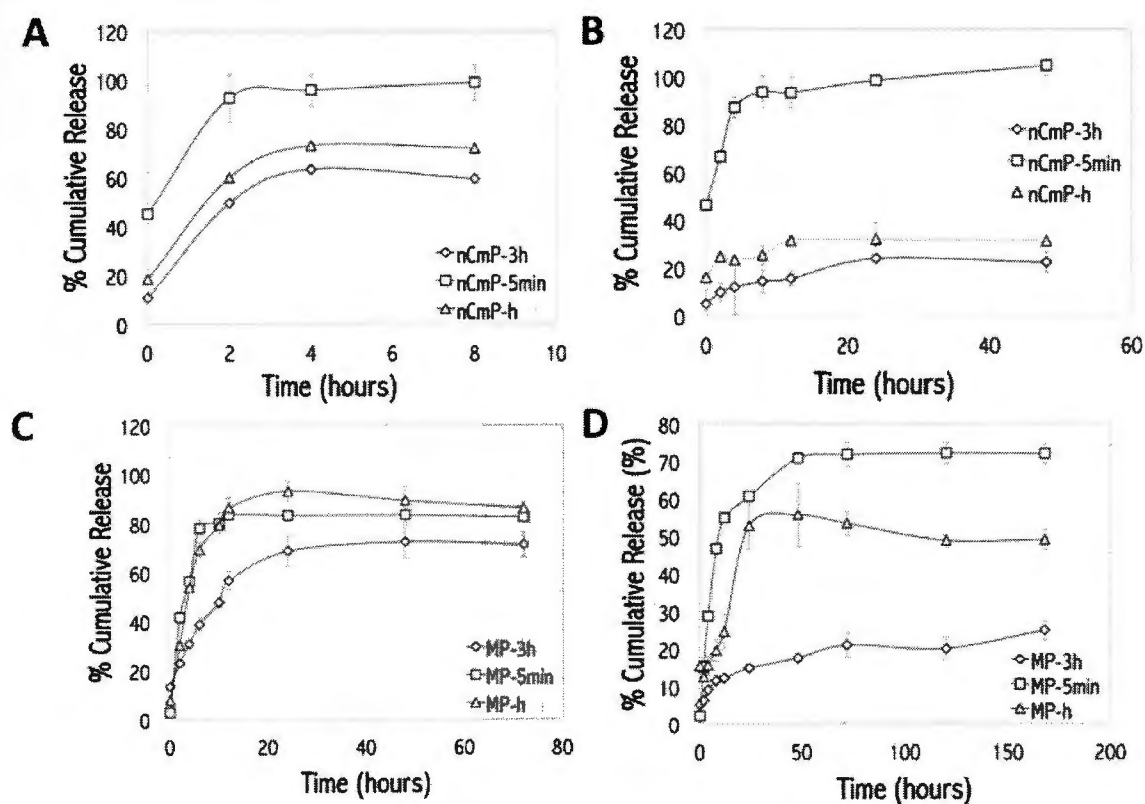


Figure 6.3. *In vitro* drug release profiles for curcumin (CUR) nanocomposite microparticle (nCmP) and microparticle (MP) systems including CUR nCmP-5min, CUR nCmP-h, CUR nCmP-3h, CUR MP-5min, CUR MP-h, and CUR MP-3h at pH 5 and 7.4.

In addition, the nCmP systems exhibited faster release than MP systems, which is likely due to the larger surface area available in the nano-sized delivery systems. Upon reaching an aqueous environment, the nCmP dissociate into nanoparticles with large surface area and a PVA coating that facilitates particle dispersity, while the MP may agglomerate due to their highly hydrophobic surfaces. As a result, the nCmP systems undergo faster polymer degradation and drug diffusion, resulting in a faster release of payloads than MP at both acidic and physiologic pH. Particles made of Ac-Dex-3h exhibited slower release rates than those comprised of Ac-Dex-5min, indicating that the drug release rate can be controlled by the polymer reaction time. At pH 7.4, particles made of Ac-Dex-h exhibited a drug release rate between Ac-Dex-5 min and Ac-Dex-3h, suggesting that the ratio of different types of Ac-Dex can also act as an important factor in adjusting the release profiles of particle systems. However, the drug release rates of the Ac-Dex particles at pH 5 did not follow this trend, which could be explained by the following two mechanisms: (1) The release profile of Ac-Dex particles is polymer degradation/erosion controlled, and the decomposition of the Ac-Dex matrix is greatly impacted by buffer pH. A study based on design of experiment will be conducted in our further research to illustrate the influence of potential factors (reaction time, polymer ratio, particle size, and pH) on the drug release profile of particle systems. (2) The release profile of Ac-Dex particles is both polymer degradation/erosion and drug diffusion controlled. In previous studies, the drug release of Ac-Dex particles is believed to be associated with Ac-Dex degradation (2, 14, 15). However, Ac-Dex degradation may cause surface erosion of particles, formation of large pores in the particles that facilitate drug diffusion, or both at the same time. As a result, the drug release profile could be

controlled by drug diffusion through water-filled pores (diffusion controlled), polymer erosion on the particle surface (erosion controlled), or both drug diffusion and surface erosion (diffusion and erosion controlled), respectively (13).

In order to further illustrate the mechanism of drug release of Ac-Dex particles, we fit the release data to several commonly utilized drug release models, including: (1) a first order model and (2) Hixson–Crowell model for drug dissolution controlled release, (3) Higuchi model modified to fit the burst release at time 0, (4) Korsmeyer–Peppas model and (5) Baker–Lonsdale for drug diffusion controlled release, (6) Hopfenberg model for surface erosion controlled, (7) Baker’s model for both degradation and diffusion controlled, and (8) Weibull model as a general empirical equation to describe a dissolution or release process (28-32). The coefficient of determinations (R^2) of all the models are summarized in **Table C.2**, and the modified Higuchi and Baker–Lonsdale models exhibited higher R^2 compared with other models, indicating that the drug release profile of Ac-Dex particles in both pH buffers was due primarily to drug diffusion. For Baker’s model (28) that describes a degradation and diffusion process, the optimal coefficient k was 0, making the Baker’s model the same with Higuchi model. Considering that the degradation of Ac-Dex was observable during the release test, the release profile of Ac-Dex particles can be explained by the mechanism of drug diffusion through water-filled pores (32). In this process, water was absorbed by Ac-Dex particles and filled in the pores of the polymer matrix, through which the drug diffused into the buffer. As polymer degraded, both pore size and number increased, leading enhanced drug release. Therefore, the reaction time of Ac-Dex affected the drug release rate significantly by controlling the formation of pores of particle matrix but not polymer

degradation on the surface. Meanwhile, the water absorption into the particles may also influence the drug release rate, which can be supported by the fact that Ac-Dex-3h had a higher ratio of total hydrophobic acetalated group conversion than Ac-Dex-5min. The fitted release curves using modified Higuchi model are shown in **Figure S6.1** along with the original data points. The model was modified to fit the burst release at time 0 of some of the particle systems, which is attributed to the CUR initially available on the surface of particles. The nCmP systems exhibited a higher release at time 0 because that the nanoparticle suspension was sonicated before spray drying to form a uniform dispersion, which may lead to CUR release in to the suspension.

3.3.2.4 Karl Fischer Titration

The residual water content of CUR nCmP and MP is shown in **Table 6.2**. The water content of nCmP system was approximately 8%, while that of MP system was approximately 6%. The lower water content of MP samples is likely due to the absence of water during the closed mode spray drying process. All the particle systems showed acceptable water content. In general, reducing the water content in inhalable dry powders can significantly improve their dispersion properties and enhance the stability of the powders during storage (33, 34). Correspondingly, low water content in inhalable dry powders is highly favorable for efficient dry powder aerosolization and effective particle delivery (34, 35).

6.3.2.5 Differential Scanning Calorimetry

Figure 6.4 shows DSC thermograms of the raw materials used in particle preparation and the final CUR nCmP and CUR MP systems. Both the raw Ac-Dex-5min and Ac-Dex-3h displayed endothermic main phase transition peaks (T_m) near 170 °C. The peaks were broad because of the wide size distribution of Ac-Dex polymer crystallites. The raw CUR powder displayed a sharp peak at 180 °C corresponding to the melting point of crystalline CUR, which is consistent with earlier studies (36). None of the CUR nCmP systems exhibited a peak corresponding to Ac-Dex melting, which indicates that the Ac-Dex was turned amorphous by rapid precipitation during NP formation. All of the CUR MP systems exhibited a broad peak near 160 °C, which corresponds to the melting of Ac-Dex. This phase transition shifted to the lower temperature range, indicating an increase in the amorphous state of Ac-Dex after the spray drying process. None of the CUR nCmP or CUR MP displayed melting peaks that would correspond to raw CUR, indicating that the crystalline CUR was converted to an amorphous phase during particle preparation.

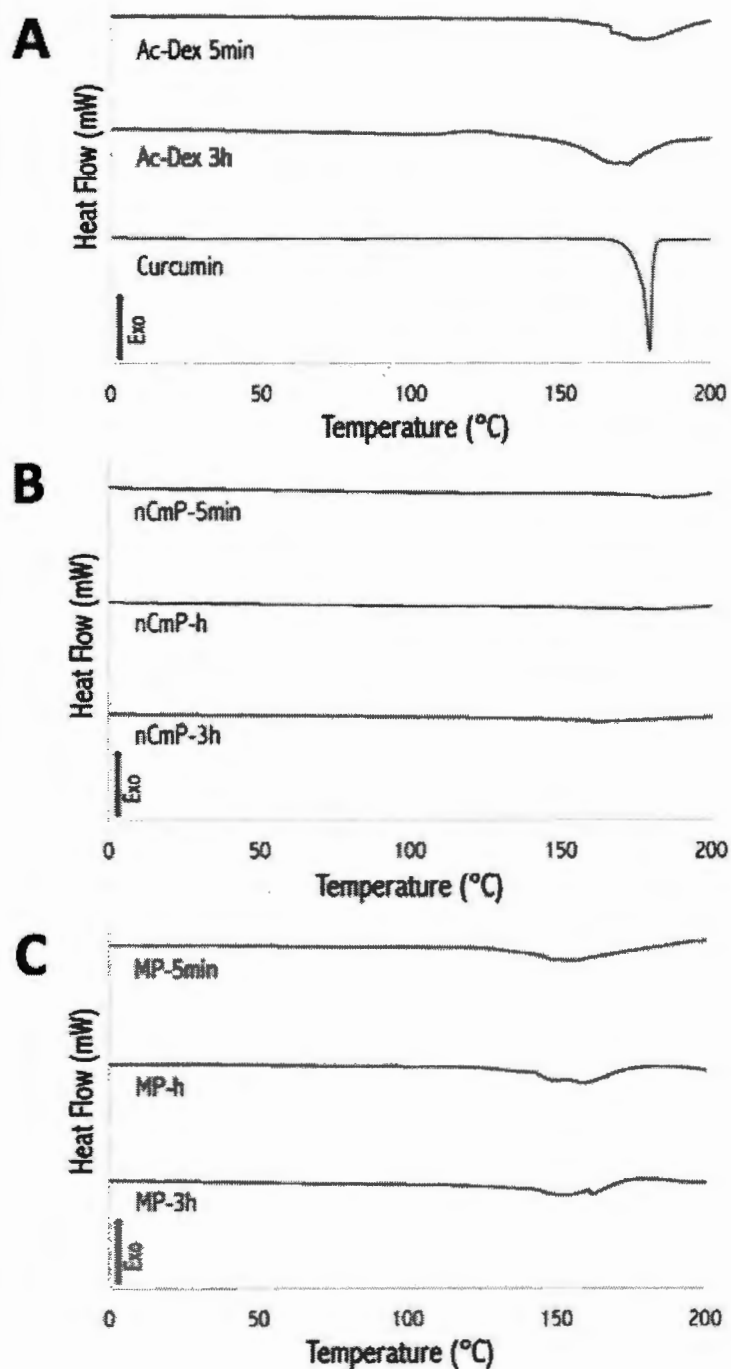


Figure 6.4. Representative differential scanning calorimetry (DSC) thermograms of raw curcumin (CUR), raw acetalated dextran-5min (Ac-Dex-5min), raw acetalated dextran-3h (Ac-Dex-3h), CUR nCmP-5min, CUR nCmP-h, CUR nCmP-3h, CUR MP-5min, CUR MP-h, and CUR MP-3h.

6.3.2.6 Powder X-ray Diffraction (PXRD)

X-ray diffraction diffractograms of the raw materials, CUR nCmP, and CUR MP are shown in **Figure 6.5**. Strong peaks were present for raw CUR indicating that it is in a crystalline form prior to spray drying. No peaks were present for either raw Ac-Dex samples, suggesting an irregular distribution of Ac-Dex crystallites. The absence of diffraction peaks from Ac-Dex is quite different from commercialized polymers such as PLGA, which exhibits strong XRD characterization peaks (34). This phenomenon is likely because the Ac-Dex was collected by rapid precipitation in water, which prevents the formation of large polymer crystallites. XRD diffractograms of the CUR nCmP and CUR MP were absent in any diffraction peaks corresponding to raw CUR, indicating that the crystalline CUR was converted to an amorphous phase in the spray drying or emulsion evaporation process. The amorphization of raw payloads into the particle matrix is suitable for the improvement in solubility of hydrophobic drugs in physiological conditions. The results obtained from the XRD diffractograms confirmed those from DSC thermograms, which proves that raw CUR was converted to amorphous forms during the particle manufacturing process.

6.3.2.8 In Vitro Aerosol Dispersion Performance Using Next Generation Impactor (NGI)

In vitro aerosol dispersion performance properties of the nCmP were evaluated using a Next Generation Impactor™ coupled with a human DPI device (**Figure 6.6 and Figure 6.7**). The results indicated that the formulated nCmP and MP are favorable for efficient dry powder aerosolization and effective targeted pulmonary delivery. The mass mean aerodynamic diameter (MMAD) value of all particle systems were approximately 2

μm , while the geometric standard deviation (GSD) value was 2 -3 μm . The MMAD value is within the range of 1 - 5 μm that is required for predominant deposition of particles into the deep lung region (37), which would be desirable to deliver therapeutics for the treatment of both local pulmonary and systematic diseases through the lung. The theoretical MMAD (MMAD_T , shown in Table 2), calculated using the geometric diameter and tapped density, was lower than the experimental results (MMAD_T). This could be due to particle agglomeration, which increased the geometric size of the dry powder. The GSD values were within the range of those previously reported and the respirable fraction (RF), fine particle fraction (FPF), and emitted dose (ED) values were all higher than reports from similar systems (10, 37, 38). The formulated Ac-Dex particle systems are expected to achieve an improved therapeutic effect with a reduced amount of payloads by effectively delivering the drug into deep lung region.

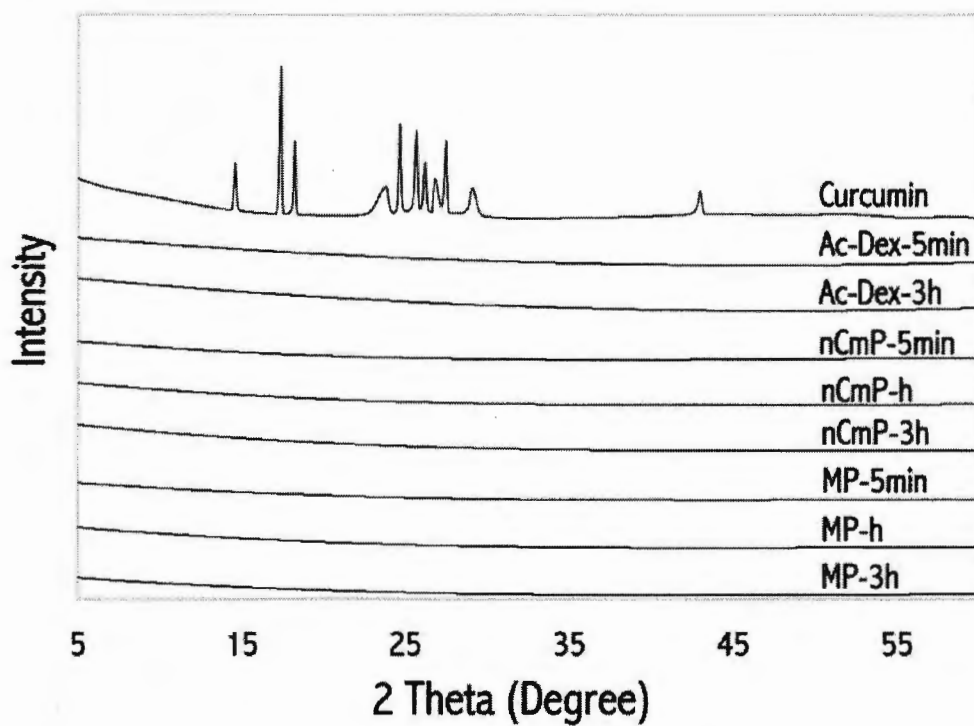


Figure 6.5. Representative powder X-ray diffractograms (PXRD) of raw curcumin (CUR), raw acetalated dextran-5min (Ac-Dex-5min), raw acetalated dextran-3h (Ac-Dex-3h), CUR nCmP-5min, CUR nCmP-h, CUR nCmP-3h, CUR MP-5min, CUR MP-h, and CUR MP-3h.

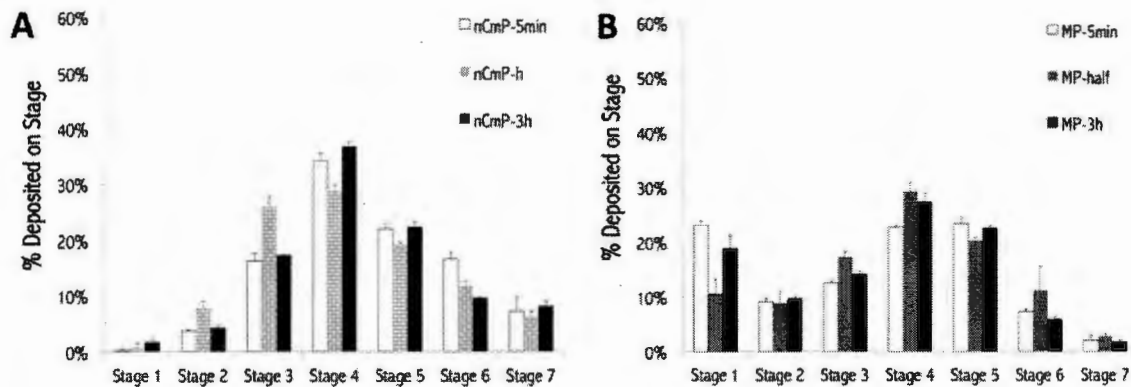


Figure 6.6. Aerosol dispersion performance of curcumin-loaded nanocomposite microparticles (CUR nCmP) and microparticles (CUR MP) as % particles deposited on each stage of the Next Generation Impactor™ (NGI™). For $Q = 60$ L/min, the effective cutoff diameters (D_{50}) for each impaction stage are as follows: stage 1 ($8.06 \mu\text{m}$), stage 2 ($4.46 \mu\text{m}$), stage 3 ($2.82 \mu\text{m}$), stage 4 ($1.66 \mu\text{m}$), stage 5 ($0.94 \mu\text{m}$), stage 6 ($0.55 \mu\text{m}$), and stage 7 ($0.34 \mu\text{m}$) (mean \pm standard deviation, $n = 3$).

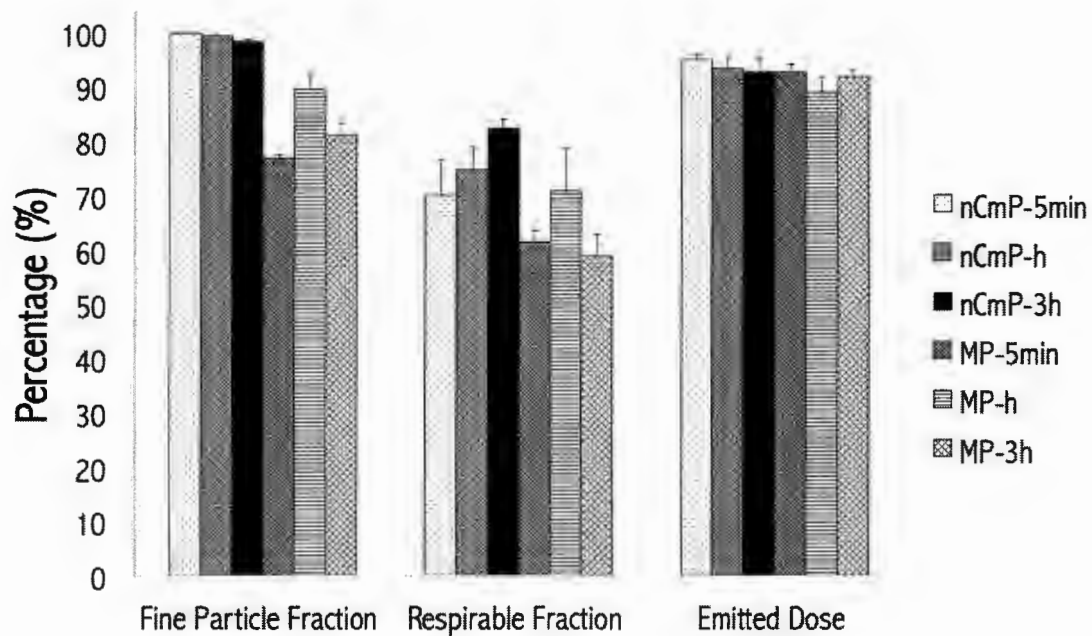


Figure 6.7. *In vitro* aerosol dispersion performance properties including fine particle dose (FPD), fine particle fraction (FPF), respirable fraction (RF), and emitted dose (ED) for curcumin loaded nanocomposite microparticles (CUR nCmP) and microparticles (CUR MP) (mean \pm standard deviation, $n = 3$).

6.4. Conclusions

Two types of pulmonary delivery systems were successfully formulated using Ac-Dex with two different degradation rates. MP were wrinkled spheres (approximately 1 μm) with smooth surfaces, while nCmP were 1.5 μm with wrinkled surfaces that dissociated into 200 nm nanoparticles upon being reconstituted in water. The variation in the drug release rates from the Ac-Dex particles were determined by the Ac-Dex reaction time, ratio of two types of Ac-Dex, and the particle size, which could be easily tuned during the manufacturing process. The pH value of environment also had a significant influence on the release profiles, allowing the Ac-Dex particles to release the payload in a controlled fashion. All nCmP and MP systems exhibited desirable properties as dry powder inhalation therapeutics, including small aerodynamic diameters, which is suitable for deep lung delivery, low water content, which is favorable for particle storage, and amorphization of a crystalline payload, which improves the efficiency of drug dissolution. Overall, the engineered Ac-Dex aerosol particle systems have the potential for targeted delivery of therapeutics in to the deep lung. Meanwhile, these dry powder formulations also provide more convenient administration, more flexible storage conditions, and lower risk of contamination in the device.

6.5 Acknowledgements

The authors gratefully acknowledge financial support from an Institutional Development Award (IDeA) from the National Institute of General Medical Sciences of the National Institutes of Health under grant number P20GM103430. The content is solely the responsibility of the authors and does not necessarily represent the official

views of the National Institutes of Health. This material is based upon work conducted at a Rhode Island NSF EPSCoR research facility, supported in part by the National Science Foundation EPSCoR Cooperative Agreement #EPS-1004057. In addition, this material is based in part upon work supported by the National Science Foundation under grant number #1508868. Any opinions, findings, and conclusions or recommendations expressed in this material are those of the authors and do not necessarily reflect the view of the National Science Foundation. Finally, the authors thank RI-INBRE for UPLC access and RIN2 for SEM, DLS, PXRD, and DSC access.

6.6 References

1. L. Cui, J.A. Cohen, K.E. Broaders, T.T. Beaudette, and J.M. Frechet. Mannosylated dextran nanoparticles: a pH-sensitive system engineered for immunomodulation through mannose targeting. *Bioconjugate chemistry*. 22:949-957 (2011).
2. S.A. Meenach, Y.J. Kim, K.J. Kauffman, N. Kanthamneni, E.M. Bachelder, and K.M. Ainslie. Synthesis, Optimization, and Characterization of Camptothecin-Loaded Acetalated Dextran Porous Microparticles for Pulmonary Delivery. *Molecular Pharmaceutics*. 9:290-298 (2012).
3. H.M. Mansour, Y.-S. Rhee, and X. Wu. Nanomedicine in pulmonary delivery. *International Journal of Nanomedicine*. 4:299-319 (2009).
4. S. Belotti, A. Rossi, P. Colombo, R. Bettini, D. Rekkas, S. Politis, G. Colombo, A.G. Balducci, and F. Buttini. Spray-dried amikacin sulphate powder for inhalation in cystic fibrosis patients: The role of ethanol in particle formation. *European Journal of Pharmaceutics and Biopharmaceutics*. 93:165-172 (2015).
5. K.V. Hoang, H.M. Borteh, M.V. Rajaram, K.J. Peine, H. Curry, M.A. Collier, M.L. Homsy, E.M. Bachelder, J.S. Gunn, L.S. Schlesinger, and K.M. Ainslie. Acetalated dextran encapsulated AR-12 as a host-directed therapy to control Salmonella infection. *Int J Pharm*. 477:334-343 (2014).
6. M.A. Collier, K.J. Peine, S. Gautam, S. Oghumu, S. Varikuti, H. Borteh, T.L. Papenfuss, A.R. Sataoskar, E.M. Bachelder, and K.M. Ainslie. Host-mediated *Leishmania donovani* treatment using AR-12 encapsulated in acetalated dextran microparticles. *Int J Pharm*. 499:186-194 (2016).

7. L. Wu, X. Miao, Z. Shan, Y. Huang, L. Li, X. Pan, Q. Yao, G. Li, and C. Wu. Studies on the spray dried lactose as carrier for dry powder inhalation. *Asian Journal of Pharmaceutical Sciences*. 9:336-341 (2014).
8. Y. Takashima, R. Saito, A. Nakajima, M. Oda, A. Kimura, T. Kanazawa, and H. Okada. Spray-drying preparation of microparticles containing cationic PLGA nanospheres as gene carriers for avoiding aggregation of nanospheres. *Int J Pharm*. 343:262-269 (2007).
9. D.M. Jensen, D. Cun, M.J. Maltesen, S. Frokjaer, H.M. Nielsen, and C. Foged. Spray drying of siRNA-containing PLGA nanoparticles intended for inhalation. *Journal of controlled release : official journal of the Controlled Release Society*. 142:138-145 (2010).
10. S.A. Meenach, K.W. Anderson, J. Zach Hilt, R.C. McGarry, and H.M. Mansour. Characterization and aerosol dispersion performance of advanced spray-dried chemotherapeutic PEGylated phospholipid particles for dry powder inhalation delivery in lung cancer. *European Journal of Pharmaceutical Sciences*. 49:699-711 (2013).
11. J.A. Cohen, T.T. Beaudette, J.L. Cohen, K.E. Broaders, E.M. Bachelder, and J.M. Fréchet. Acetal-modified dextran microparticles with controlled degradation kinetics and surface functionality for gene delivery in phagocytic and non-phagocytic cells. *Advanced materials (Deerfield Beach, Fla)*. 22:3593-3597 (2010).
12. B.D. Ulery, L.S. Nair, and C.T. Laurencin. Biomedical Applications of Biodegradable Polymers. *Journal of polymer science Part B, Polymer physics*. 49:832-864 (2011).
13. K.E. Broaders, J.A. Cohen, T.T. Beaudette, E.M. Bachelder, and J.M.J. Fréchet. Acetalated dextran is a chemically and biologically tunable material for particulate immunotherapy. *Proceedings of the National Academy of Sciences*. 106:5497-5502 (2009).
14. E.M. Bachelder, T.T. Beaudette, K.E. Broaders, J. Dashe, and J.M.J. Fréchet. Acetal-Derivatized Dextran: An Acid-Responsive Biodegradable Material for Therapeutic Applications. *Journal of the American Chemical Society*. 130:10494-10495 (2008).
15. K.J. Kauffman, N. Kanthamneni, S.A. Meenach, B.C. Pierson, E.M. Bachelder, and K.M. Ainslie. Optimization of rapamycin-loaded acetalated dextran microparticles for immunosuppression. *International Journal of Pharmaceutics*. 422:356-363 (2012).
16. N. Kanthamneni, S. Sharma, S.A. Meenach, B. Billet, J.-C. Zhao, E.M. Bachelder, and K.M. Ainslie. Enhanced stability of horseradish peroxidase encapsulated in acetalated dextran microparticles stored outside cold chain conditions. *International Journal of Pharmaceutics*. 431:101-110 (2012).

17. C. He, Y. Hu, L. Yin, C. Tang, and C. Yin. Effects of particle size and surface charge on cellular uptake and biodistribution of polymeric nanoparticles. *Biomaterials*. 31:3657-3666 (2010).
18. K. Kho, W.S. Cheow, R.H. Lie, and K. Hadinoto. Aqueous re-dispersibility of spray-dried antibiotic-loaded polycaprolactone nanoparticle aggregates for inhaled anti-biofilm therapy. *Powder Technology*. 203:432-439 (2010).
19. W.S. Rasband. ImageJ. <http://imagej.nih.gov/ij/>.
20. K. Tomoda, T. Ohkoshi, Y. Kawai, M. Nishiwaki, T. Nakajima, and K. Makino. Preparation and properties of inhalable nanocomposite particles: effects of the temperature at a spray-dryer inlet upon the properties of particles. *Colloids and surfaces B, Biointerfaces*. 61:138-144 (2008).
21. F. W. The ARLA Respiratory Deposition Calculator2008.
22. S.K. Lai, Y.-Y. Wang, and J. Hanes. Mucus-penetrating nanoparticles for drug and gene delivery to mucosal tissues. *Advanced Drug Delivery Reviews*. 61:158-171 (2009).
23. B. Gu, B. Linehan, and Y.-C. Tseng. Optimization of the Büchi B-90 spray drying process using central composite design for preparation of solid dispersions. *International Journal of Pharmaceutics*. 491:208-217 (2015).
24. I. Atalarand M. Dervisoglu. Optimization of spray drying process parameters for kefir powder using response surface methodology. *LWT - Food Science and Technology*. 60:751-757 (2015).
25. J.C. Sung, D.J. Padilla, L. Garcia-Contreras, J.L. Verberkmoes, D. Durbin, C.A. Peloquin, K.J. Elbert, A.J. Hickey, and D.A. Edwards. Formulation and pharmacokinetics of self-assembled rifampicin nanoparticle systems for pulmonary delivery. *Pharm Res*. 26:1847-1855 (2009).
26. J. Heyder. Deposition of Inhaled Particles in the Human Respiratory Tract and Consequences for Regional Targeting in Respiratory Drug Delivery. *Proceedings of the American Thoracic Society*. 1:315-320 (2004).
27. R. Vehring. Pharmaceutical Particle Engineering via Spray Drying. *Pharm Res*. 25:999-1022 (2008).
28. D. Shuwisitkul. Biodegradable implants with different drug release profiles, *Department of Biology, Chemistry and Pharmacy*, Vol. Doctor, Freie Universität Berlin2011.
29. S. Bohrey, V. Chourasiya, and A. Pandey. Polymeric nanoparticles containing diazepam: preparation, optimization, characterization, in-vitro drug release and release kinetic study. *Nano Convergence*. 3:1-7 (2016).

30. A. Seidlitz and W. Weitschies. In-vitro dissolution methods for controlled release parenterals and their applicability to drug-eluting stent testing. *The Journal of pharmacy and pharmacology*. 64:969-985 (2012).
31. P. Costa and J.M. Sousa Lobo. Modeling and comparison of dissolution profiles. *European Journal of Pharmaceutical Sciences*. 13:123-133 (2001).
32. N. Kamaly, B. Yameen, J. Wu, and O.C. Farokhzad. Degradable Controlled-Release Polymers and Polymeric Nanoparticles: Mechanisms of Controlling Drug Release. *Chemical Reviews*. 116:2602-2663 (2016).
33. A.J. Hickey, H.M. Mansour, M.J. Telko, Z. Xu, H.D. Smyth, T. Mulder, R. McLean, J. Langridge, and D. Papadopoulos. Physical characterization of component particles included in dry powder inhalers. I. Strategy review and static characteristics. *J Pharm Sci*. 96:1282-1301 (2007).
34. G. Mohammadi, H. Valizadeh, M. Barzegar-Jalali, F. Lotfipour, K. Adibkia, M. Milani, M. Azhdarzadeh, F. Kiafar, and A. Nokhodchi. Development of azithromycin-PLGA nanoparticles: physicochemical characterization and antibacterial effect against *Salmonella typhi*. *Colloids and surfaces B, Biointerfaces*. 80:34-39 (2010).
35. X. Wu, W. Zhang, D. Hayes, Jr., and H.M. Mansour. Physicochemical characterization and aerosol dispersion performance of organic solution advanced spray-dried cyclosporine A multifunctional particles for dry powder inhalation aerosol delivery. *Int J Nanomedicine*. 8:1269-1283 (2013).
36. M.A. Akl, A. Kartal-Hodzic, T. Oksanen, H.R. Ismael, M.M. Afouna, M. Yliperttula, A.M. Samy, and T. Viitala. Factorial design formulation optimization and *in vitro* characterization of curcumin-loaded PLGA nanoparticles for colon delivery. *Journal of Drug Delivery Science and Technology*. 32, Part A:10-20 (2016).
37. S.A. Meenach, F.G. Vogt, K.W. Anderson, J.Z. Hilt, R.C. McGarry, and H.M. Mansour. Design, physicochemical characterization, and optimization of organic solution advanced spray-dried inhalable dipalmitoylphosphatidylcholine (DPPC) and dipalmitoylphosphatidylethanolamine poly(ethylene glycol) (DPPE-PEG) microparticles and nanoparticles for targeted respiratory nanomedicine delivery as dry powder inhalation aerosols. *International Journal of Nanomedicine*. 8:275-293 (2013).
38. F. Ungaro, G. De Rosa, A. Miro, F. Quaglia, and M.I. La Rotonda. Cyclodextrins in the production of large porous particles: Development of dry powders for the sustained release of insulin to the lungs. *European Journal of Pharmaceutical Sciences*. 28:423-432 (2006).

CHAPTER 7

Conclusions and Future Work

7.1 Conclusions

This dissertation focuses on the development, characterization, and optimization of dry powder aerosol nanocomposite microparticle systems for the treatment of pulmonary diseases. Azithromycin and rapamycin were encapsulated in Ac-Dex nanoparticles for potential application in the treatment of cystic fibrosis-related lung infections. These nanoparticles were coated with VP5k to ensure effective dispersion in and facilitate penetrating through viscous mucus caused by cystic fibrosis. Nanoparticles coated with PVA were able to maintain a favorable dispersion and can be used to deliver tacrolimus for the treatment of pulmonary arterial hypertension.

In the production of nanoscale carriers, Ac-Dex with different degradation rates were applied to form polymer matrices with tunable release profiles. The drug release rates of the Ac-Dex particles were determined by the Ac-Dex reaction time, ratio of two types of Ac-Dex, and particle size, which could be easily tuned during the manufacturing process. The pH value of environment also had a significant influence on the release profiles, allowing the Ac-Dex particles to release the payload in a controlled fashion.

Nanocomposite microparticles were formulated using spray drying a suspension of nanoparticles. The optimal spray drying conditions were identified to prepare nCmP systems with favorable properties including: small aerodynamic diameter, effective nanoparticle redispersion, high drug loading, and low water content. Meanwhile, the safe

range of spray drying parameters were discussed to ensure the stability of therapeutics and formulations.

This is the first time that the dry powder aerosol nanocomposite microparticle systems have been comprehensively studied for the treatment of pulmonary diseases. The dissertation presents a strategy to develop nanoscale carriers with capability of protecting of drugs from degradation, enhancing of the solubility of drugs, releasing payloads at controlled rate, and overcoming physiological barriers. In addition, the optimal conditions to formulate microscale carriers with advantages including targeted deposition in the airways, high drug loading, enhanced stability, and maintenance of the favorable properties of embedded nanoparticles were elucidated.

7.2 Future Work

This dissertation provides the first comprehensive study on developing and optimizing dry powder aerosol nanocomposite microparticle systems for the treatment of pulmonary diseases. Many opportunities exist to conduct further research based on this delivery system, which may include, but are not limited to:

- Investigation of the safety and antibacterial efficacy of azithromycin-loaded Ac-dex nanoparticle with VP5k coating for the treatment of cystic fibrosis-related infections.
- Development of Ac-dex nanoparticles with various coating materials and investigation of the safety of these nanoparticles, which could be used to targeted delivery of therapeutics.

- Optimization of the spray drying conditions to formulate nCmP encapsulated with Ac-dex nanoparticles with various coating materials for pulmonary delivery or systemic delivery of therapeutics through the lungs.
- Investigation of the safety and efficacy of tacrolimus-loaded nCmP for the treatment of pulmonary arterial hypertension by *in vivo* study using an animal model.
- Development of nCmP comprised of hydrophilic encapsulated nanoparticles and a hydrophobic excipient of microscale carriers, which could be applied to provide sustained release of hydrophilic drugs with short half-lives.
- Application of the general-purpose nCmP system for protein, DNA, and RNA delivery to the lung.

APPENDIX A

Supplementary Material for Chapter 3

Table A.1. Characterization of nanoparticles after redispersion from nanocomposite microparticles in PBS including the size, polydispersity index (PDI), and zeta (ζ) potential.

System	Diameter (nm)	PDI	ζ Potential (mV)
AZI-NP	327.6 ± 3.7	0.32 ± 0.02	-7.66 ± 0.68
RAP-NP	348.2 ± 11.6	0.43 ± 0.01	-5.99 ± 0.07
Blank-NP	270.8 ± 10.8	0.26 ± 0.04	-3.98 ± 0.67

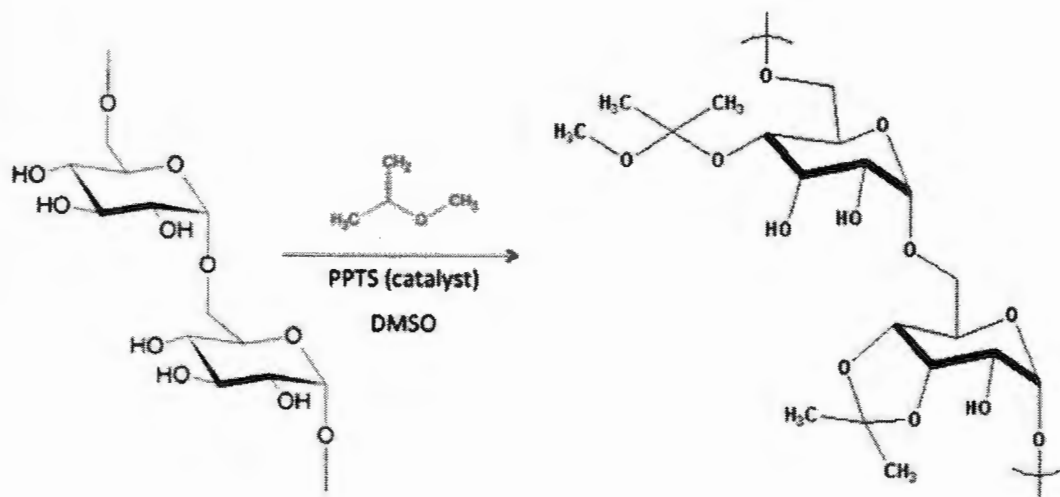


Figure A.1. Schematic of Ac-Dex synthesis

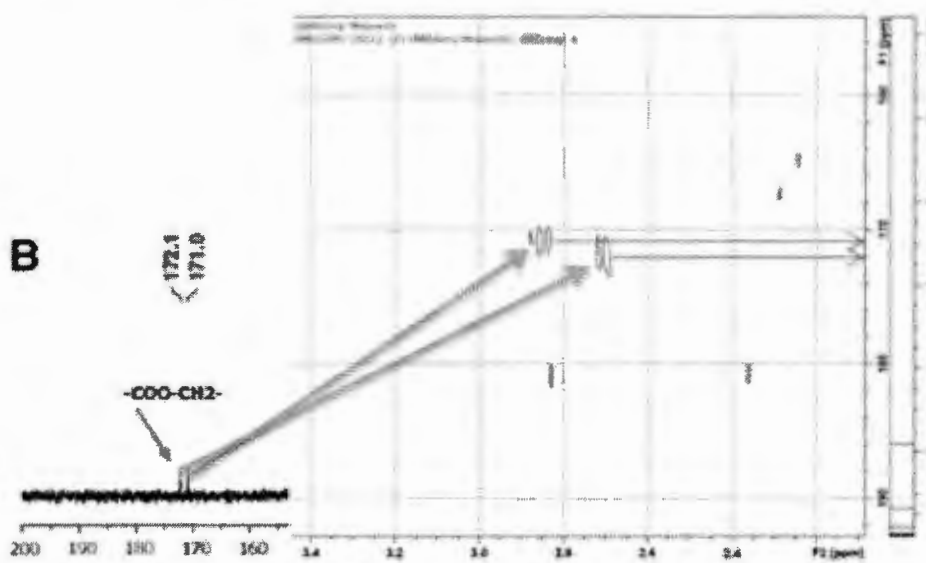
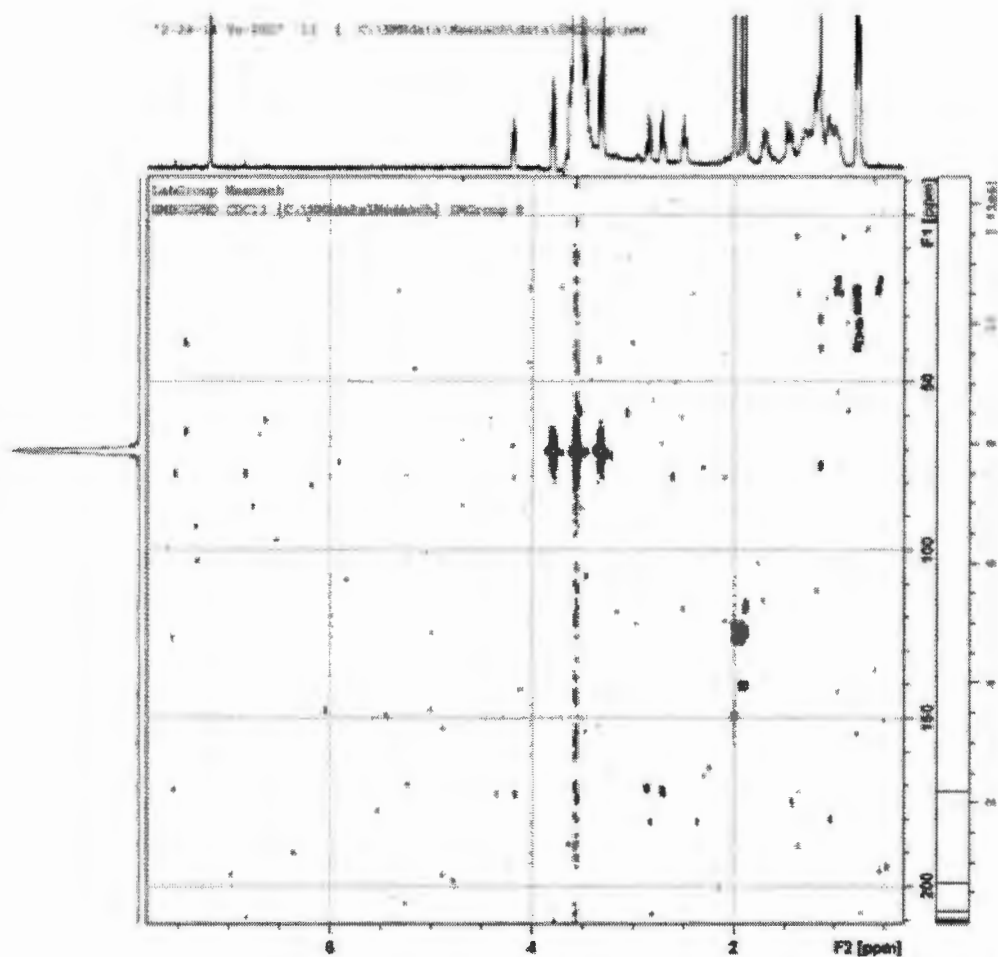


Figure A.2. NMR spectra of VP5k where (top) indicates entire spectra and (bottom) is an enlarged portion.

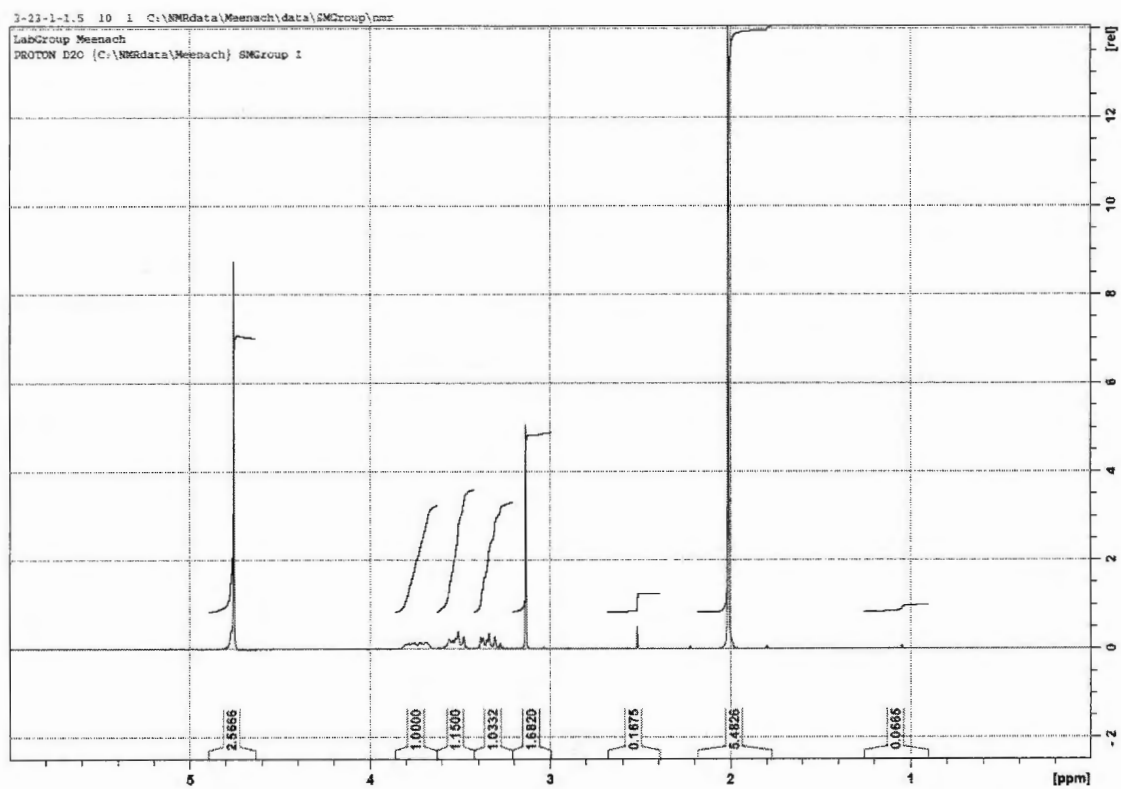


Figure A.3. NMR spectrum of acetalated dextran degradation products.

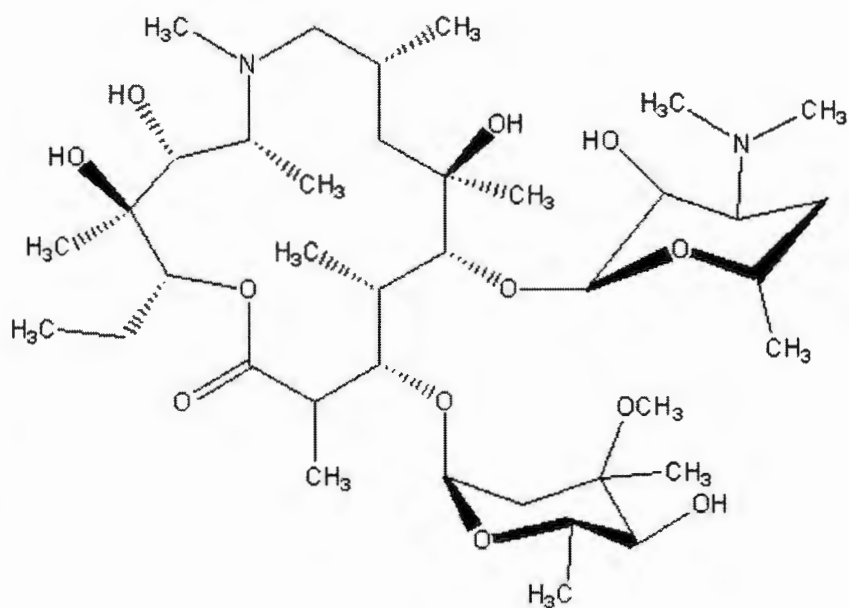


Figure A.4. Structure of azithromycin

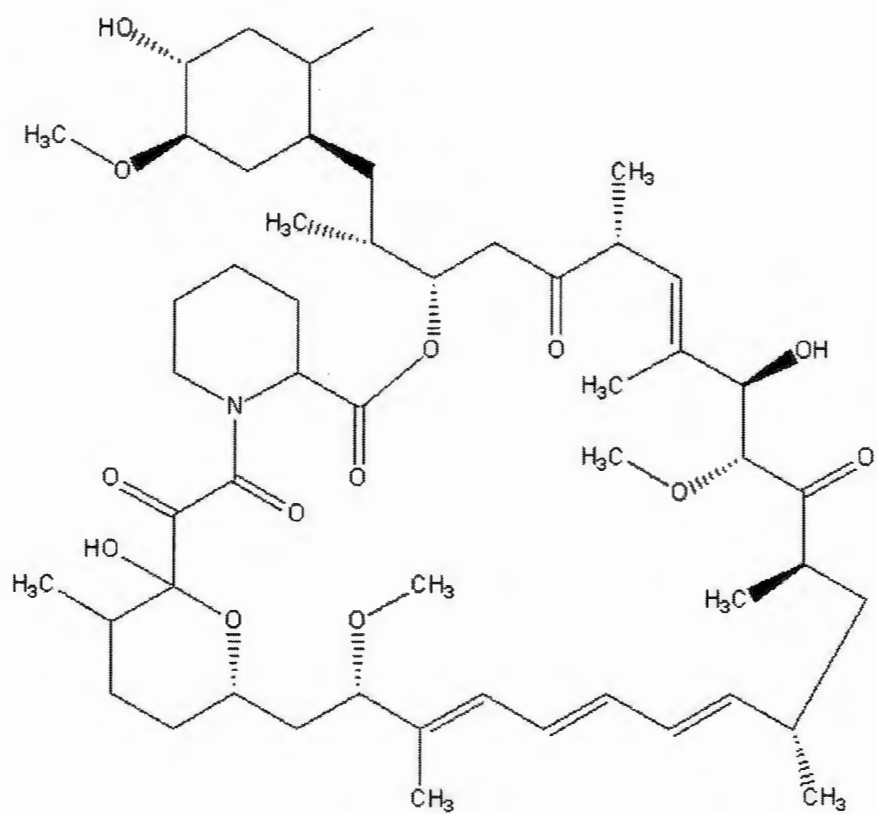


Figure A.5. Structure of rapamycin



Figure A.6. Next generation impactor (NGI) is a high-performance, precision, particle classifying cascade impactor designed for testing MDIs, DPIs, nebulizers and aerosol and nasal sprays. (www.mspcorp.com)

APPENDIX B

Supplementary Material for Chapter 4

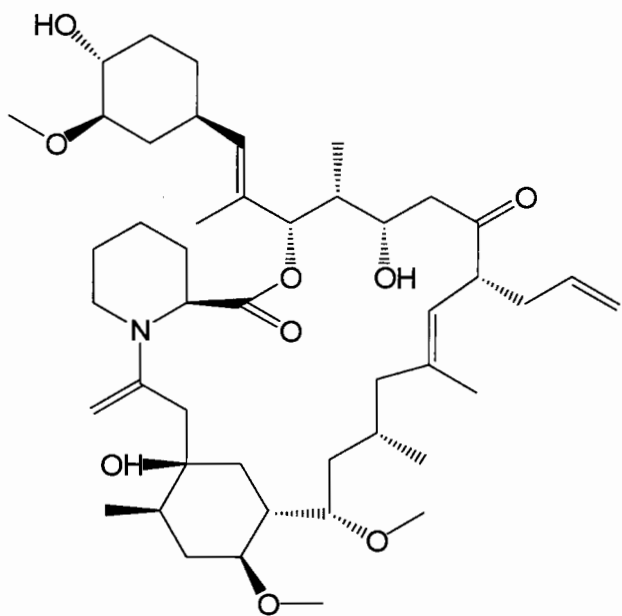


Figure B.1. Structure of tacrolimus

APPENDIX C

Supplementary Material for Chapter 5

Table C.1. Summary of curcumin-loaded nanocomposite microparticle (nCmP) systems and their corresponding inlet temperature (T_{in}), nanoparticle loading (NP %), and feed concentration (Fc).

nCmP	T_{in} (°C)	NP (%)	Fc (%)
A	50	50	2.5
B	130	50	2.5
C	90	20	2.5
D	90	80	2.5
E	50	20	1.5
F	90	50	1.5
G	50	80	1.5
H	130	80	1.5
I	130	20	1.5
J	50	50	0.5
K	90	80	0.5
L	130	50	0.5
M	90	20	0.5

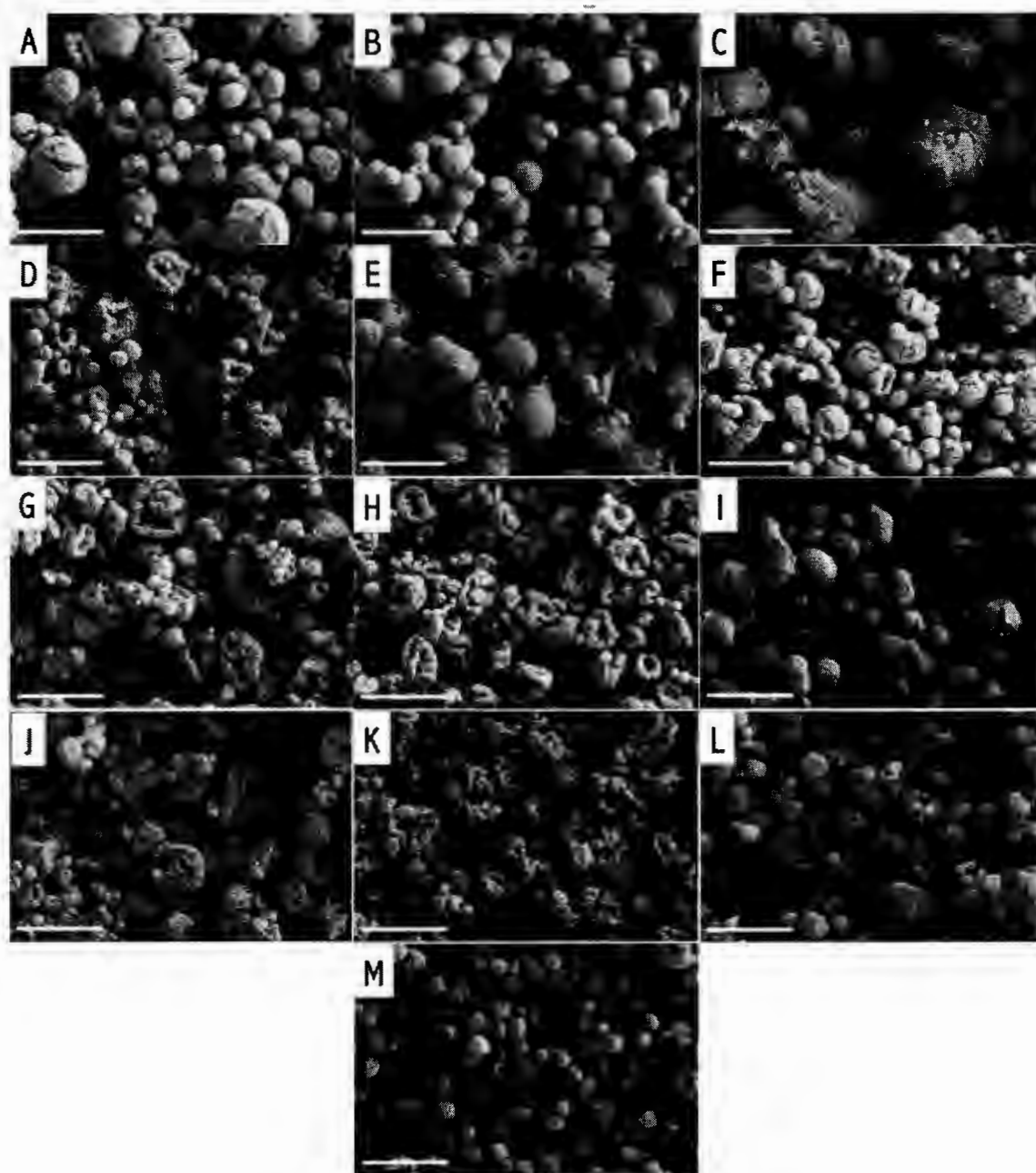


Figure C.1. Representative SEM micrographs of curcumin-loaded nanocomposite microparticle systems (CUR nCmP) corresponding to **Table B.1**. Scale bar = 5 μm .

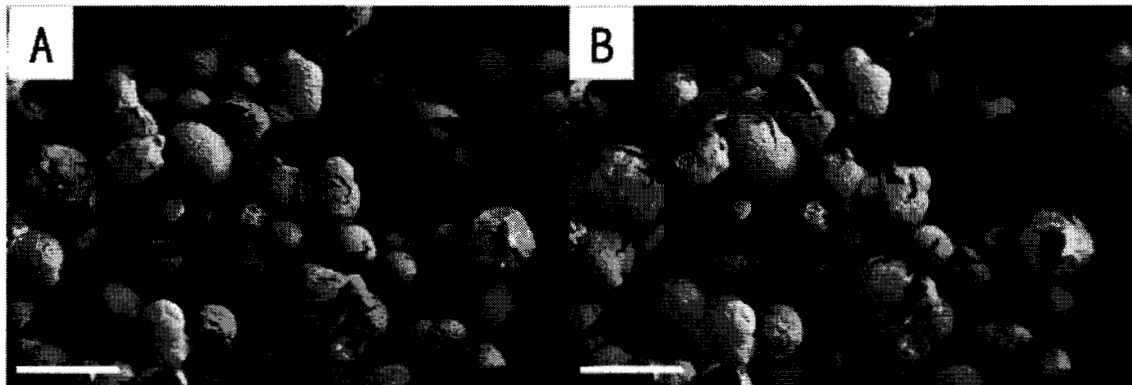


Figure C.2. Representative SEM micrographs showing the crack generation caused by the high energy electron beam where (A) was taken just after the initial focusing on the particles and (B) was taken 5 seconds after focusing. Scale bar = 5 μm .

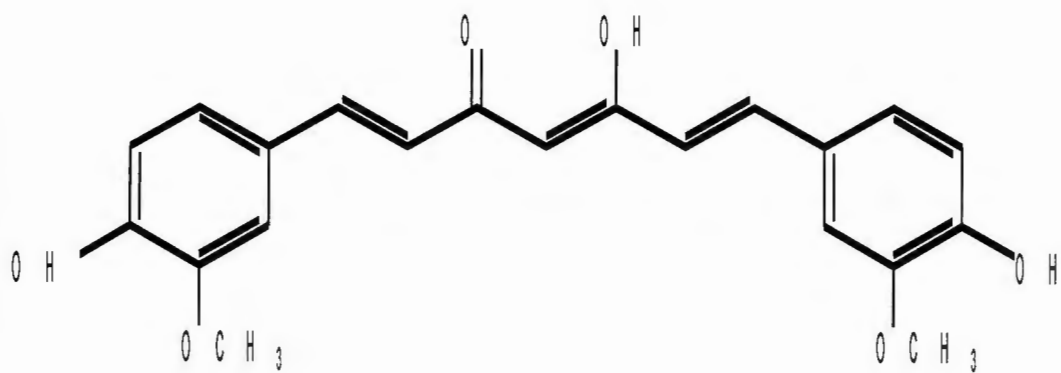


Figure C.3. Structure of curcumin

Table C.2. Summary of the nCmP properties following spray drying.

Run	Factors			Responses					
	T _{in} (°C)	NP (%)	Fc (%)	Water Content (%)	Size change (%)	PDI change (%)	Zeta Potential Change (%)	T _{out} (°C)	Yield (%)
1	130	80	1.5	4.51%	0.2%	-2.9%	-2.9%	71.5	38.8
2	50	50	0.5	5.71%	5.6%	20.0%	20.4%	30.5	59.3
3	50	50	2.5	3.82%	0.0%	31.4%	13.3%	31.5	67.0
4	90	50	1.5	2.95%	2.5%	14.3%	-32.5%	51.0	60.6
5	90	80	0.5	5.94%	9.7%	17.1%	-22.3%	51.5	50.0
6	90	50	1.5	3.41%	4.9%	14.3%	-30.1%	50.5	62.0
7	50	20	1.5	5.43%	1.0%	-21.4%	-62.2%	34.5	50.2
8	90	80	2.5	4.69%	4.9%	57.1%	-14.9%	52.5	65.9
9	130	50	0.5	5.66%	7.5%	30.0%	-61.0%	72.0	43.6
10	90	20	2.5	2.63%	4.8%	20.0%	-59.7%	49.5	41.2
11	130	50	2.5	3.84%	1.1%	-20.0%	-1.1%	69.0	53.4
12	90	50	1.5	3.23%	2.3%	-1.4%	-32.4%	50.5	60.1
13	50	80	1.5	4.68%	4.2%	15.7%	8.9%	34.5	65.8
14	90	20	0.5	6.72%	-0.2%	32.9%	-30.7%	49.0	43.4
15	130	20	1.5	4.13%	8.3%	22.9%	-38.2%	73.0	53.4

Run	Factors			Responses						
	T _{in} (°C)	NP% (%)	Fc (%)	Drug Loading (%)	EE (%)	MMAD (µm)	GSD (µm)	FPF (%)	RF (%)	EF (%)
1	130	80	1.5	0.372	72.74	2.44	2.34	98.6%	76.0%	97.7%
2	50	50	0.5	0.201	62.78	1.69	2.79	99.4%	77.2%	98.0%
3	50	50	2.5	0.192	60.14	4.49	1.95	85.0%	57.9%	99.0%
4	90	50	1.5	0.201	62.83	4.28	1.70	84.4%	60.9%	99.6%
5	90	80	0.5	0.357	69.79	1.50	2.57	98.8%	86.0%	96.3%
6	90	50	1.5	0.087	58.45	4.05	2.34	86.1%	67.4%	99.6%
7	50	20	1.5	0.074	58.12	7.44	2.34	54.2%	48.4%	99.8%
8	90	80	2.5	0.402	78.70	2.48	2.77	97.5%	70.0%	94.6%
9	130	50	0.5	0.195	61.09	3.69	2.81	83.6%	73.0%	98.8%
10	90	20	2.5	0.083	65.33	7.20	2.81	62.2%	38.0%	100.1%
11	130	50	2.5	0.172	53.71	5.78	2.50	66.2%	55.8%	99.2%
12	90	50	1.5	0.193	60.34	4.11	1.88	85.3%	61.6%	99.9%
13	50	80	1.5	0.288	56.43	2.38	2.71	98.1%	82.2%	95.7%
14	90	20	0.5	0.093	72.93	3.24	3.00	83.3%	64.4%	97.1%
15	130	20	1.5	0.113	88.07	5.46	1.88	68.8%	46.2%	100.0%

APPENDIX D

Supplemental Material for Chapter 6

D.1 Drug Release Model Description

The drug release data of the particle systems was fitted to several models (equations shown below) to aid in the determination of the type of release the systems experienced. For the models that can be linearized (all models except for Baker's model), the coefficient of determination (R^2) was utilized to determine the applicability of the release models. For Baker's model, Microsoft Excel with Solver add-in was applied to determine the parameters that minimize the sum of squares of the residues of the model. The models, equations, and their corresponding parameters for are as follows:

First order model:
$$\log M_t = \log M_0 + \frac{K}{2.303} t$$

where M_t is the amount of drug released at time t , M_0 is the initial amount of drug in the solution, and K is the first order release constant.

Weibull model:
$$m = 1 - \exp\left(\frac{-(t - T_i)^b}{a}\right)$$

where m is the accumulated fraction of the drug released at time t , a is the scale parameter, which defines the time scale of the process, T_i is the location parameter, which

represents the lag time before the onset of the dissolution or release process, and b is the shape parameter, which characterizes the shape of release curve.

Higuchi model: $M_t = Kt^{1/2} + b$

where M_t is the amount of drug released at time t , K is the Higuchi dissolution constant, and b is the amount of drug released at time 0.

Hixson–Crowell model: $W_0^{1/3} - W_t^{1/3} = Kt$

where W_0 is the initial amount of drug in the particles, W_t is the remaining amount of drug in the particles at time t , and K is a constant characterizing the surface to volume relationship.

Korsmeyer–Peppas model: $m = at^n$

where a is a constant characterizing the structural and geometric properties of the particles, n is the release exponent, indicating the drug release mechanism, and m is the accumulated fraction of the drug released at time t .

Baker–Lonsdale model: $\frac{3}{2}[1 - (1 - m)^{2/3}] - m = Kt$

where K is the release constant and m is the accumulated fraction of the drug released at time t .

Hopfenberg model: $m = 1 - [1 - Kt(t-1)]^n$

where K is a constant equal to k_0/C_0a_0 , where k_0 is the erosion rate constant, C_0 is the initial concentration of drug in the matrix, and a_0 is the initial radius for particles. m is the accumulated fraction of the drug released at time t .

Baker's model: $M_t = A(2P_0e^{kt}C_0t)^{1/2}$

where M_t is the amount of drug released in time t , P_0 is the drug permeability, A is the total area of the particle, C_0 is the drug concentration at the initial time, and k is the first-order rate constant of bond cleavage of the polymer carrier.

Table D.1. The drug release duration and total released fraction of each particle system at both pH.

Particle System	pH = 5		pH = 7.4	
	Release Duration (h)	Total Released Fraction (%)	Release Duration (h)	Total Released Fraction (%)
nCmP-5min	2	92.6	8	93.6
nCmP-h	2	63.4	12	31.5
nCmP-3h	4	73	24	23.7
MP-5min	6	78	24	60.6
MP-h	12	86.4	24	52.7
MP-3h	24	68.5	168	24.9

Table D.2. Summary of the coefficient of determinations (R^2) of all the models for all particle system. The model with relatively high R^2 for all particle systems was regarded as applicable.

pH = 5						
Model	nCmP - 5min	nCmP -h	nCmP -3h	MP - 5min	MP -h	MP -3h
First order	0.7835	0.8549	0.8511	0.573	0.4848	0.7517
Hixson- Crowell	0.8615	0.9571	0.9613	0.847	0.8899	0.949
Higuchi (modified)	0.9468	0.9968	0.9989	0.9867	0.9748	0.9715
Korsmeyer- Peppas	0.9998	0.6906	0.505	0.81	0.8843	0.9882
Baker- Lonsdale	0.8729	0.9945	0.9799	0.9065	0.9595	0.9753
Hopfenberg	0.5497	0.8743	0.9029	0.8925	0.849	0.9276
Weibull	0.9098	0.5773	0.2538	0.9387	0.9936	0.9353

pH = 7.4						
Model	nCmP - 5min	nCmP -h	nCmP - 3h	MP - 5min	MP -h	MP -3h
First order	0.8084	0.7345	0.7574	0.3797	0.829	0.6414
Hixson- Crowell	0.9312	0.8021	0.9482	0.7696	0.9117	0.8185
Higuchi (modified)	0.9573	0.8758	0.9732	0.9369	0.8288	0.9462
Korsmeyer- Peppas	0.899	0.5374	0.9457	0.8828	0.9349	0.9708
Baker- Lonsdale	0.9709	0.8172	0.9089	0.9283	0.9141	0.9079
Hopfenberg	0.8493	0.8678	0.9685	0.7462	0.8241	0.8526
Weibull	1	0.5235	0.7905	0.9783	0.8897	0.8963

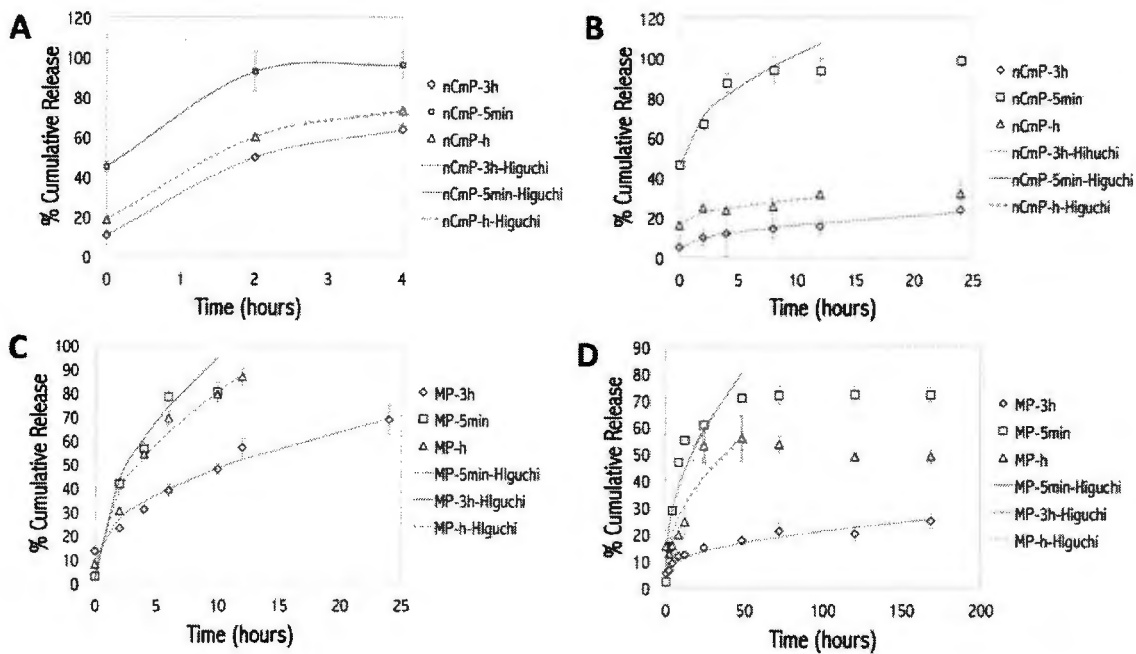


Figure D.1. Original data and fitted curves of *in vitro* drug release profiles for curcumin (CUR) nCmP and MP systems including CUR nCmP-5min, CUR nCmP-h, CUR nCmP-3h, CUR MP-5min, CUR MP-h, and CUR MP-3h at pH = 5 and pH = 7.4.

BIBLIOGRAPHY

1. B.A. Abdulrahman, A.A. Khweek, A. Akhter, K. Caution, S. Kotrange, D.H.A. Abdelaziz, C. Newland, R. Rosales-Reyes, B. Kopp, K. McCoy, R. Montione, L.S. Schlesinger, M.A. Gavrilin, M.D. Wewers, M.A. Valvano, and A.O. Amer. Autophagy stimulation by rapamycin suppresses lung inflammation and infection by *Burkholderia cenocepacia* in a model of cystic fibrosis. *Autophagy*. 7:1359-1370 (2011).
2. R.U. Agu, M.I. Ugwoke, M. Armand, R. Kinget, and N. Verbeke. The lung as a route for systemic delivery of therapeutic proteins and peptides. *Respiratory research*. 2:198-209 (2001).
3. H. AJand M. HM. *Delivery of drugs by the pulmonary route*, Taylor and Francis, New York, 2009.
4. M.A. Akl, A. Kartal-Hodzic, T. Oksanen, H.R. Ismael, M.M. Afouna, M. Yliperttula, A.M. Samy, and T. Viitala. Factorial design formulation optimization and in vitro characterization of curcumin-loaded PLGA nanoparticles for colon delivery. *Journal of Drug Delivery Science and Technology*. 32, Part A:10-20 (2016).
5. M.H. Al-Hallak, M.K. Sarfraz, S. Azarmi, W.H. Roa, W.H. Finlay, and R. Lobenberg. Pulmonary delivery of inhalable nanoparticles: dry powder inhalers. *Therapeutic delivery*. 2:1313-1324 (2011).
6. M. Ameriand Y.F. Maa. *Spray Drying of Biopharmaceuticals: Stability and Process Considerations*. *Drying Technology*. 24:763-768 (2006).
7. M.B. Antunesand N.A. Cohen. Mucociliary clearance--a critical upper airway host defense mechanism and methods of assessment. *Current Opinion in Allergy and Clinical Immunology*. 7:5-10 (2007).
8. R.P. Aquino, L. Prota, G. Auriemma, A. Santoro, T. Mencherini, G. Colombo, and P. Russo. Dry powder inhalers of gentamicin and leucine: formulation parameters, aerosol performance and in vitro toxicity on CuFil cells. *International Journal of Pharmaceutics*. 426:100-107 (2012).
9. H. Arima, K. Yunomae, K. Miyake, T. Irie, F. Hirayama, and K. Uekama. Comparative studies of the enhancing effects of cyclodextrins on the solubility and oral bioavailability of tacrolimus in rats. *Journal of Pharmaceutical sciences*. 90:690-701 (2001).
10. I. Atalarand M. Dervisoglu. Optimization of spray drying process parameters for kefir powder using response surface methodology. *LWT - Food Science and Technology*. 60:751-757 (2015).
11. S. Azarmi, W.H. Roa, and R. Löbenberg. Targeted delivery of nanoparticles for the treatment of lung diseases. *Advanced drug delivery reviews*. 60:863-875 (2008).

12. S. Azarmi, X. Tao, H. Chen, Z. Wang, W.H. Finlay, R. Löbenberg, and W.H. Roa. Formulation and cytotoxicity of doxorubicin nanoparticles carried by dry powder aerosol particles. *International Journal of Pharmaceutics*. 319:155-161 (2006).
13. E.M. Bachelder, T.T. Beaudette, K.E. Broaders, J. Dashe, and J.M.J. Fréchet. Acetal-Derivatized Dextran: An Acid-Responsive Biodegradable Material for Therapeutic Applications. *Journal of the American Chemical Society*. 130:10494-10495 (2008).
14. B. Badiani and A. Messori. Targeted Treatments for Pulmonary Arterial Hypertension: Interpreting Outcomes by Network Meta-analysis. *Heart, lung & circulation*. 25:46-52 (2016).
15. M.M. Bailey and C.J. Berkland. Nanoparticle formulations in pulmonary drug delivery. *Medicinal research reviews*. 29:196-212 (2009).
16. P. Baldrick. Pharmaceutical excipient development: the need for preclinical guidance. *Regulatory toxicology and pharmacology* 32:210-218 (2000).
17. B. Baras, M.A. Benoit, and J. Gillard. Parameters influencing the antigen release from spray-dried poly(dl-lactide) microparticles. *International Journal of Pharmaceutics*. 200:133-145 (2000).
18. E.D. Bateman, K.R. Chapman, D. Singh, A.D. D'Urzo, E. Molins, A. Leselbaum, and E.G. Gil. Acridinium bromide and formoterol fumarate as a fixed-dose combination in COPD: pooled analysis of symptoms and exacerbations from two six-month, multicentre, randomised studies (ACLIFORM and AUGMENT). *Respiratory research*. 16:92 (2015).
19. M. Beck-Broichsitter, O.M. Merkel, and T. Kissel. Controlled pulmonary drug and gene delivery using polymeric nano-carriers. *Journal of Controlled Release*. 161:214-224 (2012).
20. M. Beck-Broichsitter, C. Schweiger, T. Schmehl, T. Gessler, W. Seeger, and T. Kissel. Characterization of novel spray-dried polymeric particles for controlled pulmonary drug delivery. *Journal of Controlled Release*. 158:329-335 (2012).
21. J.H. Bell, P.S. Hartley, and J.S. Cox. Dry powder aerosols. I. A new powder inhalation device. *Journal of Pharmaceutical sciences*. 60:1559-1564 (1971).
22. S. Belotti, A. Rossi, P. Colombo, R. Bettini, D. Rekkas, S. Politis, G. Colombo, A.G. Balducci, and F. Buttini. Spray-dried amikacin sulphate powder for inhalation in cystic fibrosis patients: The role of ethanol in particle formation. *European Journal of Pharmaceutics and Biopharmaceutics*. 93:165-172 (2015).
23. S. Bohrey, V. Chourasiya, and A. Pandey. Polymeric nanoparticles containing diazepam: preparation, optimization, characterization, in-vitro drug release and release kinetic study. *Nano Convergence*. 3:1-7 (2016).

24. A. Bootz, V. Vogel, D. Schubert, and J. Kreuter. Comparison of scanning electron microscopy, dynamic light scattering and analytical ultracentrifugation for the sizing of poly(butyl cyanoacrylate) nanoparticles. *European Journal of Pharmaceutics and Biopharmaceutics*. 57:369-375 (2004).
25. C. Bosquillon, C. Lombry, V. Preat, and R. Vanbever. Influence of formulation excipients and physical characteristics of inhalation dry powders on their aerosolization performance. *Journal of Controlled Release*. 70:329-339 (2001).
26. S.-J. Bowen and J. Hull. The basic science of cystic fibrosis. *Paediatrics and Child Health*. 25:159-164 (2015).
27. N.A. Bradbury. *Cystic Fibrosis*, Academic Press 2016.
28. K.E. Broaders, J.A. Cohen, T.T. Beaudette, E.M. Bachelder, and J.M.J. Fréchet. Acetalated dextran is a chemically and biologically tunable material for particulate immunotherapy. *Proceedings of the National Academy of Sciences of the United States of America*. 106:5497-5502 (2009).
29. K.E. Broaders, J.A. Cohen, T.T. Beaudette, E.M. Bachelder, and J.M.J. Fréchet. Acetalated dextran is a chemically and biologically tunable material for particulate immunotherapy. *Proceedings of the National Academy of Sciences*. 106:5497-5502 (2009).
30. BUCHI. Mini Spray Dryer B-290 operation manual.
31. A. Burger, J.O. Henck, S. Hetz, J.M. Rollinger, A.A. Weissnicht, and H. Stöttner. Energy/temperature diagram and compression behavior of the polymorphs of D-mannitol. *Journal of Pharmaceutical Sciences*. 89:457-468 (2000).
32. P. Calvo, C. Remuñán-López, J.L. Vila-Jato, and M.J. Alonso. Novel hydrophilic chitosan-polyethylene oxide nanoparticles as protein carriers. *Journal of Applied Polymer Science*. 63:125-132 (1997).
33. Y. Capan, B.H. Woo, S. Gebrekidan, S. Ahmed, and P.P. DeLuca. Influence of formulation parameters on the characteristics of poly(d,l-lactide-co-glycolide) microspheres containing poly(l-lysine) complexed plasmid DNA. *Journal of Controlled Release*. 60:279-286 (1999).
34. M. Chacón, L. Berges, J. Molpeceres, M.R. Aberturas, and M. Guzman. Optimized preparation of poly d,l (lactic-glycolic) microspheres and nanoparticles for oral administration. *International Journal of Pharmaceutics*. 141:81-91 (1996).
35. J.M. Chen, M.G. Tan, A. Nemmar, W.M. Song, M. Dong, G.L. Zhang, and Y. Li. Quantification of extrapulmonary translocation of intratracheal-instilled particles in vivo in rats: Effect of lipopolysaccharide. *Toxicology*. 222:195-201 (2006).

36. Y.-C. Chen, C.-L. Lo, Y.-F. Lin, and G.-H. Hsiue. Rapamycin encapsulated in dual-responsive micelles for cancer therapy. *Biomaterials*. 34:1115-1127 (2013).
37. W.S. Cheow, M.W. Chang, and K. Hadinoto. The roles of lipid in anti-biofilm efficacy of lipid-polymer hybrid nanoparticles encapsulating antibiotics. *Colloids and Surfaces A: Physicochemical and Engineering Aspects*. 389:158-165 (2011).
38. N.Y. Chew and H.K. Chan. Use of solid corrugated particles to enhance powder aerosol performance. *Pharmaceutical Research*. 18:1570-1577 (2001).
39. K.M. Chin and L.J. Rubin. Pulmonary Arterial Hypertension. *Journal of the American College of Cardiology*. 51:1527-1538 (2008).
40. A. Chuchalin, E. Amelina, and F. Bianco. Tobramycin for inhalation in cystic fibrosis: Beyond respiratory improvements. *Pulmonary Pharmacology & Therapeutics*. 22:526-532 (2009).
41. A.L. Coates and C. O'Callaghan. Drug administration by aerosol in children, Saunders-Elsevier, Philadelphia, PA, 2006.
42. V. Codrons, F. Vanderbist, R.K. Verbeeck, M. Arras, D. Lison, V. Preat, and R. Vanbever. Systemic delivery of parathyroid hormone (1-34) using inhalation dry powders in rats. *Journal of Pharmaceutical sciences*. 92:938-950 (2003).
43. J.F. Coelho, P.C. Ferreira, P. Alves, R. Cordeiro, A.C. Fonseca, J.R. Góis, and M.H. Gil. Drug delivery systems: Advanced technologies potentially applicable in personalized treatments. *The EPMA Journal*. 1:164-209 (2010).
44. J.A. Cohen, T.T. Beaudette, J.L. Cohen, K.E. Broaders, E.M. Bachelder, and J.M. Frechet. Acetal-modified dextran microparticles with controlled degradation kinetics and surface functionality for gene delivery in phagocytic and non-phagocytic cells. *Advanced materials*. 22:3593-3597 (2010).
45. M.A. Collier, K.J. Peine, S. Gautam, S. Oghumu, S. Varikuti, H. Borteh, T.L. Papenfuss, A.R. Sataoskar, E.M. Bachelder, and K.M. Ainslie. Host-mediated *Leishmania donovani* treatment using AR-12 encapsulated in acetalated dextran microparticles. *International Journal of Pharmaceutics*. 499:186-194 (2016).
46. E.-M. Collnot, C. Baldes, M.F. Wempe, J. Hyatt, L. Navarro, K.J. Edgar, U.F. Schaefer, and C.-M. Lehr. Influence of vitamin E TPGS poly(ethylene glycol) chain length on apical efflux transporters in Caco-2 cell monolayers. *Journal of Controlled Release*. 111:35-40 (2006).
47. R.O. Cook, R.K. Pannu, and I.W. Kellaway. Novel sustained release microspheres for pulmonary drug delivery. *Journal of Controlled Release*. 104:79-90 (2005).

48. G.F. Cooney, B.L. Lum, M. Tomaselli, and S.B. Fiel. Absolute Bioavailability and Absorption Characteristics of Aerosolized Tobramycin in Adults with Cystic Fibrosis. *The Journal of Clinical Pharmacology*. 34:255-259 (1994).
49. K. Corkery. Inhalable drugs for systemic therapy. *Respiratory Care*. 45:831-835 (2000).
50. P. Costa and J.M. Sousa Lobo. Modeling and comparison of dissolution profiles. *European Journal of Pharmaceutical Sciences*. 13:123-133 (2001).
51. L. Cui, J.A. Cohen, K.E. Broaders, T.T. Beaudette, and J.M. Frechet. Mannosylated dextran nanoparticles: a pH-sensitive system engineered for immunomodulation through mannose targeting. *Bioconjugate chemistry*. 22:949-957 (2011).
52. R.H. Cummings. Pressurized metered dose inhalers: chlorofluorocarbon to hydrofluoroalkane transition-valve performance. *Journal of Allergy and Clinical Immunology*. 104:S230-236 (1999).
53. D. Das, E. Wang, and T.A.G. Langrish. Solid-phase crystallization of spray-dried glucose powders: A perspective and comparison with lactose and sucrose. *Advanced Powder Technology*. 25:1234-1239 (2014).
54. W.H. De Jong and P.J.A. Borm. Drug delivery and nanoparticles: Applications and hazards. *International journal of nanomedicine*. 3:133-149 (2008).
55. M.B. Dolovich, R.C. Ahrens, D.R. Hess, P. Anderson, R. Dhand, J.L. Rau, G.C. Smaildone, and G. Guyatt. Device selection and outcomes of aerosol therapy: Evidence-based guidelines*: american college of chest physicians/american college of asthma, allergy, and immunology. *Chest*. 127:335-371 (2005).
56. M.B. Dolovich and R. Dhand. Aerosol drug delivery: developments in device design and clinical use. *The Lancet*. 377:1032-1045.
57. J.F. Donohue, M.R. Maleki-Yazdi, S. Kilbride, R. Mehta, C. Kalberg, and A. Church. Efficacy and safety of once-daily umeclidinium/vilanterol 62.5/25 mcg in COPD. *Respiratory Medicine*. 107:1538-1546 (2013).
58. C. Duret, N. Wauthoz, T. Sebti, F. Vanderbist, and K. Amighi. New inhalation-optimized itraconazole nanoparticle-based dry powders for the treatment of invasive pulmonary aspergillosis. *International journal of nanomedicine*. 7:5475-5489 (2012).
59. M. Durrigl, A. Kwokal, A. Hafner, M. Segvic Klaric, A. Dumcic, B. Cetina-Cizmek, and J. Filipovic-Grcic. Spray dried microparticles for controlled delivery of mupirocin calcium: process-tailored modulation of drug release. *Journal of microencapsulation*. 28:108-121 (2011).

60. S. Edda. FK506 (Tacrolimus) in Pulmonary Arterial Hypertension (TransformPAH)2012.
61. D.A. Edwards. The macrotransport of aerosol particles in the lung: Aerosol deposition phenomena. *Journal of Aerosol Science*. 26:293-317 (1995).
62. D.A. Edwards, A. Ben-Jebria, and R. Langer. Recent advances in pulmonary drug delivery using large, porous inhaled particles. *Journal of Applied Physiology*. 85:379-385 (1998).
63. L. Ely, W. Roa, W.H. Finlay, and R. Löbenberg. Effervescent dry powder for respiratory drug delivery. *European Journal of Pharmaceutics and Biopharmaceutics*. 65:346-353 (2007).
64. J.D.W. Evans, B. Girerd, D. Montani, X.-J. Wang, N. Galiè, E.D. Austin, G. Elliott, K. Asano, E. Grünig, Y. Yan, Z.-C. Jing, A. Manes, M. Palazzini, L.A. Wheeler, I. Nakayama, T. Satoh, C. Eichstaedt, K. Hinderhofer, M. Wolf, E.B. Rosenzweig, W.K. Chung, F. Soubrier, G. Simonneau, O. Sitbon, S. Gräf, S. Kaptoge, E. Di Angelantonio, M. Humbert, and N.W. Morrell. BMPR2 mutations and survival in pulmonary arterial hypertension: an individual participant data meta-analysis. *The Lancet Respiratory Medicine*.
65. H. Fessi, F. Puisieux, J.P. Devissaguet, N. Ammoury, and S. Benita. Nanocapsule formation by interfacial polymer deposition following solvent displacement. *International Journal of Pharmaceutics*. 55:R1-R4 (1989).
66. S.Y.K. Fong, A. Ibisogly, and A. Bauer-Brandl. Solubility enhancement of BCS Class II drug by solid phospholipid dispersions: Spray drying versus freeze-drying. *International Journal of Pharmaceutics*.
67. C.F. Foundation. Patient Registry 2005 Annual Report, Bethesda, Maryland, 2005.
68. J.E. Frampton. QVA149 (indacaterol/glycopyrronium fixed-dose combination): a review of its use in patients with chronic obstructive pulmonary disease. *Drugs*. 74:465-488 (2014).
69. F.L. Fu, T.B. Mi, S.S. Wong, and Y.J. Shyu. Characteristic and controlled release of anticancer drug loaded poly (D,L-lactide) microparticles prepared by spray drying technique. *Journal of microencapsulation*. 18:733-747 (2001).
70. H.C. Gaedeand K. Gawrisch. Lateral diffusion rates of lipid, water, and a hydrophobic drug in a multilamellar liposome. *Biophysical journal*. 85:1734-1740 (2003).
71. D.E. Geller, W.H. Pitlick, P.A. Nardella, W.G. Tracewell, and B.W. Ramsey. PHarmacokinetics and bioavailability of aerosolized tobramycin in cystic fibrosis. *Chest*. 122:219-226 (2002).

72. W. Glover, H.K. Chan, S. Eberl, E. Daviskas, and J. Verschuer. Effect of particle size of dry powder mannitol on the lung deposition in healthy volunteers. *International Journal of Pharmaceutics*. 349:314-322 (2008).
73. A. Grenha, C.I. Grainger, L.A. Dailey, B. Seijo, G.P. Martin, C. Remuñán-López, and B. Forbes. Chitosan nanoparticles are compatible with respiratory epithelial cells in vitro. *European Journal of Pharmaceutical Sciences*. 31:73-84 (2007).
74. A. Grenha, B. Seijo, and C. Remunan-Lopez. Microencapsulated chitosan nanoparticles for lung protein delivery. *European journal of pharmaceutical sciences*. 25:427-437 (2005).
75. A. Grenha, B. Seijo, and C. Remuñán-López. Microencapsulated chitosan nanoparticles for lung protein delivery. *European Journal of Pharmaceutical Sciences*. 25:427-437 (2005).
76. B. Gu, B. Linehan, and Y.-C. Tseng. Optimization of the Büchi B-90 spray drying process using central composite design for preparation of solid dispersions. *International Journal of Pharmaceutics*. 491:208-217 (2015).
77. B. Gu, B. Linehan, and Y.C. Tseng. Optimization of the Buchi B-90 spray drying process using central composite design for preparation of solid dispersions. *International Journal of Pharmaceutics*. 491:208-217 (2015).
78. S. Guenneau and T.M. Puvirajesinghe. Fick's second law transformed: one path to cloaking in mass diffusion. *Journal of the Royal Society, Interface*. 10:20130106 (2013).
79. T.F. Guimarães, A.D. Lanchote, J.S. da Costa, A.L. Viçosa, and L.A.P. de Freitas. A multivariate approach applied to quality on particle engineering of spray-dried mannitol. *Advanced Powder Technology*. 26:1094-1101 (2015).
80. K. Hadinoto, P. Phanapavudhikul, Z. Kewu, and R.B.H. Tan. Novel Formulation of Large Hollow Nanoparticles Aggregates as Potential Carriers in Inhaled Delivery of Nanoparticulate Drugs. *Industrial & Engineering Chemistry Research*. 45:3697-3706 (2006).
81. K. Hadinoto, P. Phanapavudhikul, Z. Kewu, and R.B.H. Tan. Dry powder aerosol delivery of large hollow nanoparticulate aggregates as prospective carriers of nanoparticulate drugs: Effects of phospholipids. *International Journal of Pharmaceutics*. 333:187-198 (2007).
82. K. Hadinoto, K. Zhu, and R.B.H. Tan. Drug release study of large hollow nanoparticulate aggregates carrier particles for pulmonary delivery. *International Journal of Pharmaceutics*. 341:195-206 (2007).
83. D. Hayes, Jr., J.B. Zwischenberger, and H.M. Mansour. Aerosolized tacrolimus: a case report in a lung transplant recipient. *Transplantation proceedings*. 42:3876-3879 (2010).

84. C. He, Y. Hu, L. Yin, C. Tang, and C. Yin. Effects of particle size and surface charge on cellular uptake and biodistribution of polymeric nanoparticles. *Biomaterials*. 31:3657-3666 (2010).
85. H. Heijerman, E. Westerman, S. Conway, and D. Touw. Inhaled medication and inhalation devices for lung disease in patients with cystic fibrosis: A European consensus. *Journal of Cystic Fibrosis*. 8:295-315 (2009).
86. J.Y. Her, M.S. Kim, and K.G. Lee. Preparation of probiotic powder by the spray freeze-drying method. *Journal of Food Engineering*. 150:70-74 (2015).
87. D.R. Hess. Aerosol delivery devices in the treatment of asthma. *Respiratory Care*. 53:699-723; discussion 723-695 (2008).
88. J. Heyder. Deposition of Inhaled Particles in the Human Respiratory Tract and Consequences for Regional Targeting in Respiratory Drug Delivery. *Proceedings of the American Thoracic Society*. 1:315-320 (2004).
89. A.J. Hickey, Mansour, Heidi M. Delivery of Drugs by the Pulmonary Route. In J.S. A. T. Florence (ed.), *Modern Pharmaceutics: Applications and Advances*, Vol. 2, Informa Healthcare, New York, NY, 2009, pp. 191-219.
90. A.J. Hickey and H.M. Mansour. Formulation challenges of powders for the delivery of small molecular weight molecules as aerosols, Informa Healthcare, New York, 2008.
91. A.J. Hickey and H.M. Mansour. Formulation challenges of powders for the delivery of small molecular weight molecules as aerosols. In R. MJ, H. J, R. MS, and L. ME (eds.), *Modified-Release Drug Delivery Technology*, Vol. 2, Informa Healthcare, New York, 2008.
92. A.J. Hickey, H.M. Mansour, M.J. Telko, Z. Xu, H.D. Smyth, T. Mulder, R. McLean, J. Langridge, and D. Papadopoulos. Physical characterization of component particles included in dry powder inhalers. I. Strategy review and static characteristics. *Journal of Pharmaceutical sciences*. 96:1282-1301 (2007).
93. A.J. Hickey, H.M. Mansour, M.J. Telko, Z. Xu, H.D.C. Smyth, T. Mulder, R. McLean, J. Langridge, and D. Papadopoulos. Physical characterization of component particles included in dry powder inhalers. I. Strategy review and static characteristics. *Journal of Pharmaceutical Sciences*. 96:1282-1301 (2007).
94. A.M. Hillery. *Advanced Drug Delivery and targeting: An Introduction*, CRC Press 2002.
95. W.C. Hinds. *Aerosol technology: properties, behavior, and measurement of airborne particles*, Wiley-Interscience 1999.

96. T.M. Ho, T. Howes, and B.R. Bhandari. Characterization of crystalline and spray-dried amorphous α -cyclodextrin powders. *Powder Technology*. 284:585-594 (2015).
97. K.V. Hoang, H.M. Borteh, M.V. Rajaram, K.J. Peine, H. Curry, M.A. Collier, M.L. Homsy, E.M. Bachelder, J.S. Gunn, L.S. Schlesinger, and K.M. Ainslie. Acetalated dextran encapsulated AR-12 as a host-directed therapy to control Salmonella infection. *International Journal of Pharmaceutics*. 477:334-343 (2014).
98. M. Hoppentocht, P. Hagedoorn, H.W. Frijlink, and A.H. de Boer. Developments and strategies for inhaled antibiotic drugs in tuberculosis therapy: A critical evaluation. *European Journal of Pharmaceutics and Biopharmaceutics*. 86:23-30 (2014).
99. K.T. Householder, D.M. DiPerna, E.P. Chung, G.M. Wohlleb, H.D. Dhruv, M.E. Berens, and R.W. Sirianni. Intravenous delivery of camptothecin-loaded PLGA nanoparticles for the treatment of intracranial glioma. *International Journal of Pharmaceutics*. 479:374-380 (2015).
100. B.M. Ibrahim, M.D. Tsifansky, Y. Yang, and Y. Yeo. Challenges and advances in the development of inhalable drug formulations for cystic fibrosis lung disease. *Expert Opinion on Drug Delivery*. 8:451-466 (2011).
101. M. Irngartinger, V. Camuglia, M. Damm, J. Goede, and H.W. Frijlink. Pulmonary delivery of therapeutic peptides via dry powder inhalation: effects of micronisation and manufacturing. *European Journal of Pharmaceutics and Biopharmaceutics*. 58:7-14 (2004).
102. F. Iskandar, H.W. Chang, and K. Okuyama. Preparation of microencapsulated powders by an aerosol spray method and their optical properties. *Advanced Powder Technology*. 14:349-367 (2003).
103. F. Iskandar, L. Gradon, and K. Okuyama. Control of the morphology of nanostructured particles prepared by the spray drying of a nanoparticle sol. *Journal of Colloid and Interface Science*. 265:296-303 (2003).
104. N. Islam and E. Gladki. Dry powder inhalers (DPIs)--a review of device reliability and innovation. *International Journal of Pharmaceutics*. 360:1-11 (2008).
105. S. Jafarinejad, K. Gilani, E. Moazeni, M. Ghazi-Khansari, A.R. Najafabadi, and N. Mohajel. Development of chitosan-based nanoparticles for pulmonary delivery of itraconazole as dry powder formulation. *Powder Technology*. 222:65-70 (2012).
106. D.K. Jensen, L.B. Jensen, S. Koocheki, L. Bengtson, D. Cun, H.M. Nielsen, and C. Foged. Design of an inhalable dry powder formulation of DOTAP-modified PLGA nanoparticles loaded with siRNA. *Journal of Controlled Release*. 157:141-148 (2012).
107. D.M. Jensen, D. Cun, M.J. Maltesen, S. Frokjaer, H.M. Nielsen, and C. Foged. Spray drying of siRNA-containing PLGA nanoparticles intended for inhalation. *Journal of Controlled Release*. 142:138-145 (2010).

108. D.M.K. Jensen, D. Cun, M.J. Maltesen, S. Frokjaer, H.M. Nielsen, and C. Foged. Spray drying of siRNA-containing PLGA nanoparticles intended for inhalation. *Journal of Controlled Release*. 142:138-145 (2010).
109. T. Jung, W. Kamm, A. Breitenbach, E. Kaiserling, J.X. Xiao, and T. Kissel. Biodegradable nanoparticles for oral delivery of peptides: is there a role for polymers to affect mucosal uptake? *European Journal of Pharmaceutics and Biopharmaceutics*. 50:147-160 (2000).
110. W. Kaialy, H. Larhrib, G. Martin, and A. Nokhodchi. The Effect of Engineered Mannitol-Lactose Mixture on Dry Powder Inhaler Performance. *Pharmaceutical Research*. 29:2139-2156 (2012).
111. W. Kaialy and A. Nokhodchi. Dry powder inhalers: Physicochemical and aerosolization properties of several size-fractions of a promising alternative carrier, freeze-dried mannitol. *European Journal of Pharmaceutical Sciences*. 68:56-67 (2015).
112. N. Kamaly, B. Yameen, J. Wu, and O.C. Farokhzad. Degradable Controlled-Release Polymers and Polymeric Nanoparticles: Mechanisms of Controlling Drug Release. *Chemical Reviews*. 116:2602-2663 (2016).
113. N. Kanthamneni, S. Sharma, S.A. Meenach, B. Billet, J.-C. Zhao, E.M. Bachelder, and K.M. Ainslie. Enhanced stability of horseradish peroxidase encapsulated in acetalated dextran microparticles stored outside cold chain conditions. *International Journal of Pharmaceutics*. 431:101-110 (2012).
114. C. Karner, J. Chong, and P. Poole. Tiotropium versus placebo for chronic obstructive pulmonary disease. *Cochrane Database Syst Rev*. 7:CD009285 (2014).
115. K.J. Kauffman, N. Kanthamneni, S.A. Meenach, B.C. Pierson, E.M. Bachelder, and K.M. Ainslie. Optimization of rapamycin-loaded acetalated dextran microparticles for immunosuppression. *International Journal of Pharmaceutics*. 422:356-363 (2012).
116. P. Kaur, S.K. Singh, V. Garg, M. Gulati, and Y. Vaidya. Optimization of spray drying process for formulation of solid dispersion containing polypeptide-k powder through quality by design approach. *Powder Technology*. 284:1-11 (2015).
117. K. Kho, W.S. Cheow, R.H. Lie, and K. Hadinoto. Aqueous re-dispersibility of spray-dried antibiotic-loaded polycaprolactone nanoparticle aggregates for inhaled anti-biofilm therapy. *Powder Technology*. 203:432-439 (2010).
118. M. Kilicarlan, M. Gumustas, S. Yildiz, and T. Baykara. Preparation and characterization of chitosan-based spray-dried microparticles for the delivery of clindamycin phosphate to periodontal pockets. *Current drug delivery*. 11:98-111 (2014).
119. E.H.J. Kim. Surface composition of industrial spray-dried dairy powders and its formation mechanisms, *Chemical and Materials Engineering*, Vol. PhD, University of Auckland 2008.

120. E.H.J. Kim, X.D. Chen, and D. Pearce. On the Mechanisms of Surface Formation and the Surface Compositions of Industrial Milk Powders. *Drying Technology*. 21:265-278 (2003).
121. M.W. Konstan, P.A. Flume, M. Kappler, R. Chiron, M. Higgins, F. Brockhaus, J. Zhang, G. Angyalosi, E. He, and D.E. Geller. Safety, efficacy and convenience of tobramycin inhalation powder in cystic fibrosis patients: The EAGER trial. *Journal of Cystic Fibrosis*. 10:54-61 (2011).
122. M.W. Konstan, D.E. Geller, P. Minic, F. Brockhaus, J. Zhang, and G. Angyalosi. Tobramycin Inhalation Powder for *P. aeruginosa* Infection in Cystic Fibrosis: The EVOLVE Trial. *Pediatric Pulmonology*. 46:230-238 (2011).
123. K. Kramek-Romanowska, M. Odziomek, T.R. Sosnowski, and L. Gradoń. Effects of Process Variables on the Properties of Spray-Dried Mannitol and Mannitol/Disodium Cromoglycate Powders Suitable for Drug Delivery by Inhalation. *Industrial & Engineering Chemistry Research*. 50:13922-13931 (2011).
124. N.K. Kunda, I.M. Alfagih, S.R. Dennison, S. Somavarapu, Z. Merchant, G.A. Hutcheon, and I.Y. Saleem. Dry powder pulmonary delivery of cationic PGA-co-PDL nanoparticles with surface adsorbed model protein. *International Journal of Pharmaceutics*. 492:213-222 (2015).
125. N.K. Kunda, I.M. Alfagih, E.N. Miyaji, D.B. Figueiredo, V.M. Goncalves, D.M. Ferreira, S.R. Dennison, S. Somavarapu, G.A. Hutcheon, and I.Y. Saleem. Pulmonary Dry Powder Vaccine of Pneumococcal Antigen Loaded Nanoparticles. *International Journal of Pharmaceutics*(2015).
126. F. Kur, H. Reichenspurner, B.M. Meiser, A. Welz, H. Furst, C. Muller, C. Vogelmeier, M. Schwaiblmaier, J. Briegel, and B. Reichart. Tacrolimus (FK506) as primary immunosuppressant after lung transplantation. *The Thoracic and cardiovascular surgeon*. 47:174-178 (1999).
127. A. Kuzmovand T. Minko. Nanotechnology approaches for inhalation treatment of lung diseases. *Journal of Controlled Release*.
128. N.R. Labirisand M.B. Dolovich. Pulmonary drug delivery. Part I: Physiological factors affecting therapeutic effectiveness of aerosolized medications. *British Journal of Clinical Pharmacology*. 56:588-599 (2003).
129. S.K. Lai, Y.-Y. Wang, and J. Hanes. Mucus-penetrating nanoparticles for drug and gene delivery to mucosal tissues. *Advanced drug delivery reviews*. 61:158-171 (2009).
130. G. Lambert, E. Fattal, and P. Couvreur. Nanoparticulate systems for the delivery of antisense oligonucleotides. *Advanced drug delivery reviews*. 47:99-112 (2001).

131. B.L. Laube, H.M. Janssens, F.H.C. de Jongh, S.G. Devadason, R. Dhand, P. Diot, M.L. Everard, I. Horvath, P. Navalesi, T. Voshaar, and H. Chrystyn. What the pulmonary specialist should know about inhalation therapies. *European Respiratory Journal*. 37:1308-1331 (2011).
132. W.-H. Lee, C.-Y. Loo, D. Traini, and P.M. Young. Inhalation of nanoparticle-based drug for lung cancer treatment: Advantages and challenges. *Asian Journal of Pharmaceutical Sciences*. 10:481-489 (2015).
133. Y.S. Lee, P.J. Johnson, P.T. Robbins, and R.H. Bridson. Production of nanoparticles-in-microparticles by a double emulsion method: A comprehensive study. *European Journal of Pharmaceutics and Biopharmaceutics*. 83:168-173 (2013).
134. H.-Y. Li and J. Birchall. Chitosan-Modified Dry Powder Formulations for Pulmonary Gene Delivery. *Pharmaceutical Research*. 23:941-950 (2006).
135. X. Li, S. Chang, G. Du, Y. Li, J. Gong, M. Yang, and Z. Wei. Encapsulation of azithromycin into polymeric microspheres by reduced pressure-solvent evaporation method. *International Journal of Pharmaceutics*. 433:79-88 (2012).
136. X. Li and H.M. Mansour. Physicochemical Characterization and Water Vapor Sorption of Organic Solution Advanced Spray-Dried Inhalable Trehalose Microparticles and Nanoparticles for Targeted Dry Powder Pulmonary Inhalation Delivery. *AAPS PharmSciTech*. 12:1420-1430 (2011).
137. X. Li, F.G. Vogt, D. Hayes Jr, and H.M. Mansour. Physicochemical characterization and aerosol dispersion performance of organic solution advanced spray-dried microparticulate/nanoparticulate antibiotic dry powders of tobramycin and azithromycin for pulmonary inhalation aerosol delivery. *European Journal of Pharmaceutical Sciences*. 52:191-205 (2014).
138. Y.Z. Li, X. Sun, T. Gong, J. Liu, J. Zuo, and Z.R. Zhang. Inhalable microparticles as carriers for pulmonary delivery of thymopentin-loaded solid lipid nanoparticles. *Pharmaceutical Research*. 27:1977-1986 (2010).
139. Y.-Z. Li, X. Sun, T. Gong, J. Liu, J. Zuo, and Z.-R. Zhang. Inhalable microparticles as carriers for pulmonary delivery of thymopentin-loaded solid lipid nanoparticles. *Pharmaceutical Research*. 27:1977-1986 (2010).
140. M. Lippmann, D.B. Yeates, and R.E. Albert. Deposition, retention, and clearance of inhaled particles. *British Journal of Industrial Medicine*. 37:337-362 (1980).
141. E.M. Littringer, A. Mescher, S. Eckhard, H. Schröttner, C. Langes, M. Fries, U. Griesser, P. Walzel, and N.A. Urbanetz. Spray Drying of Mannitol as a Drug Carrier—The Impact of Process Parameters on Product Properties. *Drying Technology*. 30:114-124 (2011).

142. E.M. Littringer, A. Mescher, H. Schroettner, L. Achelis, P. Walzel, and N.A. Urbanetz. Spray dried mannitol carrier particles with tailored surface properties – The influence of carrier surface roughness and shape. *European Journal of Pharmaceutics and Biopharmaceutics*. 82:194-204 (2012).
143. E.M. Littringer, R. Paus, A. Mescher, H. Schroettner, P. Walzel, and N.A. Urbanetz. The morphology of spray dried mannitol particles — The vital importance of droplet size. *Powder Technology*. 239:162-174 (2013).
144. R.A. Lubet, Z. Zhang, Y. Wang, and M. You. Chemoprevention of lung cancer in transgenic mice. *Chest*. 125:144S-147S (2004).
145. Y.F. Maa, P.A. Nguyen, J.D. Andya, N. Dasovich, T.D. Sweeney, S.J. Shire, and C.C. Hsu. Effect of spray drying and subsequent processing conditions on residual moisture content and physical/biochemical stability of protein inhalation powders. *Pharmaceutical Research*. 15:768-775 (1998).
146. Y.-F. Maa, H.R. Costantino, P.-A. Nguyen, and C.C. Hsu. The Effect of Operating and Formulation Variables on the Morphology of Spray-Dried Protein Particles. *Pharmaceutical development and technology*. 2:213-223 (1997).
147. Y.-F. Maa, P.-A.T. Nguyen, and S.W. Hsu. Spray-drying of air–liquid interface sensitive recombinant human growth hormone. *Journal of Pharmaceutical Sciences*. 87:152-159 (1998).
148. S.G. Maas, G. Schaldach, E.M. Littringer, A. Mescher, U.J. Griesser, D.E. Braun, P.E. Walzel, and N.A. Urbanetz. The impact of spray drying outlet temperature on the particle morphology of mannitol. *Powder Technology*. 213:27-35 (2011).
149. S.G. Maas, G. Schaldach, P. Walzel, and N.A. Urbanetz. Tailoring dry powder inhaler performance by modifying carrier surface topography by spray drying. *Atomization and Sprays*. 20:763-774 (2010).
150. A. Mahmud and D.E. Discher. Lung Vascular Targeting Through Inhalation Delivery: Insight from Filamentous Viruses and Other Shapes. *Iubmb Life*. 63:607-612 (2011).
151. K.C. Mannix and R. Meir. Teva Announces FDA Approval of ProAir® RespiClick.
http://www.tevapharm.com/news/teva_announces_fda_approval_of_proair_respiclick_04_15.aspx.
152. H.M. Mansour, Y.S. Rhee, C.W. Park, and P.P. DeLuca. Lipid Nanoparticulate Drug Delivery and Nanomedicine. In A. Moghis (ed.), *Lipids in Nanotechnology*, American Oil Chemists Society (AOCS) Press, Urbana, Illinois, 2011, pp. 221-268.
153. H.M. Mansour, Y.S. Rhee, and X. Wu. Nanomedicine in pulmonary delivery. *International journal of nanomedicine*. 4:299-319 (2009).

154. H.M. Mansour, Y.-S. Rhee, and X. Wu. Nanomedicine in pulmonary delivery. *International journal of nanomedicine*. 4:299-319 (2009).
155. F.J. Martinez, J. Boscia, G. Feldman, C. Scott-Wilson, S. Kilbride, L. Fabbri, C. Crim, and P.M. Calverley. Fluticasone furoate/vilanterol (100/25; 200/25 mug) improves lung function in COPD: a randomised trial. *Respiratory Medicine*. 107:550-559 (2013).
156. P.H.B. Matthias Ochs, Joan Gil, and Ewald R, Weibel. Anatomy of the Chest Wall and Lungs. In J.L.I. Thomas W. Shields, Carolyn E. Reed, and Richard H. Feins (ed.), *General Thoracic Surgery*, Vol. 1, Wolters Kluwer/ Lippincott Williams and Wilkins Health, Philadelphia, 2009, p. 47.
157. M. Maury, K. Murphy, S. Kumar, A. Maurer, and G. Lee. Spray-drying of proteins: effects of sorbitol and trehalose on aggregation and FT-IR amide I spectrum of an immunoglobulin G. *European Journal of Pharmaceutics and Biopharmaceutics*. 59:251-261 (2005).
158. M. Maury, K. Murphy, S. Kumar, L. Shi, and G. Lee. Effects of process variables on the powder yield of spray-dried trehalose on a laboratory spray-dryer. *European Journal of Pharmaceutics and Biopharmaceutics*. 59:565-573 (2005).
159. D.P. McIntosh, X.Y. Tan, P. Oh, and J.E. Schnitzer. Targeting endothelium and its dynamic caveolae for tissue-specific transcytosis in vivo: a pathway to overcome cell barriers to drug and gene delivery. *Proceedings of the National Academy of Sciences of the United States of America*. 99:1996-2001 (2002).
160. S.A. Meenach, K.W. Anderson, J. Zach Hilt, R.C. McGarry, and H.M. Mansour. Characterization and aerosol dispersion performance of advanced spray-dried chemotherapeutic PEGylated phospholipid particles for dry powder inhalation delivery in lung cancer. *European Journal of Pharmaceutical Sciences*. 49:699-711 (2013).
161. S.A. Meenach, Y.J. Kim, K.J. Kauffman, N. Kanthamneni, E.M. Bachelder, and K.M. Ainslie. Synthesis, Optimization, and Characterization of Camptothecin-Loaded Acetalated Dextran Porous Microparticles for Pulmonary Delivery. *Molecular Pharmaceutics*. 9:290-298 (2012).
162. S.A. Meenach, F.G. Vogt, K.W. Anderson, J.Z. Hilt, R.C. McGarry, and H.M. Mansour. Design, physicochemical characterization, and optimization of organic solution advanced spray-dried inhalable dipalmitoylphosphatidylcholine (DPPC) and dipalmitoylphosphatidylethanolamine poly(ethylene glycol) (DPPE-PEG) microparticles and nanoparticles for targeted respiratory nanomedicine delivery as dry powder inhalation aerosols. *International journal of nanomedicine*. 8:275-293 (2013).
163. J.U. Menon, P. Ravikumar, A. Pise, D. Gyawali, C.C.W. Hsia, and K.T. Nguyen. Polymeric nanoparticles for pulmonary protein and DNA delivery. *Acta Biomaterialia*. 10:2643-2652 (2014).

164. O. Mert, S.K. Lai, L. Ensign, M. Yang, Y.-Y. Wang, J. Wood, and J. Hanes. A poly(ethylene glycol)-based surfactant for formulation of drug-loaded mucus penetrating particles. *Journal of Controlled Release*. 157:455-460 (2012).
165. C.E. Milla. Nutrition and Lung Disease in Cystic Fibrosis. *Clinics in Chest Medicine*. 28:319-330 (2007).
166. D.P. Miller, T. Tan, T.E. Tarara, J. Nakamura, R.J. Malcolmson, and J.G. Weers. Physical Characterization of Tobramycin Inhalation Powder: I. Rational Design of a Stable Engineered-Particle Formulation for Delivery to the Lungs. *Molecular Pharmaceutics*. 12:2582-2593 (2015).
167. A. Minne, H. Boireau, M.J. Horta, and R. Vanbever. Optimization of the aerosolization properties of an inhalation dry powder based on selection of excipients. *European Journal of Pharmaceutics and Biopharmaceutics*. 70:839-844 (2008).
168. T. Mizoe, T. Ozeki, and H. Okada. Preparation of drug nanoparticle-containing microparticles using a 4-fluid nozzle spray drier for oral, pulmonary, and injection dosage forms. *Journal of Controlled Release*. 122:10-15 (2007).
169. G. Mohammadi, H. Valizadeh, M. Barzegar-Jalali, F. Lotfipour, K. Adibkia, M. Milani, M. Azhdarzadeh, F. Kiafar, and A. Nokhodchi. Development of azithromycin-PLGA nanoparticles: Physicochemical characterization and antibacterial effect against *Salmonella typhi*. *Colloids and Surfaces B: Biointerfaces*. 80:34-39 (2010).
170. G. Mohammadi, H. Valizadeh, M. Barzegar-Jalali, F. Lotfipour, K. Adibkia, M. Milani, M. Azhdarzadeh, F. Kiafar, and A. Nokhodchi. Development of azithromycin-PLGA nanoparticles: physicochemical characterization and antibacterial effect against *Salmonella typhi*. *Colloids and Surfaces B: Biointerfaces*. 80:34-39 (2010).
171. D. Montani, M.-C. Chaumais, C. Guignabert, S. Günther, B. Girerd, X. Jaïs, V. Algalarrondo, L.C. Price, L. Savale, O. Sitbon, G. Simonneau, and M. Humbert. Targeted therapies in pulmonary arterial hypertension. *Pharmacology & Therapeutics*. 141:172-191 (2014).
172. L. Muand S.S. Feng. Fabrication, characterization and in vitro release of paclitaxel (Taxol®) loaded poly (lactic-co-glycolic acid) microspheres prepared by spray drying technique with lipid/cholesterol emulsifiers. *Journal of Controlled Release*. 76:239-254 (2001).
173. S.R. Mudshinge, A.B. Deore, S. Patil, and C.M. Bhalgat. Nanoparticles: Emerging carriers for drug delivery. *Saudi Pharmaceutical Journal*. 19:129-141 (2011).
174. R.H. Muller, K. Mader, and S. Gohla. Solid lipid nanoparticles (SLN) for controlled drug delivery - a review of the state of the art. *European Journal of Pharmaceutics and Biopharmaceutics* 50:161-177 (2000).

175. P. Muralidharan, M. Malapit, E. Mallory, D. Hayes Jr, and H.M. Mansour. Inhalable nanoparticulate powders for respiratory delivery. *Nanomedicine: Nanotechnology, Biology and Medicine*. 11:1189-1199 (2015).
176. K. Muzaffar and P. Kumar. Parameter optimization for spray drying of tamarind pulp using response surface methodology. *Powder Technology*. 279:179-184 (2015).
177. B.V.N.Y. Nagavarma, Hemant K. S.; Ayaz, A.; Vasudha, L. S.; Shivakumar, H. G. DIFFERENT TECHNIQUES FOR PREPARATION OF POLYMERIC NANOPARTICLES- A REVIEW. *Asian Journal of Pharmaceutical & Clinical Research*. 5:(2012).
178. S.P. Newman and W.W. Busse. Evolution of dry powder inhaler design, formulation, and performance. *Respiratory Medicine*. 96:293-304 (2002).
179. C. Nora Y.K. , Hak-Kim Chan. The Role of Particle Properties in Pharmaceutical Powder Inhalation Formulations. *Journal of Aerosol Medicine*. 15:325-330 (2002).
180. K. Ohashi, T. Kabasawa, T. Ozeki, and H. Okada. One-step preparation of rifampicin/poly(lactic-co-glycolic acid) nanoparticle-containing mannitol microspheres using a four-fluid nozzle spray drier for inhalation therapy of tuberculosis. *Journal of Controlled Release*. 135:19-24 (2009).
181. H.X. Ong, D. Traini, G. Ballerin, L. Morgan, L. Buddle, S. Scalia, and P.M. Young. Combined Inhaled Salbutamol and Mannitol Therapy for Mucus Hyper-secretion in Pulmonary Diseases. *Aaps J*. 16:269-280 (2014).
182. C.W. Park, X. Li, F.G. Vogt, D. Hayes, Jr., J.B. Zwischenberger, E.S. Park, and H.M. Mansour. Advanced spray-dried design, physicochemical characterization, and aerosol dispersion performance of vancomycin and clarithromycin multifunctional controlled release particles for targeted respiratory delivery as dry powder inhalation aerosols. *International Journal of Pharmaceutics*. 455:374-392 (2013).
183. C.W.M. Park, Heidi M.; Hayes, Don Pulmonary inhalation aerosols for targeted antibiotics drug delivery. *European Pharmaceutical Review*. 1:(2011).
184. M.D. Parkins and J.S. Elborn. Tobramycin Inhalation Powder: a novel drug delivery system for treating chronic *Pseudomonas aeruginosa* infection in cystic fibrosis. *Expert Review of Respiratory Medicine*. 5:609-622 (2011).
185. S. Parveen, R. Misra, and S.K. Sahoo. Nanoparticles: a boon to drug delivery, therapeutics, diagnostics and imaging. *Nanomedicine: Nanotechnology, Biology and Medicine*. 8:147-166 (2012).
186. J.S. Patton and P.R. Byron. Inhaling medicines: delivering drugs to the body through the lungs. *Nature Reviews Drug Discovery*. 6:67-74 (2007).

187. D. Pavia. *Aerosols and the Lung: Clinical and Experimental Aspects*. In S.W. Clarke and D. Pavia (eds.), Butterworths, London, 1984, pp. 200-229.
188. G. Pilcer and K. Amighi. Formulation strategy and use of excipients in pulmonary drug delivery. *International Journal of Pharmaceutics*. 392:1-19 (2010).
189. G. Pilcer, F. Vanderbist, and K. Amighi. Preparation and characterization of spray-dried tobramycin powders containing nanoparticles for pulmonary delivery. *International Journal of Pharmaceutics*. 365:162-169 (2009).
190. P.S. Pourshahab, K. Gilani, E. Moazeni, H. Eslahi, M.R. Fazeli, and H. Jamalifar. Preparation and characterization of spray dried inhalable powders containing chitosan nanoparticles for pulmonary delivery of isoniazid. *Journal of microencapsulation*. 28:605-613 (2011).
191. B. Pulliam, J.C. Sung, and D.A. Edwards. Design of nanoparticle-based dry powder pulmonary vaccines. *Expert Opinion on Drug Delivery*. 4:651-663 (2007).
192. W.S. Rasband. ImageJ. <http://imagej.nih.gov/ij/>.
193. J. Raula, H. Eerikäinen, and E.I. Kauppinen. Influence of the solvent composition on the aerosol synthesis of pharmaceutical polymer nanoparticles. *International Journal of Pharmaceutics*. 284:13-21 (2004).
194. S.S. Razavi Rohani, K. Abnous, and M. Tafaghodi. Preparation and characterization of spray-dried powders intended for pulmonary delivery of Insulin with regard to the selection of excipients. *International Journal of Pharmaceutics*. 465:464-478 (2014).
195. W.E. Regelman, G.R. Elliott, W.J. Warwick, and C.C. Clawson. Reduction of Sputum *Pseudomonas aeruginosa* Density by Antibiotics Improves Lung Function in Cystic Fibrosis More than Do Bronchodilators and Chest Physiotherapy Alone. *American Review of Respiratory Disease*. 141:914-921 (1990).
196. T.Z. Roham, S. Yon, S. Val, L. Yuwen, L.-B. Janel, and S. Edda. TrANsFoRM PAH: Phase II Study Of Safety And Efficacy Of FK-506 (Tacrolimus) In Pulmonary Arterial Hypertension. *MANAGEMENT OF PULMONARY HYPERTENSION*, American Thoracic Society 2013, pp. A3275-A3275.
197. D. Roy, X. Guillon, F. Lescure, P. Couvreur, N. Bru, and P. Breton. On shelf stability of freeze-dried poly(methylidene malonate 2.1.2) nanoparticles. *International Journal of Pharmaceutics*. 148:165-175 (1997).
198. L.J. Rubin and N. Galiè. Pulmonary arterial hypertension: a look to the future. *Journal of the American College of Cardiology*. 43:S89-S90 (2004).
199. R. Sand S. L. Pulmonary infections in patients with cystic fibrosis. *Seminars in Respiratory Infections* 17:47-56 (2002).

200. S. Sand H. AJ. Drug properties affecting aerosol behavior. *Respiratory Care*. 45:652-666 (2000).
201. L. Saiman, B.C. Marshall, N. Mayer-Hamblett, and et al. Azithromycin in patients with cystic fibrosis chronically infected with pseudomonas aeruginosa: A randomized controlled trial. *JAMA*. 290:1749-1756 (2003).
202. J. Sanchis, C. Corrigan, M.L. Levy, J.L. Viejo, and A. Group. Inhaler devices - from theory to practice. *Respiratory Medicine*. 107:495-502 (2013).
203. P. SC, D. LH, and R. KA. Clarithromycin and azithromycin: new macrolide antibiotics. *Clinical Pharmacology*. 11:137-152 (1992).
204. N. Schafroth, C. Arpagaus, U.Y. Jadhav, S. Makne, and D. Douroumis. Nano and microparticle engineering of water insoluble drugs using a novel spray-drying process. *Colloids and Surfaces B: Biointerfaces*. 90:8-15 (2012).
205. A. Seidlitz and W. Weitschies. In-vitro dissolution methods for controlled release parenterals and their applicability to drug-eluting stent testing. *The Journal of pharmacy and pharmacology*. 64:969-985 (2012).
206. J.O.H. Sham, Y. Zhang, W.H. Finlay, W.H. Roa, and R. Löbenberg. Formulation and characterization of spray-dried powders containing nanoparticles for aerosol delivery to the lung. *International Journal of Pharmaceutics*. 269:457-467 (2004).
207. X. Shi and Q. Zhong. Crystallinity and quality of spray-dried lactose powder improved by soluble soybean polysaccharide. *LWT - Food Science and Technology*. 62:89-96 (2015).
208. W.S. Shim, J.-H. Kim, K. Kim, Y.-S. Kim, R.-W. Park, I.-S. Kim, I.C. Kwon, and D.S. Lee. pH- and temperature-sensitive, injectable, biodegradable block copolymer hydrogels as carriers for paclitaxel. *International Journal of Pharmaceutics*. 331:11-18 (2007).
209. S.A. Shoyele and S. Cawthorne. Particle engineering techniques for inhaled biopharmaceuticals. *Advanced drug delivery reviews*. 58:1009-1029 (2006).
210. D. Shuwisitkul. Biodegradable implants with different drug release profiles, Department of Biology, Chemistry and Pharmacy, Vol. Doctor, Freie Universität Berlin 2011.
211. K.M. Skubitz and P.M. Anderson. Inhalational interleukin-2 liposomes for pulmonary metastases: a phase I clinical trial. *Anticancer Drugs*. 11:555-563 (2000).
212. A.R. Smyth, S.C. Bell, S. Bojcin, M. Bryon, A. Duff, P. Flume, N. Kashirskaya, A. Munck, F. Ratjen, S.J. Schwarzenberg, I. Sermet-Gaudelus, K.W. Southern, G. Taccetti, G. Ullrich, S. Wolfe, and S. European Cystic Fibrosis. *European Cystic Fibrosis*

Society Standards of Care: Best Practice guidelines. *Journal of Cystic Fibrosis*. 13 Suppl 1:S23-42 (2014).

213. H.C. Smyth and A.J. Hickey. Carriers in drug powder delivery. *Am J Drug Deliv*. 3:117-132 (2005).

214. F. Soubrier, W.K. Chung, R. Machado, E. Grünig, M. Aldred, M. Geraci, J.E. Loyd, C.G. Elliott, R.C. Trembath, J.H. Newman, and M. Humbert. Genetics and Genomics of Pulmonary Arterial Hypertension. *Journal of the American College of Cardiology*. 62:D13-D21 (2013).

215. K.W. Southern and P.M. Barker. Azithromycin for cystic fibrosis. *European Respiratory Journal*. 24:834-838 (2004).

216. E. Spiekerkoetter, Y.K. Sung, D. Sudheendra, M. Bill, M.A. Aldred, M.C. van de Veerdonk, A. Vonk Noordegraaf, J. Long-Boyle, R. Dash, P.C. Yang, A. Lawrie, A.J. Swift, M. Rabinovitch, and R.T. Zamanian. Low-Dose FK506 (Tacrolimus) in End-Stage Pulmonary Arterial Hypertension. *American journal of respiratory and critical care medicine*. 192:254-257 (2015).

217. E. Spiekerkoetter, X. Tian, J. Cai, R.K. Hopper, D. Sudheendra, C.G. Li, N. El-Bizri, H. Sawada, R. Haghighat, R. Chan, L. Haghighat, V. de Jesus Perez, L. Wang, S. Reddy, M. Zhao, D. Bernstein, D.E. Solow-Cordero, P.A. Beachy, T.J. Wandless, P. ten Dijke, and M. Rabinovitch. FK506 activates BMPR2, rescues endothelial dysfunction, and reverses pulmonary hypertension. *The Journal of Clinical Investigation*. 123:3600-3613 (2013).

218. K. Ståhl, M. Claesson, P. Lilliehorn, H. Lindén, and K. Bäckström. The effect of process variables on the degradation and physical properties of spray dried insulin intended for inhalation. *International Journal of Pharmaceutics*. 233:227-237 (2002).

219. S. Stanojevic, V. Waters, J.L. Mathew, L. Taylor, and F. Ratjen. Effectiveness of inhaled tobramycin in eradicating *Pseudomonas aeruginosa* in children with cystic fibrosis. *Journal of Cystic Fibrosis*. 13:172-178 (2014).

220. S. Stegemann, S. Kopp, G. Borchard, V.P. Shah, S. Senel, R. Dubey, N. Urbanetz, M. Cittero, A. Schoubben, C. Hippchen, D. Cade, A. Fuglsang, J. Morais, L. Borgström, F. Farshi, K.H. Seyfang, R. Hermann, A. van de Putte, I. Klebovich, and A. Hincal. Developing and advancing dry powder inhalation towards enhanced therapeutics. *European journal of pharmaceutical sciences*. 48:181-194 (2013).

221. S. Stegemann, S. Kopp, G. Borchard, V.P. Shah, S. Senel, R. Dubey, N. Urbanetz, M. Cittero, A. Schoubben, C. Hippchen, D. Cade, A. Fuglsang, J. Morais, L. Borgström, F. Farshi, K.H. Seyfang, R. Hermann, A. van de Putte, I. Klebovich, and A. Hincal. Developing and advancing dry powder inhalation towards enhanced therapeutics. *European Journal of Pharmaceutical Sciences*. 48:181-194 (2013).

222. N.A. Stocke, S.A. Meenach, S.M. Arnold, H.M. Mansour, and J.Z. Hilt. Formulation and characterization of inhalable magnetic nanocomposite microparticles (MnMs) for targeted pulmonary delivery via spray drying. *International Journal of Pharmaceutics*. 479:320-328 (2015).
223. S. Suarez and A.J. Hickey. Drug properties affecting aerosol behavior. *Respiratory Care*. 45:652-666 (2000).
224. T. Sun, Y.S. Zhang, B. Pang, D.C. Hyun, M. Yang, and Y. Xia. Engineered Nanoparticles for Drug Delivery in Cancer Therapy. *Angewandte Chemie International Edition*. 53:12320-12364 (2014).
225. J.C. Sung, D.J. Padilla, L. Garcia-Contreras, J.L. Verberkmoes, D. Durbin, C.A. Peloquin, K.J. Elbert, A.J. Hickey, and D.A. Edwards. Formulation and pharmacokinetics of self-assembled rifampicin nanoparticle systems for pulmonary delivery. *Pharmaceutical Research*. 26:1847-1855 (2009).
226. J.C. Sung, B.L. Pulliam, and D.A. Edwards. Nanoparticles for drug delivery to the lungs. *Trends in Biotechnology*. 25:563-570 (2007).
227. D. T, M. N, and W. P. Nebuliser systems for drug delivery in cystic fibrosis. *Cochrane Database of Systematic Reviews*(2013).
228. Y. Takashima, R. Saito, A. Nakajima, M. Oda, A. Kimura, T. Kanazawa, and H. Okada. Spray-drying preparation of microparticles containing cationic PLGA nanospheres as gene carriers for avoiding aggregation of nanospheres. *International Journal of Pharmaceutics*. 343:262-269 (2007).
229. B.C. Tang, M. Dawson, S.K. Lai, Y.Y. Wang, J.S. Suk, M. Yang, P. Zeitlin, M.P. Boyle, J. Fu, and J. Hanes. Biodegradable polymer nanoparticles that rapidly penetrate the human mucus barrier. *Proceedings of the National Academy of Sciences of the United States of America*. 106:19268-19273 (2009).
230. B.C. Tang, M. Dawson, S.K. Lai, Y.-Y. Wang, J.S. Suk, M. Yang, P. Zeitlin, M.P. Boyle, J. Fu, and J. Hanes. Biodegradable polymer nanoparticles that rapidly penetrate the human mucus barrier. *Proceedings of the National Academy of Sciences*. 106:19268-19273 (2009).
231. M.J. Telko and A.J. Hickey. Dry Powder Inhaler Formulation. *Respiratory Care*. 50:1209-1227 (2005).
232. P. Tewa-Tagne, S. Briançon, and H. Fessi. Preparation of redispersible dry nanocapsules by means of spray-drying: Development and characterisation. *European Journal of Pharmaceutical Sciences*. 30:124-135 (2007).
233. R.M. Thursfield and J.C. Davies. Cystic Fibrosis: therapies targeting specific gene defects. *Paediatric Respiratory Reviews*. 13:215-219 (2012).

234. T.-Y. Ting, I. Gonda, and E. Gipps. Microparticles of Polyvinyl Alcohol for Nasal Delivery. I. Generation by Spray-Drying and Spray-Desolvation. *Pharmaceutical Research*. 9:1330-1335 (1992).
235. K. Tomoda, T. Ohkoshi, Y. Kawai, M. Nishiwaki, T. Nakajima, and K. Makino. Preparation and properties of inhalable nanocomposite particles: Effects of the temperature at a spray-dryer inlet upon the properties of particles. *Colloids and Surfaces B: Biointerfaces*. 61:138-144 (2008).
236. K. Tomoda, T. Ohkoshi, T. Nakajima, and K. Makino. Preparation and properties of inhalable nanocomposite particles: Effects of the size, weight ratio of the primary nanoparticles in nanocomposite particles and temperature at a spray-dryer inlet upon properties of nanocomposite particles. *Colloids and Surfaces B: Biointerfaces*. 64:70-76 (2008).
237. N. Tsapis, D. Bennett, B. Jackson, D.A. Weitz, and D.A. Edwards. Trojan particles: Large porous carriers of nanoparticles for drug delivery. *Proceedings of the National Academy of Sciences*. 99:12001-12005 (2002).
238. B.D. Ulery, L.S. Nair, and C.T. Laurencin. Biomedical Applications of Biodegradable Polymers. *Journal of polymer science Part B, Polymer physics*. 49:832-864 (2011).
239. F. Ungaro, I. d'Angelo, C. Coletta, R. d'Emmanuele di Villa Bianca, R. Sorrentino, B. Perfetto, M.A. Tufano, A. Miro, M.I. La Rotonda, and F. Quaglia. Dry powders based on PLGA nanoparticles for pulmonary delivery of antibiotics: Modulation of encapsulation efficiency, release rate and lung deposition pattern by hydrophilic polymers. *Journal of Controlled Release*. 157:149-159 (2012).
240. F. Ungaro, I. d'Angelo, A. Miro, M.I. La Rotonda, and F. Quaglia. Engineered PLGA nano- and micro-carriers for pulmonary delivery: challenges and promises. *The Journal of pharmacy and pharmacology*. 64:1217-1235 (2012).
241. F. Ungaro, G. De Rosa, A. Miro, F. Quaglia, and M.I. La Rotonda. Cyclodextrins in the production of large porous particles: Development of dry powders for the sustained release of insulin to the lungs. *European Journal of Pharmaceutical Sciences*. 28:423-432 (2006).
242. R. Vanbever, J.D. Mintzes, J. Wang, J. Nice, D. Chen, R. Batycky, R. Langer, and D.A. Edwards. Formulation and physical characterization of large porous particles for inhalation. *Pharmaceutical Research*. 16:1735-1742 (1999).
243. J. Varshosaz, F. Hassanzadeh, A. Mardani, and M. Rostami. Feasibility of haloperidol-anchored albumin nanoparticles loaded with doxorubicin as dry powder inhaler for pulmonary delivery. *Pharmaceutical development and technology*. 20:183-196 (2015).

244. S.K. Vaswani and P.S. Creticos. Metered dose inhaler: past, present, and future. *Ann Allergy Asthma Immunol.* 80:11-19; quiz 19-20 (1998).
245. R. Vehring. Pharmaceutical particle engineering via spray drying. *Pharmaceutical Research.* 25:999-1022 (2008).
246. R. Vehring, W.R. Foss, and D. Lechuga-Ballesteros. Particle formation in spray drying. *Journal of Aerosol Science.* 38:728-746 (2007).
247. A.S. Verkman, Y.L. Song, and J.R. Thiagarajah. Role of airway surface liquid and submucosal glands in cystic fibrosis lung disease. *American Journal of Physiology-Cell Physiology.* 284:C2-C15 (2003).
248. M. Vicari-Christensen, S. Repper, S. Basile, and D. Young. Tacrolimus: review of pharmacokinetics, pharmacodynamics, and pharmacogenetics to facilitate practitioners' understanding and offer strategies for educating patients and promoting adherence. *Progress in transplantation.* 19:277-284 (2009).
249. F. W. The ARLA Respiratory Deposition Calculator 2008.
250. T. Wagner, G. Soong, S. Sokol, L. Saiman, and A. Prince. Effects of azithromycin on clinical isolates of *Pseudomonas aeruginosa* from cystic fibrosis patients*. *Chest.* 128:912-919 (2005).
251. Q. Wang, J. Zhang, and A. Wang. Freeze-drying: A versatile method to overcome re-aggregation and improve dispersion stability of palygorskite for sustained release of ofloxacin. *Applied Clay Science.* 87:7-13 (2014).
252. Z. Wang, J.L. Cuddigan, S.K. Gupta, and S.A. Meenach. Nanocomposite Microparticles (nCmP) for the Delivery of Tacrolimus in the Treatment of Pulmonary Arterial Hypertension. *International Journal of Pharmaceutics.* 512:305-313 (2016).
253. Z. Wang and S.A. Meenach. Synthesis and Characterization of Nanocomposite Microparticles (nCmP) for the Treatment of Cystic Fibrosis-Related Infections. *Pharmaceutical Research.* 33:1862-1872 (2016).
254. Z. Wang, E.A. Torrico-Guzman, S.K. Gupta, and S.A. Meenach. Nanocomposite Microparticles (nCmP) for Pulmonary Drug Delivery Applications. In R. Keservani (ed.), *In Strategies of Nanotechnology in Drug Delivery*, Apple Academic Press, New Jersey, In Press July 2016.
255. A.B. Watts and R.O. Williams. Nanoparticles for Pulmonary Delivery. In D.C.H. Smyth and J.A. Hickey (eds.), *Controlled Pulmonary Drug Delivery*, Springer New York, New York, NY, 2011, pp. 335-366.
256. J. West, E. Austin, J.P. Fessel, J. Loyd, and R. Hamid. Rescuing the BMP2 signaling axis in pulmonary arterial hypertension. *Drug Discovery Today.* 19:1241-1245 (2014).

257. A.Z. Wilczewska, K. Niemirowicz, K.H. Markiewicz, and H. Car. Nanoparticles as drug delivery systems. *Pharmacological Reports*. 64:1020-1037 (2012).
258. L. Willis, D. Hayes, and H.M. Mansour. Therapeutic Liposomal Dry Powder Inhalation Aerosols for Targeted Lung Delivery. *Lung*. 190:251-262 (2012).
259. E.B. Wilms, D.J. Touw, H.G.M. Heijerman, and C.K. van der Ent. Azithromycin maintenance therapy in patients with cystic fibrosis: A dose advice based on a review of pharmacokinetics, efficacy, and side effects. *Pediatric Pulmonology*. 47:658-665 (2012).
260. C.A. Wolfe, P.S. James, A.R. Mackie, S. Ladha, and R. Jones. Regionalized lipid diffusion in the plasma membrane of mammalian spermatozoa. *Biology of reproduction*. 59:1506-1514 (1998).
261. L. Wu, X. Miao, Z. Shan, Y. Huang, L. Li, X. Pan, Q. Yao, G. Li, and C. Wu. Studies on the spray dried lactose as carrier for dry powder inhalation. *Asian Journal of Pharmaceutical Sciences*. 9:336-341 (2014).
262. X. Wu, D. Hayes, Jr., J.B. Zwischenberger, R.J. Kuhn, and H.M. Mansour. Design and physicochemical characterization of advanced spray-dried tacrolimus multifunctional particles for inhalation. *Drug design, development and therapy*. 7:59-72 (2013).
263. X. Wu, W. Zhang, D. Hayes, and H.M. Mansour. Physicochemical characterization and aerosol dispersion performance of organic solution advanced spray-dried cyclosporine A multifunctional particles for dry powder inhalation aerosol delivery. *International journal of nanomedicine*. 8:1269-1283 (2013).
264. M.E. Wylam, R. Ten, U.B. Prakash, H.F. Nadrous, M.L. Clawson, and P.M. Anderson. Aerosol granulocyte-macrophage colony-stimulating factor for pulmonary alveolar proteinosis. *European Respiratory Society*. 27:585-593 (2006).
265. W. Xu, P. Ling, and T. Zhang. Toward immunosuppressive effects on liver transplantation in rat model: Tacrolimus loaded poly(ethylene glycol)-poly(D,L-lactide) nanoparticle with longer survival time. *International Journal of Pharmaceutics*. 460:173-180 (2014).
266. Z. Xu, H.M. Mansour, and A.J. Hickey. Particle Interactions in Dry Powder Inhaler Unit Processes. *Journal of Adhesion Science and Technology*. 25:451-482 (2011).
267. N.R. Yacobi, N. Malmstadt, F. Fazlollahi, L. DeMaio, R. Marchelletta, S.F. Hamm-Alvarez, Z. Borok, K.-J. Kim, and E.D. Crandall. Mechanisms of Alveolar Epithelial Translocation of a Defined Population of Nanoparticles. *American Journal of Respiratory Cell and Molecular Biology*. 42:604-614 (2010).
268. M.S. Yang, H. Yamamoto, H. Kurashima, H. Takeuchi, T. Yokoyama, H. Tsujimoto, and Y. Kawashima. Design and evaluation of inhalable chitosan-modified

- poly (DL-lactic-co-glycolic acid) nanocomposite particles. *European Journal of Pharmaceutical Sciences*. 47:235-243 (2012).
269. X.-F. Yang, Y. Xu, D.-S. Qu, and H.-Y. Li. The influence of amino acids on aztreonam spray-dried powders for inhalation. *Asian Journal of Pharmaceutical Sciences*. 10:541-548 (2015).
270. P. York. Strategies for particle design using supercritical fluid technologies. *Pharmaceutical Science & Technology Today*. 2:430-440 (1999).
271. Y. You, M. Zhao, G. Liu, and X. Tang. Physical characteristics and aerosolization performance of insulin dry powders for inhalation prepared by a spray drying method. *The Journal of pharmacy and pharmacology*. 59:927-934 (2007).
272. J. Zhang, L. Wu, H.-K. Chan, and W. Watanabe. Formation, characterization, and fate of inhaled drug nanoparticles. *Advanced drug delivery reviews*. 63:441-455 (2011).
273. Z. Zhang, L. Xu, H. Chen, and X. Li. Rapamycin-loaded poly(ϵ -caprolactone)-poly(ethylene glycol)-poly(ϵ -caprolactone) nanoparticles: preparation, characterization and potential application in corneal transplantation. *Journal of Pharmacy and Pharmacology*. 66:557-563 (2014).
274. M. Zhao, Y. You, Y. Ren, Y. Zhang, and X. Tang. Formulation, characteristics and aerosolization performance of azithromycin DPI prepared by spray-drying. *Powder Technology*. 187:214-221 (2008).
275. S. Ziffels, N.L. Bemelmans, P.G. Durham, and A.J. Hickey. In vitro dry powder inhaler formulation performance considerations. *Journal of Controlled Release*. 199:45-52 (2015).
276. G.S. Zijlstra, W.L.J. Hinrichs, A.H.d. Boer, and H.W. Frijlink. The role of particle engineering in relation to formulation and de-agglomeration principle in the development of a dry powder formulation for inhalation of cetorelix. *European Journal of Pharmaceutical Sciences*. 23:139-149 (2004).